


12-2016

Bridge maintenance to enhance corrosion resistance and performance of steel girder bridges

Luis M. Moran Yanez
Purdue University

Follow this and additional works at: https://docs.lib.purdue.edu/open_access_dissertations

 Part of the [Civil Engineering Commons](#), and the [Materials Science and Engineering Commons](#)

Recommended Citation

Moran Yanez, Luis M., "Bridge maintenance to enhance corrosion resistance and performance of steel girder bridges" (2016). *Open Access Dissertations*. 977.
https://docs.lib.purdue.edu/open_access_dissertations/977

This document has been made available through Purdue e-Pubs, a service of the Purdue University Libraries. Please contact epubs@purdue.edu for additional information.

**PURDUE UNIVERSITY
GRADUATE SCHOOL
Thesis/Dissertation Acceptance**

This is to certify that the thesis/dissertation prepared

By LUIS MIGUEL MORAN YANEZ

Entitled

BRIDGE MAINTENANCE TO ENHANCE CORROSION RESISTANCE AND PERFORMANCE OF STEEL GIRDER BRIDGES

For the degree of Doctor of Philosophy

Is approved by the final examining committee:

DR. MARK D. BOWMAN

Chair

DR. AYHAN IRFANOGLU

DR. JUDY LIU

DR. MICHAEL E. KREGER

DR. ROBERT H. SPITZER

To the best of my knowledge and as understood by the student in the Thesis/Dissertation Agreement, Publication Delay, and Certification Disclaimer (Graduate School Form 32), this thesis/dissertation adheres to the provisions of Purdue University's "Policy of Integrity in Research" and the use of copyright material.

Approved by Major Professor(s): DR. MARK D. BOWMAN

Approved by: DR. DULCY ABRAHAM

Head of the Departmental Graduate Program

10/4/2016

Date

BRIDGE MAINTENANCE TO ENHANCE CORROSION RESISTANCE AND
PERFORMANCE OF STEEL GIRDER BRIDGES

A Dissertation

Submitted to the Faculty

of

Purdue University

by

Luis M. Moran Yañez

In Partial Fulfillment of the

Requirements for the Degree

of

Doctor of Philosophy

December 2016

Purdue University

West Lafayette, Indiana

the Indiana Department of Transportation and its staff, by supporting my research with information, materials and guidance.

My deeply thanks to my mother, brothers and sister, because I always have in mind all what they did for me. To Clarita, Luis Miguel and Paquito, for being with me in this project, for their love and affection. To Clara, my wife, by joining me in my dreams and goals, for her love and constant encouragement.

TABLE OF CONTENTS

	Page
LIST OF TABLES	xi
LIST OF FIGURES	xiv
ABSTRACT	xxi
CHAPTER 1. INTRODUCTION	1
1.1 General	1
1.2 Problem Statement	1
1.3 Objectives of the Research	6
1.4 Scope of the Research	7
CHAPTER 2. LITERATURE REVIEW	9
2.1 Research on Atmospheric Corrosion of Steel Girder Highway Bridges	9
2.2 Research in Bridge Maintenance Activities	12
2.3 Research on Accelerated Corrosion Tests	15
2.4 Research on Structural Analysis and Design of Corroded Composite Steel Girders	16
CHAPTER 3. CORROSION OF STEEL BRIDGE HIGHWAY GIRDERS	18
3.1 Introduction	18
3.2 Structural Steel	18
3.2.1 Characteristics of Structural Steel	18
3.2.2 Types of Structural Steel for Bridges	20
3.3 Corrosion of Structural Steel	22
3.3.1 Definition of Corrosion	22
3.3.2 Atmospheric Corrosion	23
3.3.3 Electrochemical Corrosion Process	24

	Page
3.3.4 Forms of Corrosion.....	26
3.3.5 Atmospheric Environments	27
3.4 Corrosion of Composite Steel Girders	28
3.4.1 Causes of Steel Girder Corrosion	28
3.4.2 Problems Due to Steel Girder Corrosion.....	30
3.5 Deterioration Model of Steel Girder Corrosion	32
3.5.1 Model to Predict the Rate of Corrosion.....	32
3.5.2 Model to Predict Location of Corrosion.....	37
3.6 Corrosion Protection of Steel Girders	40
CHAPTER 4. MAINTENANCE ACTIVITIES OF STEEL GIRDER BRIDGES....	42
4.1 Introduction	42
4.2 Bridge Superstructure Washing.....	43
4.2.1 Bridge Superstructure Washing Programs at State DOTs.....	45
4.2.2 Bridge Superstructure Washing Benefits	49
4.3 Spot Painting	50
4.3.1 Spot Painting Benefits	51
4.3.2 Service Life of Spot Painting.....	52
4.4 Summary	53
CHAPTER 5. ACCELERATED CORROSION TEST.....	54
5.1 Introduction	54
5.2 Accelerated Corrosion Test Program	56
5.2.1 Accelerated Corrosion Test – ASTM B117	56
5.2.2 Materials	57
5.2.3 Equipment.....	59
5.2.4 Salt Solution Application.....	63
5.3 ACT for Steel Washing Evaluation.....	64
5.3.1 Number of Coupons and Identification	64
5.3.2 Schedule for Washing Process	65
5.3.3 Initial Data Acquisition	67

	Page
5.3.4 Procedure for the ACT Regime for Steel Washing Evaluation.....	69
5.3.5 Results from ACT for Steel Washing Evaluation	74
5.4 ACT for Spot Painting Evaluation	91
5.4.1 Number of Coupons and Identification	91
5.4.2 Scribing Coupon Procedure.....	92
5.4.3 Initial Data Acquisition	93
5.4.4 Procedure for the ACT Regime for Spot Painting Evaluation	93
5.4.5 Results from ACT for Spot Painting Evaluation.....	96
5.5 Discussion of Results	105
5.5.1 Accelerated Corrosion Test (ACT)	105
5.5.2 Steel Washing Evaluation.....	106
5.5.3 Spot Painting Evaluation	107
CHAPTER 6. CORRELATION BETWEEN AN ACCELERATED CORROSION TEST AND ATMOSPHERIC CORROSION	108
6.1 Introduction	108
6.2 Control Test.....	110
6.2.1 Number of Coupons and Identification	110
6.2.2 Schedule for Control Test.....	110
6.2.3 Initial Data Acquisition	111
6.2.4 Procedure for the Control Test	111
6.2.5 Results from Control Test	112
6.3 Correlation between ACT and Atmospheric Corrosion.....	118
6.3.1 Correlation between the Weight Increment and Corrosion Penetration during ACT	118
6.3.2 Correlation between Time inside the Chamber and Time at Real Environments.....	120
6.3.3 Correlation between Corrosion Penetration from ACT to Atmospheric Corrosion	124
6.4 Sensitivity Analysis between Control Test Data and ACT Data.....	131

	Page
CHAPTER 7. STRUCTURAL ANALYSIS, DESIGN, AND LOAD RATING.....	139
7.1 Introduction	139
7.2 Bridge Load and Resistant Models	140
7.2.1 Dead Load	140
7.2.2 Live Load.....	141
7.2.3 Dynamic Load	142
7.2.4 Bridge Resistance Model.....	143
7.3 Structural Analysis and Design According to AASHTO LRFD.....	143
7.3.1 Representative I-Girder Steel Bridges Considered.....	144
7.3.2 Design Parameters and Loading Considerations.....	148
7.3.3 Load and Resistance Factor Design (AASHTO LRFD)	149
7.3.4 Limit States.....	150
7.3.5 Design for Flexural Capacity.....	151
7.3.6 Design for Shear Capacity.....	153
7.3.7 Elastic Deflections.....	154
7.3.8 Steel Highway Bridge Design using a FE Package.....	154
7.3.9 Analysis and Design of Typical Steel Girder Bridge	157
7.4 Steel Bridge Load Rating According to AASHTO MBE	163
7.4.1 Load and Resistance Factor Rating (LRFR).....	163
7.4.2 General Load-Rating Equation.....	166
7.4.3 Levels of Evaluation.....	168
7.4.4 Load Rating for Representative Bridges Considered	172
7.5 Results and Discussion.....	175
7.5.1 Effect of Stress Type	177
7.5.2 Effect of Local Environment	181
7.5.3 Effect of Number of Spans	183
7.5.4 Effect of Span Length.....	185
7.5.5 Effect of Steel Type.....	187
7.5.6 Effect on Live-Load Deflections	189

	Page
7.5.7 Effect of Maintenance Alternative	193
CHAPTER 8. ECONOMIC EVALUATION OF CORRODED STEEL BRIDGES	198
8.1 Introduction	198
8.2 Life Cycle Cost Analysis.....	199
8.2.1 Bridge Service Life.....	200
8.2.2 Cost of Bridge Maintenance Activities, Rehabilitation, and Replacement	200
8.2.3 Discount Rate	201
8.2.4 Present Value.....	201
8.2.5 Bridge Load Rating	202
8.3 Economic Analysis for Bridge Maintenance Activities	205
8.3.1 Effect of Steel Girder Washing Activity for Uncoated Carbon Steel	205
8.3.2 Effect of Steel Girder Washing Activity for Coated Carbon Steel	209
8.3.3 Effect of Washing on Coated and Re-coated Carbon Steel Members.....	213
8.3.4 Effect of Steel Washing Activity for Uncoated and Coated Weathering Steel	215
8.4 Results from LCCA.....	217
CHAPTER 9. SUMMARY, CONCLUSIONS AND RECOMMENDATIONS	219
9.1 Summary	219
9.2 Conclusions	221
9.3 Recommendations	224
LIST OF REFERENCES	226
APPENDICES	
Appendix A Corrosion Penetration Data	235
Appendix B Product Certificate.....	239
Appendix C Identification of Coupons for ACT	243
Appendix D Weight Change During ACT.....	246
Appendix E Initial Dimensions of Coupons.....	264
Appendix F Thickness Change During ACT	268
Appendix G Photographs During ACT.....	284

	Page
Appendix H Creepage Area Change of Scribed Coupons During ACT.....	288
Appendix I Control Test.....	294
Appendix J Rating Factors RF _m and RF _v	298
VITA.....	323

LIST OF TABLES

Table	Page
3.1: Minimum mechanical properties of structural steel by shape, strength, and thickness (AASHTO, 2012)	21
3.2: Statistical parameters for A and B (Kayser, 1988)	34
4.1: DOTs information reported on bridge washing programs (Berman et al., 2013)....	46
4.2: Service life of spot painting (Bowman and Moran, 2015)	53
5.1: Matrix for washing program	66
6.1: Results of Control Test for coupons from steel Type A.	114
6.2: Results of Control Test for coupons from steel Type C	116
6.3: Corrosion penetration values from ACT for steel Type A	119
6.4: Corrosion penetration values from ACT for steel Type C.....	120
6.5: Correlating weeks in Control Test - years at real environments – (Type A).....	121
6.6: Correlating weeks in Control Test - years at real environments – (Type C).....	122
6.7: Correlating values between ACT and real environments – steel Type A.....	123
6.8: Correlating values between ACT and real environments - steel Type C.....	124
6.9: Corrosion penetration C for steel Type A versus time measured in weeks at ACT and years at real environments	126
6.10: Corrosion penetration C for steel Type C versus time measured in weeks at ACT and years at real environments	127
6.11: Weight increment data from control test and Group A10	131
6.12: Ratio of corrosion penetration to weight increment for control test data	132
6.13: Corrosion penetration from weight increment for Group A10	132
6.14: Corrosion penetration values from Group A10	134
6.15: Correlating penetration from Group A10 with years at real environments	135

Table	Page
6.16: Correlating years at real environments for 3.5 weeks at ACT – Steel Type A	136
6.17: Corrosion penetration C for steel type A versus time measured in weeks at ACT and years at real environments	136
7.1: Typical values for materials weight.....	140
7.2: Dynamic load allowance (AASHTO, 2012).....	143
7.3: Material properties assumed for composite steel girder bridges	148
7.4: Multiple presence factors, m (AASHTO, 2012).....	149
7.5: Dead load moment values for CSiBridge and hand solution and analysis	156
7.6: Live load moment values for hand solution and CSiBridge analysis	157
7.7: Maximum Demand/Capacity ratios for stresses and deflections.....	162
7.8: Generalized live load factors for commercial routine vehicles - Evaluation for strength I limit state (AASHTO, 2011).....	172
7.9: Generalized live load factors for specialized hauling vehicles - Evaluation for strength I limit state (AASHTO, 2011).....	172
8.1: Unit costs for bridge maintenance activities (Sobanjo, 2001; Hearn, 2012).....	201
8.2: Bridge’s service age (years) when reaching RFv=1.0 - Industrial/urban	204
8.3: Bridge’s service age (years) when reaching RFv=1.0 - Marine	204
8.4: Bridge’s service age (years) when reaching RFv=1.0 - Rural.....	205
8.5: Bridge models reaching legal load rating limit RFv = 1.00	209
8.6: Three-coat paint system service life	210
8.7: Summary of PV for bridge cases of carbon steel, uncoated and coated.....	213
 Appendix Table	
A.1: Parameters A and B – Industrial environment. Albrecht and Naeemi (1984).....	235
A.2: Parameters A and B –Marine environment. Albrecht and Naeemi (1984).....	235
A.3: Parameters A and B – Rural environment. Albrecht and Naeemi (1984)	236
C.1: Identification of steel coupons from steel types A, B, C, and D.....	244
D.1: Weight change during ACT for coupons from steel Type A.....	247
D.2: Weight change during ACT for coupons from steel Type B.....	252
D.3: Weight change during ACT for coupons from steel Type C.....	257

Appendix Table	Page
D.4: Weight change during ACT for coupons from steel Type D.....	262
E.1: Initial dimensions of coupons from steel Type A	265
E.2: Initial dimensions of coupons from steel Type B.....	266
E.3: Initial dimensions of coupons from steel Type C.....	267
F.1: Thickness change during ACT for coupons from steel Type A	269
F.2: Thickness change during ACT for coupons from steel Type B	274
F.3: Thickness change during ACT for coupons from steel Type C	279
H.1: Creepage area change during ACT for coupons from steel Type D.....	291
I.1: Identification for Control Test coupons, Groups X and W	295
I.2: Weight change for Control Test, Groups X.....	296
I.3: Weight change for Control Test, Groups W.....	296

LIST OF FIGURES

Figure	Page
1.1: US bridge inventory by year of construction (FHWA, 2015)	2
1.2: US steel bridges condition at 2005 (Eom, 1024)	3
1.3: Service life extension: a) Performing simple preventive maintenance activities, b) Performing only important rehabilitation processes (NYSDOT, 2008).....	5
3.1: Engineering stress-strain curve for structural steel (FHWA, 2012)	20
3.2: Classification of corrosion process (Syed, 2006)	23
3.3: Schematic representation of the corrosion mechanism for steel (Corus, 2005)	25
3.4: Sketches for the principal forms of steel corrosion (Landolfo, 2010).....	27
3.5: Typical corrosion process of steel girders: 1) at the web and bottom flange (Zaffetti, 2010), 2) Next to a pin and hanger connection (WisDOT, 2011)	30
3.6: Debris accumulation at a steel superstructure connection point (Kogler, 2012).....	30
3.7: Mean of Time-Corrosion penetration curves for carbon steel (Kayser, 1988).....	36
3.8: Corrosion penetration curves (Park et al., 1998)	37
3.9: Typical corrosion locations on a steel girder bridge (Kayser, 1988).....	38
3.10: Corrosion on typical steel girder sections, at midspan (left), and at supports (right) (Park, 1999)	39
3.11: Corrosion on typical steel girder section (Czarnecki, 2006)	40
4.1: Damaged steel girder due to extended corrosion (Zaffetti, 2010)	44
4.2: Steel bridge superstructure washing (Crampton et al., 2013).....	45
4.3: Interior of lower chord from truss. Before (left) and after (right) cleaning and washing (Berman et al., 2013).....	50
4.4: Portion of a steel girder candidate for spot painting (Myers et al., 2010)	51

Figure	Page
5.1: Steel coupons before and after epoxy coating application. Left: uncoated coupon, Right: coated coupon.....	58
5.2: Steel coupons supported by PVC racks.....	58
5.3: Front and lateral view of acrylic box.....	59
5.4: Interior view of weather chamber with acrylic boxes (left). Misting system installed (right).....	61
5.5: Power washer.....	62
5.6: Abrasive blast cabinet.....	62
5.7: Milling machine scribing a steel plate.....	63
5.8: Components for salt solution preparation: Sodium chloride and scale (left), distilled water and graduated plastic bucket (center), and pH-meter (right).....	64
5.9: Location of thickness measuring positions.....	68
5.10: Coupon data acquisition. From left to right: weight, side dimensions, thickness, photograph.....	69
5.11: Weather chamber with steel coupons under ACT regime.....	70
5.12: Power washing steel coupons.....	71
5.13: Drying wet coupons after washing.....	72
5.14: Flow chart for ACT program for steel washing evaluation.....	74
5.15: Weight change versus time for steel Type A groups.....	77
5.16: Weight change versus time for mean values from Groups A02-A05 and Group A10.....	79
5.17: Weight change versus time for steel Type C groups.....	80
5.18: Weight change versus time for mean values from Groups C02-C05 and Group C10.....	81
5.19: Weight change versus time for steel Type C groups.....	82
5.20: Weight change versus time for mean values from Groups B02-B05 and Group B10.....	83
5.21: Thickness change versus time for steel Type A groups.....	84

Figure	Page
5.22: Thickness change versus time for mean values from Groups A02-A05 and Group A10.....	85
5.23: Thickness change versus time for steel Type C groups.....	87
5.24: Thickness change versus time for mean values from Groups C02-C05 and Group C10.....	87
5.25: Thickness change versus time for steel Type B groups.....	89
5.26: Thickness change versus time for mean values from Groups B02-B05 and Group B10.....	89
5.27: Rust formation over uncoated steel coupon (coupon A01-a).....	90
5.28: Lack of rust formation over coated steel coupon (coupon B05-a).....	91
5.29: Left: Scribed steel coupon (D01-a). Right: Scribe mark magnified with (mm) scale.....	92
5.30: Flow chart for ACT program for spot painting evaluation.....	94
5.31: Tools and products used to eliminate the rust and protect the scribe.	95
5.32: Process to clean and protect the scribe. From left to right: Clean the scribe with sandpaper and rust dissolver application; cover all coupon face but scribe mark; spray paint; coupon with covered scribe.	96
5.33: Weight change versus time for steel Type D groups.....	98
5.34: Weight change versus time for mean values from Groups D01-D04 and Group D06.....	99
5.35: Creepage area measurement (ASTM Standard D7087-05a).....	100
5.36: Trace of rust creepage area. Complete scribed coupon image and two magnifications after six weeks of ACT.....	102
5.37: Net Mean Creepage versus time for steel Type D groups.....	103
5.38: Net Mean Creepage versus time for mean values from Groups D02-D04 and Group D06.....	104
5.39: Coupons from Groups D05 and D07 after the ACT ended.....	105
6.1: Dimensions for exposed area of a Control Test coupon.....	113
6.2: Correlation weight increment-corrosion penetration for steel Type A.....	115

Figure	Page
6.3: Correlating weight increment-corrosion penetration for steel Type C	117
6.4: Correlating weeks in Control Test - years at real environments - steel Type A.....	123
6.5: Correlating weeks in Control Test - years at real environments - steel Type C	124
6.6: Corrosion penetration vs. time - steel Type A - Industrial/Urban environment	128
6.7: Corrosion penetration vs. time - steel Type A - Marine environment	128
6.8: Corrosion penetration vs. time - steel Type A - Rural environment.....	129
6.9: Corrosion penetration vs. time - steel Type C - Industrial/Urban environment	129
6.10: Corrosion penetration vs. time - steel Type C - Marine environment	130
6.11: Corrosion penetration vs. time - steel Type C - Rural environment.....	130
6.12: Correlation weight increment-corrosion penetration for steel Type A.....	133
6.13: Correlating weeks in the ACT with years at real environments – Type A.....	135
6.14: Corrosion penetration vs. time – steel Type A – Industrial/urban environment....	137
6.15: Corrosion penetration vs. time – steel Type C – Industrial/urban environment....	138
7.1: AASHTO LRFD design live load (HL-93) (AASHTO, 2011)	142
7.2: Typical bridge cross section (Barth, 2012).....	145
7.3: Sketch of longitudinal view for typical one-span and two-span bridges	147
7.4: Sketch of typical steel girder elevation (Barth, 2012)	156
7.5: Sketch of the typical 70' one-span composite steel I-girder bridge	158
7.6: Sketch of the typical 90' one-span composite steel I-girder bridge	158
7.7: Sketch of the typical 110' one-span composite steel I-girder bridge	158
7.8: Sketch of the typical 130' one-span composite steel I-girder bridge	159
7.9: Sketch of the typical 70'-70' two-span composite steel I-girder bridge.....	160
7.10: Sketch of the typical 90'-90' two-span composite steel I-girder bridge.....	160
7.11: Sketch of the typical 110'-110' two-span composite steel I-girder bridge.....	161
7.12: Sketch of the typical 130'-130' two-span composite steel I-girder bridge.....	161
7.13: Load and resistance factor rating flow chart (AASHTO, 2011).....	165
7.14: AASHTO legal trucks (AASHTO, 2011).....	170
7.15: Bridge posting loads for single-unit SHVs (AASHTO, 2011)	171
7.16: Notional rating load (AASHTO, 2011)	171

Figure	Page
7.17: RF _m and RF _v versus time for bridge case 2CSIN.....	175
7.18: RF _m and RF _v variation on time (inventory, operating, legal) – Cases 1ASIN and 1ASIW	180
7.19: RF _m and RF _v variation on time (inventory, operating, legal) – Cases 2CTMN and 2CTMW.....	180
7.20: RF _v versus time for bridge cases 1AT_ and for the three local environments.....	182
7.21: RF _v versus time for bridge cases 2BT_ and for the three local environments.....	182
7.22: RF _v for one-span and two-span configurations and no washing alternative	184
7.23: RF _v for one-span and two-span configurations and steel washing alternative.....	185
7.24: RF _v vs. time for bridge cases of one-span (70', 90', 110', and 130').....	186
7.25: RF _v vs. time for bridge cases of two-span (70', 90', 110', and 130').....	187
7.26: RF _v versus time for bridge cases 1_SIN and 1_TIN	189
7.27: RF _v versus time for bridge cases 1_SIW and 1_TIW	189
7.28: Live-load elastic deflections versus time for cases 1_SIN and 1_SIW	192
7.29: Live-load elastic deflections versus time for cases 2_SIN and 2_SIW	192
7.30: RF _v versus time for bridge cases 1CSIN/W and 2CSIN/W	196
7.31: RF _v versus time for bridge cases 1DSIN/W and 2DSIN/W	196
8.1: Load rating factor for shear capacity - bridge case 1CSIN, uncoated steel.....	207
8.2: LCCA for bridge 1CSIN uncoated steel - alternative with no maintenance	207
8.3: Load rating factor for shear capacity - bridge case 1CSIW, uncoated steel.....	208
8.4: LCCA for bridge 1CSIW uncoated steel - alternative with maintenance.....	208
8.5: LCCA for bridge 1CSIN coated steel - alternative with no maintenance	211
8.6: LCCA for bridge 1CSIW coated steel - alternative with maintenance.....	211
8.7: LCCA for bridge 1CSIN coated steel - alternative with washing and re-coating ...	214
8.8: 1-Span x 110' – Weathering steel – Industrial – No washing/Washing.....	215
8.9: 2-Span x 110' – Weathering steel – Industrial – No washing/Washing.....	216
8.10: 1-Span x 130' – Weathering steel – Marine – No washing/Washing.....	216
8.11: 2-Span x 130' – Weathering steel – Marine – No washing/Washing.....	216

Appendix Figure	Page
A.1: Corrosion penetration for carbon steel - Linear axis	236
A.2: Corrosion penetration for carbon steel – Log-Log axis	237
A.3: Corrosion penetration for weathering steel - Linear axis.....	237
A.4: Corrosion penetration for weathering steel – Log-Log axis	238
B.1: Material test report for carbon steel GR50 from EVRAZ, INC.....	240
B.2: Report of test and analyses for weathering steel GR50W from ARCELORMITTAL STEEL USA	241
B.3: Certificate of analysis for sodium chloride from MORTON SALT, INC.	242
D.1: Weight change versus time during ACT for coupons from steel Type A	250
D.2: Weight change versus time during ACT for coupons from steel Type B.....	255
D.3: Weight change versus time during ACT for coupons from steel Type C.....	260
D.4: Weight change versus time during ACT for coupons from steel Type D	263
F.1: Thickness change versus time during ACT for coupons from steel Type A.....	272
F.2: Thickness change versus time during ACT for coupons from steel Type B.....	277
F.3: Thickness change versus time during ACT for coupons from steel Type C	282
G.1: Photographs showing physical aspect change during ACT - Coupon A01-a.....	285
H.1: Photographs of creepage area change during ACT - Coupon D01-a.....	289
H.2: Photographs of creepage area change during ACT - Coupon D02-b	290
H.3: Graphs for NMC change during ACT for coupons from steel Type D	292
I.1: Photographs from Control Test - Coupon X01-a	297
I.2: Photographs from Control Test - Coupon W05-a	297
J.1: RFm and RFv versus time for 1-Span x 70', Industrial/urban	299
J.2: RFm and RFv versus time for 1-Span x 90', Industrial/urban	300
J.3: RFm and RFv versus time for 1-Span x 110', Industrial/urban	301
J.4: RFm and RFv versus time for 1-Span x 130', Industrial/urban	302
J.5: RFm and RFv versus time for 2-Span x 70', Industrial/urban	303
J.6: RFm and RFv versus time for 2-Span x 90', Industrial/urban	304
J.7: RFm and RFv versus time for 2-Span x 110', Industrial/urban	305
J.8: RFm and RFv versus time for 2-Span x 130', Industrial/urban	306

Appendix Figure	Page
J.9: RFm and RFv versus time for 1-Span x 70', Marine	307
J.10: RFm and RFv versus time for 1-Span x 90', Marine	308
J.11: RFm and RFv versus time for 1-Span x 110', Marine	309
J.12: RFm and RFv versus time for 1-Span x 130', Marine	310
J.13: RFm and RFv versus time for 2-Span x 70', Marine	311
J.14: RFm and RFv versus time for 2-Span x 90', Marine	312
J.15: RFm and RFv versus time for 2-Span x 110', Marine	313
J.16: RFm and RFv versus time for 2-Span x 130', Marine	314
J.17: RFm and RFv versus time for 1-Span x 70', Rural.....	315
J.18: RFm and RFv versus time for 1-Span x 90', Rural.....	316
J.19: RFm and RFv versus time for 1-Span x 110', Rural.....	317
J.20: RFm and RFv versus time for 1-Span x 130', Rural.....	318
J.21: RFm and RFv versus time for 2-Span x 70', Rural.....	319
J.22: RFm and RFv versus time for 2-Span x 90', Rural.....	320
J.23: RFm and RFv versus time for 2-Span x 110', Rural.....	321
J.24: RFm and RFv versus time for 2-Span x 130', Rural.....	322

ABSTRACT

Moran Yañez, Luis M.. Ph.D., Purdue University, December 2016. Bridge Maintenance to Enhance Corrosion Resistance and Performance of Steel Girder Bridges. Major Professor: Mark Bowman.

The integrity and efficiency of any national highway system relies on the condition of the various components. Bridges are fundamental elements of a highway system, representing an important investment and a strategic link that facilitates the transport of persons and goods. The cost to rehabilitate or replace a highway bridge represents an important expenditure to the owner, who needs to evaluate the correct time to assume that cost. Among the several factors that affect the condition of steel highway bridges, corrosion is identified as the main problem. In the USA corrosion is the primary cause of structurally deficient steel bridges.

The benefit of regular high-pressure superstructure washing and spot painting were evaluated as effective maintenance activities to reduce the corrosion process. The effectiveness of steel girder washing was assessed by developing models of corrosion deterioration of composite steel girders and analyzing steel coupons at the laboratory under atmospheric corrosion for two alternatives: when high-pressure washing was performed and when washing was not considered. The effectiveness of spot painting was assessed by analyzing the corrosion on steel coupons, with small damages, unprotected and protected by spot painting

A parametric analysis of corroded steel girder bridges was considered. The emphasis was focused on the parametric analyses of corroded steel girder bridges under two alternatives: (a) when steel bridge girder washing is performed according to a particular

frequency, and (b) when no bridge washing is performed to the girders. The reduction of structural capacity was observed for both alternatives along the structure service life, estimated at 100 years. An economic analysis, using the Life-Cycle Cost Analysis method, demonstrated that it is more cost-effective to perform steel girder washing as a scheduled maintenance activity in contrast to the no washing alternative

CHAPTER 1. INTRODUCTION

1.1 General

The integrity and efficiency of any national highway system relies on the condition of the various components. Bridges are fundamental elements of a highway system, representing an important investment and a strategic link that facilitates the transport of persons and goods. The cost to rehabilitate or replace a highway bridge represents an important expenditure to the owner, who needs to evaluate the correct time to assume that cost. But most significant, any highway system interruption due to partial or total closure of bridges represents a considerable indirect cost to the users, caused by delays and loss of productivity that could be estimated to be several times the direct cost of the bridge rehabilitation (Koch, 2002). A policy of performing simple, scheduled bridge maintenance activities is expected to extend the service lives of highway bridges at a low-cost, and with traffic service that is interrupted only for short periods of time. Consequently, prolonging the service lives of highway bridges requiring only short interruptions is an effective way to provide outstanding service for the users and to make more efficient use of the owner's scarce resources.

1.2 Problem Statement

Highway bridges constitute vital links in any transportation system. According to the Federal Highway Administration (FHWA), as of December 2013, there are 607,751 bridges across the country (FHWA, 2015). Most of them were constructed after World War II, sponsored and funded under President Eisenhower's Interstate Highway Act of

1956, as seen in Figure 1.1. The National Bridge Inventory (NBI) shows that steel bridges represent more than 30% of the entire system. Steel bridges have been widely considered as an adequate alternative in the USA highway system, based on the outstanding characteristics of structural steel, such as economy, speed of construction, versatility, and aesthetics. Nevertheless, when a steel bridge is not properly designed, constructed or maintained, deterioration of the steel components became a critical issue in the bridge service life. From the steel bridges inventory, 26% are classified as structurally deficient and 19% are functionally obsolete, as shown in Figure 1.2 (Eom, 2014). The number of structurally deficient bridges will be likely to continue increasing if measures are not implemented to reduce the rate of the deterioration process.

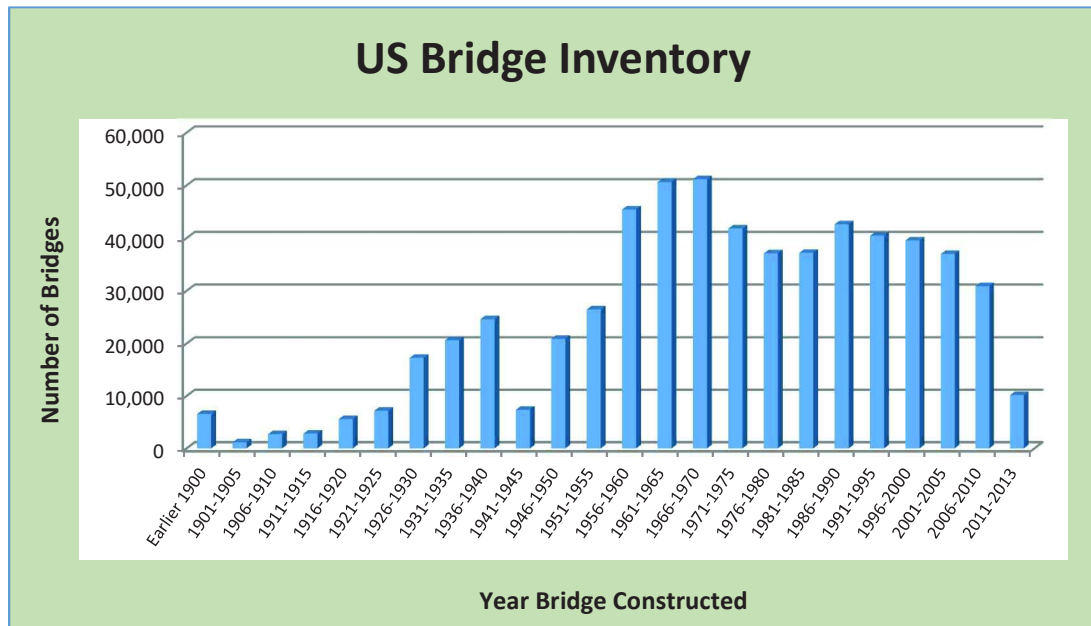


Figure 1.1: US bridge inventory by year of construction (FHWA, 2015)

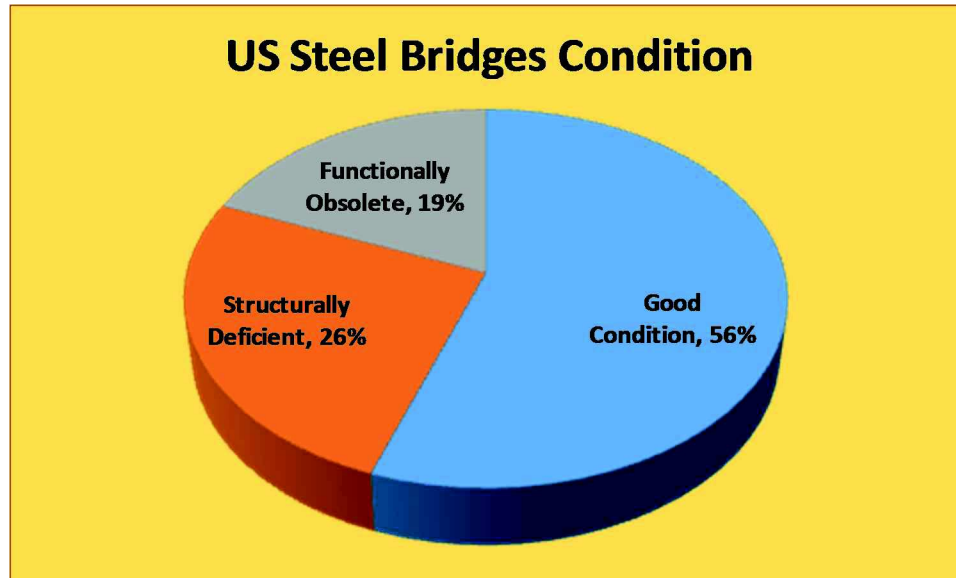


Figure 1.2: US steel bridges condition at 2005 (Eom, 1024)

A structurally deficient bridge will typically require it to be posted, rehabilitated or replaced, implying safety hazards and future funds allocations. There are many factors affecting steel bridge condition, such as an excessive live load regime, an aggressive environment, aging, and bridge maintenance operations. These factors, among others, produce different types of deterioration problems.

Among the several factors that affect the condition of steel highway bridges, corrosion is identified as the main problem by State Departments of Transportations (DOTs). From a report by the FHWA (Koch, 2002), corrosion is the primary cause of structurally deficient steel bridges. By the 1960s, many Snow Belt states introduced the use of deicing products to reduce snow accumulation on the bridge decks during winter seasons (Kepler et al., 2000). The corrosion process initiates when deicing products reach the steel structural elements under the deck by leakage through deck joints or salt solution is sprayed from roads under the bridge by passing traffic. The process is based on a chloride-induced corrosion, produced by the attack of chloride ions present in the deicing products. In a similar manner, steel bridges exposed to marine environments are susceptible to corrosion by the high concentration of chloride ions in the air. As a

consequence of corrosion, a structural steel member loses part of its mass and section thickness, causing it to be susceptible to partial failure of the member or the total collapse of the structural system.

Bridge preservation can be defined as the ability to keep a bridge structure in good condition as long as possible, thereby slowing the process of deterioration. Bridge preservation can be achieved through the performance of some selected bridge maintenance activities, at some regular frequency and following appropriate practices. It has been shown in different studies that a program of low cost maintenance activities, performed with some regular frequency, is a cost-effective practice, instead of performing few expensive bridge repairs, rehabilitations or even replacements, during the bridge service life (Hopwood, 1999; Purvis, 2003; NYSDOT, 2008; Spuler et al, 2012). Figure 1.3 depicts the performance level for a bridge under two different programs: one considering a maintenance program with frequent low-cost activities, versus a program with no maintenance considerations but the performance of a few expensive rehabilitations.

Life-cycle cost analysis (LCCA) is an efficient tool to analyze and select the best alternative from different options (Hawk, 2003; Azizinamini et al., 2013). The application of LCCA has proven that performing frequently low-cost bridge maintenance alternatives is more cost-effective than alternatives expecting only high-cost rehabilitations or replacements (Weyers et al., 1993; Chang et al., 1999; RIDOT, 2002). Consequently, bridge maintenance activities are expected to be an effective alternative to prolong the bridge service life at a low cost.

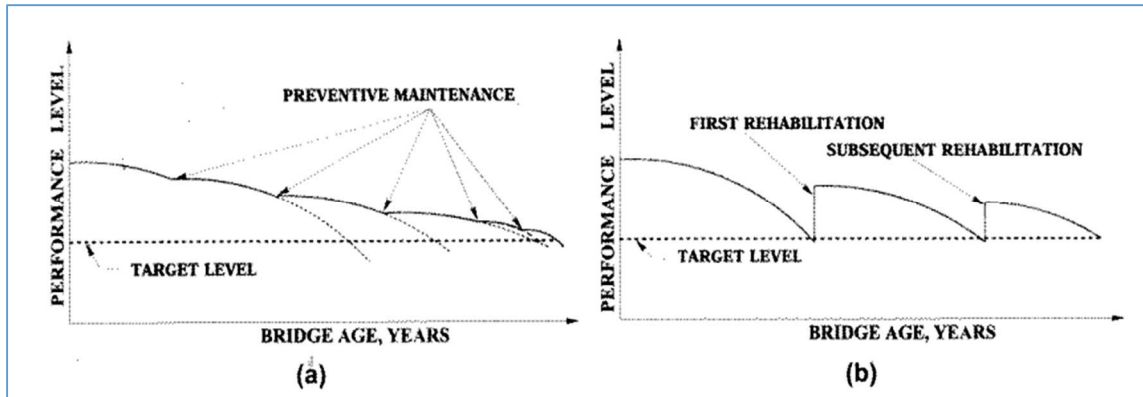


Figure 1.3: Service life extension: a) Performing simple preventive maintenance activities, b) Performing only important rehabilitation processes (NYSDOT, 2008)

To reduce the corrosion of steel highway bridge girders, the two most common alternatives have been either the application of a coating system to the surfaces of carbon steel or the use of weathering steel (Nickerson, 1995; Corus, 2012). Nevertheless, it has been found that both protection systems fail to prevent corrosion when chloride compounds accumulate on the surface of steel girders during extended periods. The application of regular high-pressure washing is believed to be an effective alternative to eliminate or reduce the accumulation of chloride ions on the steel girder surfaces, thereby reducing or slowing the corrosion process. Regrettably, this is a fact based mostly on empirical data provided by State DOTs maintenance crews, bridge inspectors, and transport experts, with no scientific evidence supporting this belief.

Another source of corrosion is small, spot damage on the girder's coat surface, commonly developed during transport from the shop to the bridge site or during the bridge assembly. This small damaged surface is prone to develop corrosion at a faster rate due to steel surface exposure to the environment and aggressive compounds such as chloride ions. Spot painting is considered an effective maintenance activity to address surface coating damage, since only a small girder area has to be repaired.

Therefore, there is a need to study superstructure washing and spot painting as effective low-cost bridge maintenance activities for steel girders, since they are able to reduce or

delay the corrosion process. The effectiveness of these activities should be justified by an economic analysis supported by methods such as the Life Cycle Cost Analysis.

1.3 Objectives of the Research

The objective of this research was to understand, model, and assess the structural capacity degradation of typical steel girder highway bridges due to the atmospheric corrosion, so that the benefit of regular high-pressure superstructure washing and spot painting can be evaluated as effective maintenance activities to reduce the corrosion process. The effectiveness of steel girder washing was assessed by developing models of corrosion deterioration of composite steel girders and analyzing steel coupons at the laboratory under atmospheric corrosion for two alternatives: when high-pressure washing was performed and when washing was not considered. The effectiveness of spot painting was assessed by analyzing the corrosion on steel coupons, with small damages, unprotected and protected by spot painting.

Corrosion models were developed to estimate the loss of mass and reduction of section thickness with aging. The corrosion models also considered the corrosion penetration patterns exhibited by typical steel highway bridge girders. A series of accelerated corrosion laboratory tests were performed on small steel samples to reproduce the effect of both high-pressure washing and spot painting in reducing the corrosion. From the accelerated tests a series of curves relating aging time with corrosion penetration were established.

Based on the section reduction by corrosion, the structural capacity reduction of steel highway bridge girders was analyzed. The reduction of structural capacity of steel girder bridges due to environmental corrosion was assessed by performing a parametric study on typical steel highway bridges of one and two spans, with different span lengths, different steel types, exposed to different environments, and under different maintenance alternatives. The structural capacity reduction was estimated by performing a structural

analysis on composite steel girder bridge models using a finite element software. The reduction of bending and shear capacity, and the increment of deflections, were estimated using the limit state functions given by the AASHTO LRFD Bridge Design Specifications (AASHTO, 2012), and performing the bridge load rating based on specifications from the Manual for Bridge Evaluation (AASHTO, 2011).

1.4 Scope of the Research

Steel corrosion is a complex problem due to the influence of several factors, all of them with significant variations and uncertainties involved during the process. Corrosion is a combination of physical and chemical processes that requires considerable time to be developed, sometimes months or even years, according to the surrounding atmospheric conditions and steel properties. This study was limited to consider the effect of uniform corrosion as the only factor for structural degradation of the steel highway bridge girders. The atmospheric corrosion was studied considering three macro-environments: Industrial/Urban, Marine, and Rural. The analyzed girders were constructed from carbon steel and weathering steel, both uncoated and coated using a three-layer system (inorganic zinc primer, epoxy intermediate coat and a polyurethane finish coat). The structural analysis considered typical steel girder highway bridges, of one and two spans. The following tasks were performed to achieve the objective of this research:

- Perform a literature review of studies related to steel corrosion process in general, corrosion processes on steel girder highway bridges, accelerated corrosion tests, structural analysis of corroded steel girder bridges, bridge load rating process, bridge maintenance activities, high-pressure washing/flushing of steel girder, spot painting, and cost/benefit analysis.
- Implement an accelerated corrosion process to replicate corrosion degradation of steel samples in the laboratory.
- Develop a set of experimental curves to relate the frequency of high-pressure washing treatments with corrosion rates at different typical environments.

- Identify a corrosion rate model based on reliable documented experiences to be related with curves of corrosion rates obtained from laboratory tests.
- Analyze the effect of spot painting on scribed plates.
- Define typical steel girder highway bridge models of one and two spans, of different span lengths, and for different types of steel, to be analyzed under different levels of corrosion.
- Study the loss of structural capacity and serviceability of steel highway bridges with time due to general corrosion effects.
- Evaluate the cost/benefit ratio for two alternatives: when steel girders are treated with high-pressure washing to reduce the corrosion process and when washing is not performed.
- Propose an efficient frequency for periodic washing/flushing maintenance activities that minimize the loss of structural capacity of steel bridges due to corrosion and maximize the allocated resources.

CHAPTER 2. LITERATURE REVIEW

Part of this research was a review of relevant literature on corrosion of steel beam and girder highway bridges, maintenance activities for steel highway bridges, accelerated corrosion tests, and structural analysis, design, and load rating of corroded steel highway bridges. Abundant literature and research on steel corrosion was found; limited information on atmospheric corrosion of steel highway bridges was located; and very few documents were found on the effectiveness of bridge maintenance activities in reducing the rate of atmospheric corrosion of steel girders.

2.1 Research on Atmospheric Corrosion of Steel Girder Highway Bridges

According to Czarnecki (2006) steel bridges deteriorate during their service life due to several effects, with the most influential involving the surrounding environment, changes in live loads, and structural fatigue. Size and capacity of modern trucks have increased in the last few decades, requiring greater bridge resistant capacities. Evaluation of bridge capacities focuses on structure and material capacities and resistances. Steel highway bridge design requires special considerations with respect to material degradation due to environmental effects, especially atmospheric corrosion attack. The resistances of steel bridge members change in time due to environmental attack (Kayser, 1988; Czarnecki, 2006; Rahgozar, 2009).

In the National Cooperative Highway Research Program Report 272, Albrecht and Naeemi (1984) studied the performance of weathering steel in bridges, and also the performance for other steel types, such as carbon steel and copper steel. The main

concern in this study was atmospheric corrosion attack, their causes, consequences, and alternatives to reduce the problems. The document emphasizes the influence of the environment surrounding the bridge as the main factor for corrosion degradation. The study by Albrecht and Naeemi (1988) indicated that the use of deicing salts is one of the leading causes of corrosion in steel bridge members. They mentioned that especially in the “snow belt” states of the USA, steel bridges are exposed to corrosion attack due to contamination from deicing salt compounds in different ways. Albrecht and Naeemi (1984), Kayser (1988), and Czarnecki (2006) mentioned that debris accumulation on the horizontal surfaces of steel members is another source for corrosion attack since they are able to retain moisture, chloride and sulfate compounds in contact with the steel surface for a prolong period of time. In the same sense, Kogler (2012) indicated that the time of wetness is an issue for steel bridge member areas that trap or retain water or debris. “The severity of the deterioration depends upon how much water gets to the steel and how long it remains there (Kayser, 1988).” Morcillo (2011) indicated that steel bridge members will corrode at different rates during their exposure in different environments.

Corrosion is developed in several forms in steel bridge members. General (uniform) corrosion is the most common, causing gradual reduction in section thicknesses (Rahgozar, 2009). For instance, the Michigan DOT investigated the corrosion of steel bridges in the state of Michigan (McCrum et al., 1985). The study found a rate of uniform corrosion at exposed surfaces that ranged from 0.2 mils per year to 6 mils per year. In the same study it was reported that pitting corrosion in shielded areas can be as high as 16 mils per year. The estimation of steel loss of thickness from atmospheric corrosion has been a serious concern and several models have been developed.

Various corrosion models, developed from different approaches, can be classified as first level and second level models. First level models are based on the relationships from the steel and microenvironment components and the application of laws from physics and chemistry. The second level models are oriented to engineering applications and estimate the corrosion penetration from the loss of mass with time (Landolfo et al., 2010). Due to

the most direct application to the solution of engineering problems, the second level models were used in this study.

Townsend and Zoccola (1982) found that corrosion penetration results, obtained from atmospheric tests, were well predicted using a power function of the form $C = At^B$. In this expression, C is the corrosion penetration, t is the exposure time, and A and B are constants. McCuen and Albrecht (1994) recommended a composite power-linear model that consisted of two expressions, the first a power function similar to that from Townsend and Zoccola and the second a linear expression. McCuen and Albrecht (1994) also presented a composite power-power model, comprised of two power equations to describe the corrosion penetration in time.

To consider the delay of corrosion initiation, due to coating protection, Park et al. (1998) presented a modified corrosion model, with near zero corrosion for the first fifteen to twenty years, until the paint or protective cover deteriorates and then corrosion damage starts to develop. From several studies (Kayser, 1988; Park et al., 1998; Czarnecki, 2006) there is an agreement that steel girders corrode at higher rates at the upper face of the bottom flange along all the span, over the entire web near the supports, and at the lower portion of the web away from the supports.

The main effects of atmospheric corrosion on steel bridge members have been identified by many researchers. Those effects are mostly linked to degradation of the bridge safety, capacity, and serviceability (Kayser and Nowak, 1989; Park et al., 1998; Czarnecki, 2006; Rahgozar, 2009). Rahgozar (2009) pointed out that loss of material due to corrosion produces a change in the section properties of a steel member (area, moment of inertia, radius of gyration, etc.), hence causing a reduction in the member carrying capacity, and therefore, reducing the entire structural capacity. Park et al. (1998) indicated that steel girder corrosion may affect the bridge resistant capacity in bending, shear and bearing.

2.2 Research in Bridge Maintenance Activities

Appropriate bridge maintenance activities can prolong the bridge service life at relative low costs if they are routinely conducted (FHWA, 2011). The necessity for effective bridge maintenance treatments is widely recognized, but they are often limited by constrained allocations (Kim 2005). There are several maintenance activities recognized by State DOTs and federal agencies as effective alternatives to reduce the corrosion on steel highway bridges (MnDOT, 2006; NYSDOT, 2008; MDOT, 2010; FHWA, 2011). Ford et al. (2012) referenced the work by Sinha et al. (2009), who indicated that the service life of a bridge in Indiana could vary between 35 to 80 years based on the program of maintenance/preservation activities provided for the bridge. Effective inspections and appropriate maintenance activities are required to ensure a bridge will reach its expected service life (ITD, 2008). Czarnecki (2006) indicated that “if a steel highway bridge is not maintained properly (regular cleaning, inspection, repainting, and repair) steel corrosion occurs.”

In 1988 the Federal Highway Administration sponsored a Weathering Steel Forum, with specialists from throughout the US (FHWA, 1989). The speakers presented histories and data from studies on the use of weathering steel in highway structures. As a result of the event, suggested guidelines were presented as recommendations to achieve the greatest potential of the product. One of the recommendations from the guidelines was focused on maintenance actions, indicating that “effective inspection and maintenance programs are essential to ensure that all bridges reach their intended service life. This is especially true in the case of uncoated weathering steel bridges” (FHWA, 1989). Some specific maintenance activities recommended by the document were: “Remove dirt, debris and other deposits that hold moisture and maintain a wet surface condition on the steel. In some situations, hosing down a bridge to remove debris and contaminants may be practical and effective. Some agencies have a regularly scheduled program to hose down their bridges”.

A study from the Rhode Island Department of Transportation (RIDOT, 2002) analyzed the effectiveness of washing Interstate highway bridges. The analysis was done applying PONTIS (Golabi et al., 1993), a bridge management software developed by AASHTO, to a random sample of 96 steel bridges from the state inventory. PONTIS utilizes mathematical formulas and probability estimates to predict future bridge conditions, based on current condition and the application of hypothetical actions on the structure. In this case, an eight years period (arbitrary) was considered as a framework for two alternatives. One alternative was the “Do Nothing” (DN) alternative during the eight years period, while the other alternative was the implementation of a regular bridge cleaning and washing program, performed each two years during the eight years. The PONTIS element No. 107 “Painted steel open girder” was utilized for the analysis. The PONTIS program classifies the condition of a “Painted steel open girder” in a five levels scale (1 to 5). Based on transitional probabilities, the study assumed the percentages of probability that one element remains on its current state or decreases one level when nothing is done to protect it. On the other hand, there is a 100% (certainty) that an element in conditions 1 or 2 will remain in its current condition when using a regular washing program. After applying the transitional probabilities to the selected bridges, each two years for a period of eight years, the predicted conditions of the bridges were obtained for both alternatives. An economic analysis for the total cost of both alternatives showed that providing a regular maintenance program to a painted steel open girder, consisting of cleaning and washing, would be more cost-effective than the Do Nothing alternative.

The Shikoku Regional Bureau of Japan Highway Public Co. (JH) conducted a pilot study from 2001 to 2004 based on the behavior of two weathering steel bridges under an experimental bridge washing program (Hara et al., 2005). The focus of the study was to analyze the effect of bridge superstructure washing as a mean to eliminate corrosive products derived from deicers applied on bridge decks. During the study fixed points on the bridge girders were observed and documented once a year, before and after the application of deicers products. For those points in the steel surface the loss of mass and

rust characteristics were analyzed. The researchers concluded that washing the steel surface had the effect of suppressing the increase of rust particles size, and this was a way to reduce the corrosion due to deicer products.

The Iowa Department of Transportation (Iowa DOT) together with Wiss, Janney, Elsnor Associates, Inc. (WJE), studied the behavior of steel weathering bridge structures (Crampton et al., 2013). The research considered methods to assess the quality of the weathering steel patina layer and chloride contamination, and the possible benefits from regular bridge washing. The study concluded that high-pressure washing (3,500 psi) is an adequate procedure to reduce chloride ion concentrations on weathering steel patinas; however, not all chlorides could be completely eliminated. This could indicate that bridge superstructure washing mainly removes chlorides from the patina surface, while some amount of chlorides remains under the patina surface, inside the pores and voids of the patina. WJE found that when performed immediately after the winter deicing season, bridge washing will be able to remove the majority of chloride products, before they migrate under the patina layer, as predicted by Fick's Law. Therefore, the study concluded that repeating bridge washing on a regular basis will reduce the corrosion process on the steel girders, but qualified this conclusion and indicated that further study needs to be conducted on this topic.

A study sponsored by the Washington State Department of Transportation (WSDOT) and the Federal Highway Administration (FHWA) analyzed the costs and benefits of regular washing of steel bridges (Berman et al., 2013). The study was implemented in 2011, consisting in washing some bridges annually while some other would not be washed. WSDOT inspectors will annually inspect each bridge from the project and will record steel coating condition and corrosion level, for both, washed and unwashed bridges. Processing the data obtained annually will indicate the cost effectiveness of bridge washing for extending steel coating life and retarding the corrosion process. The project is at present under development. As part of the study, Berman et al. (2013) conducted a national survey

to all DOT agencies, reporting that seven State DOTs agencies performed some type of steel bridge washing on a regular basis.

2.3 Research on Accelerated Corrosion Tests

Accelerated corrosion tests are used with the aim to produce atmospheric corrosion in the laboratory in a greatly reduced time (Guthrie, 2002; Lin, 2005). There are three main types of corrosion tests according to Guthrie (2002): service testing, field testing, and laboratory testing. Service testing is the most reliable since it provides actual results from the actual in situ corrosion processes. Regrettably, the results from service tests are limited to the period of time the test lasts, which normally is far too short to achieve useful results. Field tests also offer excellent results on reproducing corrosion but they have the same limitations as service tests. Hence, accelerated corrosion tests are an adequate alternative to achieve appropriate results in a very short period of time (Guthrie, 2002). The results from accelerated tests are always an approximation to reality and they are only as good as the laboratory conditions approached the service conditions (Carlsson, 2006).

At the moment there are several standard procedures to perform accelerated corrosion tests, with most of them developed for the coating automotive industry. “The oldest and most widely used method for laboratory accelerated corrosion testing is the continuous neutral salt spray test (Carlsson, 2006).” Originally published in 1939, the ASTM B117 procedure has been used for many years as an accelerated corrosion test for all types of applications (Cremer, 1996). Since corrosion processes include several variations, other standardized accelerated tests have been developed and implemented, with the aim to approach certain specific corrosion characteristics (Guthrie, 2002).

Given the several assumptions established during accelerated corrosion tests, the results have to be accepted with an adequate margin of error. Lin (2005) applied the ASTM B117 standard to perform an accelerated corrosion tests to study three types of steel: soft

steel (hot rolled), carbon steel, and weathering steel. The research objective was to establish a correlation between corrosion rates and corrosion factors such as chloride deposition fluxes, time of wetness, and temperature at real environments. Measuring the weight loss from specimens at real environment and in the laboratory, Lin (2005) established the correlations between predicted and measured thickness losses due to atmospheric corrosion. The results from the study showed the following margin of errors: for soft steel 29.0%, carbon steel 28.7%, and weathering steel 37.2%. Clearly, some degree of error always exists when an accelerated test is used to model corrosion.

2.4 Research on Structural Analysis and Design of Corroded Composite Steel Girders

Several studies in relation to the structural analysis and design of steel girder bridges under the effects of atmospheric corrosion attack have been conducted. All those studies had to define several parameters and model some structural characteristics, such as: the types of corrosion affecting the steel superstructure, the rate of corrosion penetration with time, identify the steel member zones where corrosion develops, define appropriate limit state functions, specify load and resistant models, and identify the effects of corrosion attack to structural members and to structural systems (Kayser, 1988; Park, 1999; Czarnecki, 2006). In general, the studies analyzed the corrosion progression on structural steel members and its effect on the structural capacity and serviceability of the bridge system.

Kayser (1988) studied the effect of atmospheric corrosion on typical steel girder highway bridges. The study examined four, single span, composite steel girder bridges. The bridge spans ranged from 40 ft. to 100 ft. with increments of 20 ft. The superstructure comprised a concrete deck supported by five steel A36 girders, carrying two traffic lanes. The study by Kayser (1988) focused on the structural deterioration in an unprotected marine environment for a service life of fifty years. The study concluded that: 1) the environment surrounding the bridge has a significant influence on the deterioration of safety and capacity, 2) corrosion affects the bending, shear, and bearing resistance of the structure,

3) a reduction of the bridge resistance (bending, shear, and bearing) occurs at different rates, changing the original bridge configuration.

Park (1999) implemented a series of structural analyses on typical steel girder highway bridges to investigate the effect of corrosion on composite steel girders. The analysis included the variation of several parameters, such as: span length, deck thickness, number of girders, girder spacing, and degree of corrosion. The research performed a parametric analysis for a service life of 120 years. From his research, Park (1999) observed that corroded steel girders are more affected in their shear capacity than their bending capacity. This conclusion was justified due to the thickness reduction of the web. Shear buckling on steel girders was found as the governing failure mode at the end of the bridge service life.

The research performed by Czarnecki (2006) evaluated composite steel girder bridges under atmospheric corrosion. The study comprised the analysis of fifty-four, single span, typical steel highway bridges. The study took into account the variation of span length, number of steel girders, girder spacing, type of environment, and load carrying capacity. Czarnecki (2006) concluded that corroded steel girders produce a reduction in the structure strength capacity, increasing the probability of failure. The study also showed that the bridge resistance capacity is reduced in larger proportion in shorter spans than for longer spans.

CHAPTER 3. CORROSION OF STEEL BRIDGE HIGHWAY GIRDERS

3.1 Introduction

Corrosion is one of the most significant problems a highway system must confront. Steel girder bridges are crucial components of any highway system and they are constantly threatened by exposure to aggressive environments. To establish adequate, practical, and economical solutions, it is necessary to understand how corrosion develops on structural steel bridge members. Understanding the cause of corrosion and the problems corrosion generates are basic requirements to propose solution alternatives for existing bridges. This chapter presents a review of those causes and problems of corrosion on steel girders. Also, some mathematical models are proposed to predict the amount of corrosion penetration and the location in the steel girder where corrosion takes place.

3.2 Structural Steel

3.2.1 Characteristics of Structural Steel

Structural steel is a product extensively used in the construction of buildings, bridges, factories, and many other structures. Steel used in construction typically conforms to specific standard specifications such as sections dimensions, chemical composition, and physical and mechanical properties. Structural steel is mainly composed of a combination of iron (Fe), carbon (C), and manganese (Mn). The addition of extra constituents (chromium, copper, etc.) as alloy elements, enhances certain steel capabilities, for example higher strength, higher corrosion resistance, etc. Carbon is the element

responsible for steel resistance; however, an excessive content of carbon reduces other important steel properties, such as toughness and weldability (Barker and Puckett, 2007).

Structural steel is recognized as an advantageous construction material due to its controlled production, light weight, and rapid on-site assembly. Also, structural steel is the most recyclable construction material, since more than 93% of structural steel in the USA is produced from recycled steel scrap (AISC, 2015).

Structural steel used in steel bridge construction is exposed to more stringent conditions than steel used for buildings or other structural facilities. Steel bridges require special capabilities to support exposure to: aggressive environments, fatigue under millions of load-unload cycles, daily strong temperature changes, and corrosive compounds from deicing products (FHWA, 2012). Consequently, the structural steel material and environmental requirements for bridges are more rigorous than those for general structural steel.

Both, the American Association of State Highway Transportation Officials (AASHTO) and the American Society for Testing and Materials (ASTM) publish structural steel standards for bridges. The AASHTO specifications for structural steel for bridges are presented as standards M 270(US units) and M 270M(metric units), while the ASTM specifications are given in the standards A 709(US units) and A 709M(metric units). The standards from both organizations are quite similar, with very few differences. Most State DOTs agencies require that steel bridge design and construction adheres to AASHTO standard specifications, and are often supplemented with ASTM requirements.

A typical structural steel is best represented by its stress-strain curve, as shown in Figure 3.1. The steel's modulus of elasticity (Young's modulus) is defined by the slope of the elastic part of the stress-strain curve. A conservative value for this modulus is specified to $E = 29,000 \text{ ksi}$ (200 GPa), while the yield strength F_y is defined by the 0.2% offset line

method. After yielding, structural steel will show plastic deformation at almost constant load, what is called the yield plateau.

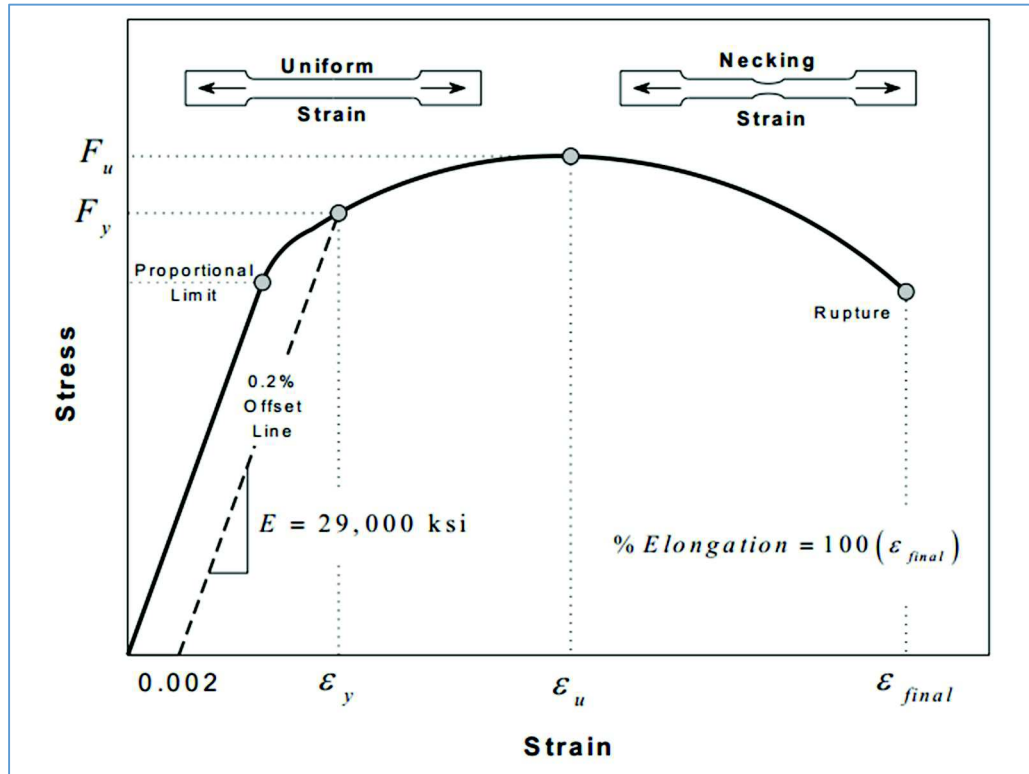


Figure 3.1: Engineering stress-strain curve for structural steel (FHWA, 2012)

3.2.2 Types of Structural Steel for Bridges

Four different types of structural steel are identified according to AASHTO (AASHTO, 2012), based on their chemical composition, heat treatment, and yielding stress: a) structural carbon steel (Grade 36/250) (ksi/MPa), b) high-strength low-alloy steel (Grade 50/345), c) quenched and tempered low-alloy steel (Grade 70/485), and d) high-yield strength, quenched and tempered alloy steel (Grade 100/690). Table 3.1 shows detailed information corresponding to each type of structural steel. The suffix W indicates a weathering steel, a type of steel with more improved capabilities than carbon steel to

resist atmospheric corrosion. The HPS suffix indicates a high-performance steel that has improved toughness, weathering, and welding characteristics.

Table 3.1: Minimum mechanical properties of structural steel by shape, strength, and thickness (AASHTO, 2012)

AASHTO Designation	M 270M/ M 270 Grade 36	M 270M/ M 270 Grade 50	M 270M/ M 270 Grade 50S	M 270M/ M 270 Grade 50W	M 270M/ M 270 Grade HPS 50W	M 270M/ M 270 Grade HPS 70W	M 270M/ M 270 Grade HPS 100W	
Equivalent ASTM Designation	A709/ A709M Grade 36	A709/ A709M Grade 50	A709/ A709M Grade 50S	A709/ A709M Grade 50W	A709/ A709M Grade HPS 50W	A709/ A709M Grade HPS 70W	A709/ A709M Grade HPS 100W	
Thickness of Plates, in.	Up to 4.0 incl.	Up to 4.0 incl.	Not Applicable	Up to 4.0 incl.	Up to 4.0 incl.	Up to 4.0 incl.	Up to 2.5 incl.	Over 2.5 to 4.0 incl.
Shapes	All Groups	All Groups	All Groups	All Groups	Not Applicable	Not Applicable	Not Applicable	Not Applicable
Minimum Tensile Strength, F_u , ksi	58	65	65	70	70	85	110	100
Specified Minimum Yield Point or Specified Minimum Yield Strength, F_y , ksi	36	50	50	50	50	70	100	90

Carbon steel and weathering steel are the two most common structural steel types for most bridge structures and, therefore, a brief discussion of both types of steels is given in the following.

Carbon Steel

All structural steel types contain carbon. Carbon steel particularly, refers to a steel when no minimum content of any element is specified to obtain a desired alloying effect, the specified minimum content of copper does not exceed 0.40%, or the maximum content specified for any of the following elements does not exceed: manganese 1.65%, silicon 0.60%, and copper 0.60% (AISI, 1985, cited by Barker, 2007). A typical construction grade carbon steel is ASTM A36, which shows a marked yielding stress at $F_y = 36$ ksi (250 MPa). Sometimes this carbon steel is just called “mild” steel.

When carbon steel is exposed to moisture and oxygen, a loose rust surface is formed, which allows more water and air accumulation, producing more rust and weakening the steel surface (McDad, 2000). When used for steel bridges, carbon steel must be protected with a coating system to resist corrosion attack from aggressive environments.

Weathering Steel

Weathering steel is typically a high-strength low-alloy steel which contains 2 percent or less of alloying components such as copper, phosphorus, chromium, nickel, and silicon (Albrecht and Naeemi, 1984). In its bare, mature state, weathering steel in contact with moisture and oxygen is able to develop a dense and adherent oxide film known as “patina”, which seals the base metal and acts as a protective coat to minimize further atmospheric corrosion (McDad, 2000). The characteristics of this protective film is a function of several factors, such as steel age, degree of exposure, and environment conditions. When properly specified, weathering steel can provide an alternative to reduce the maintenance cost of bridge painting.

To form its protective film weathering steel needs to be exposed to environments with continuous wet-dry cycles and free of an atmosphere with salt contents. Otherwise, when exposed to prolong periods of wetness and high levels of deicing salts, weathering steel will corrode as plain carbon steel (Albrecht and Naeemi, 1984).

3.3 Corrosion of Structural Steel

3.3.1 Definition of Corrosion

The word corrosion is derived from the Latin *corrosus* which means eaten away or consumed by degrees (Syed, 2006). Corrosion is defined as the degradation of a material by interaction with its surrounded environment (Jones, 1996). The corrosion process is

mainly related to the attack of metals but also can be considered the corrosion of other materials such as ceramics, plastics, rubber, paints, and other nonmetallic materials (Fontana, 1986). The oxide produced by metal corrosion is a material that loses adherence to the base metal and flakes off, causing the loss of mass and reduction of section thicknesses, and consequently the reduction of structural capacity (Czarnecki, 2006). According to the process corrosion undergoes, they can be classified as presented in Figure 3.2

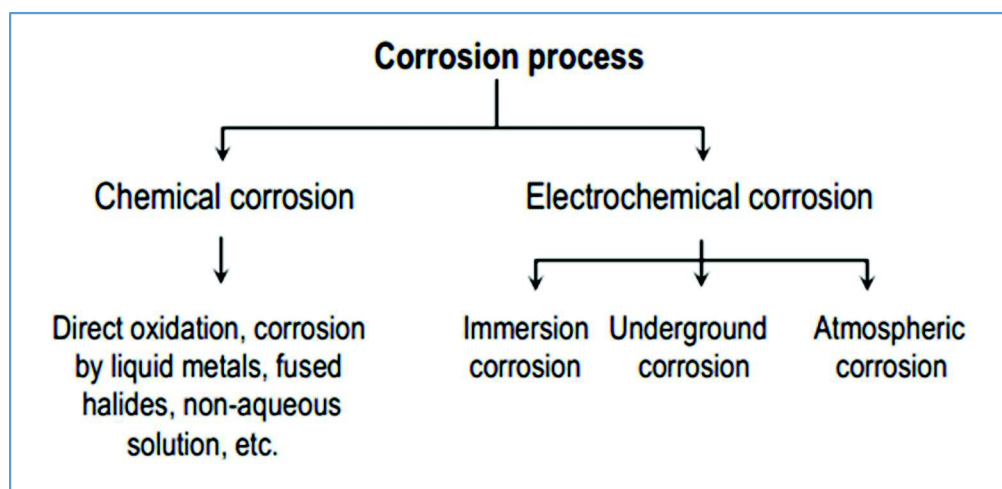


Figure 3.2: Classification of corrosion process (Syed, 2006)

Steel bridges members are predominantly exposed to atmospheric corrosion, a type of electrochemical corrosion, produced by the chemical interaction between steel and environmental components, and promoted by the electromotive force due to the interchange of electrons and ions at the metal-oxide interface.

3.3.2 Atmospheric Corrosion

The metallurgy process to produce metal alloys requires huge amounts of energy, which is stored into the refined metal. Because all transformed systems in nature tend to return

to their original condition, at lower states of energy, refined metals deteriorate by corrosion (metal oxidation) to return to their original components (Kayser, 1988).

“Corrosion of metals is a natural process. For the most part, corrosion is quiet, gradual, and unspectacular, unlike other forces of nature such as earthquakes and tornados. These natural, dramatic processes we can do very little about except to watch for them, but corrosion can be prevented or at least controlled so that the metals can perform their required tasks (Bradford, 1998).”

Structural steel components from bridges are prone to corrode when exposed to local atmospheric conditions, specifically to the presence of moisture (water) and oxygen in contact with the steel surface. The corrosion process under this condition is known as “atmospheric corrosion”, and it is responsible for almost all corrosion problems on steel bridges. When one of these elements is absent, the corrosion process will not develop. For instance, corrosion is negligible in dry regions, such as the hot deserts, or in very cold regions under the freezing point, such as the Polar Regions (Park, 2004). Steel atmospheric corrosion is the result of an electrochemical process due to the interaction of the steel and its environment, resulting in a cathodic-anodic reaction (Landolfo, 2010).

3.3.3 Electrochemical Corrosion Process

Structural steel corrosion is an electrochemical process that requires moisture and oxygen as indicated previously. In this process the steel reacts in the aqueous environment while transferring electrons between components. This process requires that the portion of steel to be corroded will conform a corrosion cell to one area acting as an anode, and another area as a cathode, as represented in Figure 3.3.

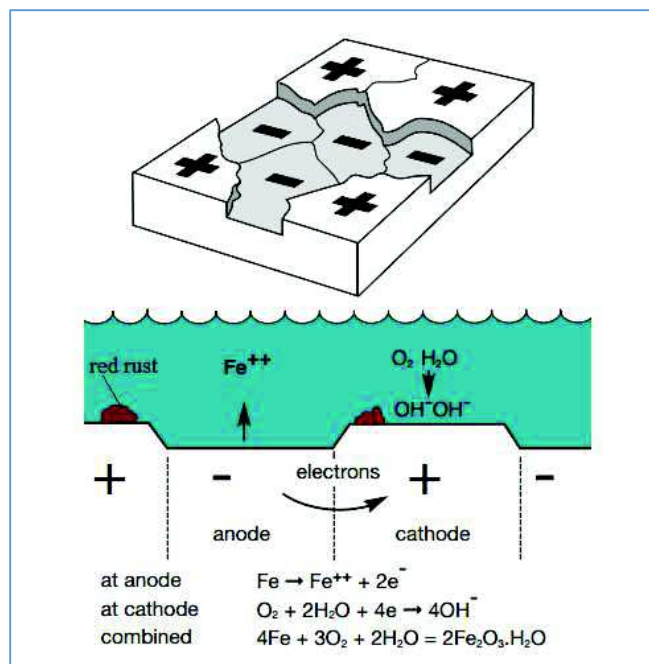


Figure 3.3: Schematic representation of the corrosion mechanism for steel (Corus, 2005)

The corrosion process is described in the following stages with the corresponding chemical reactions (Albrecht and Naeemi, 1984; Czarnecki, 2006):

- The initial degradation occurs at anode areas, with iron being dissolved in ferrous ions (Fe^{++}) that go to the aqueous solution, while electrons (e^-) are released and moved through the steel structure to the cathode area (iron oxidation):



- To balance the reaction at the anode area, the cathode area receives the electrons (e^-) and combines them with water and oxygen to form hydroxyl ions (OH^-) (oxygen reduction):



- Those hydroxyl ions (OH^-) react in the solution with the ferrous ions (Fe^{++}), producing ferrous hydroxide $\text{Fe}(\text{OH})_2$:



- Finally, the fresh ferrous hydroxide is oxidized by air, producing hydrated ferric oxide, most common known as “red rust”



Due to polarization, corrosion in the anodic area is reduced after some time and then a new reactive anodic area starts to corrode, replicating the aforementioned process. After a long period, this corrosion process produces a quasi-uniform loss of mass, known as general corrosion or uniform corrosion.

The rate of corrosion penetration, which is the amount of thickness that it is lost due to uniform corrosion, is influenced by several factors, such as the steel composition, the steel surface homogeneity, the time of wetness (TOW) of the steel surface to be corroded, and the micro-atmosphere composition as the main factors. The content of pollutants (sulfurs and chlorides) in the atmosphere surrounding the steel member has significant influence in the level of corrosion.

3.3.4 Forms of Corrosion

According to Fontana (1986), corrosion attack can be classified into eight forms, based on the appearance and damage produced on the corroded metal. Based on visual observations corrosion can be classified as: 1) Uniform or general corrosion. 2) Galvanic corrosion, 3) Crevice corrosion, 4) Pitting corrosion, 5) Intergranular corrosion, 6) Selective leaching corrosion. 7) Erosion corrosion. 8) Stress corrosion. Other identified

forms of corrosion are cavitation and fatigue corrosion. Figure 3.4 presents sketches for the indicated forms of corrosion. This research focused on uniform corrosion, a diffuse corrosion penetration that is spread over the steel surface. Uniform corrosion represents the most common and severe form of corrosion in steel girder bridges.

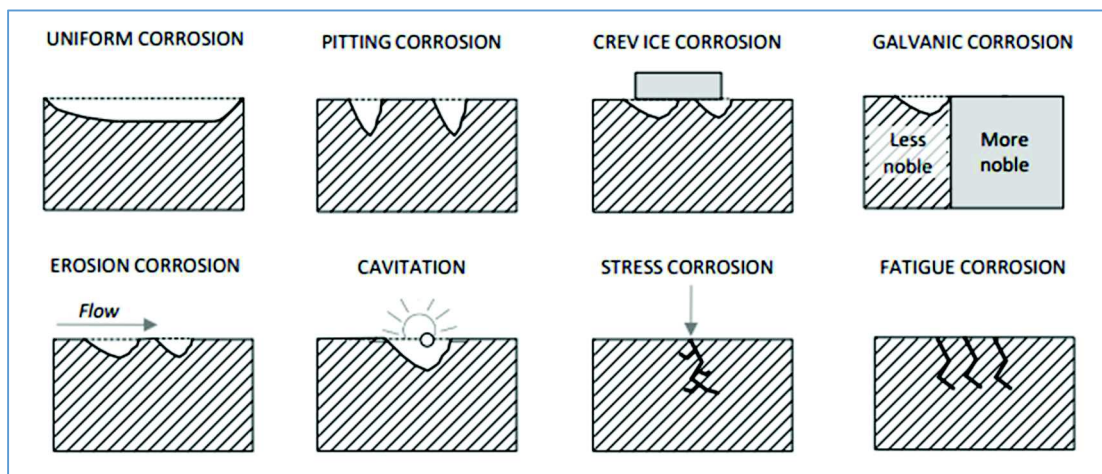


Figure 3.4: Sketches for the principal forms of steel corrosion (Landolfo, 2010)

3.3.5 Atmospheric Environments

The corrosion process on steel bridge girders is decisively influenced by the characteristics of the local environment surrounding the structure. The system protection for steel members must be defined accordingly to the site environment. Kayser (1988), Albrecht and Hall (2003), and Kogler (2012) identified three particular environments for highway bridges: Industrial/Urban, Marine, and Rural.

- **Industrial/Urban Environments**

Environments containing pollutants such as sulfur oxides and nitrogen oxides as a result of the combustion of fossil fuels from motor vehicles and some industrial emissions. Chloride compounds from deicing products are spread to the air by passing traffic during the winter seasons.

- **Marine Environments**

Environments with high contents of salt in the air due to a close proximity to a seacoast, combined with high levels of humidity and moisture.

- **Rural Environments**

Environments with a very low rate of pollutants in the air. Their corrosiveness is produced by moisture, and small compounds of sulfurs and carbon dioxide.

As part of this research, the influence of these three generic environments over steel girder bridges was analyzed.

3.4 Corrosion of Composite Steel Girders

Corrosion of the structural steel members is one of the most significant factors in reducing the bridge service life. Steel corrosion could reduce the bridge load-carrying capacity, and as a consequence, reduce its safety and eventually could collapse during service. To mitigate or reduce those threats, corrosion should be reduced as much as possible. To address the reduction of corrosion on steel girders requires a better understanding of the pattern that the corrosion process follows when attacking a typical steel girder. The most common causes and problems of steel girder corrosion on typical highway bridges are presented in the following sections.

3.4.1 Causes of Steel Girder Corrosion

Steel girder bridges commonly involve a reinforced concrete deck supported by steel girders. The girder and the concrete deck are generally connected by steel shear studs, forming a composite system. Structural steel corrosion is a time-dependent process. This

corrosion process develops with the aging of steel member at a rate depending on the steel composition, atmospheric characteristics, and bridge maintenance conditions.

Kayser (1988) indicates that a primary cause of corrosion in steel girders is the accumulation of water on the steel surface, and the rate of corrosion is related to the time the water remains accumulated. The study identified deck leakage, through damaged deck joints or deck cracks, as the most common paths for water to reach girders surfaces. Failure of deck drainage systems is also a very common problem, and as a result, accumulated water on the deck surface ends flowing through the deck, to the bridge superstructure elements, including steel girders (Kogler, 2012).

Another way steel girders become wet is due to truck traffic passing under the bridge. The trucks splash water from the road, creating water plume with sufficient height to wet the steel girders of the bridge. The corrosion process can be exacerbated during winter seasons, when deicing products are spread in significant quantities on roads and bridge decks to facilitate snow and ice removal. The chloride compounds from deicing products mixed with the water that reaches the steel girder surfaces will significantly increase the rate of corrosion (Albrecht and Naeemi, 1984).

Debris formations are another source of corrosion problems on steel girders. Debris can buildup on horizontal surfaces of steel girder and at corners formed by horizontal and vertical elements. Debris retains moisture, and keep chloride and sulfate compounds in contact with steel members for a longer period of time, increasing the rate of corrosion on those areas of contact (Albrecht and Naeemi, 1984; Kogler, 2012).

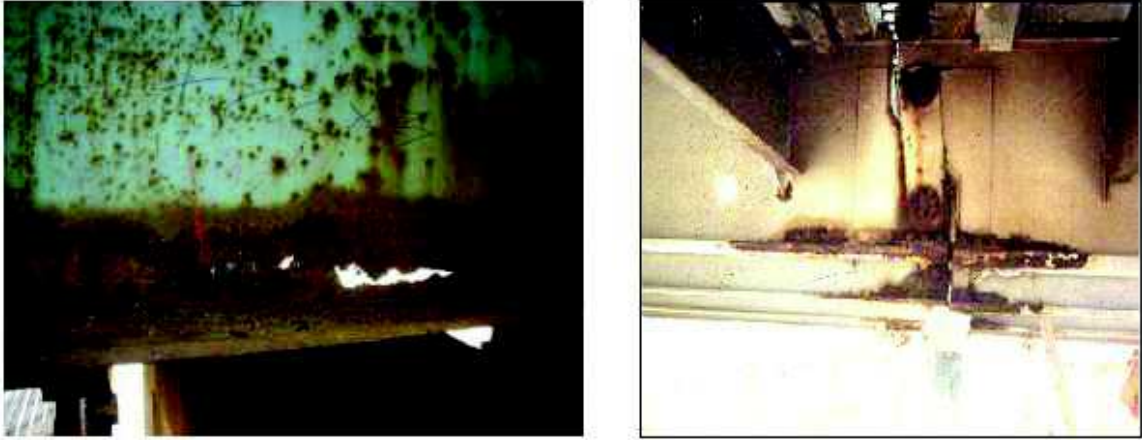


Figure 3.5: Typical corrosion process of steel girders: Left) at the web and bottom flange (Zaffetti, 2010), Right) Next to a pin and hanger connection (WisDOT, 2011)



Figure 3.6: Debris accumulation at a steel superstructure connection point (Kogler, 2012)

3.4.2 Problems Due to Steel Girder Corrosion

Kulicki et al. (1990) indicates that corrosion can produce four kinds of effects on structural elements: loss of material, creation of undesired stress concentration, introduction to unintended fixity, and generation of unintended movements.

The loss of material due to corrosion is the most significant effect on structural members from steel girder bridges because of the reduction in cross section thicknesses. The reduction of section thicknesses will generate the reduction on the members' section properties. Reduction of the area, radius of gyration, and moment of inertia, will thereby reduce the strength, stiffness and ductility of the corroded structural elements. Under these conditions, a structural member designed as a particular class of section (plastic, compact, semi-compact, or slender) may change its conditions, producing stresses not considered during the design. Hence, the development of the corrosion process could cause an initial compact section to turn into a semi-compact, or even in a slender section. These changes will lead to a reduction in the bending, shear, and bearing capacities of the structural elements, and consequently result in the reduction of both the load-carrying capacity of the bridge structure and its service capabilities due to larger deflections (Kayser, 1989, Rahgozar, 2009).

Localized corrosion can also reduce the web thickness of steel girders, introducing new eccentricities, thus increasing the effect of local buckling, principally near to the supports. Under millions of cyclic loads as experienced by bridge members, corrosion can reduce the fatigue strength capacity, especially in zones where high stresses are concentrated. The buildup of corrosion products can generate changes in the bridge flexibility, freezing supposed movable parts such as free bearing supports, hinge connections, or pin-hanger assemblies. These movement restrictions will introduce undesired stresses into the structural members. Those additional stresses, not considered during the bridge design, could produce localized damage, or even the failure of a structural element and possible the total collapse of the bridge. Corrosion products can also induce unintended movements, affecting some steel members or in occasions the entire bridge structure (Prucz, 1998; Czarnecki, 2006, Landolfo 2010).

The controlling failure on a corroded structural member can be affected due to corrosion attack, by reducing its section thicknesses, introducing additional stresses, or changing

the original structural configuration. Consequently, the residual capacity of a corroded member should be evaluated considering all possible modes of failure and verifying their capacity for strength, stability, serviceability, fatigue and fracture.

3.5 Deterioration Model of Steel Girder Corrosion

To predict the development of corrosion on structural steel bridge members, several factors have to be taken into account, making the task quite complicated and with a high degree of uncertainty. The influence of the environment at the bridge location, the position of steel member within the bridge configuration, the steel composition, and the presence of sulfurs or chlorides are decisive factors in the corrosion pattern that develops in a steel member.

Various researchers have developed mathematical models to predict the amount of corrosion penetration, based on the type of steel and the environment at which the steel member is exposed (Townsend and Zoccola, 1980; Albrecht and Naeemi, 1984; Komp, 1987). Also, researchers have found that corrosion on steel girders follows some particular patterns in the steel section and along the span length (Mc Crum et al., 1985; Kayser, 1988; Kayser and Novak, 1989).

3.5.1 Model to Predict the Rate of Corrosion

There are several studies in relation to models to predict the rate of corrosion penetration on steel alloys when exposed to different atmospheric conditions (Larrabee and Coburn, 1962; Townsend and Zoccola, 1982; McCuen et Albrecht, 1994). Most of those models define the rate of corrosion as a function of mass loss or thickness reduction with time. Generally, the studies are based on the observation of corrosion penetration on steel coupons exposed to selected atmospheric conditions for certain periods of time, sometimes months or even years. That limited empirical information is calibrated with data from laboratory tests and then extrapolated to develop mathematical expressions to

generalize their findings (Czarnecki, 2006; Landolfo, 2010). These empirical or semi-empirical expressions try to capture the actual corrosion process, including some regression coefficients, and commonly taking the form of a power function.

A comprehensive assessment of steel corrosion was performed by Albrecht and Naeemi (1984) in a study for the National Cooperative Highway Research Program (NCHRP). The NCHRP study collected data from several atmospheric corrosion tests on coupons from different steel types, performed at several locations around the world, and lasting from three to eighteen years in some cases. The study considered three different environments: Industrial, Marine, and Rural. Each location was identified with certain specific environment, and different types of steel alloys were exposed to atmospheric corrosion. According to the NCHRP study and other references (Townsend and Zoccola, 1982), a power function is the curve that best fit the time-penetration data collected from all test sites. A power function is of the form presented in Equation 3.5.

$$C = A t^B \quad \text{Equation 3.5}$$

Equation 3.5 can also be expressed in a logarithmic form, becoming in a straight-line function as presented in Equation 3.6.

$$\log C = \log A + B \log t \quad \text{Equation 3.6}$$

where:

- C = average corrosion penetration determined from weight loss;
- T = exposure time;
- A = regression coefficient numerically equal to the penetration after a unit of time;
- B = regression coefficient numerically equal to the slope of Equation 3.6 in a log-log plot.

The study from Albrecht and Naeemi (1984), presented the average values for regression coefficients A and B obtained from the several coupons tested at each location and for each type of steel. These parameters A and B were evaluated for each type of steel and test location considered in the study. The data collected in this study, corresponding to carbon and weathering steel, are presented in Appendix A.

Kayser (1988) also studied steel corrosion and applied a power function to estimate the rates of corrosion penetration. The average values of regression coefficients A and B from Albrecht and Naeemi (1984) were averaged in the study by Kayser (1988). Kayser determined a unique set of values A and B for each one of the three environments considered. Therefore, the values proposed by Kayser (1988) resulted in the averages from the averages values determined by Albrecht and Naeemi (19984). The mean and coefficient of variation of parameters A and B determined in the study by Kayser are presented in Table 3.1. In his study, Kayser (1988) identified as Urban the type of environments identified as Industrial in Albrecht and Naeemi (1988) study. In this dissertation, that type of environment was identified as Industrial/Urban.

Table 3.2: Statistical parameters for A and B (Kayser, 1988)

Parameters	Carbon Steel		Weathering Steel	
	A (μm)	B	A (μm)	B
Rural Environment				
Mean value, μ	34.0	0.65	33.3	0.50
Coefficient of variation, σ/μ	0.09	0.10	0.34	0.09
Coefficient of correlation, ρ_{AB}	N.A.		-0.05	
Urban Environment				
Mean value, μ	80.2	0.59	50.7	0.57
Coefficient of variation, σ/μ	0.42	0.40	0.30	0.37
Coefficient of correlation, ρ_{AB}	0.68		0.19	
Marine Environment				
Mean value, μ	70.6	0.79	40.2	0.56
Coefficient of variation, σ/μ	0.66	0.49	0.22	0.10
Coefficient of correlation, ρ_{AB}	-0.31		-0.45	

Kayser (1988) reported a wide range of variation for parameters A and B between environments. The same tendency was found for the coefficient of correlation between A and B . Therefore, Kayser emphasized that corrosion penetration will be approximated when the A and B are estimated without high confidence. Kayser used the mean values A and B to extrapolate, the data acquired during Albrecht and Naeemi (1984) tests to 50 years of corrosion penetration values on steel highway bridge girders for the considered environments. The curves for mean time-corrosion penetration corresponding to carbon steel when exposed to the three typical environments (Rural, Urban, and Marine) and projected to 50 years are depicted in Figure 3.7. Actual data collected by Albrecht and Naeemi (1984) are presented in Figure 3.7 in solid lines, while extrapolated values to 50 years evaluated by Kayser (1988) are presented in dotted lines. Figure 3.7 shows that the higher corrosion rates are developed at marine environments, followed by rates at urban environments, and the lower corrosion rates are presented at rural environments. Also, can be noticed that initial corrosion rates decay in time for the three considered environments. In Appendix A are presented the complete set of corrosion penetration curves for the three considered environments.

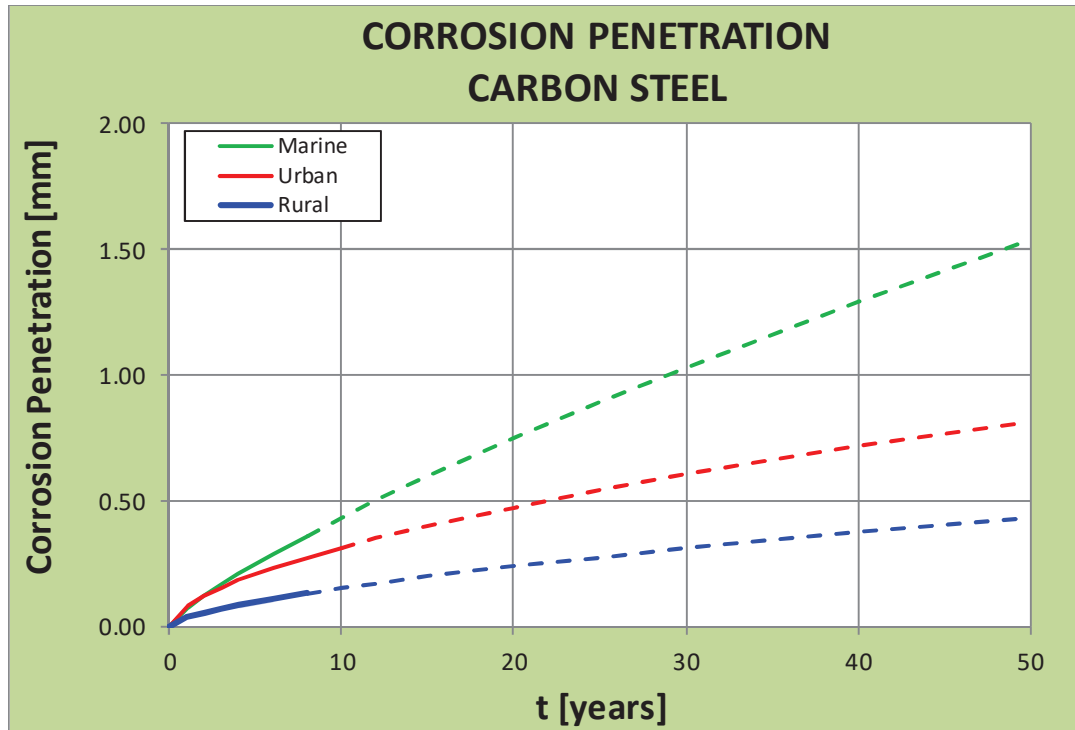


Figure 3.7: Mean of Time-Corrosion penetration curves for carbon steel (Kayser, 1988)

Kayser (1988) identified some limitations on his work and had to consider two assumptions. Firstly, penetration rates obtained using the mean values of parameters A and B will include certain inaccuracies, due to the high variation found when the parameters were evaluated. Secondly, some deviations are expected in the corrosion analysis when the mean values of regression coefficients A and B are used to estimate actual penetrations on large steel bridge members, since those parameters were obtained from testing small coupons,

Other authors have presented different penetration models than the power function. Park et al. (1998) proposed three curves (high, medium, and low) for corrosion penetration rates. The curves considered initially the steel girders were painted, therefore, the paint coat provided protection that last the first ten to twenty years, depending on the environment. The high corrosion rate was assumed for marine environment or heavy industrial conditions; the low corrosion rate was considered to be developed at dry

conditions with no salt or aggressive compounds acting on the metal; and medium corrosion rate represented the average conditions. The model considered that after the coating was damaged by corrosion, the girder will not be repainted. Figure 3.8 shows the corrosion curves suggested by Park et al. (1998) with the initial corrosion protection provided by paint until corrosion start to progress. Lee et al. (2006) modified the power function for corrosion penetration, introducing periodic repainting periods.

In this study the model and the statistical parameters A and B from Kayser (1988) were selected to predict the corrosion penetration in time.

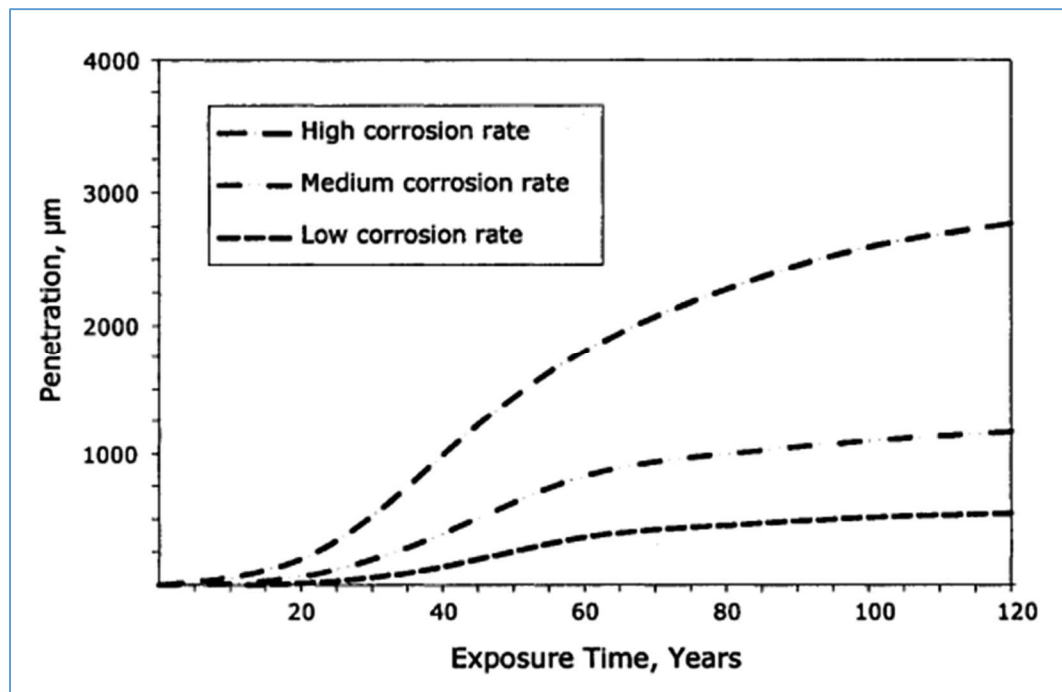


Figure 3.8: Corrosion penetration curves (Park et al., 1998)

3.5.2 Model to Predict Location of Corrosion

Some studies have found that corrosion damage in steel girders follows particular patterns according to the section location in the bridge. These patterns strongly depend on

bridge configuration, construction details, and maintenance conditions. As indicated previously, deck joint failures, inadequate deck slopes, clogged drainage systems, deck cracking, etc., are bridge problems with high influence on corrosion of the steel girders. Girder zones exposed to accumulate and retain moisture, debris, and pollutants are also prone to corrode at a greater rate than those zones more protected from those agents.

Data gathered from field surveys by Kayser (1988) indicated that corrosion is more likely to occur along the top surface of the bottom flange. Also, the study noted that web surfaces tend to corrode just at the bottom part, close to the bottom flange. However, in zones close to the supports the corrosion was observed to develop over the entire web surface. Figure 3.9 shows a sketch representing typical girder corrosion for a simple span bridge (Kayser, 1988).

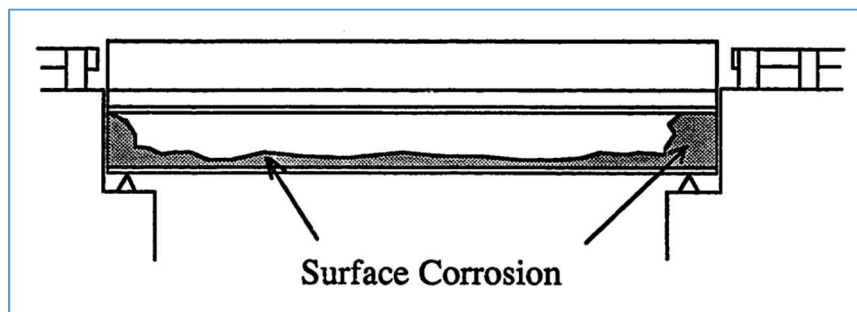


Figure 3.9: Typical corrosion locations on a steel girder bridge (Kayser, 1988)

The research presented by Kayser (1988) indicates that girders location in the bridge system also influences the rate and pattern of corrosion. Outside girders facing the oncoming traffic are more likely to corrode than interior girders, which are more protected to water spray produced by traffic passing under the bridge.

Park (1999) assumed in his research a model for location of corrosion similar to the Kayser model. Park's model, however, was more specific, limiting the web surface corrosion at midspan to the bottom quarter of the web height. The study defined the

length of end support zones to ten percent of the span length. Figure 3.10 shows sketches for typical corrosion patterns in the cross section based on Park's research.

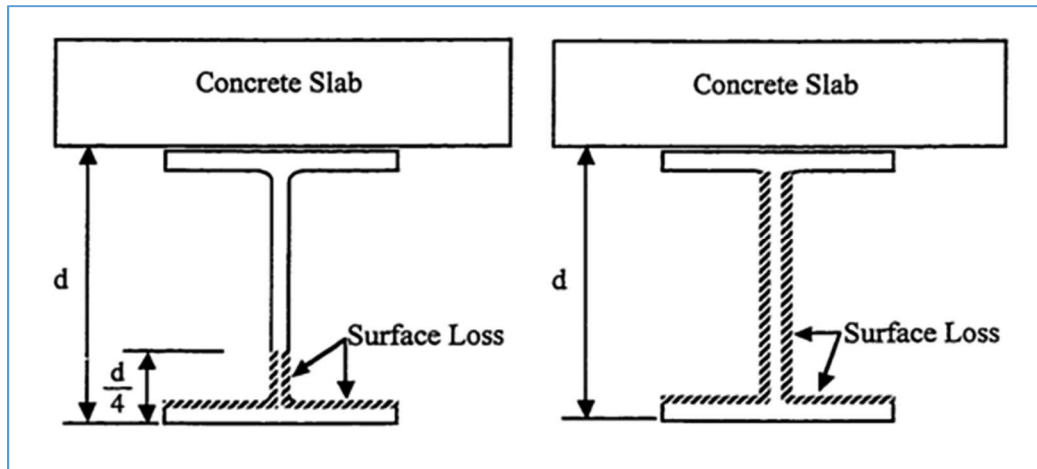


Figure 3.10: Corrosion on typical steel girder sections, at midspan (left), and at supports (right) (Park, 1999)

Czarnecki (2006) modified the model for corrosion location presented by Kayser. According to this study, there are several factors influencing the corrosion pattern as mentioned by Kayser. The complexities and uncertainties involved in determining the corrosion patterns are a significant limitation to define a very detailed corrosion model. As a consequence, the study assumed a model with corrosion located on the top surface of the bottom flange and on the entire web surfaces. The study also assumed that corrosion develops in the same pattern on all steel girders, regardless their location in the bridge. Figure 3.11 presents a sketch of a typical steel girder section with the corrosion location pattern assumed by Czarnecki (2006). The simplified model from Czarnecki (2006) was followed to model the corrosion penetration in the present research.

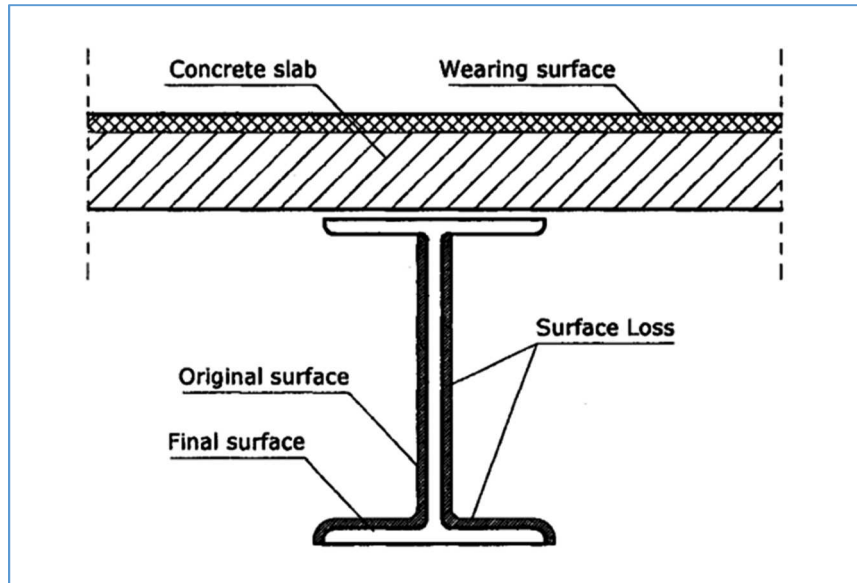


Figure 3.11: Corrosion on typical steel girder section (Czarnecki, 2006)

3.6 Corrosion Protection of Steel Girders

There are several proven strategies for corrosion protection of steel girders. The most accepted systems can be classified into three main groups: surface coating systems, cathodic treatments, and corrosion resistance steels (Albrecht and Hall, 2003). Selection of an appropriate corrosion protection system must be based on some influence factors such as site environment, system cost, system availability, service life, and maintenance possibilities (Kogler, 2012).

The use of a surface coating system has been the predominant protection method used by State DOTs for many years. A coating system works as a barrier between the steel surface and the environment. The components conforming a coating system have evolved since initial basic lead-based paints to current modern three-coat systems. The evolution has been driven by the search for the most effective corrosion protection products that are also economical and environmentally friendly. Most of the State DOTs in the USA recommend corrosion protection of steel highway bridges using a 3-coat system,

consisting of a zinc-rich primer as the main protection coat, combined with an intermediate epoxy coat, and a finishing urethane topcoat.

The use of weathering steel has also been recommended in the last three decades as an alternative instead of the use of coating systems to protect steel bridges from corrosion. As indicated in section 3.2.2, this type of steel produces an adherent film that acts as a protective coat, allowing the owner to reduce initial costs by mostly eliminating the use of a coating protection system.

CHAPTER 4. MAINTENANCE ACTIVITIES OF STEEL GIRDER BRIDGES

“Preventive maintenance is a planned strategy of cost-effective treatments to an existing roadway system and their appurtenance that preserves the system, retards future deterioration, and maintains or improves the functional condition of the system (without substantially increasing structural capacity).”

AASHTO Subcommittee on Maintenance (FHWA, 2011)

4.1 Introduction

Department of Transportation agencies need to develop and implement additional requirements for bridge preservation, rehabilitation, or replacement. According to the National Bridge Inventory (NBI) 26% of the steel bridge inventory is classified as structurally deficient and 19% as functionally obsolete (FHWA 2005, cited by Laumet, 2006). The condition of the Indiana highway bridge system is similar to the national trend. This situation is expected to increase if adequate measures are not implemented, since appropriate allocations are not enough to solve the entire problem. From the research by Bowman and Moran (2015), bridge preventive maintenance activities were analyzed as alternatives to preserve and extend the bridge service life. In that study, previous studies on bridge preventive maintenance activities were analyzed and discussed. From that study, several bridge preventive maintenance activities were found as efficient alternatives to prolong the bridge service life at a low cost. In particular, the study found that, when properly applied at a regular frequency, bridge superstructure washing and spot painting are two maintenance activities that are capable of extending

the service life of steel girders. Therefore, those activities are viewed as low-cost alternatives to preserve the bridge serviceability. The objective of the present dissertation is oriented to study the benefits of these two bridge maintenance activities as alternatives to enhance corrosion resistance and performance of steel girder bridges. In the next sections a brief description of these bridge maintenance activities and their benefits are presented.

4.2 Bridge Superstructure Washing

Steel bridges require an adequate protective system to retard the development of corrosion attack. In recent years the application of a coating system and/or the use of weathering steel have been the most common alternatives for corrosion protection (AISI, 1995; Corus, 2012). There are several factors to initiate corrosion attack on steel girders. Exposure to polluted environments, leaking of deicing compounds from the deck, the accumulation of dirt, debris, or sand, and water spray produced by moving vehicles are common sources to initiate the process of corrosion on steel elements (Kayser, 1988; RIDOT, 2002; Crampton et al., 2013).

Significant corrosion damage of a steel girder due to extended corrosion attack is shown in Figure 4.1. The loss of section for the extent of corrosion damage shown in Figure 4.1 can compromise the girder strength capability and, in some occasions, the entire bridge integrity. Consequently, corrosion control is a paramount responsibility for highway bridge owners.



Figure 4.1: Damaged steel girder due to extended corrosion (Zaffetti, 2010)

Rehabilitation or replacement of corroded steel girders is an expensive procedure that can interrupt or stop the traffic for several weeks or months. For that reason, the bridge owner has to select this option when other alternatives are not possible. On the other hand, bridge superstructure washing is considered as an efficient alternative to reduce the rate of atmospheric corrosion on steel girders.

A common method for superstructure bridge washing includes the collection and cleaning of solid materials from the superstructure, followed by the spray of pressured clean water to remove the contaminant compounds from the girder surface. Chloride compounds from deicing products are the most common and aggressive substances attacking a steel girder. Also the accumulation of dirt, debris, and dust is the source for corrosion initiation and should be cleaned from the steel girder surfaces (Berman et al., 2013). Figure 4.2 shows a maintenance crew member performing superstructure washing.

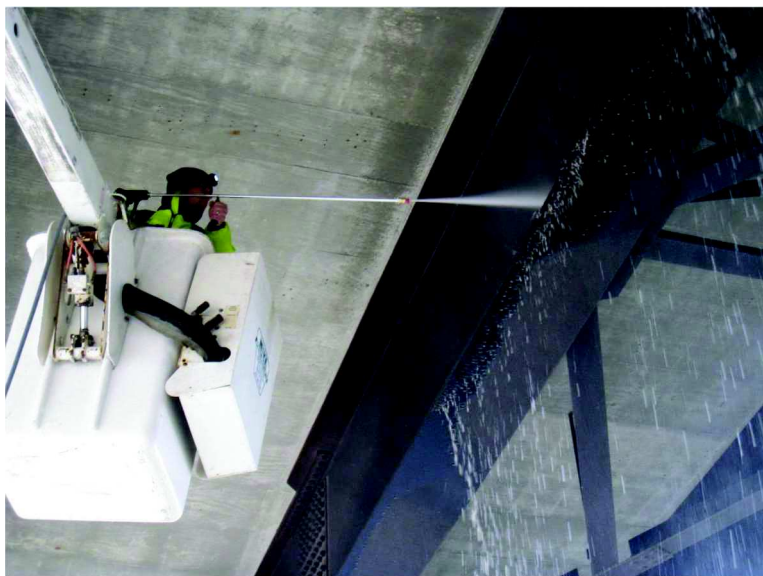


Figure 4.2: Steel bridge superstructure washing (Crampton et al., 2013)

4.2.1 Bridge Superstructure Washing Programs at State DOTs

Several DOT agencies consider bridge superstructure washing as an effective alternative to extend the steel girder bridge service life (Berman et al., 2013; Crampton et al., 2013). According to a national survey performed in the Berman et al. study (2013) some DOT agencies routinely perform superstructure washing, considering this activity as an alternative to reduce the rate of corrosion in steel girders and to prolong the service life of steel coatings. In the same study it was emphasized that there is a lack of supporting evidence for the effectiveness of superstructure washing in reducing the rate of corrosion process in steel girders. In general, superstructure washing is a commonly accepted bridge maintenance practice, with no rigorous studies supporting its effectiveness. Table 4.1 presents the most pertinent information reported from the DOT agencies that perform bridge superstructure washing according to the study from Berman et al. (2013).

Table 4.1: State DOTs information reported on bridge washing programs (Berman et al., 2013)

AGENCY	WASHING PROGRAM CHARACTERISTICS	WASHING METHOD	FREQUENCY OF WASHING	CORRELATION
Iowa Department of Transportation (IowaDOT)	IowaDOT has had a bridge washing program in place for 20 years. There is no specific selection process for bridges.	The process involves collecting, bagging, and disposing of dry debris before washing.	Every weathering steel bridge located along the East and West borders are slated to be washed every year.	IowaDOT has not studied any correlation between bridge washing and paint life or corrosion.
Alaska Department of Transportation and Public Facilities (ADOT&PF)	Started a bridge inspection program in 2004 labeled the Fracture Critical Inspection Program (FCIP). There is rarely an issue with regulations as salt is rarely used.	Bridges at the interior of the state have debris cleared off with compressed air. Bridges located in the coastal regions are washed with low pressure hoses, without any dry debris collected beforehand, and then a spray washing is applied.	Every bridge under FCIP is cleaned and inspected every 2 years.	The Alaska DOT has not studied any correlation between bridge washing and paint life or corrosion.
Kentucky Transportation Cabinet (KYTC)	Started a bridge washing program beginning in 2010. Only bridges in moderately good condition are chosen to be cleaned. Focused on washing the lower chords, abutments, joints, and any other problem/splash areas	The KYTC collects the majority of solid waste with brooms and shovels before spray washing.	Paint and corrosion do not specifically determine when a bridge is scheduled to be washed.	The KYTC have drawn no correlation between paint life/corrosion and bridge washing.

Table 4.1: Continued

AGENCY	WASHING PROGRAM CHARACTERISTICS	WASHING METHOD	FREQUENCY OF WASHING	CORRELATION
New York State Bridge Authority (NYSBA)	The NYSBA initiated their bridge washing program in the 1960's. Salt is not used on bridge decks as a deicer, but instead they use sand.	There is a dry-cleaning process in which the sand and other debris is swept and shoveled up and disposed of before spraying. The bridge is then sprayed at garden hose pressure with water.	All bridge sections are washed annually. Paint condition and corrosion are assessed visually on an annual basis.	The NYSBA has no documented correlation between bridge washing and paint life. They have only needed about 25,000 pounds of steel replacement in the past 80 years.
New Hampshire Department of Transportation (NHDOT)	NHDOT has had a bridge washing program since the 1970's.	There is a dry-cleaning process that involves sweeping, shoveling, and collecting debris before spraying. Dry cleaning and spray washing focus mainly on splash areas (spray from tires) and only occasionally move to the underside of the bridge deck.	According to the program, every bridge is ideally washed every other year. Paint condition and corrosion are assessed visually during inspection.	The NHDOT has completed no studies on the correlation between bridge washing and paint life.

Table 4.1: Continued

AGENCY	WASHING PROGRAM CHARACTERISTICS	WASHING METHOD	FREQUENCY OF WASHING	CORRELATION
Missouri Department of Transportation (MoDOT)	MoDOT has had a bridge washing program in effect since 2002.	There is a dry-cleaning process that involves sweeping, shoveling, and removal of debris before spraying but this is not performed during every washing.	Every bridge is washed twice per year; once in the spring and once in the fall. Paint condition and corrosion are assessed visually during inspection and given a rating. These two attributes do not determine if a bridge is slated to be washed.	The MoDOT has no documented correlation between bridge washing and paint life.

From Table 4.1 is observed that some DOT agencies perform a regular bridge washing program. Some State DOTs started their washing program early in the 1960's and 1970's, while other State DOTs started more recently in the 2000's. Most of the washing programs include a previous dry-cleaning, collecting debris and solid waste before spray washing the steel girders with pressured water. The most common frequency for bridge washing is every other year, while only New York State Bridge Authority performs the activity every year. The most relevant observation from Table 4.1 is that none of the referred State DOTs have studied or documented a correlation between bridge washing activity and paint life performance. This is the fact that justify a research to find some type of correlation between those two parameters.

4.2.2 Bridge Superstructure Washing Benefits

Bridge superstructure washing is accepted by several DOT agencies as an effective maintenance activity that can reduce the rate of corrosion on steel members. Extending the steel girders service life has a direct influence on bridge structure preservation and integrity. Appleman et al. (1995), Hara et al. (2005), and Crampton et al. (2013) concluded that superstructure water washing is a useful activity to suppress corrosion due to deicing salt products and other compounds. Additionally, bridge superstructure washing has positive effects on bridge inspection quality, providing a safe and clean steel surface to be inspected and rated (RIDOT, 2002; Crampton et al. 2013). Figure 4.3 shows the interior of a steel truss member with accumulated debris and the same section with the corroded surface found after the debris was eliminated.



Figure 4.3: Interior of lower chord from truss. Before (left) and after (right) cleaning and washing (Berman et al., 2013)

4.3 Spot Painting

To protect steel highway bridge girders from corrosion attack, the application of a coating system when the girders are built is the most common practice. The coating systems used 20 – 30 years ago were lead-based paint systems without surface treatment. Due to environmental concerns, the coating systems composition changed in the last couple of decades to include the use of more environmentally friendly compounds. The environmental and safety requirements for removing lead-based paints and other chemical pollutants from the surfaces of steel bridge members have increased exponentially, along with the cost of these abatement activities. Because of the ostensible cost, many DOT agencies have decided not to repaint steel highway bridges. Due to expected coat damages on structural steel members, a paint repair is frequently required. As an alternative to a total bridge re-coating, spot painting is considered an efficient solution when only few, and very small, portions of the coating are damaged. Spot painting is expected as an economical alternative when no more than 1% of the total surface area is damaged or it is rated on grade 7 or less in the scale presented in the standard ASTM D610 “Standard Practice for Evaluating Degree of Rusting on Painted Steel Surface” (ASTM, 2012).

Basically, spot painting involves these activities: 1) cleaning the damaged surface, using hand/power tools, until all corrosion material has been eliminated, 2) prepare the area to receive the new protecting coat, and 3) application of a new coating system, compatible with the original coat system, using a brush, roller or spray. Several DOT agencies include spot painting in their bridge maintenance programs, since they consider it an efficient activity to protect steel members from corrosion attack. Among those states performing spot painting routinely are New York, New Jersey, Virginia, Pennsylvania, Washington, Oregon, New Hampshire, Maine, and Minnesota. Figure 4.4 illustrates a portion of a steel girder that is a good candidate for spot painting.



Figure 4.4: Portion of a steel girder candidate for spot painting (Myers et al., 2010)

4.3.1 Spot Painting Benefits

When applied properly, spot painting is an economical alternative due to the small area treated and the simplicity of the operation. Since spot painting is applied to reduced areas, no great expenditures are needed to prepare the area and perform the job. In contrast, high costs are expected when a total bridge is painted, such as the costs related to big containments, scaffoldings, or prolonged traffic suspension. Also, fairly limited amount

of debris and pollutants are expected to be eliminated. Due to the relatively small area to be treated in spot painting work, little material is required, and it can be prepared at the site without complicated procedures. The spot painting crew could move rapidly to treat several spots in the same girder and the same bridge in a simple journey. Due to the basic equipment required to perform spot painting, the traffic under the bridge is not interrupted or it has to be partially interrupted for short periods of time only (Lanterman, 2009; Rea, 2014).

According to Lanterman (2009) and Rossow (2014), spot painting should be performed as soon as possible to obtain maximum benefits from this activity. When not performed at an early stage, the corrosion progress in the damaged area will be more significant and the repair will require a more complex and expensive treatment.

4.3.2 Service Life of Spot Painting

The study from Chang (1999) indicated that several factors influence the service life of a coating system, including: climate, coating age, traffic conditions, and maintenance practices. Based on coating specifications, the most important requirement to achieve the maximum service life from a coating system is the application process, including an appropriate surface treatment prior to the coating application. Table 4.2 shows the estimated service life of spot painting from several research studies, presented in the study from Bowman and Moran (2015). It can be observed from Table 4.2 a wide variation in the mean and range of expected values for the service life of spot painting, according to those different studies. The large variation on the service life of spot painting could be explained by the influence of the several factors that affect the coating performance.

Table 4.2: Service life of spot painting (Bowman and Moran, 2015)

Researcher/DOT	Service Life (years)
Chang, 1999	15
Zayed et al., 2001	15
Chan, 2003	10 - 15
Yuan, 2005	10 - 15
Hesel et al., 2008	4 - 5
Petcherdchoo et al., 2008	10 - 15
MDOT, 2011	5
Yunovich et al., 2014	4

4.4 Summary

Although there is a lack of conclusive evidence, superstructure bridge washing is considered for several DOT agencies as an efficient alternative to prolong the coating system service life and reduce the corrosion attack on steel girders. There is an extensive agreement between bridge inspectors, engineers, and maintenance crews, that regular cleaning and washing of steel bridges is beneficial and will extend the structure service life. Since this accepted agreement is based on opinions, beliefs and some performances, more rigorous studies should be implemented on bridge washing. It is necessary to study the benefits of bridge washing and the appropriate frequency of washing to obtain the best benefits from the allocated resources when performing this activity.

Spot painting is a more studied activity, but predominantly from the automotive paint sector. From the literature review it was found there is not a general agreement in the expected service life for spot painting coats on steel girders. Therefore, more studies applied on spot painting systems are required to support the benefits this maintenance activity offers to extend the bridge service life.

CHAPTER 5. ACCELERATED CORROSION TEST

5.1 Introduction

Steel bridges are exposed to very aggressive environments and must resist dead and live loads throughout their entire service life, therefore, they require an adequate corrosion protective system. “The most common corrosion protective systems have been the use of either coating systems or weathering steel” (Bowman and Moran, 2015). Even the best steel coating systems suffer damage due to manipulation during girder erection or corrosion attack during their service life. Many State Department of Transportation (DOTs) consider that regular bridge superstructure washing is an effective alternative to reduce the damage due to atmospheric corrosion on steel substrate or coating layers (Berman et al., 2013; Crampton et al., 2013). Also, spot painting has been identified as an economical option to repair small and localized coating damage, avoiding the progress of corrosion beyond the spot (Lanterman, 2009). The main objective of this study was to analyze the performance of bridge superstructure washing and spot painting to determine if these are effective maintenance activities to reduce the atmospheric corrosion process on steel girder bridges.

The effect of superstructure washing was studied by performing a set of tests using steel coupons under corrosion attack. The test program utilized two identical groups of samples, one of them under a regular washing program and the second group without washing.

The effectiveness of spot painting was studied in the same way, performing a set of tests over two similar groups of coated steel plates exposed to corrosion attack. One group of plates was prepared with a small coating damage, which were repaired by spraying a coat of Rust-Oleum® over the scribe, and the other group of coupons remained without any type of repair to the damage.

Atmospheric corrosion on steel members is a combination of physical and chemical processes that could take months or even years to develop, based on several factors, such as the type of steel, the surrounding environment, the position of the member in the bridge, the type of corrosion protection, its exposure to deicing products or pollutants, etc. As a consequence, the most reliable information about atmospheric steel corrosion is that obtained from samples made from the same steel to be studied and exposed outdoor at the same environmental conditions for a long period of time -months or years- until enough corrosion has developed as expected (Drazic, 1989; Itoh, 2006). The requirement of such a long period of analysis, which also implies considerable expense, precludes the study of steel corrosion under real service conditions.

As an alternative to atmospheric corrosion in a real environment, several accelerated corrosion tests (ACT) were developed to mimic the atmospheric corrosion process in the laboratory, over a much shorter period of time (Carlson, 2006; Cambier, 2014). In an ACT the conditions are intensified, with the aim to produce corrosion deterioration on steel samples in a short period of time and as similar as possible to the corrosion from real conditions. By the nature of ACTs, the correlation between laboratory test results and real service conditions is not totally accurate. Actual atmospheric corrosion is affected by many complex factors that cannot be faithfully duplicated by the few simple and controlled variables considered under ACTs. Nevertheless, under appropriate test conditions, an ACT may offer useful information to be related to actual atmospheric corrosion, and in a shorter time of exposure (Guthrie, 2002).

In the present study, an ACT regimen based on a salt spray cabinet system under the ASTM B117-11 “Standard Practice for Operating Salt Spray (Fog) Apparatus” (ASTM, 2011) was used to reproduce atmospheric corrosion on steel coupons. The ACT regimen was applied to steel coupons to analyze and evaluate the performance of both steel washing and spot painting as effective options to reduce the rate of corrosion on steel girders.

5.2 Accelerated Corrosion Test Program

The following sections describe the test practices applied, the materials tested, the equipment used, and all the processes performed during the accelerated corrosion tests in the laboratory. The results from those tests were employed to analyze and evaluate the effectiveness of washing and spot painting as effective alternatives to reduce the rate of atmospheric corrosion on steel highway girder bridges.

5.2.1 Accelerated Corrosion Test – ASTM B117

This research utilized ASTM B117-11 (ASTM, 2011), a standard practice for salt spray (fog) test that has been designed to provide a controlled corrosive environment, and produces an accelerated corrosion attack of metal pieces located inside a test chamber. A misting system injects to the chamber a salt solution of sodium chloride (NaCl) at 5% in weight, with a pH ranging from 6.5 to 7.2. The solution is atomized over the exposed coupons inside the chamber by nozzles. The exposure zone should be kept at $95\pm 3^{\circ}\text{F}$ ($35\pm 2^{\circ}\text{C}$) and at relative humidity RH of 95-98%. The coupons shall be supported with an inclination from 15° to 30° from the vertical. The salt solution fog is spread uniformly over the coupons, with a rate of 0.034 to 0.068 fl-oz. (1.0 to 2.0 mL) of solution collected per hour, upon and horizontal area of 12.4 in^2 (80 cm^2). The test shall be continuous for the duration of the entire test period.

5.2.2 Materials

The study considered two types of structural steel: carbon (plain) steel and weathering steel. Two plates of carbon steel A709 Grade 50 with dimensions 4' x 3' x 0.5" and two plates of weathering steel A709 Grade 50W with the same dimensions, were provided by the Indiana Department of Transportation (INDOT) as part of their support for this research. The mill test report for the two types of steel are presented in Appendix B, detailing the mechanical properties and chemical composition for both steel types. For each type of steel, one plate was coated and the other plate remained uncoated. The coating system was applied by a certified INDOT contractor, in accordance to the requirements established by INDOT standards (INDOT, 2012), consisting in a three-coat system: an inorganic zinc primer, an epoxy intermediate coat, and a polyurethane finish coat. The steel plates were cut in small coupons of 3" x 6" at the Central Machine Shop at Purdue University.

The steel coupons were then protected with a casing made of a thick layer of 3M Scotchkote Liquid Epoxy Coating 323, a two-part system designed to protect steel pieces from harsh corrosion. The epoxy was applied to protect completely one face of the coupon, all four edges, and the borders in the other face. Corrosion from cut edges produces more rust than rolled surfaces, therefore all cut edges were protected to avoid distortions due to this effect. The uncoated coupons presented a surface of 2 ½" x 5 ½" and the coated coupons presented a surface of 2 ¼" x 5 ¼", totally free to be exposed to corrosion attack during tests. In this manner, the steel coupons offered only one face to be exposed to corrosion while the rest of the plate was effectively protected. Figure 5.1 shows typical steel coupons before and after application of epoxy casing protection.

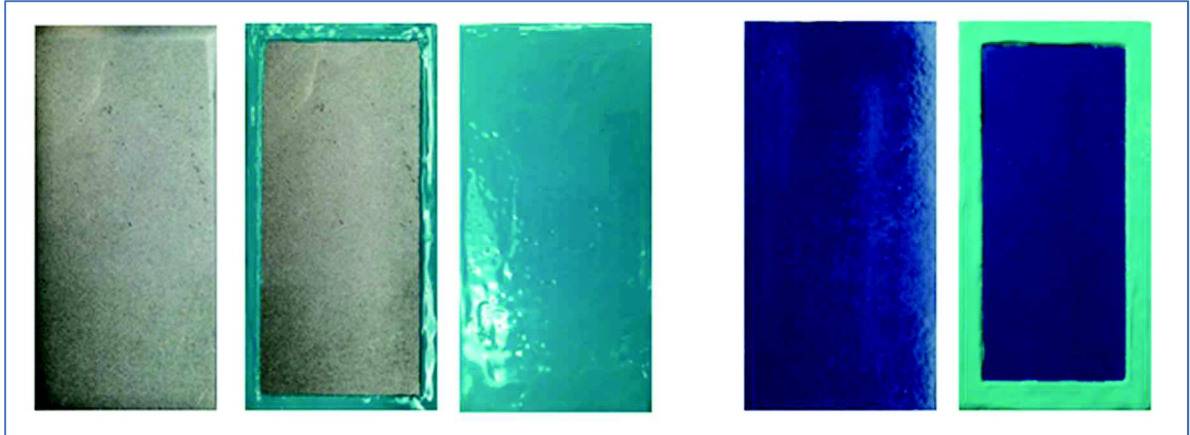


Figure 5.1: Steel coupons before and after epoxy coating application. Left: uncoated coupon, Right: coated coupon.

Polyvinyl chloride (PVC) racks were built to hold the steel coupons in a steady position during tests. The material was chosen to prevent galvanic couples when in contact with the metal pieces. Grooves were drilled with a tilt angle of 15° from the vertical and enough separation between them to avoid overlap of the plates. Figure 5.2 shows a group of racks holding steel coupons.



Figure 5.2: Steel coupons supported by PVC racks.

Acrylic boxes (25" high, 20" wide, and 27" deep) were built to contain the steel coupons inside the chamber under controlled temperature and relative humidity, as required by ASTM B117. The boxes had space to contain 40 coupons supported by racks. Each box had attachments to affix the misting system and keep 4 nozzles in a vertical position over the coupons. The ceiling had a marked inclination, such that any drop of solution accumulated in the upper inner surface would be directed to the sides. Figure 5.3 shows an acrylic box with tubing connections to conduct the pumped salt solution to the nozzles.

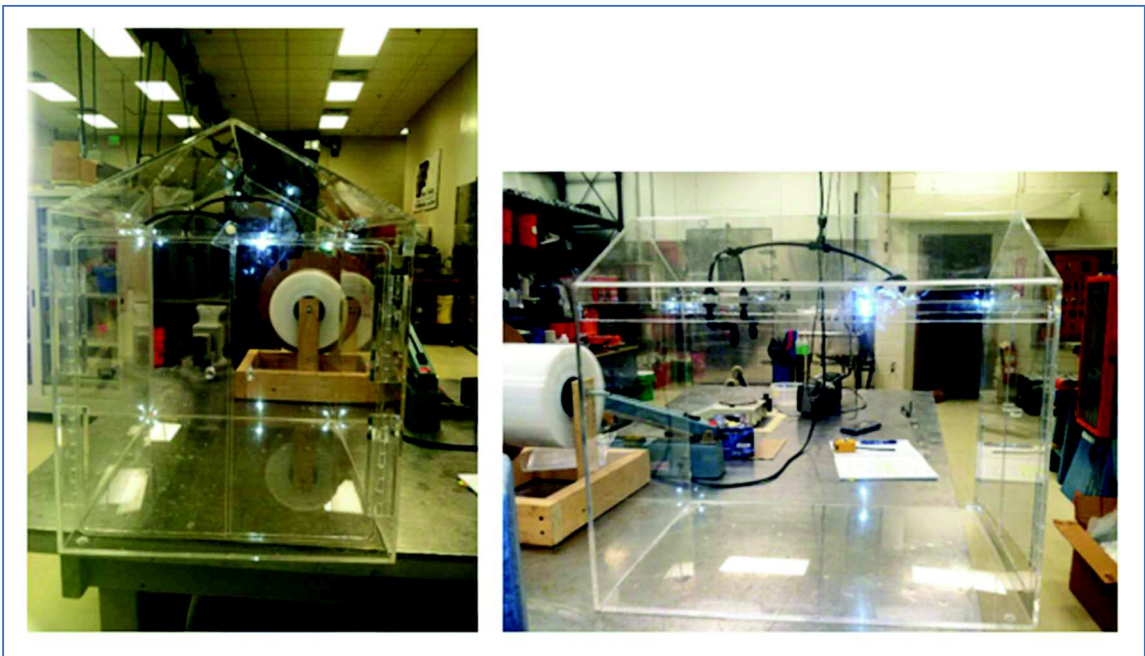


Figure 5.3: Front and lateral view of acrylic box

5.2.3 Equipment

5.2.3.1 Chamber

To perform the ACT following the ASTM B117 practice, a salt spray chamber was adapted at the Pankow Materials Laboratory at Purdue University. A weather chamber with automated controlled temperature from Darwin Chambers was assembled with a

misting system to periodically spray a salt solution to steel coupons located inside the chamber. A time controller device was set up to regulate the spray of a salt solution during specific periods of time throughout the day, every day, for the duration of the entire test period. The chamber had automatic temperature control and it was set up to keep an interior temperature of 95°F (35°C) during the entire test period of 24-weeks. Inside the chamber were positioned four acrylic boxes to contain the steel coupons during the ACT. The boxes were connected to the misting system to inject the salt fog through the nozzles and spray all coupons. The boxes were positioned with a slight slope downward to the front to facilitate the drainage of the solution after spraying the steel coupons. The solution was conducted through an orifice and tubing installed in the box's floor towards plastic containers located below the acrylic boxes. The sprayed solution was collected in those containers and periodically discharged from the chamber.

5.2.3.2 Misting System

A misting system from MistKing was connected to the weather chamber to spray the salt solution periodically under a controlled regime. A 125 psi (0.86 MPa) misting pump was installed to inject the salt solution to the weather chamber. PVC tubing ¼ in. diameter was used to link a plastic bucket containing the salt solution to the misting pump, and from the misting pump to each one of the four ¼ in. nozzles located on each acrylic box. The nozzles atomized the salt solution to spray it as a fine mist over the steel coupons. A ZipDrip valve was installed to eliminate falling drops from nozzles immediately after stopping each pumping cycle. A digital time-control device with 8 programmable events was used to modulate the misting system. The time-control device controlled the run/stop pumping cycle of the salt solution according to an established schedule for the entire day. Various accessories such as T and Y unions, manifolds, and valves, were installed to fit the misting system to the acrylic boxes.

Figure 5.4 shows the interior of the weather chamber with the four acrylic boxes in position and the misting system installed.



Figure 5.4: Interior view of weather chamber with acrylic boxes (left). Misting system installed (right)

5.2.3.3 Power Washer

Corroded steel coupons were treated by washing them to analyze its effect on the corrosion process. A 2500 - 3100 psi (17.24 - 21.37 MPa) Power Washer from Generac was utilized to wash the corroded steel plates at high pressure. This equipment takes water from a water source and ejects it at a high pressure; it is commonly used to clean and wash surfaces such as floors and walls. A strip pressure nozzle was recommended to produce medium rinsing, with higher pressure and medium flow. This type of nozzle was ideal for removing stains and rust without damage to the work surface. Figure 5.5 shows the power washer equipment.

5.2.3.4 Abrasive Blast Cabinet

An abrasive blast cabinet from Ruemelin Manufacturing Co. from the Bowen Laboratory for Large-Scale Civil Engineering Research at Purdue University was used to clean

selected corroded steel coupons. The cabinet propells fine grains of abrasive material at high velocity by an air compressor. Exposing a corroded steel plate to the sandblast eliminates all the rust from the surface, producing a white metal blast surface. Figure 5.6 shows the Ruemelin blast cabinet.



Figure 5.5: Power washer



Figure 5.6: Abrasive blast cabinet

5.2.3.5 Milling Machine

Steel coated coupons were scribed by a 2ML milling machine from The Cincinnati Milling Machine Co. at the Bowen Laboratory at Purdue University. The mill produced a controlled and artificial damage on coated steel samples in order to simulate damage in the field. A hard nail attached to a rotating axis produces an homogeneous cut in the sample. Figure 5.7 shows the milling machine used to scribe the steel coupons.



Figure 5.7: Milling machine scribing a steel plate

5.2.3.6 Small Equipment and Tools

Additional small equipment and tools used during the tests were the following:

- A Sartorius ENTRIS3202-1S Top loading electronic balance to weigh test samples.
- A Pittsburgh digital caliper (0.001” precision) and a Federal C81S dial gage (0.001” precision) to measure thicknesses.
- An 8-megapixel digital camera from Apple iPhone to take photographs of all coupons.

5.2.4 Salt Solution Application

The salt solution was prepared mixing 10 L of distilled water with 530.0 gr. of Culinox 999 Food Grade Sodium Chloride from Morton Salt Inc., to obtain a saltwater solution at 5% in weight. The water used in the mix was distilled water acquired at Walmart stores. The sodium chloride composition was in accordance with the ASTM-B117 requirements. A copy of the Certificate of Analysis from the sodium chloride presented by the provider is shown in Appendix B. The prepared mix was stored in a plastic bucket and injected to the chamber by the pump for 1.25 minutes each 2.5 hours. The steel coupons were

sprayed eight times each day at the following times: 00:30am., 7:00am., 9:30am., 12:00m., 2:30pm., 5:00pm., 7:30pm., 10:00pm. The total spray cycle per day resulted in an average rate of 1.55mL/h collected in an horizontal area of 12.4 in². The pH level in the mix was controlled for each load using a Symphony DB70P pH-meter, keeping the pH level at an average value of 7. Figure 5.8 shows the elements employed to prepare the salt solution in accordance to ASTM B117. Every three days the residual solution collected was eliminated from the chamber.



Figure 5.8: Components for salt solution preparation: Sodium chloride and scale (left), distilled water and graduated plastic bucket (center), and pH-meter (right)

5.3 ACT for Steel Washing Evaluation

5.3.1 Number of Coupons and Identification

The procedure to test the effect of steel washing was based on regularly washing steel coupons at different frequencies. The objective was to measure the effect of washing and the influence of the washing frequency in the reduction of corrosion rates. To achieve this objective forty 3”x6”x0.5” coupons from each type of steel were considered to test the effect of washing. For an easy and simple identification, each coupon from a type of steel was labeled with a capital letter A, B, and C, corresponding to uncoated carbon steel (A), coated carbon steel (B), and uncoated weathering steel (C). Due to a confusion when the steel plates were sent for coating, the weathering steel plate was not coated. For that reason, coated weathering steel was not a type of steel tested. For an easier identification

of data corresponding to different steel types, a color code was implemented. Each table and graph from a specific steel type was identified with a specific color: uncoated carbon steel type (A) = green, coated carbon steel type (B) = blue, and uncoated weathering steel type (C) = red.

Ten groups of coupons were utilized for each type of steel to be tested. To seek better confidence in the mean results, four steel coupons were considered for each group. The groups were identified by a number from 01 to 10, and each coupon belonging to certain group was identified by an additional lowercase letter, such as a, b, c, or d. Therefore, each coupon was identified by a compound label, consisting first in a capital letter indicating the type of steel (A, B or C), followed by a number indicating the group to which the coupon belongs (01 to 10), and finally a lowercase letter (a, b, c, or d) referring to one of the four individual coupons within that group. As an example, the label A-04c refers to the third coupon (c), from Group 04, of the uncoated carbon steel (steel Type A). All coupons were labeled according to this identification system on the top side and the back face of the plate, on the epoxy casing surfaces, using a Sharpie permanent marker. Appendix C presents the identification for all coupons from all steel types considered.

5.3.2 Schedule for Washing Process

At the beginning of the ACT there was not an exact period of time for which the test should be run to achieve the expected levels of corrosion. After twenty four weeks of running the ACT, the uncoated coupons from steel Types A and C developed a large amount of corrosion in the form of flaking and loose rust. Therefore, it was decided to stop the ACT at the end of week twenty four.

The ACT strategy was to set up several groups of coupons, which should be washed at different frequencies, to obtain a wide and trusted data base. Based on the size of the acrylic boxes it was estimated that forty (40) was the maximum number of coupons to be hold inside each box. Given the maximum capacity from each box, it was decided that

the test program would consist of ten groups of four coupons for each group. Four coupons for each group was believed to be an adequate size of sample to obtain an adequate level of accuracy from the test results.

For each type of steel, nine groups of steel coupons were washed regularly at a different frequency, while one group was never washed. Steel coupons from Group 01 were withdrawn from the chamber and washed every week; coupons from Group 02 were withdrawn from the chamber and washed every 2 weeks; coupons from Group 03 were washed every 3 weeks; and, in the same way, each group was washed every number of weeks as its group number identification, until Group 09 that was washed every 9 weeks. Coupons from Group 10 were never washed. Therefore, 3 steel types x 10 groups of coupons x 4 coupons per group, resulted in 120 steel coupons exposed to the ACT regime to analyze the effect of washing and the frequency of washing in reducing the rate of corrosion.

Table 5.1 presents the washing program, indicating the assigned week for washing each group of coupons. The same schedule is valid for steel Types A, B, and C. For instance, under this program all coupons from Groups A04, B04 and C04 should be washed every four weeks, at week 4, 8, 12, 16, 20 and 24, following the procedure explained in the following sections.

Table 5.1: Matrix for washing program

GROUP	WEEK																							
	01	02	03	04	05	06	07	08	09	10	11	12	13	14	15	16	17	18	19	20	21	22	23	24
01	X	X	X	X	X	X	X	X	X	X	X	X	X	X	X	X	X	X	X	X	X	X	X	X
02		X		X		X		X		X		X		X		X		X		X		X		X
03			X			X			X			X			X			X			X			X
04				X				X				X				X				X				X
05					X					X						X					X			
06						X						X						X						X
07							X							X							X			
08								X								X								X
09									X									X						
10																								

Note: X indicates a week when the corresponding group should be washed

5.3.3 Initial Data Acquisition

The initial physical characteristics from each coupon were taken and registered before beginning the ACT regimen. The weight, dimensions, thickness, and a photograph from each steel coupon were registered before and after the application of the protective epoxy casing used to expose only one coupon's face to corrosion. The procedures for data acquisition are presented in the next sections.

5.3.3.1 Weight

All coupons were weighed using the electronic balance, repeating the measurement three times for a better precision. The initial weight of each coupon, after epoxy casing application, are presented in Appendix D as data at week 0.

5.3.3.2 Dimensions

The top and bottom side dimensions for all coupons were measured using the digital caliper. The initial side dimensions of all coupons, before epoxy casing application, are presented in Appendix E.

5.3.3.3 Thickness

The thickness of each coupon was measured using two dial gages mounted in special acrylic frames. One dial gage was attached to a frame fixed to measure the thicknesses at points located at one fourth of the coupon width. The second dial gage was mounted to a frame fixed to measure the thicknesses of points at the middle of the coupon width. A plastic piece, the size of the steel coupon's area was used as a template, with four perforations at the one-fourth location of the coupon width and four perforations at the middle of the coupon width. Using this template, the coupon thickness was measured at twelve selected points, four at each one-fourth width and four at the middle of the coupon width. Figure 5.9 shows the twelve points on a coupon where the thickness was measured. The perforations in the plastic template were a little larger than the tip of the spindle's gage, enough to allow the spindle to fit the holes always in the same position.

The use of the plastic template helped to measure the thickness of a coupon in the same twelve positions every time. The initial thickness of all the coupons, after epoxy casing application, are presented in Appendix F.

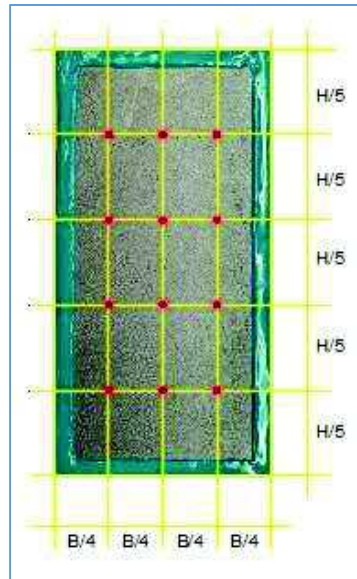


Figure 5.9: Location of thickness measuring positions

5.3.3.4 Photographs

Each steel coupon was photographed using the digital camera from a smartphone. The equipment was mounted in a special acrylic frame that helped to take photographs of the coupons from the same distance and position each time. The initial photographs for each coupon, before and after epoxy casing application, were registered and recorded in the research database. Figure 5.10 shows the instruments utilized for coupon data acquisition, such as weight, side dimensions, thickness, and photograph capture. In Appendix G are presented all the photographs corresponding to coupon A01-a, for the twenty four weeks the ACT lasted.

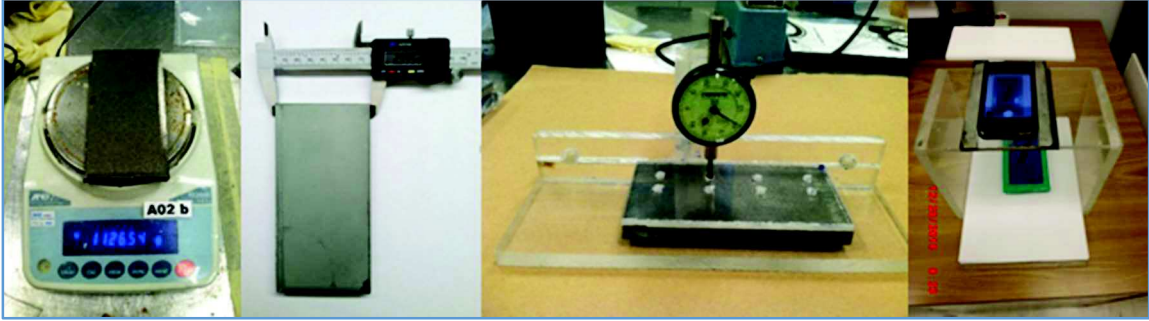


Figure 5.10: Coupon data acquisition. From left to right: weight, side dimensions, thickness, photograph.

5.3.4 Procedure for the ACT Regime for Steel Washing Evaluation

The 120 steel coupons from Groups A, B, and C, were supported on the PVC racks and placed inside the acrylic boxes. Each group of steel coupons was placed in one acrylic box, forming four lines of racks, and containing ten coupons in each line. After the spray process was initiated, the ACT continued every day for twenty four weeks, following the indicated program of eight spray cycles per day. The salt solution bucket was loaded with the 5% by weight of sodium chloride (NaCl) mix each three days to ensure a continuing fog spray of the coupons inside the boxes. The spray system was controlled in a way that never ran out of salt solution. Figure 5.11 shows the weather chamber with the acrylic boxes containing the steel coupons during the ACT regime.



Figure 5.11: Weather chamber with steel coupons under ACT regime.

Every week, for the twenty four weeks (approximately 4000 hours) that the ACT lasted, the groups of coupons were programmed for washing according to Table 5.1. The programmed coupons were carefully removed from the chamber and submitted to a protocol, which consisted of a series of treatments and data acquisition, as presented in the next sections.

5.3.4.1 Removal from Chamber

Weekly every Thursday the coupons from the selected groups (see Table 5.1), corresponding to the three steel Types A, B, and C, were withdrawn from the test chamber to perform a series of treatments and physical observations. The remaining coupons continued with the ACT process.

5.3.4.2 Power Washing

The selected steel coupons were placed on the floor, outside the laboratory for washing. The steel coupons were kept an adequate distance between each other, with the corroded face side up. The coupons were pressure-washed with the power washer machine,

ejecting potable water at approximately 2500 psi (17.24 MPa), from a distance of one foot (0.30 m). The pressured water was applied during two seconds to remove the salt compounds from the coupon surface. The time of washing was estimated following the recommendations from the study by Crampton et al. (2013). This activity was performed only to coupons belonging to Groups 01 to 09, since coupons from Group 10 were never washed. Figure 5.12 shows a series of steel coupons under pressure washing.



Figure 5.12: Power washing steel coupons

5.3.4.3 Air Drying

After finishing power washing, the steel coupons were dried using a portable fan. Inside the laboratory, the washed coupons were placed over a table and air-dried during 15 minutes. Figure 5.13 shows steel coupons that are being air-dried with a portable fan.



Figure 5.13: Drying wet coupons after washing

5.3.4.4 Data Acquisition

a) Weight

After dried, all coupons were weighed and the information recorded. Each measure was taken three times and the average value was registered in a master spreadsheet for subsequent calculations. The weight of all coupons corresponding to each week of treatment of the ACT regime are presented in charts in Appendix D. Tables in Appendix D present the weight for each coupon, measured each week the coupon was washed; the tables are organized for each steel Type (A, B, and C), and for each Group (01 to 10).

b) Thickness

Next, the thickness of all programmed steel coupons were measured, using the dial gages mounted in plastic frames and the template described before. Twelve points over each coupon were identified using the template and the corresponding thicknesses were registered. Each measure was done three times and the average value was registered in a master spreadsheet for subsequent calculations. The mean value of the twelve measured thicknesses from each coupon is presented in tables in Appendix F. Tables in Appendix F

present the thickness for each coupon, measured each week the coupon was washed, and they are organized for each steel Type (A, B, and C), and for each Group (01 to 10).

c) Photograph Capture

All analyzed coupons were photographed to keep a visual record from physical changes during the ACT. The photographs for all coupons tested during the ACT were registered and recorded in the research database. In Appendix G are presented, as a manner of example, all the photographs corresponding to coupon A01-a, for the twenty four weeks the ACT lasted.

5.3.4.5 Return to Chamber

Finally, all the analyzed coupons were returned to the test chamber to continue the ACT regime. The coupons were returned to the chamber in a different order than the original. The position of coupons inside the box were changed every week to reduce some possible influence of the location within the box on the rate of corrosion. Figure 5.14 presents a flow chart with all the activities that are performed under the protocol of the ACT for steel washing evaluation.

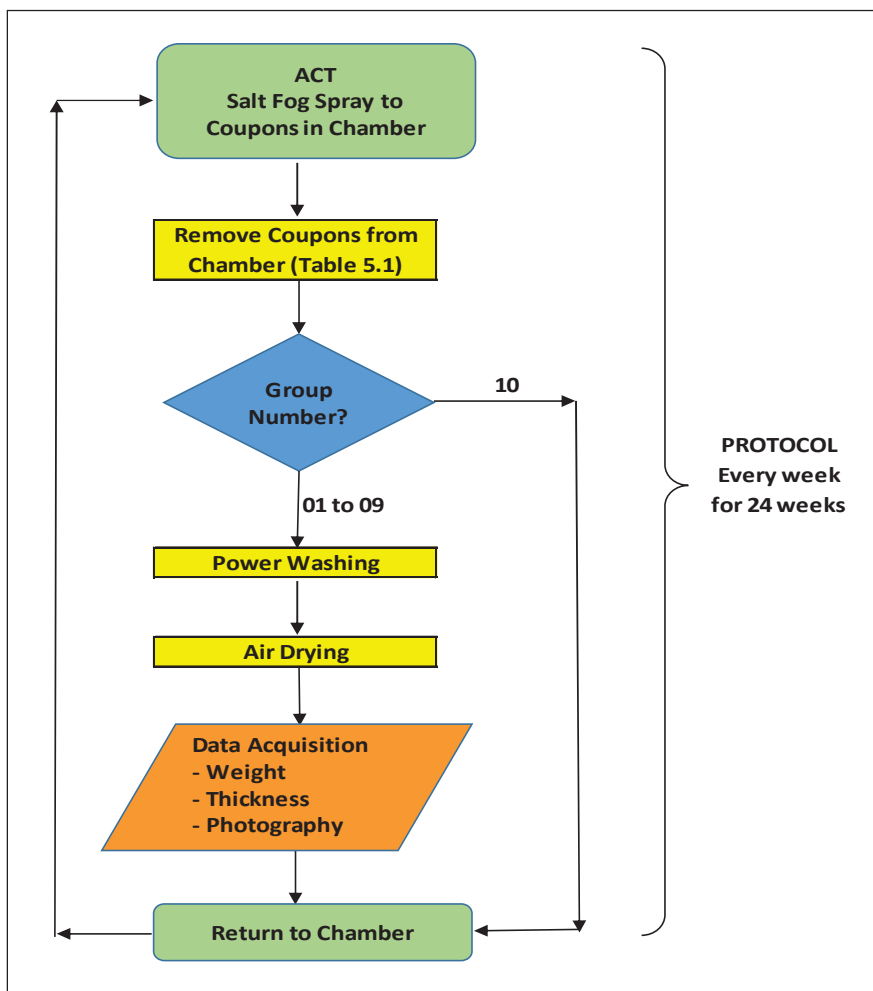


Figure 5.14: Flow chart for ACT program for steel washing evaluation

5.3.5 Results from ACT for Steel Washing Evaluation

The results from the ACT for steel washing evaluation are presented in this section. First, some details from the test procedure are described, the most significant observations are noted, and the corresponding results obtained from all coupons submitted to the ACT for steel washing evaluation are presented in tabulated and graphical form. A summary of the relevant results is presented, interpreted, and commented.

Few hours after the ACT started, the formation of the first spots of rust were observed on the surfaces of both uncoated carbon and uncoated weathering steel coupons (steel Types A and C respectively). The rust product was easily visualized and identified by its characteristic orange to brown color in contrast to the steel gray color. The corrosion degradation progressed gradually with time for the uncoated coupons, since the test started and continued during the twenty four weeks the ACT lasted. During the salt spray test the continuous fog caused the formation of drops in the corroded surface. With the ACT progress, rough and flaky rust products grew on the surfaces of the uncoated coupons (steel Types A and C). As could be observed from the photo-documented evidence in Appendix G for coupon A01-a, the uncoated coupons developed significant amount of rust products after the 24-weeks of exposure. The bottom edge of all uncoated coupons showed a high grade of rust stain due to accumulation of corrosion products between the coupons and the racks. A small formation of rust under the edges of the epoxy casing, producing some cracks but without breaking the casing were observed in a few uncoated coupons. The significant state of corrosion developed by the uncoated coupons was the main reason to establish the end of the ACT at week 24.

Coated carbon steel coupons, labeled as steel Type B, showed no rust formation, blistering, or any type of corrosion degradation in their exposed surface during the 24-weeks the ACT lasted. Visual observation of all coated coupons showed undamaged surfaces, even keeping almost the same gloss the coupons had at the beginning of the ACT. The lack of corrosion defects on the coated surfaces after 4,000 hours of ACT could be explained because the salt spray test did not include exposure to ultraviolet (UV) light. UV light is considered a critical environmental factor affecting the paint gloss and fading (Chong, 2007).

5.3.5.1 Weight Change

Data corresponding to the weight change from all steel coupons under the ACT are presented in Appendix D. The recorded weight for each one of the 120 coupons submitted to the ACT are presented in tabulated form. The tables present the weight for

each coupon measured each week the coupon was washed, classified by steel Types A, B, and C, and by groups, from Group 01 to Group 10 respectively. Data for week 0 referred to the initial weight, before the ACT started. Data were registered from week 0 to week 24, which is the last week of testing.

The weight change is also presented in graphical manner, showing the weight change normalized by the coupon area exposed to corrosion. For each group of steel coupons a graph is presented. Each graph represents the variation in time of the mean value of the weight change corresponding to the four coupons for each group. The data were fitted using functions from MS Excel to determine a representative curve for each group. For steel Types A and C the data were best represented by a power function, which has a line trace when it is plotted in log-log axes. For steel Type B, which shows values with little variation, the data were best represented by a second order polynomial function, which is showed in linear axes. In both cases the type of function was selected based on a relatively high correlation parameter R^2 .

A review of the graphs in Appendix D, corresponding to steel Types A and C, shows a similar pattern between groups of the same number (e.g. A04 with C04), with slightly higher increment of weight on steel Type C coupons. For both steel Types A and C, the pattern is an increment of coupon's weight in time. There is a direct relationship between the increments of weight with the increment of corrosion rates, since the increment of weight is generated by the production of rust due to underneath steel corrosion.

Observing the graphs for steel Type B coupons, the weight change values are almost insignificant when compared to the values corresponding to steel Groups A or C. For that reason, the graphs for steel Type B coupons are presented at a magnified scale for the vertical axis. In the plots for steel Type B coupons, the common pattern is a slightly increment of weight during the first few weeks of the test, followed by a continued decrease of weight until the end of the test.

A summary of data corresponding to weight change from steel Type A coupons is presented in Figure 5.15. Figure 5.15 shows the weight change variation in time for the mean values of the four coupons conforming each group (Groups A01 to A10).

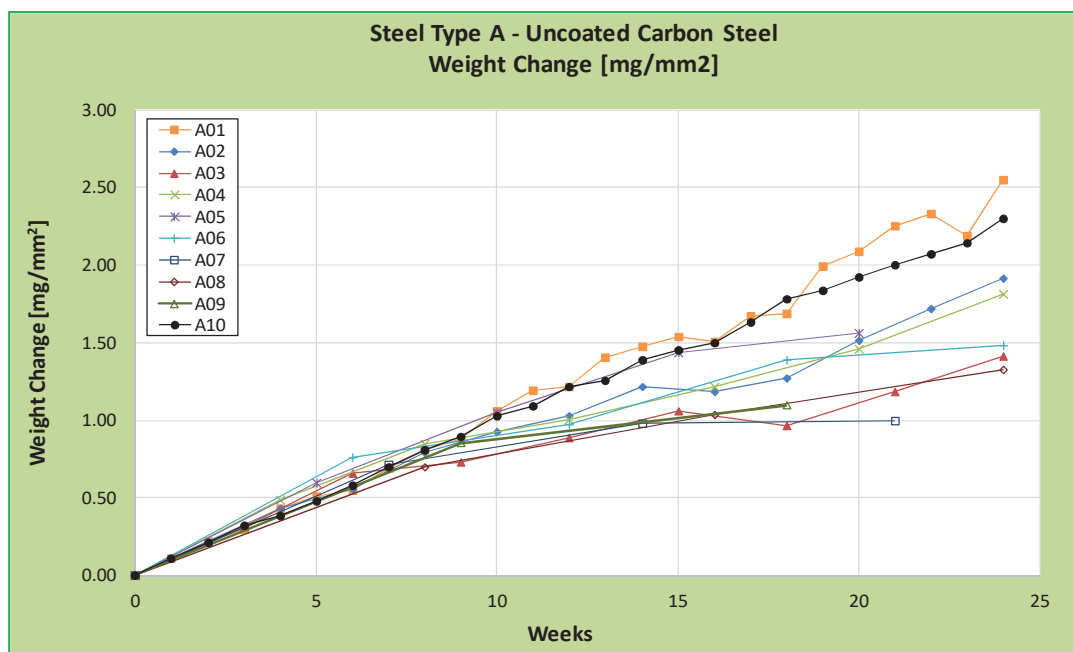


Figure 5.15: Weight change versus time for steel Type A groups

In figure 5.15 there is not a clear and distinct pattern between wash frequency and weight change. In fact, some curves corresponding to different frequencies of washing crossed each other during the test duration. It can be observed that the curve corresponding to the one-week washing frequency (Group A01) produces a higher weight increment than the no washing alternative (Group A10). This situation was contrary to the hypothesis of investigation, that steel washing will reduce the corrosion rates. On the other hand, in the long time, all other frequency alternatives showed reduced rates of corrosion than the no washing alternative, which was in agreement with the hypothesis of investigation.

Analyzing the behavior for Group A01, it was concluded that those steel coupons presented a higher increment of weight, and consequently a higher rate of corrosion, due to the larger number of wet-dry cycles the coupons experienced. Group A01 coupons

were washed every week, therefore following the ACT test protocol, the coupons were retired from the chamber and dried every week. Wet-dry cycles exacerbate the process of corrosion on steel coupons as it is considered in the ASTM G85, the modified salt spray test, or the SAE J2334, an ACT developed for the automotive industry (SAE, 2003). Regardless the ASTM B107 test does not consider wet-dry cycles as a factor for corrosion acceleration, the frequency of washing each week for Group A01 required a weekly dry stage. Consequently, Group A01 coupons could be affected by two effects, a corrosion reduction effect due to weekly washing and a corrosion increment effect due to frequent wet-dry cycles. This possible double effect is a consideration out of the limits of this dissertation and therefore it was not studied. Based on this possible double effect over Group A01 coupons, it was decided do not consider this group in the study of steel washing.

Since the group of coupons with low washing frequency resulted in very few data values, it was also decided not to consider the data from those groups. Groups A06, A07, A08, and A09, with four or less data values, resulted in mean values with low confidence, and consequently were not considered. Group A05 had four values but it was considered since presented the same regular tendency than Groups A02 to A04.

After the indicated considerations, data from Groups A02, A03, A04 and A05 were combined, averaged, and plotted along with data corresponding to Group A10. Figure 5.16 presents the data for the mean of weight change values from combined Groups A02-A05 and data from Group A10. In Figure 5.16 can be observed that the average of weight change values for combined Groups A02-A05 is quite similar to values from Group A10 at the beginning of the test. After the first seven weeks the values start a marked difference, with a reduction on the increment of weight for the average values from combined Groups A02-A05.

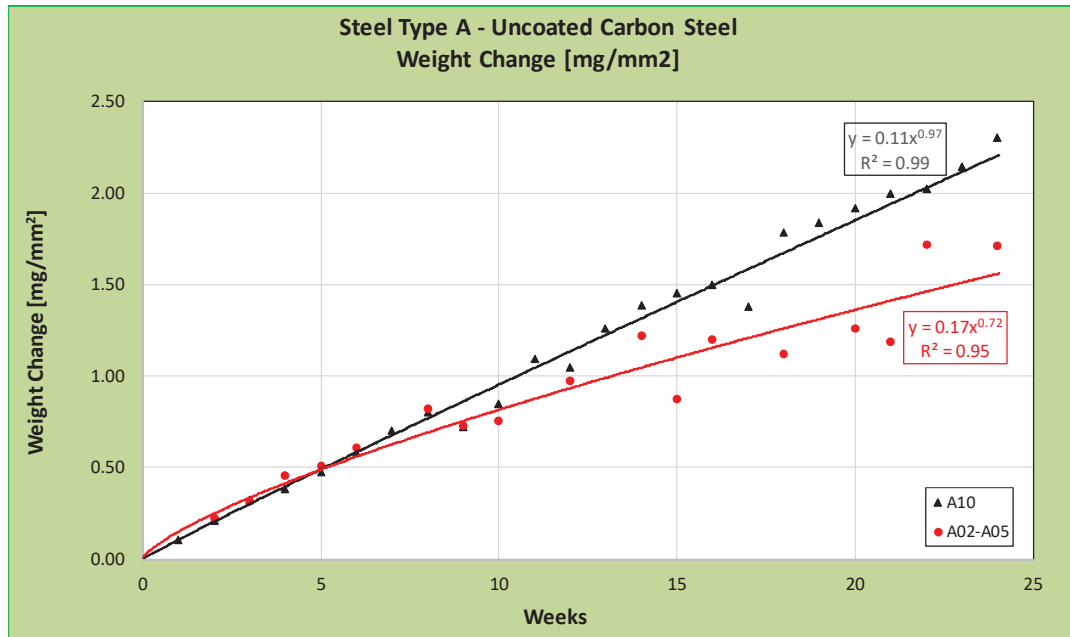


Figure 5.16: Weight change versus time for mean values from Groups A02-A05 and Group A10

Reducing the analyzed data to Groups A02 to A05 shows a more clear effect of steel washing on reducing the rate of weight increment, and therefore, as explained previously, a reduction of corrosion rates. In Figure 5.16 data corresponding to Group A10 present higher rates of weight increment, and consequently, higher corrosion rates than data from combined Groups A02-A05. Data points from the two plots in Figure 5.16 were fitted using the least-squares function from MS Excel to determine a representative curve for each group. Equations 5.1 and 5.2 show the power functions representing the weight change for Groups A02-A05 and Group A10 respectively. In both cases the type of function was selected based on a relatively high correlation parameter R^2 .

$$W1 = 0.17 t^{0.72} \quad \text{Equation 5.1}$$

$$W2 = 0.11 t^{0.97} \quad \text{Equation 5.2}$$

where:

$W1$ = weight change for combined Groups A02-A05 [mg/mm²]

W_2 = weight change for Group A10 [mg/mm^2]
 t = exposure time in ACT [weeks]

The same analysis and considerations applied to steel Type A coupons were applied to the analysis for steel Type C coupons. Figure 5.17 shows the data corresponding to the mean values of weight change variation in time for each group of coupons corresponding to steel Type C (Groups C01 to C10). Figure 5.18 shows the data for the mean of weight change values from combined Groups C02-C05 and data from Group C10. Again, it is observed that there is less weight increment, and hence lower corrosion rates, from steel washing alternatives (Groups C02-C05) versus the no washing alternative (Group C10). Data points from the two plots were fitted using the least-squares function from MS Excel to determine a representative curve for each group. Equations 5.3 and 5.4 show the power functions representing the weight change for Groups C02-A05 and Group C10 respectively. In both cases the type of function was selected based on a relatively high correlation parameter R^2 .

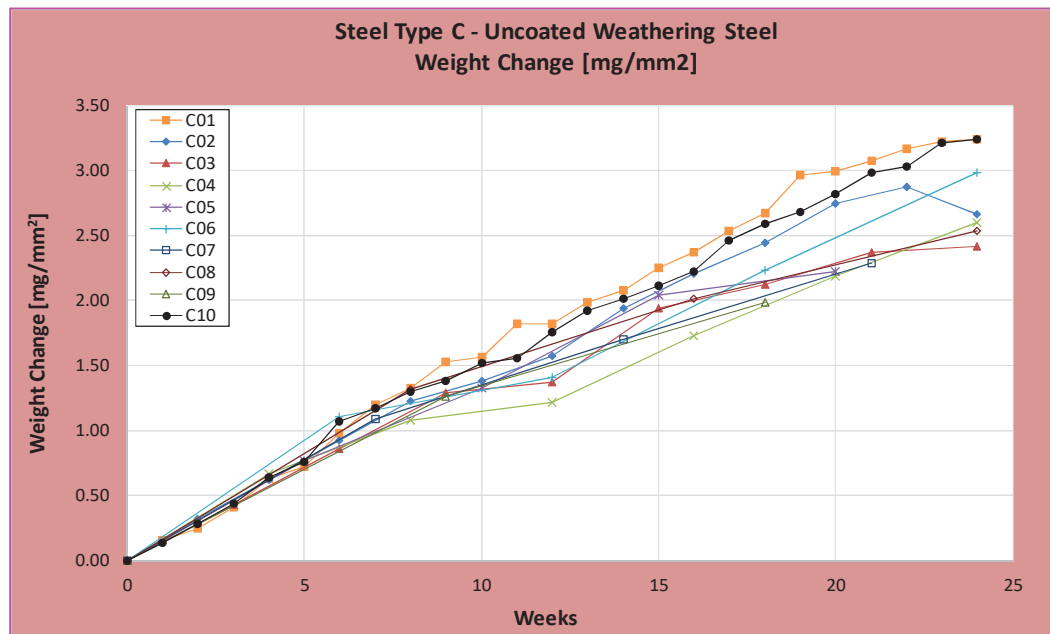


Figure 5.17: Weight change versus time for steel Type C groups

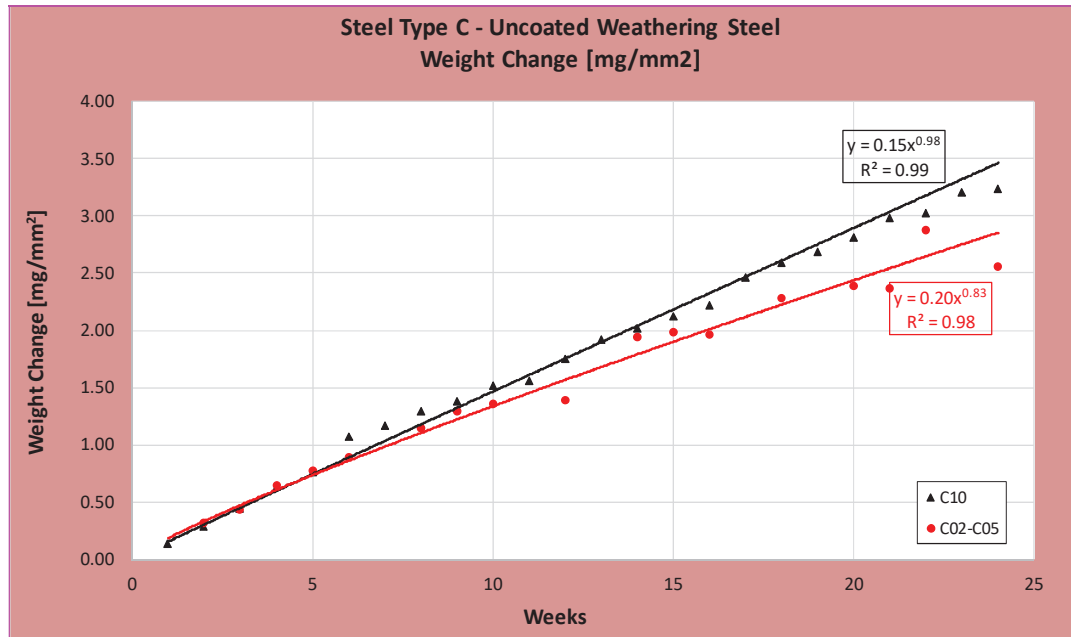


Figure 5.18: Weight change versus time for mean values from Groups C02-C05 and Group C10

$$W3 = 0.20 t^{0.83} \quad \text{Equation 5.3}$$

$$W4 = 0.15 t^{0.98} \quad \text{Equation 5.4}$$

where:

$W3$ = weight change for combined Groups C02-C05 [mg/mm²]

$W4$ = weight change for Group C10 [mg/mm²]

t = exposure time in ACT [weeks]

Data corresponding to weight change variation in time for the mean values of steel Type B coupons are summarized in Figure 5.19. Plots from all Groups B01 to B10 do not show a consistently pattern between wash frequency and weight change. From Figure 5.19 it is observed a small tendency in all coupons to increase the weight at the beginning of the test, and approximately after the week twelve to fifteen, the tendency is to reduce the weight. It is important to emphasize the fact that weight changes for steel coupons from steel Type B are very small (max. value of 0.10 mg/mm²) and irrelevant when compared

with values corresponding to coupons from steel Types A and C (max. values of 2.5 and 3.5 mg/mm²).

Following the methodology from steel Types A and C, Figure 5.20 shows the data for the mean of weight change values from combined Groups B02-B05 and also data from Group B10. In Figure 5.20 is observed that even for steel Type B, performing steel washing frequently is a convenient alternative to reduce weight change and corrosion rates. Data points from the two plots were fitted using the least-squares function from MS Excel to determine a representative curve for each group. Those fitting curves resulted in second order polynomial functions. In this case, for steel Type B (coated carbon steel) the negative weight change values mean a reduction of the coating layer, but in very small amounts.

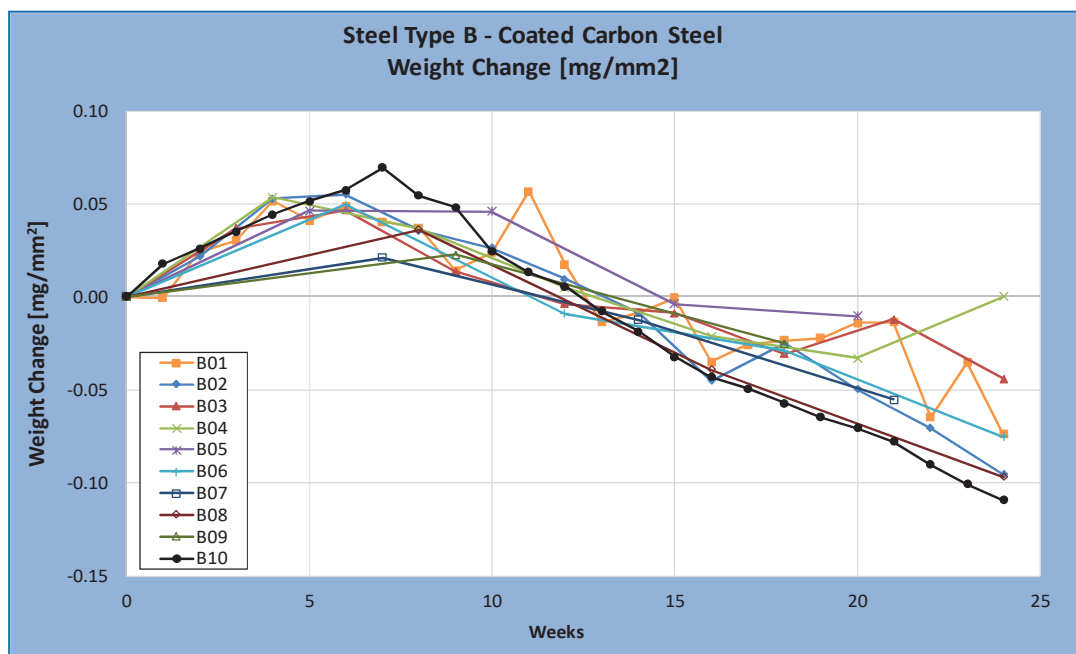


Figure 5.19: Weight change versus time for steel Type C groups

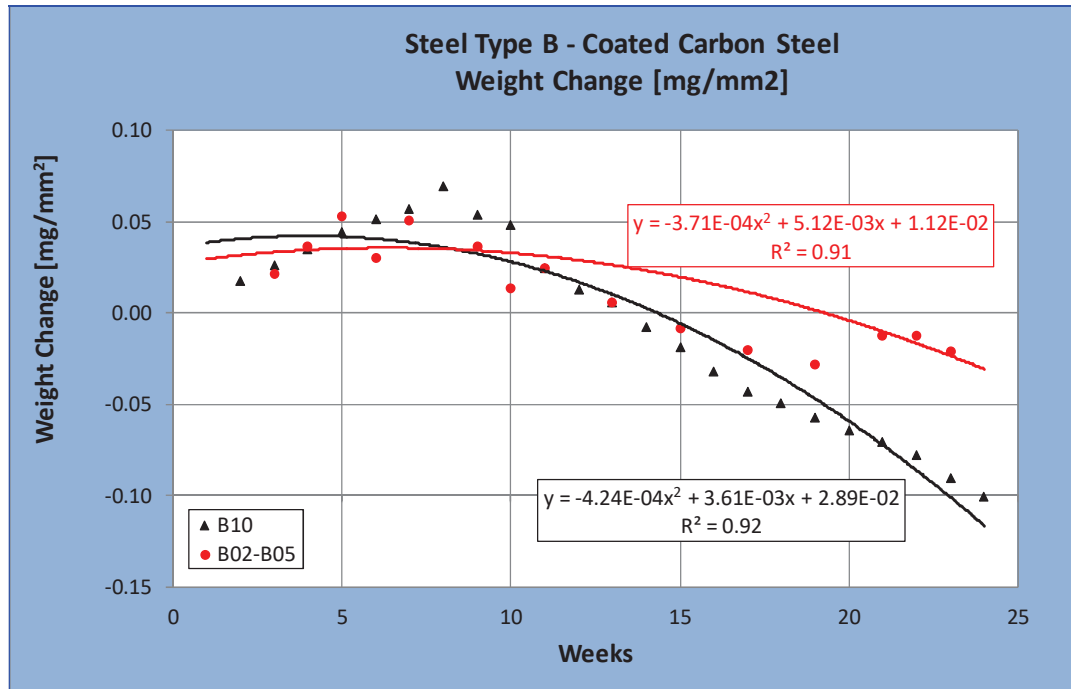


Figure 5.20: Weight change versus time for mean values from Groups B02-B05 and Group B10

5.3.5.2 Thickness Change

Data corresponding to thickness change from all steel coupons under the ACT are presented in Appendix F. Thickness change data are classified by steel Types A, B, and C, and by Groups 01 to 10 respectively. Data corresponding to coupons thickness change are presented in Appendix F by means of tables and graphs. Data are reported in tables for all the 120 coupons submitted to the ACT. For each group of steel coupons, a graph is presented in Appendix F. The graphs show the variation in time of the mean value of the thickness change corresponding to the four coupons for each group. On each graph the mean values were fitted using the least-squares function from MS Excel to determine a representative curve for the group. For steel Types A and C the data are best represented by a power function, which has a line trace when it is plotted in log-log axes. For steel Type B the data are best represented by a second order polynomial function.

The graphs in Appendix F for steel Types A and C present a similar pattern between groups of the same number (e.g. A04 with C04), with slightly higher increment of thickness on steel Type C coupons. For both steel Types A and C, the pattern is an increment of coupon's thickness in time. There is a direct relationship between the increment of thickness with the increment of corrosion rates, since the increment of thickness is generated by the production of rust due to underneath steel corrosion. Observing the graphs for steel Type B coupons, the thickness change values are almost insignificant when compared to the values corresponding to steel Groups A or C. For that reason, the graphs for steel Type B coupons are presented on a magnified scale for the vertical axis. In the plots for steel Type B coupons, the common pattern is a slight increase of thickness during the first weeks of the test, followed by a decrease of thickness until the end of the test.

Figure 5.21 presents a summary of data corresponding to thickness change from steel Type A coupons. Figure 5.21 shows the thickness change variation in time for the mean values of the four coupons for each group (Groups A01 to A10).

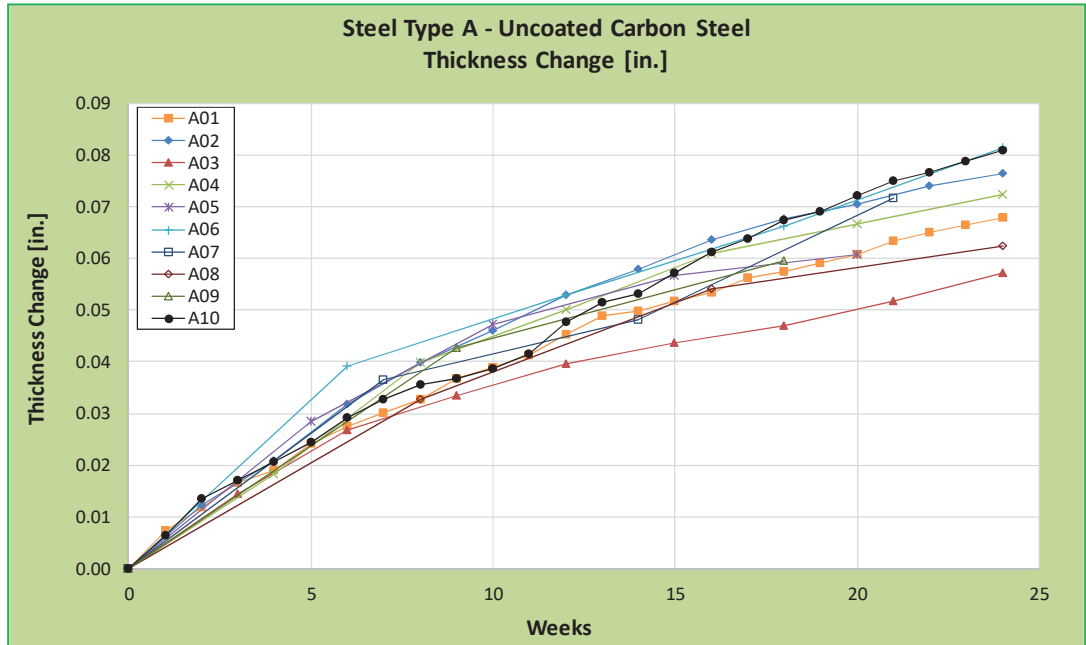


Figure 5.21: Thickness change versus time for steel Type A groups

Figure 5.21 presents an unclear pattern between wash frequency and thickness change. It can be observed that some curves corresponding to different frequencies of washing crossed each other during the test duration. To simplify the analysis, again, only Groups A02 to A05 were considered to analyze the effect of steel washing over thickness change. Figure 5.22 shows the data for the mean of thickness change values from combined Groups A02-A05 and data from Group A10. In Figure 5.22 it could be observed that the average of thickness change values for combined Groups A02-A05 is quite similar to values from Group A10 at the beginning of the test. After the first weeks the values start a marked difference, with a reduction on the increment of thickness for the average values from combined Groups A02-A05. Data points from the two plots were fitted using the least-squares function from MS Excel to determine a representative curve for each group. Equations 5.5 and 5.6 show the power functions representing the thickness change for combined A02-A05 and A10 groups respectively. In both cases the type of function was selected based on a relatively high correlation parameter R^2 .

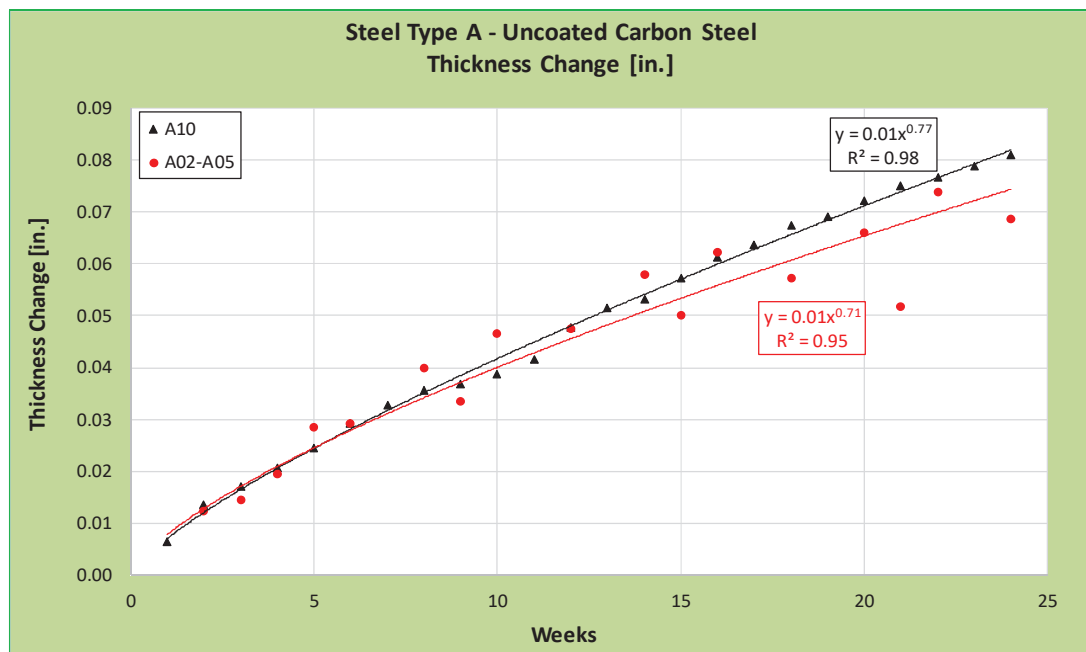


Figure 5.22: Thickness change versus time for mean values from Groups A02-A05 and Group A10

$$T1 = 0.01 t^{0.71} \quad \text{Equation 5.5}$$

$$T2 = 0.01 t^{0.77} \quad \text{Equation 5.6}$$

where:

$T1$	=	thickness change for combined Groups A02-A05 [in]
$T2$	=	thickness change for Group A10 [in]
t	=	exposure time in ACT [weeks]

From Figure 5.22 it can be observed that data points for steel washing alternative (Groups A02-A05) show more dispersion than data from Group A10. The tendency from Groups A02-A05 is to produce less thickness increment than the no washing alternative (Group A10). These results are in agreement with the results obtained from weight change analysis, as showed in Figure 5.16.

The data corresponding to thickness change variation in time from steel Type C coupons are shown in Figures 5.23 and 5.24. Figure 5.23 presents the thickness change variation in time for the mean values of the four coupons for each group from steel Type C. Figure 5.24 shows the data for the mean of thickness change values from combined Groups C02-C05 and data from Group C10. Again, the results show an agreement with the results from weight change for the same type of steel, as showed in Figures 5.17 and 5.18. Data points from the two plots were fitted using the least-squares function from MS Excel to determine a representative curve for each group. Equations 5.7 and 5.8 show the power functions representing the thickness change for C02-C05 and C10 groups respectively. In both cases the type of function was selected based on a relatively high correlation parameter R^2 .

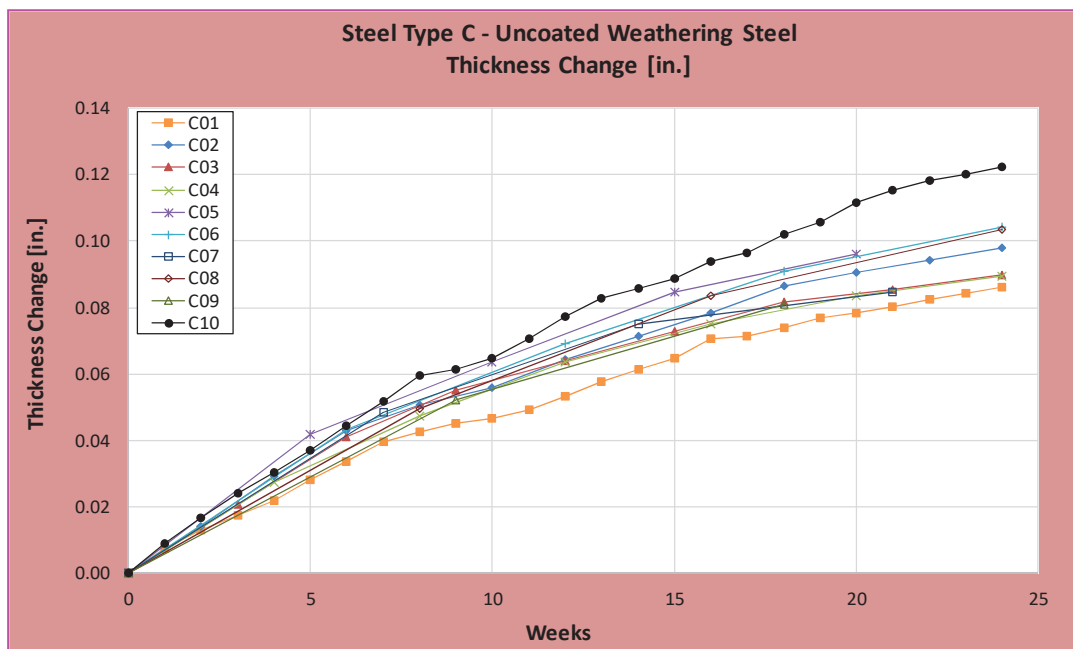


Figure 5.23: Thickness change versus time for steel Type C groups

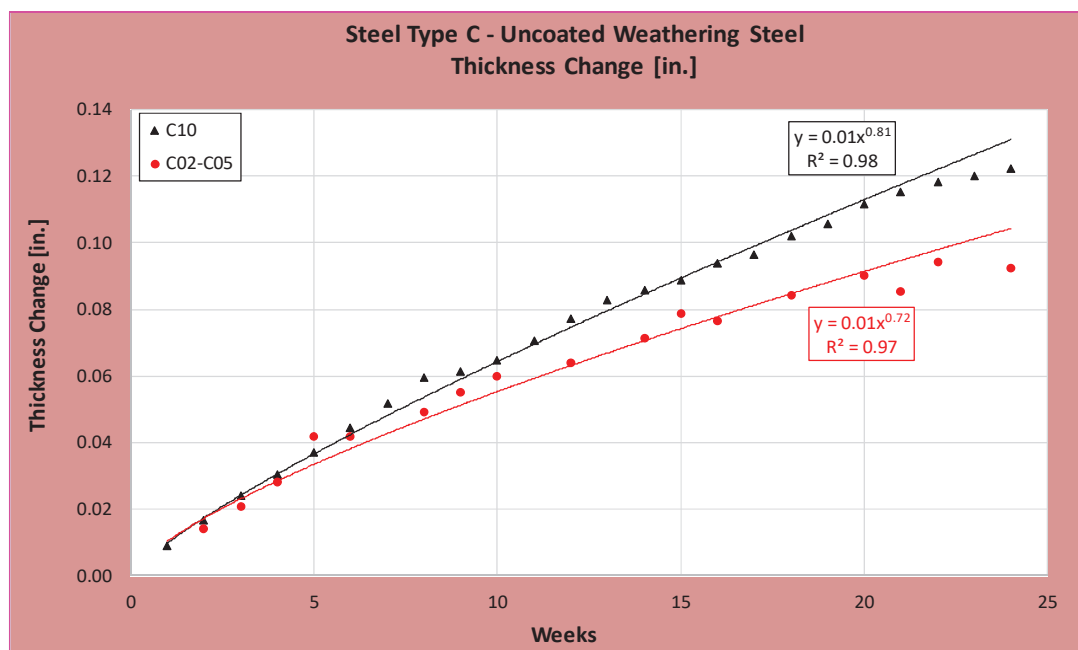


Figure 5.24: Thickness change versus time for mean values from Groups C02-C05 and Group C10

$$T3 = 0.01 t^{0.72}$$

Equation 5.7

$$T4 = 0.01 t^{0.81} \quad \text{Equation 5.8}$$

where:

- $T3$ = thickness change for combined Groups C02-C05 [in]
 $T4$ = thickness change for Group C10 [in]
 t = exposure time in ACT [weeks]

Data corresponding to thickness change variation in time for the steel Type B coupons are summarized in Figures 5.25 and 5.26. In Figure 5.25 it is observed that plots from all Groups B01 to B10 do not show a consistent pattern between wash frequency and thickness change. From Figure 5.25 it is observed that there is a tendency in all coupons to increase the thickness at the beginning of the test, and after some weeks, the tendency is to reduce the thickness. Thickness changes for steel coupons from steel Type B are very small and irrelevant when compared with values corresponding to coupons from steel Types A and C. Figure 5.26 shows the data for the variation in time of the mean of thickness change values from combined Groups B02-B05 and from Group B10. From Figure 5.26 it is observed that performing steel washing frequently is a convenient alternative to reduce thickness changes, and consequently, to reduce corrosion rates. In this case, for steel Type B (coated carbon steel) the negative thickness change values mean a reduction of the coating layer, but in very small amounts. Data points from the two plots were fitted using the least-squares function from MS Excel to determine a representative curve for each group. Those fitting curves resulted in second order polynomial functions.

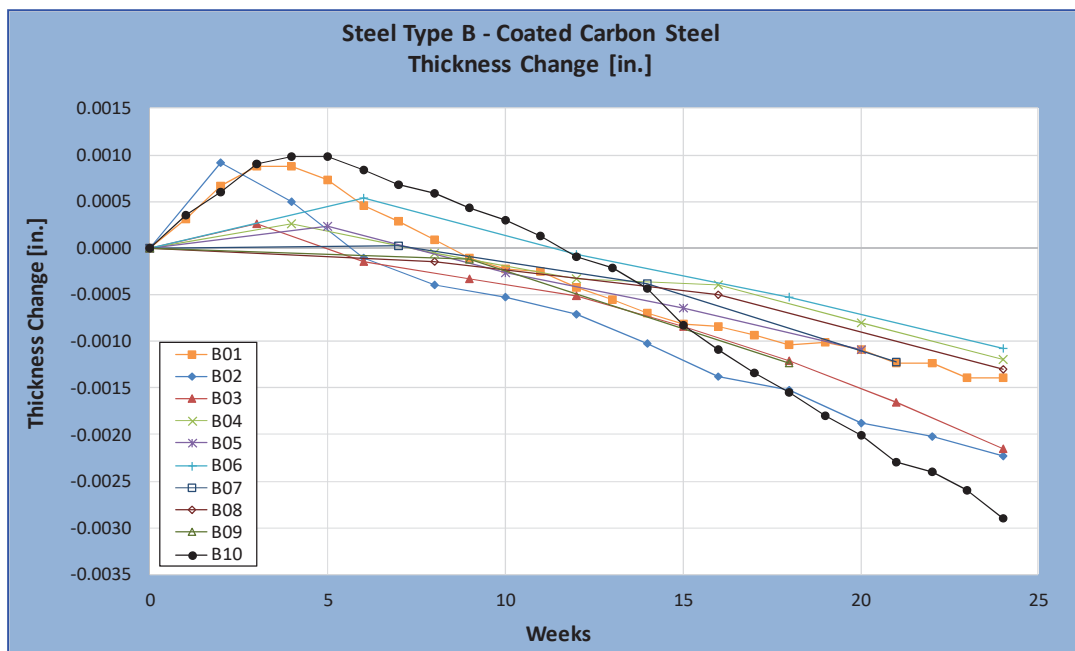


Figure 5.25: Thickness change versus time for steel Type B groups

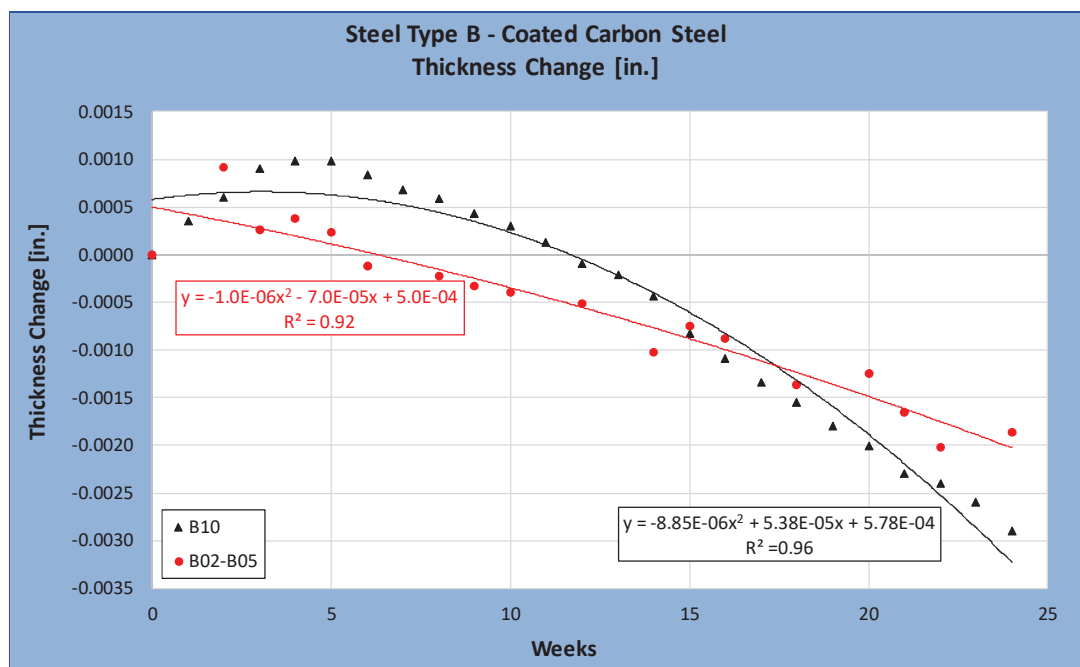


Figure 5.26: Thickness change versus time for mean values from Groups B02-B05 and Group B10

5.3.5.3 Physical Aspect Change

Visual inspection from all uncoated coupons showed a rapid and continuous formation of rust product over the exposed area. As fast as after two to three days of ACT, the exposed area of all uncoated coupons (uncoated carbon and uncoated weathering steels) were covered by brown-to-orange rust stains. Coupons from steel Types A and C showed a regular and continuous formation of rough and flaky rust products in time. The physical aspect change from all coupons were registered by photographs and were recorded at the research database. Figure 5.27 presents some selected photographs showing the formation of rust products over exposed area to corrosion for coupon A-01a. In Appendix G is presented the chronological formation of rust product of coupon A-01a.

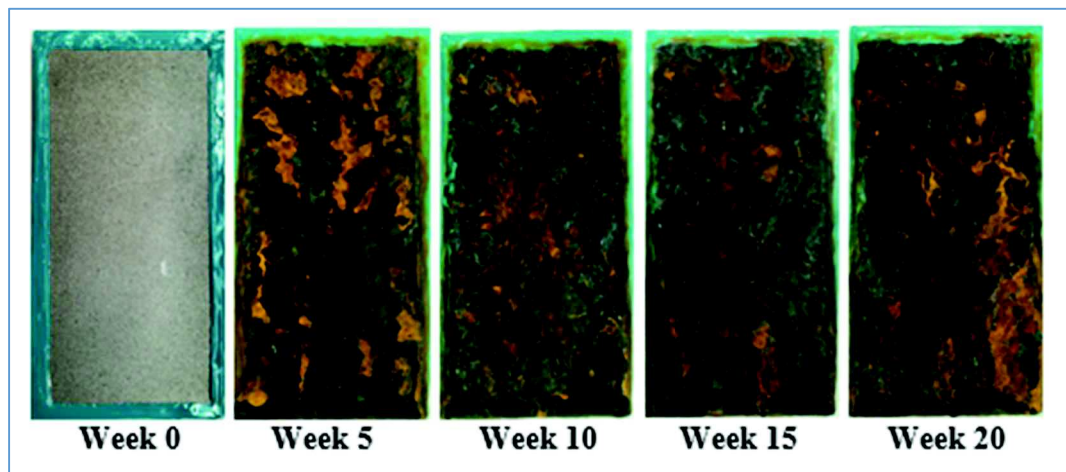


Figure 5.27: Rust formation over uncoated steel coupon (coupon A01-a)

Visual inspection of coupons from steel Type B showed a lack of rust formation. The coating layer worked properly in avoiding the attack of corrosion to the steel substrate during the entire duration of the ACT. After the twenty four weeks the ACT lasted, all the steel Type B coupons kept the exposed surface without showing any damage due to corrosion attack, even keeping almost the same gloss the plate had before the test started. However, as stated earlier, there was some small loss in coating thickness experienced. Figure 5.28 shows some photographs from a typical coated plate from steel Type B.

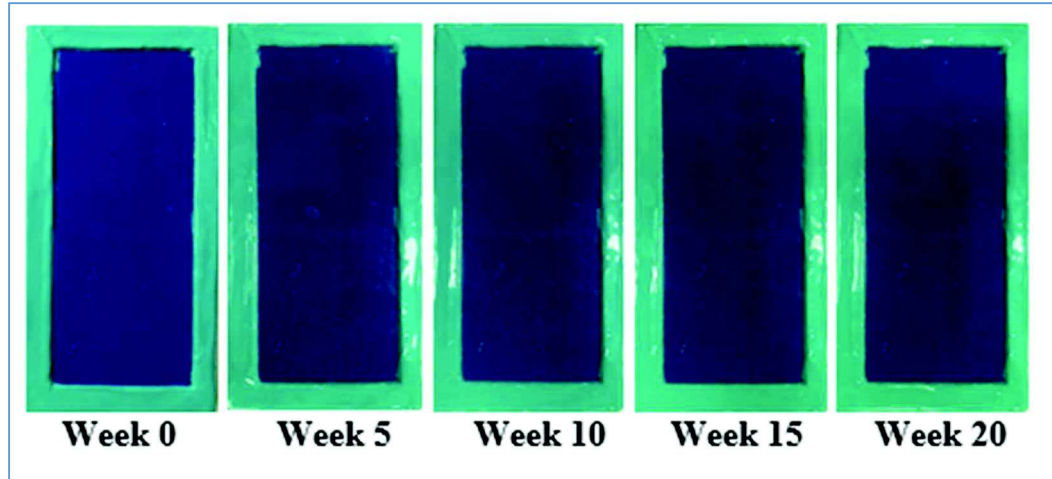


Figure 5.28: Lack of rust formation over coated steel coupon (coupon B05-a)

5.4 ACT for Spot Painting Evaluation

5.4.1 Number of Coupons and Identification

After 15 weeks of the ACT for steel washing evaluation, coupons from steel Type B (coated carbon steel) showed no trace of obvious damage in the coating. In fact, at week 15 of the ACT those coupons showed the same surface condition as observed before the test started, presenting even the same initial gloss. Based on this situation, it was decided to continue the ACT for steel washing evaluation with only two plates for each group from steel Type B. Consequently, only the samples *a* and *b* from each group of steel Type B continued the ACT for steel washing evaluation. The remaining samples *c* and *d* from each group of steel Type B were renamed to constitute a new steel type, called steel Type D, to be tested specifically for spot painting evaluation. The twenty coupons for the steel Type D were renamed to form seven groups, each group consisting of three or two coupons. Groups D01 to D05 contained three coupons, while Groups D06 and D07 contained two coupons. Each steel coupon belonging to steel Type D was identified with a lower case letter *a*, *b* or *c*. Following the color identification rule, data from steel Type D were assigned with the orange color. Appendix C presents the identification for all coupons conforming the seven groups for steel Type D, to be tested under the ACT for spot painting evaluation.

5.4.2 Scribing Coupon Procedure

To evaluate the effect of spot painting in reducing the corrosion on localized damaged areas, all coupons from steel Type D were scribed in their coated face with a 2 in. (5 cm.) length mark. The width of the scribe was 0.04 in. (1 mm.) and a depth great enough to reach the steel substrate. This procedure followed the requirements from the ASTM D1654-08, “Standard Test for Evaluation of Painted or Coated Specimens Subjected to Corrosive Environments” (ASTM, 2008), which provides a detailed procedure to scribe a coated piece of steel. Each scribe was centered at the coupon diagonal that follows the direction from the upper right corner to the bottom left corner. The scribes were made using a milling machine from the Bowen Laboratory at Purdue University. The scribes had the objective to simulate a defect that penetrates the coating and serves as a starting spot for corrosion. Figure 5.29 shows a coated steel coupon with a scribe mark on its surface and a detail of it magnified with an attached scale [mm].

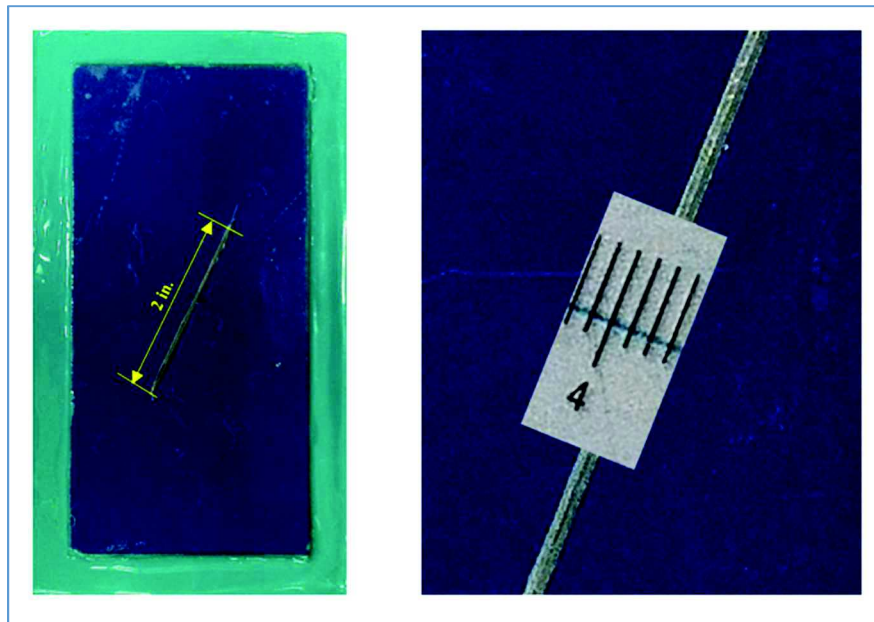


Figure 5.29: Left: Scribed steel coupon (D01-a). Right: Scribe mark magnified with scale (mm).

5.4.3 Initial Data Acquisition

All coupons from steel Type D (Groups D01 to D07) were weighed and photographed after scribing and the data were recorded to follow the progress of corrosion in the spot damage during the ACT. Initial weights from all coupons from steel Type D are presented in Appendix D. All coupons from steel Type D were photographed before the test started and the photographs were recorded in the research database. Appendix H presents the photographs for coupons D01-a and D02-b before exposure to the ACT.

5.4.4 Procedure for the ACT Regime for Spot Painting Evaluation

During six weeks the scribed coupons from steel Type D followed a similar ACT to that used for the steel washing evaluation, as explained in section 5.3.3. The coupons from Groups D01 to D04 were washed, dried, weighed, and photographed, with a frequency according to Table 5.1. The coupons from Groups D05 to D07 were never washed, but weighed and photographed, following the same schedule from Table 5.1. In this ACT regime the coupon thickness change was not a variable to be measured. Each week, after all data were acquired, the analyzed coupons were returned to the chamber, in a position different from which they occupied previously. For each coupon from steel Type D, the weights and photographs corresponding to each week of treatment of the ACT regime are presented in Appendices D and H respectively. Figure 5.30 shows a flow chart for the activities performed during the ACT regime for spot painting evaluation.

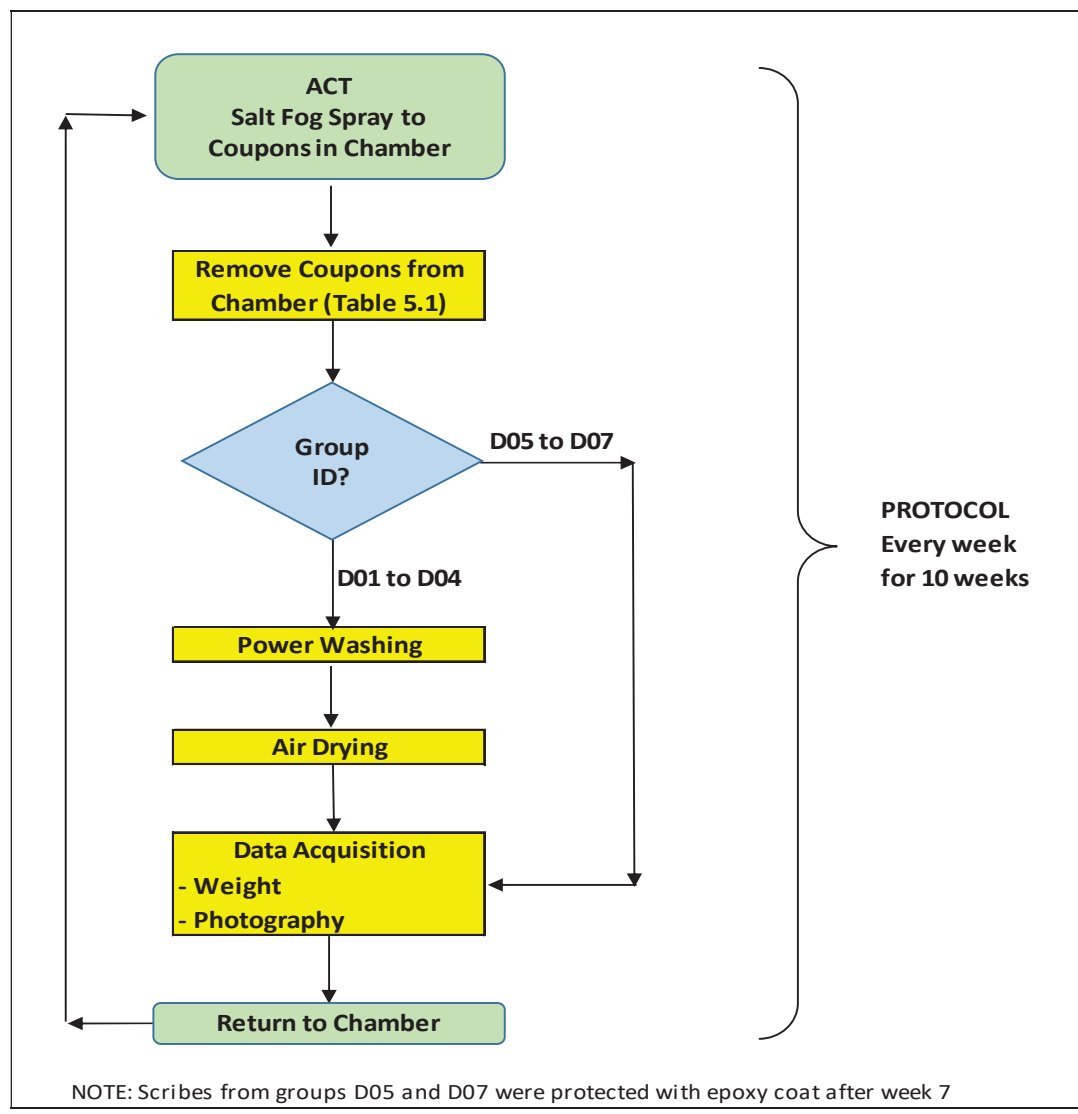


Figure 5.30: Flow chart for ACT program for spot painting evaluation

As could be observed from the sequence of photographs in Appendix H, the scribe in a coupon from steel Type D developed some grade of corrosion with time. As the ACT developed in time, the corrosion process produced more rust creepage from the scribe on the coupon. After six weeks of this ACT, the steel coupons from Groups D05 and D07 had developed enough rust creepage at scribes, and consequently were selected to study the effect of spot painting.

At the sixth week of the ACT to evaluate spot painting, coupons from Groups D05 and D07 were treated with a protective coat to cover their scribe mark. First, the rust creepage from scribe was cleaned using sandpaper and a small steel nail. Next, the rust remaining in the scribe was removed applying a Loctite - Rust Dissolver, a treatment formula that eliminates rust from metal surfaces. When the scribe mark was completely cleaned from rust, a protective paint was sprayed onto the surface to cover the scribe mark. Scribe from coupons of Group D05 were covered with one application of Rust Reformer from Rust-Oleum, while coupons from Group D07 received two applications of Rust Reformer. Figure 5.31 shows the different tools and products used to eliminate the rust from a scribe and to protect it against future corrosion. Figure 5.32 presents the process followed to apply Rust-Oleum® products to clean and protect the scribe.



Figure 5.31: Tools and products used to eliminate the rust and protect the scribe.

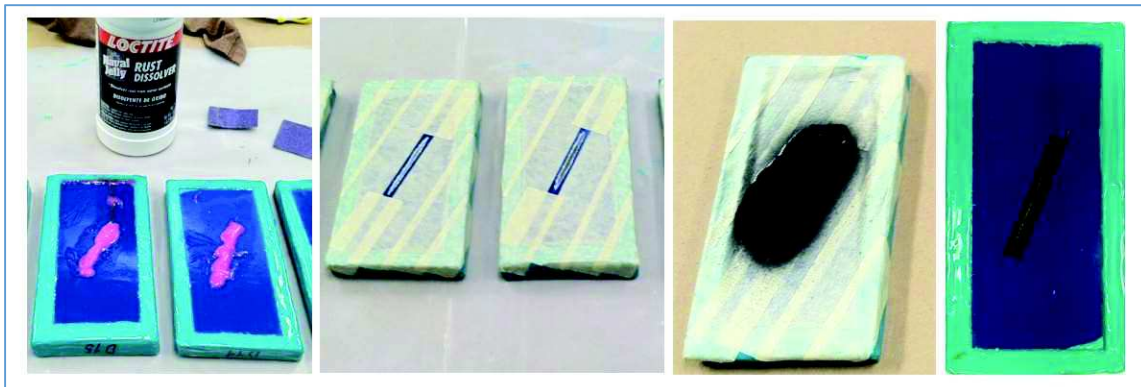


Figure 5.32: Process to clean and protect the scribe. From left to right: Clean the scribe with sandpaper and rust dissolver application; cover all coupon face but scribe mark; spray paint; coupon with covered scribe.

Steel coupons from Groups D01 to D04 and D06 remained with their scribes uncovered and were left to continue their ACT for four more weeks, until week 10. Coupons from Groups D01 to D04 continued being washed according to Table 5.1 while coupons from Group D06 were never washed. Coupons from Groups D05 and D07 with their scribes protected using the Rust-Oleum system were left exposed to the ACT for ten more weeks, until week 16.

5.4.5 Results from ACT for Spot Painting Evaluation

The results from the ACT for spot painting evaluation are presented in this section. A summary of the relevant results is presented, interpreted, and discussed. The complete information from the data obtained during the ACT is presented in tabulated and graphical form in the corresponding appendices.

After the first week the ACT started, most of the coupons developed some rust creepage from the scribe mark. Due to the effect of gravity, the creepage area extended downward. Each steel coupon had a particular creepage shape, but in general they were a thin stain at the top of the scribe, and gradually became wider towards the bottom part of the scribe. The creepage made a notorious stain over the coated surface, with origin in the scribe, and showing an orange-to-brown color that contrasted with the blue paint color.

5.4.5.1 Weight Change

Data corresponding to weight change of coupons under the ACT from Groups D01, D02, D03, D04 and D06 are presented in Appendix D. These scribed coupons were exposed to the ACT for ten weeks. The tables in Appendix D present the weight for each coupon, measured each week the coupon was washed, and classified by groups. Data were registered from week 0 to week 10, which was the last week of testing for Groups D01, D02, D03, D04 and D06. Weight change of coupons from Groups D05 and D07 were not registered since those coupons were selected to be covered by the protective coat in order to analyze the effect of spot painting.

The weight changes from Groups D01, D02, D03, D04 and D06 are also presented in a graphical manner in Appendix D. For each group of steel coupons, a graph is presented. Each graph represents the variation in time of the mean value of the weight change corresponding to the coupons that conformed each group. The data were fitted using the least-squares function from MS Excel to determine a representative curve for each group. The weight change from these coupons was best represented by a second order polynomial function.

A summary of the weight change versus time from steel Type D coupons is shown in Figure 5.33 for the mean values of the coupons for each group (Groups D01 to D04 and D06). The review of Figure 5.33 shows a clear tendency for weight increase with time. However, there is not a clear pattern between wash frequency and weight increment, since some curves crossed each other during the test duration. All groups present a similar curve of weight increment in time with the exception of Group D03, which showed a higher rate of weight increment the entire test. In order to appreciate the combined effect of the different wash frequencies, the weight change from Groups D01 to D04 were averaged and grouped.

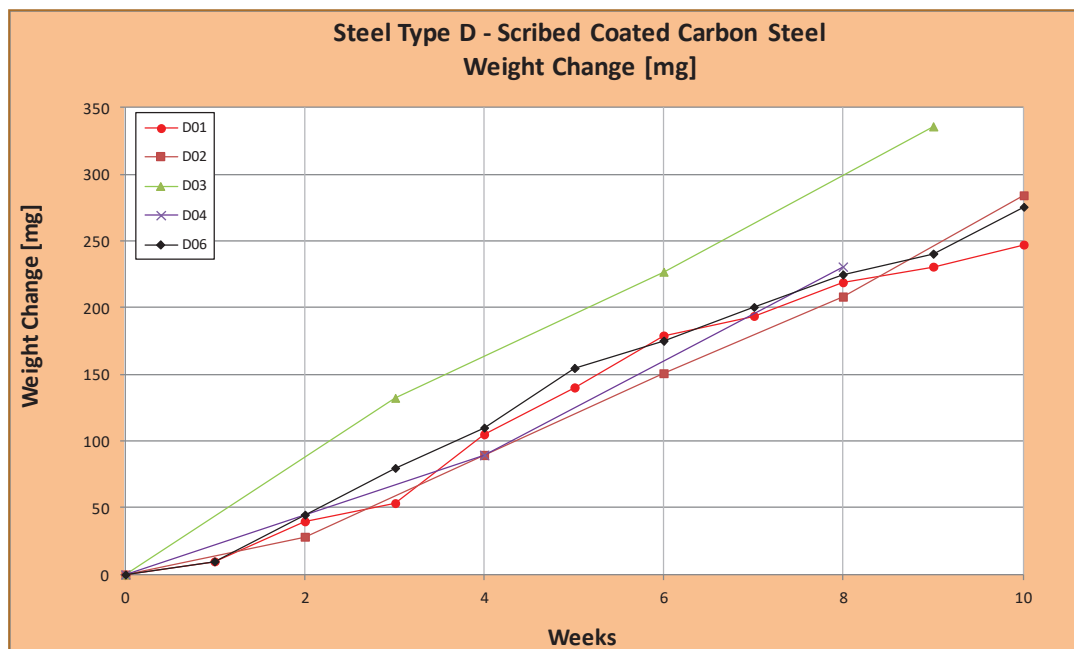


Figure 5.33: Weight change versus time for steel Type D groups

The data for the mean of weight change values from combined Groups D01-D04 and data from Group D06 (never washed coupons) are shown in Figure 5.34. It can be observed that the average of weight change values for combined Groups D01-D04 is similar to values from Group D06 during the entire test. From this observation could be concluded that wash frequency is not a factor that affects the weight change on the scribed coupons.

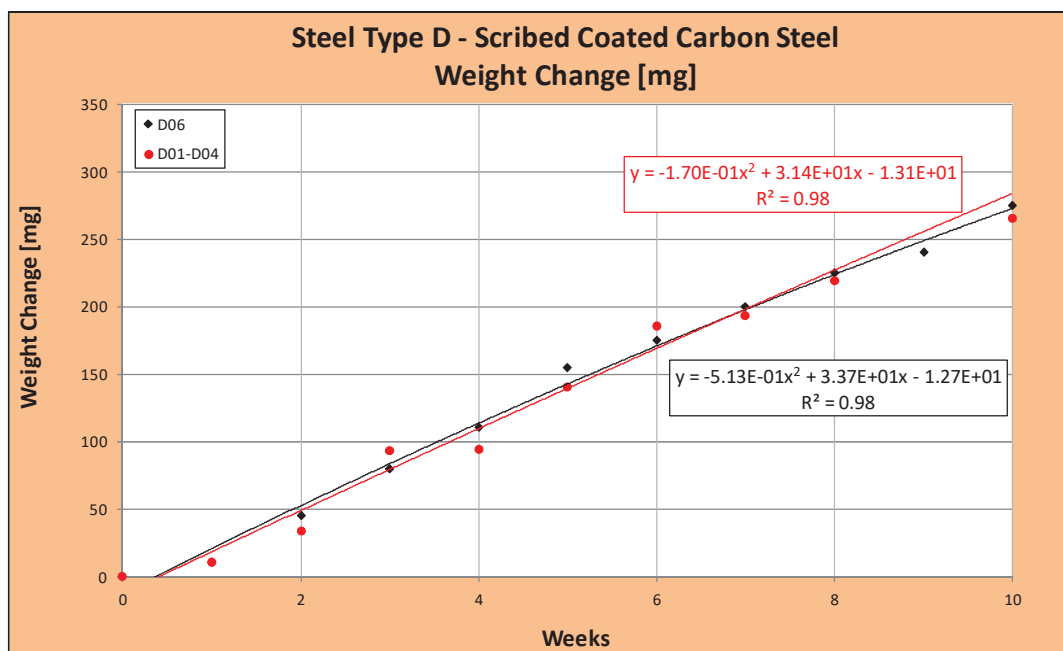


Figure 5.34: Weight change versus time for mean values from Groups D01-D04 and Group D06

5.4.5.2 Rust Creepage Change

Coupons from Groups D01 to D07 were scribed mechanically with a milling machine to obtain a uniform scratch in the coat layer to reach the steel substrate. The scribing method followed the requirements given in ASTM D1654-08 (ASTM, 2008). This is a common practice to obtain a break in the coating to accelerate the corrosion process on painted steel. The scribe mark is an artificial defect that is made to simulate the damage that a structural coated member could experience, during handling, transportation, or erection.

During the ACT progress, corrosion products emanated from the scribe. The extent of rust creepage was registered by regular photographs of the steel coupon. The creepage area extension gave a rate of the corrosion level. In this research the rust creepage was measured following the method described in ASTM D7087-05a “Standard Test Method for an Imaging Technique to Measure Rust Creepage at Scribe on Coated Test Panels Subjected to Corrosive Environments” (ASTM, 2010). According to this standard, the scribed coupon is scanned or photographed and the image is analyzed using an imaging

software to obtain the creepage area. The creepage area is defined as the area limited by the perimeter of the creepage and two perpendicular lines to the original scribe line. The distance between these two lines represents the center 80% of the scribe line. Figure 5.35 presents the sketch of a creepage from the ASTM Standard D7087-05a, indicating the method to obtain the creepage area. In Figure 5.35 the creepage area is defined by the closed region marked by the points i-j-l-k.

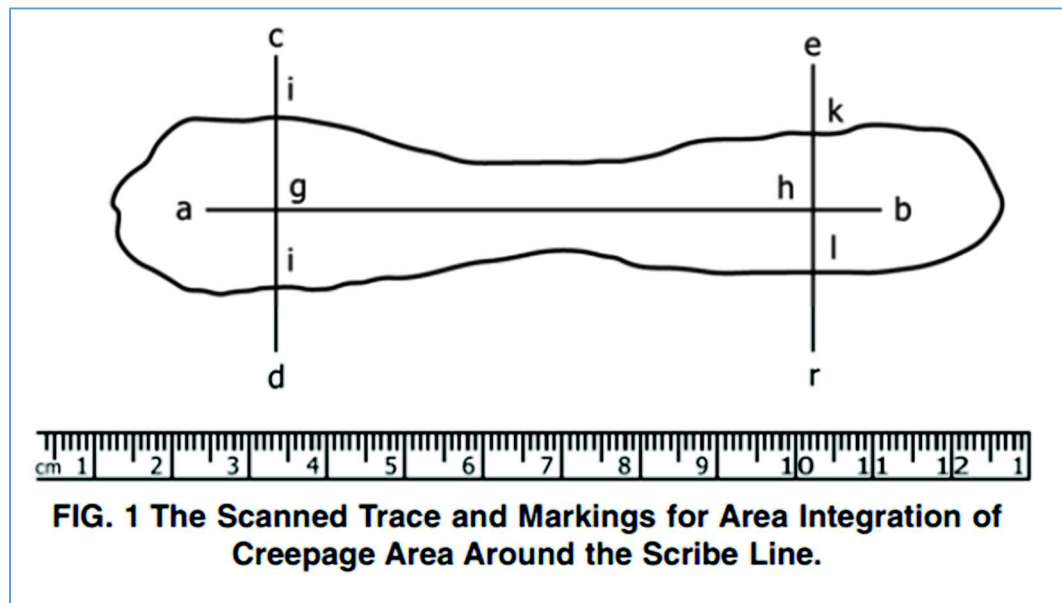


Figure 5.35: Creepage area measurement (ASTM Standard D7087-05a)

The ASTM D7087-05a Standard defines two parameters to characterize the corrosion level, called Mean Creepage and Net Mean Creepage. The Net Mean Creepage parameter was selected herein to evaluate the corrosion level reached by a scribed coupon. The Net Mean Creepage is defined by Equation 5.9

$$C_{net} = (A_{ijkl} - A_0)/(2L) \quad \text{Equation 5.9}$$

where:

C_{net} = net mean creepage [mm]
 A_{ijkl} = integrated area inside the boundary of i-j-k-l by tracing and imaging

A_0 = integrated area of scribe line before exposure
 L = length of scribe line from which creepage (or undercutting) is extended and area is integrated.

After the coupons from steel Type D were scribed, they were placed inside the weather chamber to start the ACT for spot painting evaluation. All coupons were photographed each week the coupons were washed according to the schedule from Table 5.1. A visual record of coupons D01-a and D02-b, ordered by weeks and showing the development of rust creepage is shown in Appendix H. All coupons were photographed each week they were analyzed and the information was recorded in the research database. Those photographs were uploaded to AutoCAD 2016 (Autodesk, 2016), a graphical software that allows the user to edit an image, trace a boundary, and evaluate an area inside a boundary. Hence, using AutoCAD 2016 (Autodesk, 2016), for each photograph of scribed coupon, the rust creepage boundary was traced using a closed polyline -a connected sequence of segments- following the prescription from the ASTM D7087-05a Standard. Figure 5.36 shows a scribed coupon with the trace of the creepage area using AutoCAD 2016 (Autodesk, 2016); in the same figure two magnifications from the traced area are also shown. Coupons from Groups D05 and D07 were photographed until week 4, since at week 6 those coupons were selected to coat their scribes.

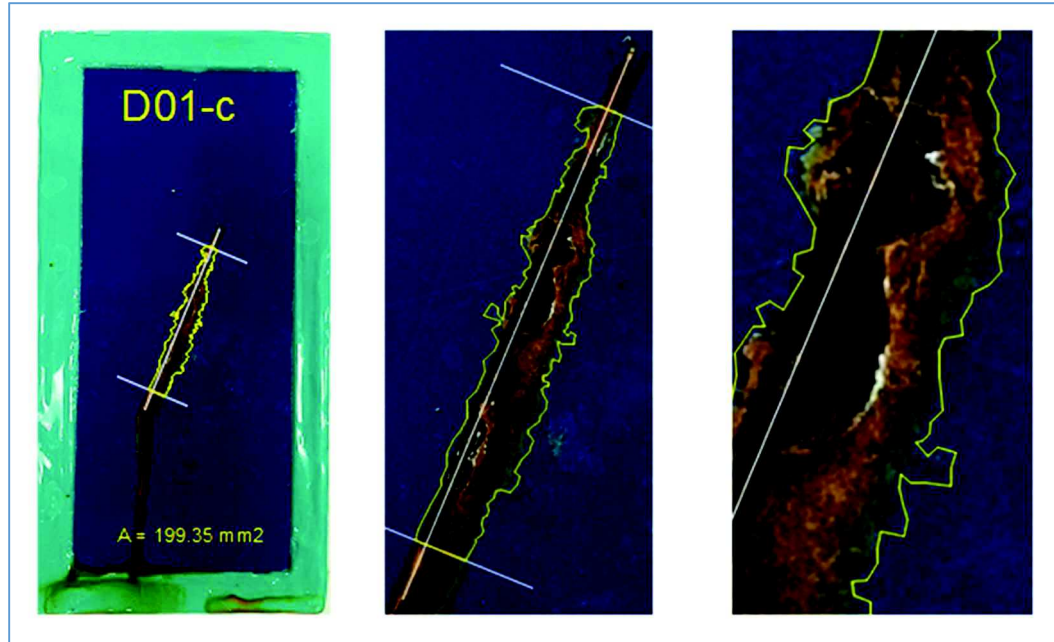


Figure 5.36: Trace of rust creepage area. Complete scribed coupon image and two magnifications after six weeks of ACT.

In Appendix H are presented, in tabulated form, the data corresponding to the change of creepage areas from all steel Type D coupons. The tables present the rust creepage area for each coupon, week by week, and organized by groups, from D01 to D07 respectively. Data for week 0 referred to the initial scribe area, before the ACT started. Data were registered from week 0 to week 10, which was the last week of testing. From the creepage area evaluated using AutoCAD 2016 (Autodesk, 2016), and applying Equation 5.9, the variation of Net Mean Creepage (NMC) in time were calculated for each coupon. The change of NMC in time were plotted in graphs presented in Appendix H. Each graph represents the variation in time of the mean value of the NMC corresponding to the coupons that formed each group. The data from those graphs were fitted using the least-squares function from MS Excel to determine a representative curve for each group. The data were best represented by a second order polynomial function.

A summary of data corresponding to NMC versus time for steel Type D coupons is shown in Figure 5.37. The graph presents the NMC variation for the mean values of the coupons for each group, D01 to D04 and D06.

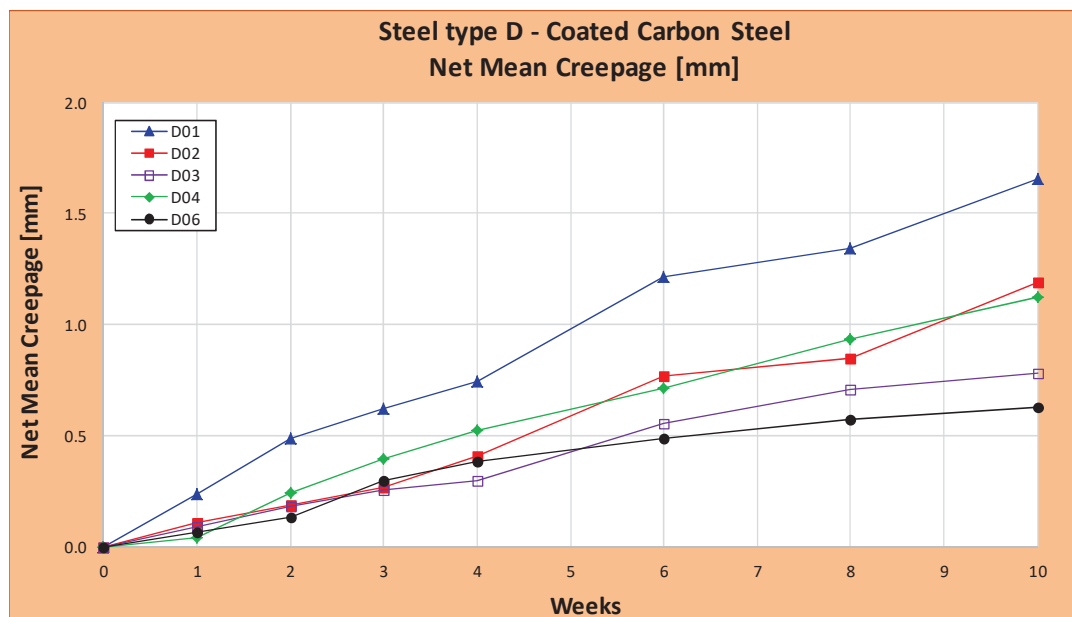


Figure 5.37: Net Mean Creepage versus time for steel Type D groups

From Figure 5.37 can be observed that the curve corresponding to the one-week washing frequency (Group D01) produces a higher NMC increment than the other groups (Groups D02 to D04 and D06). Moreover, the no washing alternative (Group D06) shows the lowest NMC increment for almost the entire test. This pattern was contrary to the hypothesis of investigation.

Considering as before, that Group D01 had the influence of many wet-dry cycles, data from this group were discharged. Then, data from Groups D02 to D04 were combined, averaged, and plotted along with data from the no washing alternative (Group D06), as shown in Figure 5.38. Analyzing Figure 5.38 it could be concluded that washing a scribed steel coupon enhances the NMC value. This can be understood as the corrosion products on a scribe, in some way, helps to protect the scribe from more corrosion, while washing the scribe enhances the development of more NMC. Therefore, washing a scribe is not an adequate alternative.

Data from the two plots, Groups D02-D04 and D06 were fitted using the least-squares function from MS Excel to determine a representative curve for each group. Those fitting

curves resulted in power functions as presented in Figure 5.38. In both cases the type of function was selected based on a relatively high correlation parameter R^2 .

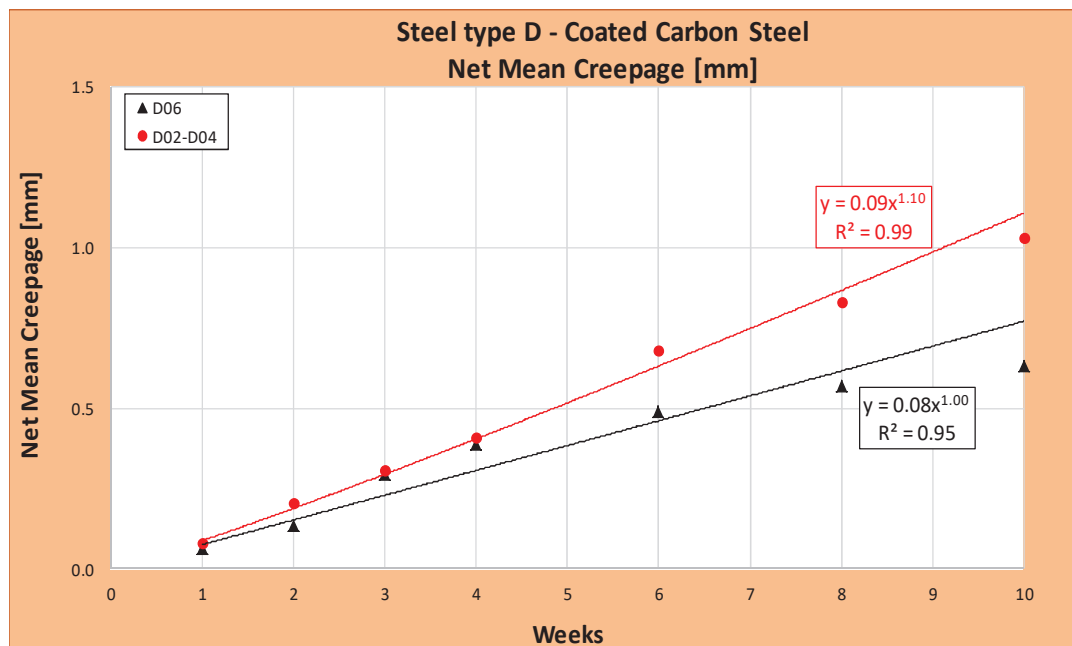


Figure 5.38: Net Mean Creepage versus time for mean values from Groups D02-D04 and Group D06

The next step in the study was to analyze the effect of spot painting in reducing the corrosion level in the scribed coupons. To study the effect of spot painting, coupons from Groups D05 and D07 were covered with a coat of Rust-Oleum paint, following the procedure described in section 5.4.4. Coupons from Group D05 received one coat of paint and coupons from Group D07 received two coats of paint. The coats of paint were applied to the scribes according to the manufacturer specifications. After the spot paint application, coupons from Groups D05 and D07 were returned to the weather chamber and continued the ACT for ten more weeks. At the end of the test, coupons from Groups D05 and D07 showed no damage, degradation, or loss of paint protection. The scribes showed no signs of rust products. Figure 5.39 shows the five coupons protected with the Rust-Oleum paint after the ten weeks these coupons were exposed to the ACT and no signs of corrosion were detected in the protected scribe marks.

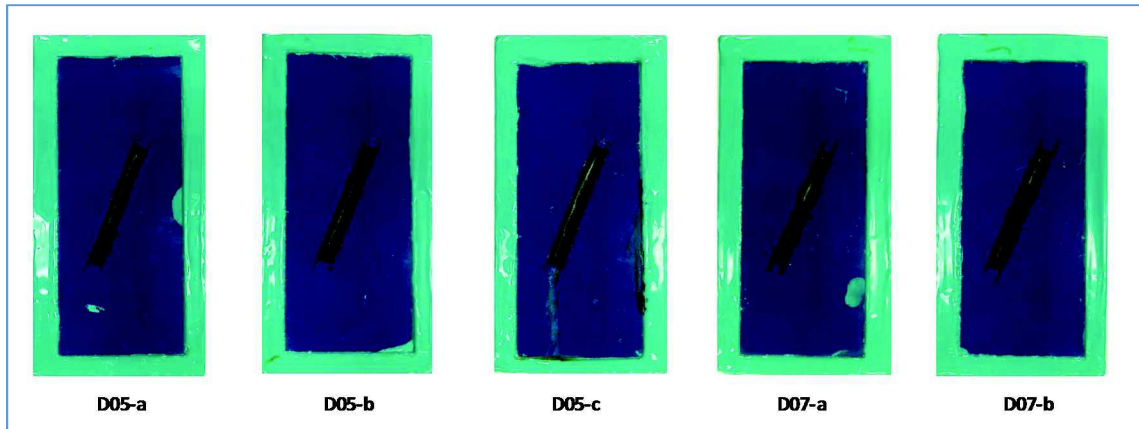


Figure 5.39: Coupons from Groups D05 and D07 after the ACT ended

From the physical inspection of coupons conforming Groups D05 and D07, it could be concluded that spot painting the scribe marks is an adequate alternative to stop the corrosion process of damaged plates. The weight change experienced by the coupons from Groups D05 and D07 was minimum, and in the same rate they have before scribing. Physical comparison between coupons from Groups D05 and D07 resulted in no differences. Both groups showed the same level of protection for the ACT period conducted. Therefore, one coat of spot paint protection was observed to produce similar results as for the two coats alternative in this test. Although, the two coat protection may be superior if a long duration is needed before the structure will be re-coated.

5.5 Discussion of Results

5.5.1 Accelerated Corrosion Test (ACT)

As indicated from several references (Albrecht and Naeemi, 1984; Kayser, 1988; Park 1999) an ACT is a useful tool to analyze the corrosion of metal elements in a shorter period of time and in a simplified manner. Replicating the complex electrochemical process through atmospheric corrosion developed inside a test chamber is extremely difficult. Based on that, the use of data collected from ACT should be used cautiously, keeping in mind the limitations assumed during the test. Nevertheless, an ACT is

accepted as the best method to perform corrosion analysis under limitations of time and resources.

In this research the results from the ACT showed a good tendency when analyzed. Some important assumptions had to be compromised to make adequate use of such a data.

The ACT rapidly produced corrosion effects over the uncoated steel Types (Groups A and C). The ACT did not produce any appreciable damage to coated steel Type B. From those results, it can be concluded that the ACT implemented in this study is adequate to study uncoated pieces of metal but is not suitable for coated elements. Testing coated elements could require variations in the ACT, such as the application of UV light to facilitate the deterioration of the coating.

According to specialized literature, weathering steel has a higher resistant to atmospheric corrosion than carbon steel. During the ACT the coupons from uncoated weathering steel showed a higher weight increment than uncoated carbon steel. This situation could be explained based on the fact that during the ACT, the uncoated weathering steel pieces did not develop the patina protecting layer.

5.5.2 Steel Washing Evaluation

The analysis of ACT results indicated that steel washing is an effective alternative to reduce the rates of corrosion in steel members. From the data collected, corrosion rates from the combined washed Groups A02-A05 and C02-C05 demonstrated lower corrosion rates than results from Groups A10 and C10 corresponding to the no washing alternatives.

From the results obtained during the ACT on scribed coupons, it can be concluded that washing spot damage on coated steel members is not an adequate alternative. It was

found that the rate of rust creepage area increased when a damaged coated coupon was subjected to frequent washing.

5.5.3 Spot Painting Evaluation

Painting a small scribe on coated steel members with a simple commercial metal spray paint product resulted in significant corrosion protection. From the results in this test, the progression of rust creepage emanating from the scribe was completely eliminated after the paint cover was applied. The protected scribed coupons did not show any sign of new corrosion for the remaining time the ACT lasted.

The spot painting test showed that a one-coat application of paint gave similar results than the two-coat application. However, the use of a two-coat paint protection for spot damage is recommended to provide adequate long-term protection against corrosion.

CHAPTER 6. CORRELATION BETWEEN AN ACCELERATED CORROSION TEST AND ATMOSPHERIC CORROSION

6.1 Introduction

An accelerated corrosion test (ACT) is a controlled test that seeks to reproduce the atmospheric corrosion process at the laboratory, in a shorter period of time than at real environment. Atmospheric corrosion is the result of the combination of several atmospheric factors that corrode an exposed piece of metal. An ACT seeks to reproduce the atmospheric corrosion process as accurately as possible, but based on the control of just a few factors in the laboratory. Based on those limitations, the results obtained from an ACT should be considered and used with appropriate judgement and discretion. Nevertheless, an ACT is an appropriate tool to approach the study of real corrosion when limited by the time and the resources to reproduce actual corrosion process.

In this research, an ACT was developed to reproduce the effect of atmospheric corrosion on steel coupons under a washing program. The objective of the research was to study the benefit of steel washing in reducing the corrosion rate of steel highway bridge girders. Several sets of steel coupons were subjected to different washing frequencies in order to characterize and model the effect of washing and the frequency of washing in the reduction of corrosion rates. The ACT process performed in the laboratory and the results obtained were presented in detail in Chapter 5. In summary, the primary results from the ACT were the weight change and thickness change of each individual coupon during the test performance. The weight change was found to be the most accurate parameter to describe the level of corrosion penetration in a coupon. The weight change resulted in an increment of weight for the uncoated coupons (steel Types A and C) due to the formation

of rust material on the exposed surface. The effect of weight change for coupons from steel Type B was negligible, and therefore, is not considered in this analysis.

Every week the programmed coupons from steel Types A and C under the ACT were washed, weighed, and then returned to the chamber. Under this protocol, it was impossible to measure the corresponding loss of thickness after washing the coupon, since that action could be done only by cleaning and eliminating all the rust from the coupon. A cleaned coupon, with all the rust material eliminated, would not be useful to continue on the ACT, as they were actually used. Therefore, a different set of steel coupons were required for the ACT to provide a relationship between the weight increment in steel coupons during the ACT with the corresponding level of corrosion penetration. Also, this new set of coupons subjected to the ACT should offer enough information in order to properly apply the results from the ACT to the study of real problems. Those expected relationships are enounced in the following:

- a) A relationship was required to obtain the actual level of corrosion corresponding to each amount of weight increment of a coupon inside the chamber. This relationship should correlate each value of weight increment to the corresponding level of corrosion during the ACT, and consequently, the corresponding amount of corrosion penetration in the steel coupon.
- b) A relationship between a unit time in the chamber during the ACT and the corresponding time for a real environment. This will be useful in order to correlate the results obtained from the ACT to real problems.
- c) A relationship to extrapolate the results from the ACT during a short period of time to real problems of larger periods of time, such as the bridge service life.

To achieve all these required relationships, it was necessary to perform an ACT to a new group of steel coupons. The new ACT was named “Control Test”, and the details of the tested coupons, the test protocol, and the results obtained are presented in the next sections.

6.2 Control Test

The Control Test was an ACT performed using a new series of steel coupons, from steel Types A and C, in order to develop the necessary relationships between the results from an ACT and the corrosion occurring in a real environment.

6.2.1 Number of Coupons and Identification

The Control Test was designed to expose a set of steel coupons to an ACT and to measure the increment of weight and the thickness loss experienced by the coupons under the test. Steel coupons in the Control Test were exposed to an ACT, and at a certain frequency, a group of coupons were withdrawn from the chamber to be analyzed.

Five groups of coupons were assembled for each type of steel to be tested (steel Types A and C). The groups of coupons from steel Type A were identified from X01 to X05, while groups from steel Type C were identified from W01 to W05. To seek better confidence in the mean results, three coupons were used for each group. The identification for all control group coupons considered in this test are described in Appendix I. All coupons tested during the Control Test were protected with an epoxy coat to expose only one surface for corrosion development, similar to the coupons tested in the ACT for steel washing evaluation.

6.2.2 Schedule for Control Test

The Control Test was designed to analyze each group at a bi-weekly frequency. Thus, each two weeks a group of coupons from each steel type was withdrawn from the chamber for analysis. At week 2, the groups designated with number 01 (X01 and W01) were analyzed as explained in the next sections. At week 4 the groups numbered 02 (X02 and W02) were analyzed, and in the same way, until groups numbered 05 (X05 and W05) were analyzed at week number 10.

6.2.3 Initial Data Acquisition

The initial physical characteristics from each coupon were taken and registered before the beginning of the Control Test. The weight and a photography from each steel coupon were registered. All coupons were weighed using the electronic balance; the measurement was repeated three times for a better precision. Each steel coupon was photographed using the digital camera from a smartphone. The initial weight of each coupon, identified as the weight at week 0, is shown in Appendix I. The photographs from all coupons before the Control Test started were registered as part of the research database. In Appendix I a few selected photographs from coupons before the Control Test started are shown.

6.2.4 Procedure for the Control Test

The five groups of steel coupons from steel Types A and C respectively were supported on racks and placed inside the weather chamber for an ACT. This test followed almost the same process that followed the ACT for steel washing evaluation. The coupons were exposed to a cyclic spray process, every day during ten weeks, using the same type of sodium chloride solution (NaCl) at 5% by weight. In this test the bi-weekly selected coupons were not power washed but were cleaned by sandblasting to eliminate all of the excess material from the corroded surfaces. The protocol followed in this Control Test is detailed in the next sections.

6.2.4.1 Data before Sandblasting

After removal from the chamber the selected coupons were air-dried and weighed. The weight from each coupon was registered in a master spreadsheet for subsequent calculations. The registered weights are presented in Appendix I. Then, a photograph from each selected coupon was captured, to record its corroded condition. All photographs were registered in the research database. The photographs from selected groups of coupons are shown in Appendix I.

6.2.4.2 Sandblasting

To eliminate all corrosion material from a corroded coupon a mechanical process was employed. Following the ASTM G1-03 “Standard Practice for Preparing, Cleaning, and Evaluating Corrosion Test Specimens” (ASTM, 2011), a sandblasting method was used. An abrasive blast cabinet from the Bowen Laboratory at Purdue was used to remove the corrosion products from the coupon. During the sandblasting process, proper care was exercised to eliminate only the corrosion products, and avoided the removal of any base metal.

6.2.4.3 Data after Sandblasting

The tested coupons after sandblasting were weighed and photographed. The final weights were recorded in the master spreadsheet. The weights after sandblasting corresponding to all the coupons are presented in tables in Appendix I, classified by steel types and by groups. The photographs after sandblasting were also recorded in the research database. As before, selected photographs corresponding to some groups of coupons after sandblasting are provided in Appendix I.

6.2.5 Results from Control Test

The mean values of the weight change, measured bi-weekly, of the tree coupons that conformed each group of steel Type A (uncoated carbon steel) are shown in Table 6.1. As indicated previously, at week 2 the coupons from Group X01 were tested, at week 4 the Group X02 was tested, until week 10 when the coupons from Group X05 were tested.

The weight increment due to corrosion during control test was registered before the sandblasting work, and the weight loss due to cleaning the corroded surface was registered after the sandblasting was performed. The weight increment and weight loss are presented in absolute values and as value per unit of exposed area. The normalized weight increment and loss values were calculated considering an exposed surface of 2.5 in. (63.5 mm) by 5.5 in. (139.7 mm) as shown in Figure 6.1.

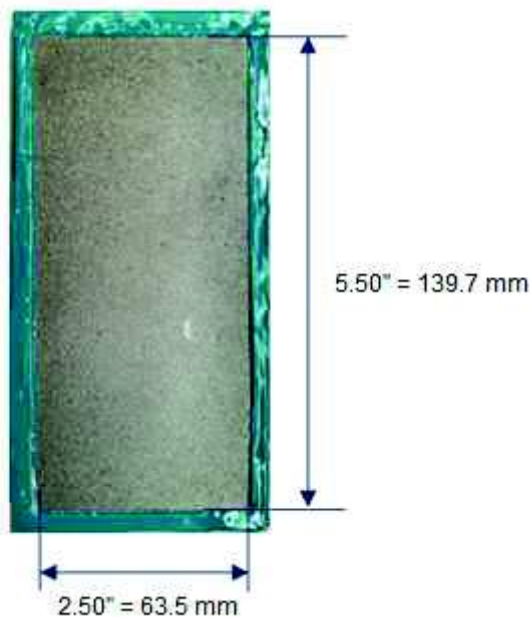


Figure 6.1: Dimensions for exposed area of a Control Test coupon

The thickness loss or corrosion penetration C is presented in Table 6.1. This corrosion penetration parameter is obtained from the weight loss experienced by the coupons and assuming a uniform corrosion over the corroded surface. From the coupon initial weight (Appendix D) and initial dimensions (Appendix E), both before epoxy coating, an average specific weight of 7.85 mg/mm^3 was obtained for carbon steel and weathering steel. Hence, the approximate corrosion penetration value C was obtained applying Equation 6.1.

$$C = W/A\gamma \quad \text{Equation 6.1}$$

where:

- C = corrosion penetration [mm]
- W = weight loss [mg]
- A = exposed area = 8871 mm^2
- γ = specific weight = 7.85 mg/mm^3

Table 6.1: Results of Control Test for coupons from steel Type A.

From Control Test					
(1)	(2)	(3)	(4)	(5)	(6)
Week	Weight Increment [g]	Weight Loss [g]	Weight Increment [mg/mm ²]	Weight Loss [mg/mm ²]	Corrosion Penet. [mm]
0	0.00	0.00	0.00	0.00	0.00
2	1.46	4.77	0.16	0.54	0.07
4	3.90	7.73	0.44	0.87	0.11
6	8.57	12.53	0.97	1.41	0.18
8	10.85	17.25	1.22	1.94	0.25
10	17.23	21.27	1.94	2.40	0.31

(1) = # of weeks from Control Test

(2) = Weight Increment due to corrosion during Control Test

(3) = Weight Loss due to sandblasting

(4) = (2)*1000/Area

(5) = (3)*1000/Area

(6) = (5)/ γ

The values obtained for weight increment [mg/mm²] for steel Type A were plotted versus the values calculated for corrosion penetration C [mm] – see Figure 6.2. Figure 6.2 shows the data points from those two parameters and a power function, fitting the parameters, was plotted using the least-squares function from MS Excel. The potential function was chosen due to the relatively high correlation given by the R^2 factor.

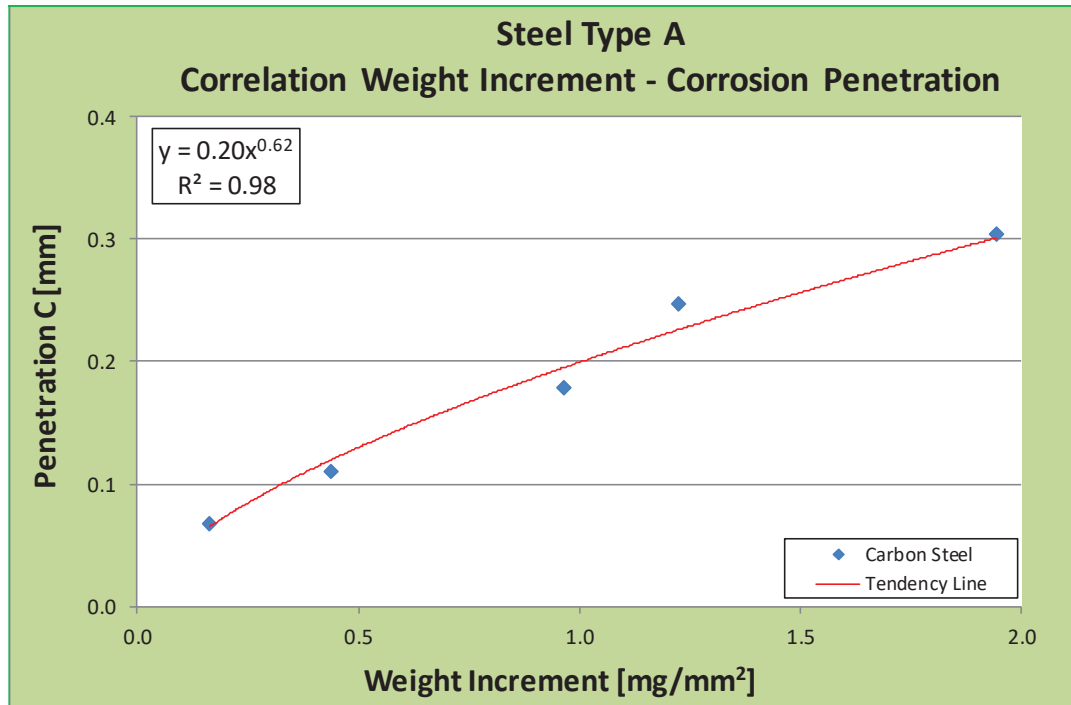


Figure 6.2: Correlation weight increment-corrosion penetration for steel Type A

The expression correlating the weight increment with the corrosion penetration for steel Type A is presented in Equation 6.2.

$$C_A = 0.20 W_A^{0.62} \quad \text{Equation 6.2}$$

where:

- C_A = corrosion penetration for steel Type A [mm]
- W_A = weight increment for steel Type A [mg/mm²]
- A = exposed area = 8871 mm²
- γ = specific weight = 7.85 mg/mm³

The results from the Control Test corresponding to the coupons from steel Type C are presented in Table 6.2. Data from Table 6.2 were obtained following the same procedure applied for Table 6.1.

Table 6.2: Results of Control Test for coupons from steel Type C

From Control Test					
(1)	(2)	(3)	(4)	(5)	(6)
Week	Weight Increment [g]	Weight Loss [g]	Weight Increment [mg/mm ²]	Weight Loss [mg/mm ²]	Corrosion Penet. [mm]
0	0.00	0.00	0.00	0.00	0.00
2	1.31	4.89	0.15	0.55	0.07
4	4.04	8.62	0.46	0.97	0.12
6	6.82	11.25	0.77	1.27	0.16
8	9.89	15.38	1.11	1.73	0.22
10	13.25	18.22	1.49	2.05	0.26

(1) = # of weeks from Control Test

(2) = Weight Increment due to corrosion during Control Test

(3) = Weight Loss due to sandblasting

(4) = (2)*1000/Area

(5) = (3)*1000/Area

(6) = (5)/ γ

The data corresponding to the values obtained for weight increment versus the values calculated for corrosion penetration from the steel Type C coupons are plotted in Figure 6.3.

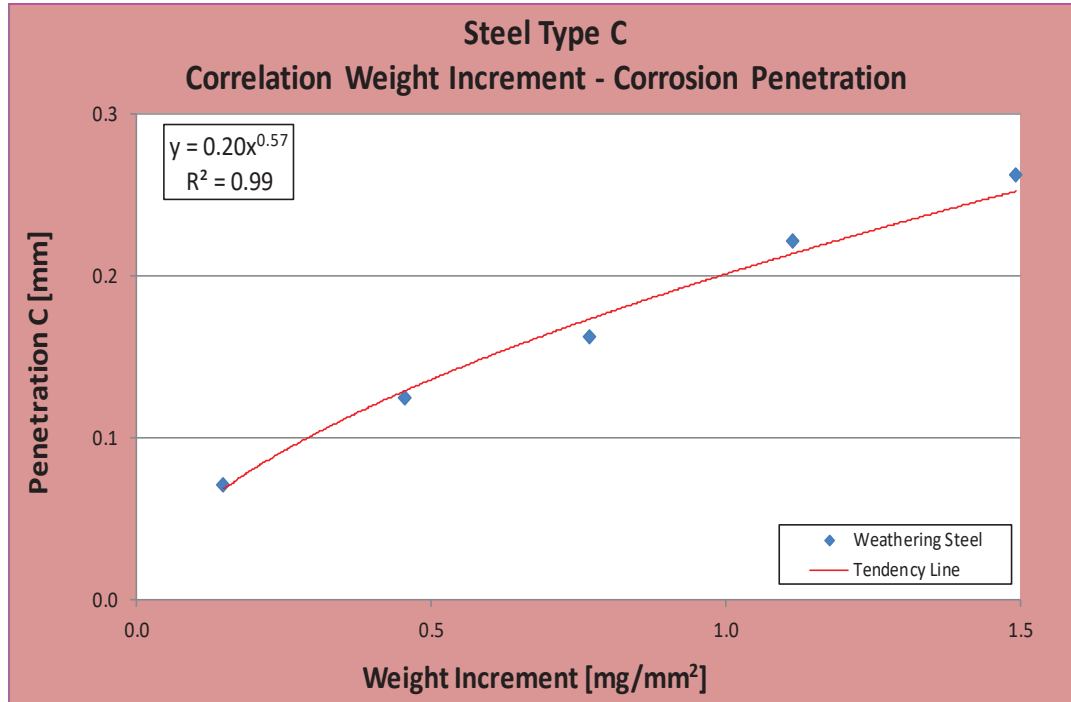


Figure 6.3: Correlating weight increment-corrosion penetration for steel Type C

The expression correlating the weight increment with the corrosion penetration C for steel Type C is presented in Equation 6.3.

$$C_C = 0.20 W_C^{0.57} \quad \text{Equation 6.3}$$

where:

- C_C = corrosion penetration for steel Type C [mm]
- W_C = weight increment for steel Type C [mg/mm²]
- A = exposed area = 8871 mm²
- γ = specific weight = 7.85 mg/mm³

Note that a comparison of Equations 6.2 and 6.3 shows that the primary difference is the exponent value for the weight increment variable.

6.3 Correlation between ACT and Atmospheric Corrosion

The results from the Control Test, together with the data obtained during the ACT for steel washing evaluation were used to evaluate the length of time to develop corrosion penetration. The linkage to corrosion for real environments was based on the studies from Albrecht and Naeemi (1984) and Kayser (1988). The correlation expressions are provided in the following sections.

6.3.1 Correlation between the Weight Increment and Corrosion Penetration during ACT

The first step was to obtain the corrosion penetration values during the ACT for steel coupons from washing evaluation for the twenty four weeks the test lasted. To obtain the corrosion penetration values, Equations 6.2 and 6.3 were used for steel Type A and C respectively, and the results are presented in Tables 6.3 and 6.4.

Table 6.3: Corrosion penetration values from ACT for steel Type A

Week	Measured from ACT			
	Weight Increment [mg/mm ²]		Corrosion Penetration [mm]	
	A02-A05	A10	A02-A05 (*)	A10 (*)
0	0.000	0.000	0.000	0.000
1	0.171	0.106	0.067	0.050
2	0.282	0.207	0.091	0.075
3	0.377	0.306	0.109	0.096
4	0.464	0.404	0.124	0.114
5	0.545	0.502	0.137	0.130
6	0.621	0.598	0.149	0.145
7	0.694	0.694	0.159	0.160
8	0.764	0.790	0.169	0.173
9	0.832	0.885	0.178	0.185
10	0.897	0.980	0.187	0.198
11	0.961	1.075	0.195	0.209
12	1.023	1.169	0.203	0.220
13	1.084	1.263	0.210	0.231
14	1.143	1.357	0.217	0.242
15	1.202	1.450	0.224	0.252
16	1.259	1.543	0.231	0.262
17	1.315	1.637	0.237	0.271
18	1.370	1.729	0.243	0.281
19	1.425	1.822	0.249	0.290
20	1.478	1.915	0.255	0.299
21	1.531	2.007	0.260	0.308
22	1.583	2.099	0.266	0.317
23	1.635	2.191	0.271	0.325
24	1.686	2.283	0.276	0.334

(*) Using Equation 6.2

Table 6.4: Corrosion penetration values from ACT for steel Type C

Week	Measured from ACT		Corrosion Penetration [mm]	
	Weight Increment [mg/mm ²]		Corrosion Penetration [mm]	
	C02-C05	C10	C02-C05 (*)	C10 (*)
0	0.000	0.000	0.000	0.000
1	0.200	0.150	0.080	0.068
2	0.356	0.296	0.111	0.100
3	0.498	0.440	0.134	0.125
4	0.632	0.584	0.154	0.147
5	0.761	0.726	0.171	0.167
6	0.885	0.868	0.187	0.185
7	1.006	1.010	0.201	0.201
8	1.124	1.151	0.214	0.217
9	1.239	1.292	0.226	0.231
10	1.352	1.432	0.238	0.245
11	1.463	1.573	0.248	0.259
12	1.573	1.713	0.259	0.272
13	1.681	1.852	0.269	0.284
14	1.788	1.992	0.279	0.296
15	1.893	2.131	0.288	0.308
16	1.997	2.271	0.297	0.319
17	2.100	2.410	0.305	0.330
18	2.202	2.548	0.314	0.341
19	2.304	2.687	0.322	0.351
20	2.404	2.826	0.330	0.362
21	2.503	2.964	0.337	0.372
22	2.602	3.102	0.345	0.381
23	2.699	3.240	0.352	0.391
24	2.796	3.378	0.359	0.400

(*) Using Equation 6.3

6.3.2 Correlation between Time inside the Chamber and Time at Real Environments

The following step was to find a correlation between a unit of time inside the chamber during the ACT and an equivalent time in real environments. To obtain this correlation, the corrosion penetration produced on coupons inside the chamber during the Control Test was equated with the corrosion penetration produced on coupons of the same steel type at real environments (Industrial/Urban, Marine, and Rural). The corrosion penetration at real environments were evaluated using a power function with the

statistical parameters derived by Kayser (1988), which were presented in Table 3.1 and plotted in Figure 3.7. Table 6.5 presents the corrosion penetration C [mm] obtained for steel type A during the ten weeks for the Control Test and the corresponding time (in years) to develop the same corrosion penetration for the three environments considered by Kayser (1988). The number of years corresponding to each environment were calculated by solving for t from equation 3.5, which is presented in equation 6.4. Since parameters A and B were statistical values with standard deviations, Equation 6.4 resulted in the most likely value of the time of exposure to real environments.

$$t_A = \sqrt[B]{\frac{C}{A}} \quad \text{Equation 6.4}$$

where:

- t_A = most likely value of the time of exposure to real environment for steel Type A to produce penetration C [years]
- A, B = statistics parameters evaluated by Kayser (1988)
for Industrial/urban environment: $A = 80.2, B = 0.59$
for Marine environment: $A = 70.6, B = 0.79$
for Rural environment: $A = 34.0, B = 0.65$
- C = corrosion penetration [mm]

Table 6.5: Correlating weeks in Control Test - years at real environments – (Type A)

Corrosion Penetration C [mm]	Steel Type A - Carbon Steel			
	Time at Control Test Weeks	Time at Real Environments		
		Industrial/Urban Years	Marine Years	Rural Years
0.00	0	0.0	0.0	0.0
0.07	2	0.8	1.0	2.9
0.11	4	1.7	1.8	6.2
0.18	6	3.9	3.3	13.0
0.25	8	6.7	4.9	21.2
0.31	10	9.6	6.4	29.3

Table 6.6 presents the time correlation between the Control Test and real environments for steel Type C, using equation 6.5 with the appropriate parameters.

$$t_C = \sqrt[B]{\frac{C}{A}} \quad \text{Equation 6.5}$$

where:

- t_C = most likely value of the time of exposure to real environment for steel Type C to produce penetration C [years]
- A, B = statistics parameters evaluated by Kayser (1988)
 for Industrial/urban environment: $A = 50.7, B = 0.57$
 for Marine environment: $A = 40.2, B = 0.56$
 for Rural environment: $A = 33.3, B = 0.50$
- C = corrosion penetration [mm]

Table 6.6: Correlating weeks in Control Test - years at real environments – (Type C)

Corrosion Penetration C [mm]	Steel Type C - Weathering Steel			
	Time at Control Test Weeks	Time at Real Environments		
		Industrial/Urban Years	Marine Years	Rural Years
0.00	0	0.0	0.0	0.0
0.07	2	1.8	2.7	4.6
0.12	4	4.8	7.6	14.2
0.16	6	7.6	12.3	24.3
0.22	8	13.3	21.5	45.5
0.26	10	17.9	29.1	63.9

The ACT for steel washing evaluation was analyzed in Chapter 5. In that chapter it was concluded that averaging the results from steel washing with frequencies of 2, 3, 4, and 5 weeks resulted in a better alternative than the no steel washing option. This steel washing alternative was named as A02-A05 for coupons from steel Type A, and as C02-C05 for coupons from steel Type C. For practical implementation, the mean value for the frequency of the four combined groups resulted in an average frequency of washing each 3.5 weeks. Assuming this washing frequency at the ACT as representative for the

combined Groups A02-A05 and C02-C05, the corresponding number of years at real environments were estimated from Tables 6.5 and 6.6 for steel Types A and C respectively. Data from Table 6.5 are plotted in Figure 6.4, where the number of weeks inside the chamber during the Control Test for steel Type A are related with an equivalent number of years of exposure in real environments - Industrial/Urban, Marine, and Rural. From the plots in Figure 6.4 the equivalent number of years corresponding to the washing frequency of 3.5 weeks were determined, and the results are presented in Table 6.7 for each of the three different environments.

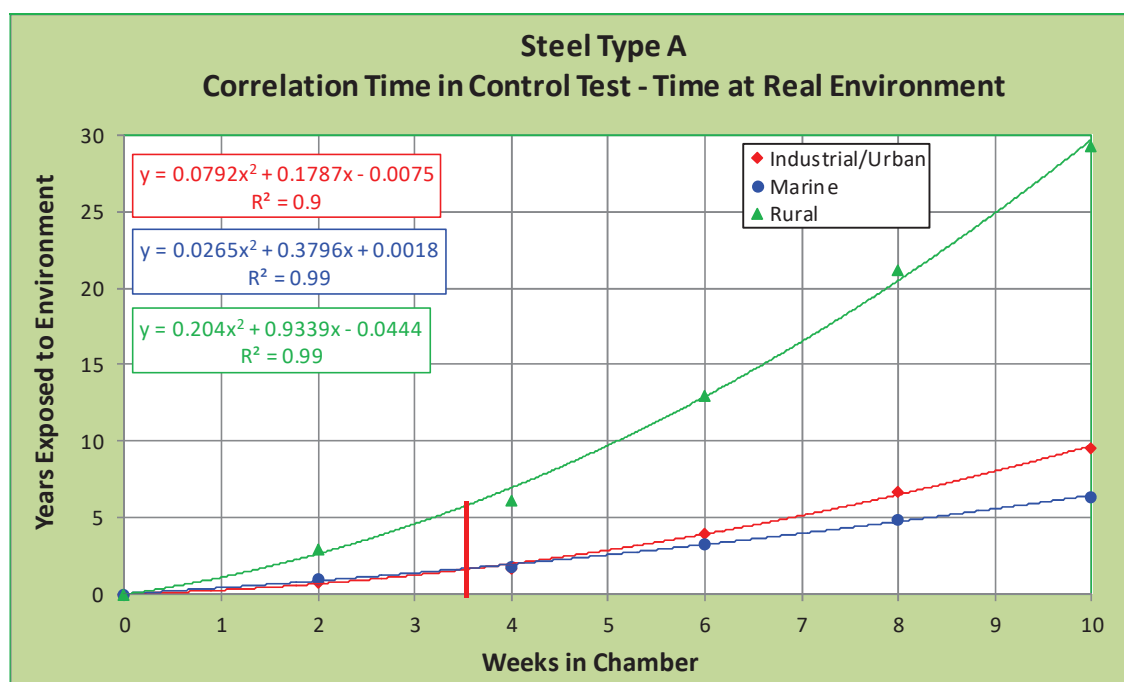


Figure 6.4: Correlating weeks in Control Test - years at real environments - steel Type A

Table 6.7: Correlating values between ACT and real environments – steel Type A

Weeks at ACT	Steel Type A - Years at Real Environments		
	Industrial/Urban	Marine	Rural
3.5	1.59	1.66	5.72

The previous analysis was also applied to the data from steel Type C. Figure 6.5 shows the data from Table 6.6, corresponding to the correlation between the number of weeks inside the chamber during the Control Test and the number of years at real environments for steel Type C. The number of years at real environments correlated to 3.5 weeks inside the chamber for steel Type C are presented in Table 6.8.

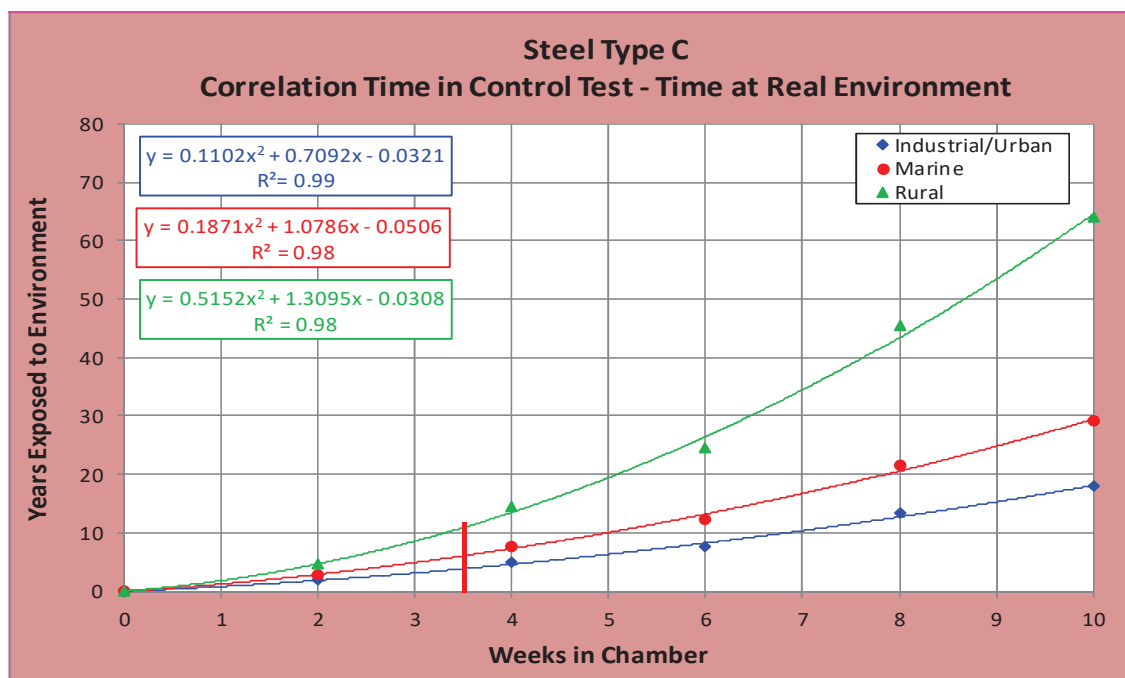


Figure 6.5: Correlating weeks in Control Test - years at real environments - steel Type C

Table 6.8: Correlating values between ACT and real environments - steel Type C

Weeks at ACT	Steel Type C - Years at Real Environments		
	Industrial/Urban	Marine	Rural
3.5	3.80	6.02	10.86

6.3.3 Correlation between Corrosion Penetration from ACT to Atmospheric Corrosion

The final stage was to correlate the corrosion penetration from coupons inside the chamber during the 24-weeks the ACT lasted (evaluated in Tables 6.3 and 6.4) to

corrosion penetration developed during an equivalent number of years of exposure to real environments. The time measured by weeks during the ACT was transformed to an equivalent number of years for each environment considered. The transformation was performed using the equivalence between weeks from ACT and years at real environments presented in Tables 6.7 and 6.8. Then, the corrosion penetration values from Tables 6.3 and 6.4 were expressed to their equivalent number of years at real environments (Industrial/Urban, Marine, and Rural) for steel Types A and C.

The corrosion penetration values C [mm] and the corresponding time required to produce that level of corrosion on steel Type A, expressed as the number of weeks during the ACT and the number of years of exposure to real environments are presented in Table 6.9. In the same manner, the data for corrosion penetration C [mm] for steel Type C, expressed in weeks at the ACT and years of exposure to real environments are presented in Table 6.10.

Table 6.9: Corrosion penetration C for steel Type A versus time measured in weeks at ACT and years at real environments

ACT	Corrosion Penetration C [mm]		Industrial/ urban environment	Marine environment	Rural environment
	Weeks	A02-A05	A10	Years	Years
0	0.00	0.000	0.00	0.00	0.00
1	0.067	0.050	0.45	0.47	1.64
2	0.091	0.075	0.91	0.95	3.27
3	0.109	0.096	1.36	1.42	4.91
4	0.124	0.114	1.82	1.89	6.54
5	0.137	0.130	2.27	2.37	8.18
6	0.149	0.145	2.72	2.84	9.81
7	0.159	0.160	3.18	3.31	11.45
8	0.169	0.173	3.63	3.79	13.08
9	0.178	0.185	4.09	4.26	14.72
10	0.187	0.198	4.54	4.73	16.35
11	0.195	0.209	4.99	5.21	17.99
12	0.203	0.220	5.45	5.68	19.62
13	0.210	0.231	5.90	6.15	21.26
14	0.217	0.242	6.36	6.63	22.89
15	0.224	0.252	6.81	7.10	24.53
16	0.231	0.262	7.26	7.57	26.17
17	0.237	0.271	7.72	8.05	27.80
18	0.243	0.281	8.17	8.52	29.44
19	0.249	0.290	8.63	8.99	31.07
20	0.255	0.299	9.08	9.47	32.71
21	0.260	0.308	9.54	9.94	34.34
22	0.266	0.317	9.99	10.41	35.98
23	0.271	0.325	10.44	10.88	37.61
24	0.276	0.334	10.90	11.36	39.25

Table 6.10: Corrosion penetration C for steel Type C versus time measured in weeks at ACT and years at real environments

ACT	Corrosion Penetration C [mm]		Industrial/Urban environment	Marine environment	Rural environment
	A02-A05	A10	Years	Years	Years
0	0.00	0.000	0.00	0.00	0.00
1	0.080	0.068	1.08	1.72	3.10
2	0.111	0.100	2.17	3.44	6.21
3	0.134	0.125	3.25	5.16	9.31
4	0.154	0.147	4.34	6.88	12.41
5	0.171	0.167	5.42	8.60	15.52
6	0.187	0.185	6.51	10.32	18.62
7	0.201	0.201	7.59	12.04	21.73
8	0.214	0.217	8.68	13.76	24.83
9	0.226	0.231	9.76	15.48	27.93
10	0.238	0.245	10.85	17.20	31.04
11	0.248	0.259	11.93	18.92	34.14
12	0.259	0.272	13.02	20.64	37.24
13	0.269	0.284	14.10	22.36	40.35
14	0.279	0.296	15.19	24.08	43.45
15	0.288	0.308	16.27	25.80	46.56
16	0.297	0.319	17.36	27.52	49.66
17	0.305	0.330	18.44	29.24	52.76
18	0.314	0.341	19.53	30.96	55.87
19	0.322	0.351	20.61	32.68	58.97
20	0.330	0.362	21.70	34.40	62.07
21	0.337	0.372	22.78	36.12	65.18
22	0.345	0.381	23.87	37.84	68.28
23	0.352	0.391	24.95	39.56	71.39
24	0.359	0.400	26.04	41.28	74.49

Data from Table 6.9 are plotted in Figures 6.6, to 6.8, where the corrosion penetration C [mm] for steel Type A is plotted as a function of the equivalent number of years exposed to industrial/rural, marine, and rural environments, respectively. The data from Table 6.10 corresponding to corrosion penetration for steel Type C, expressed in weeks for the ACT and years of exposure to real environments, are presented in Figures 6.9 to 6.11.

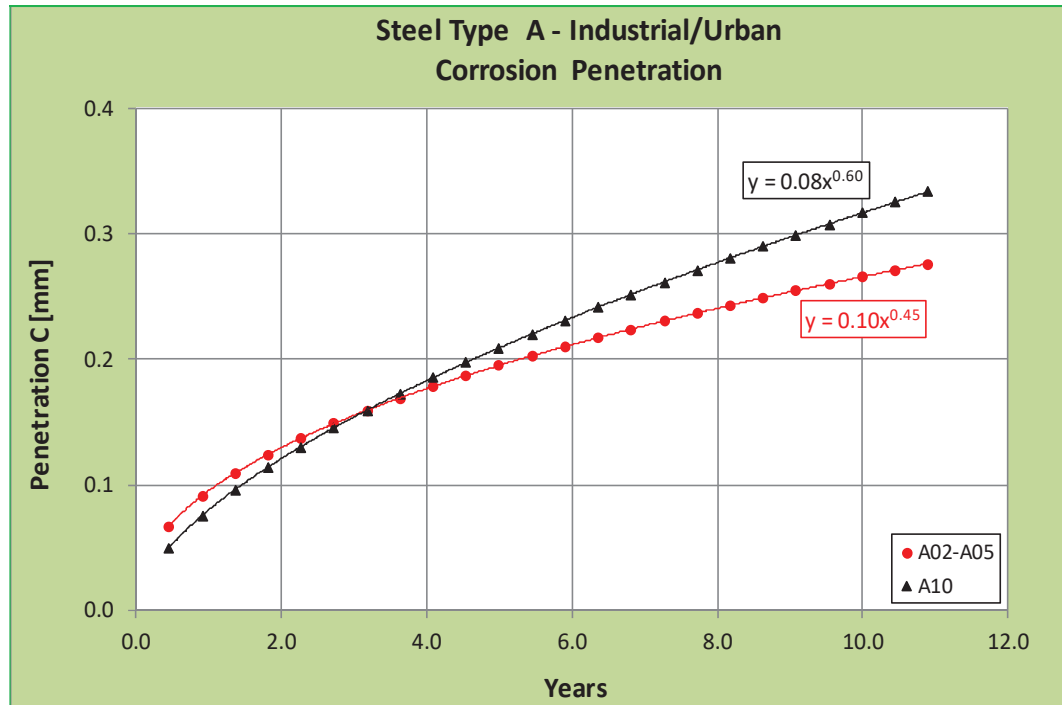


Figure 6.6: Corrosion penetration vs. time - steel Type A - Industrial/Urban environment

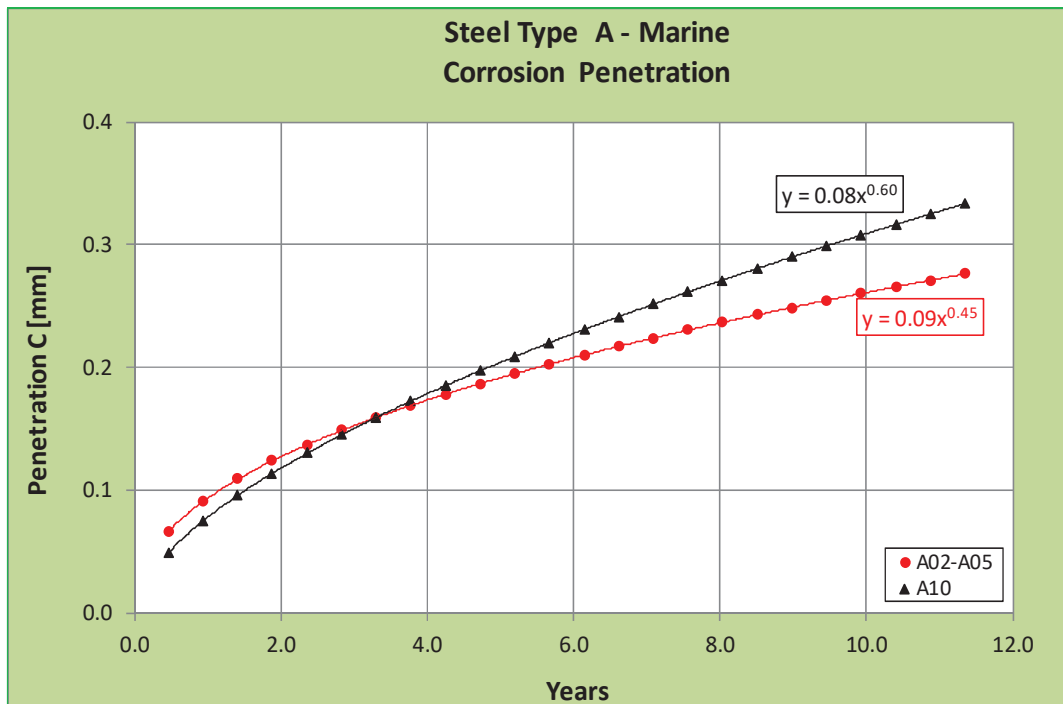


Figure 6.7: Corrosion penetration vs. time - steel Type A - Marine environment

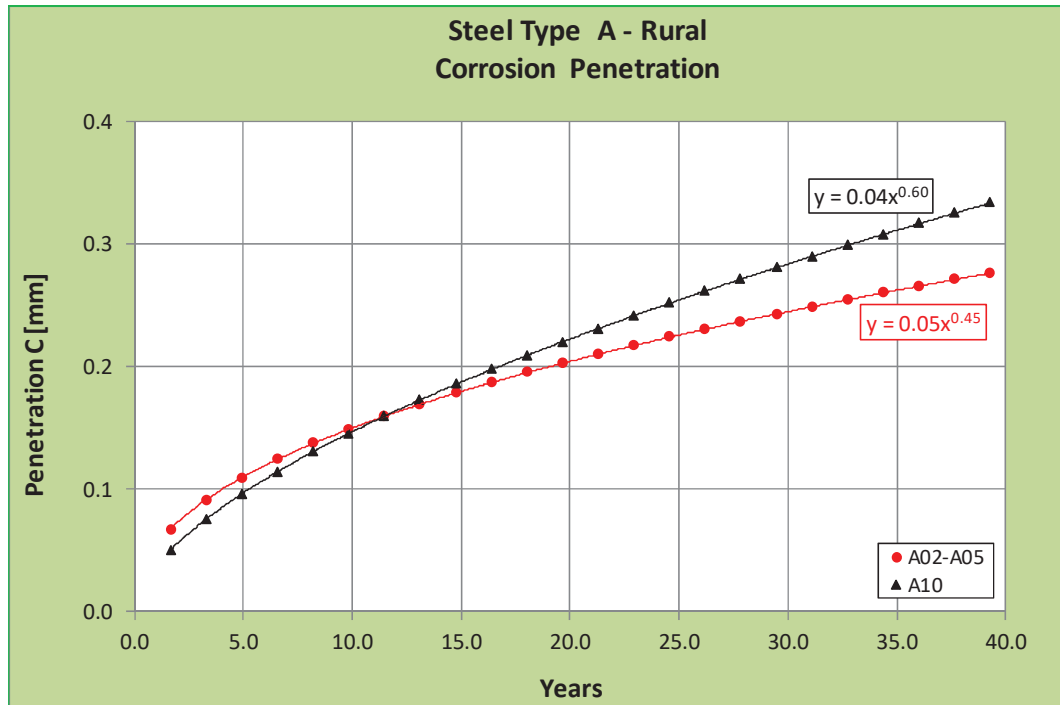


Figure 6.8: Corrosion penetration vs. time - steel Type A - Rural environment

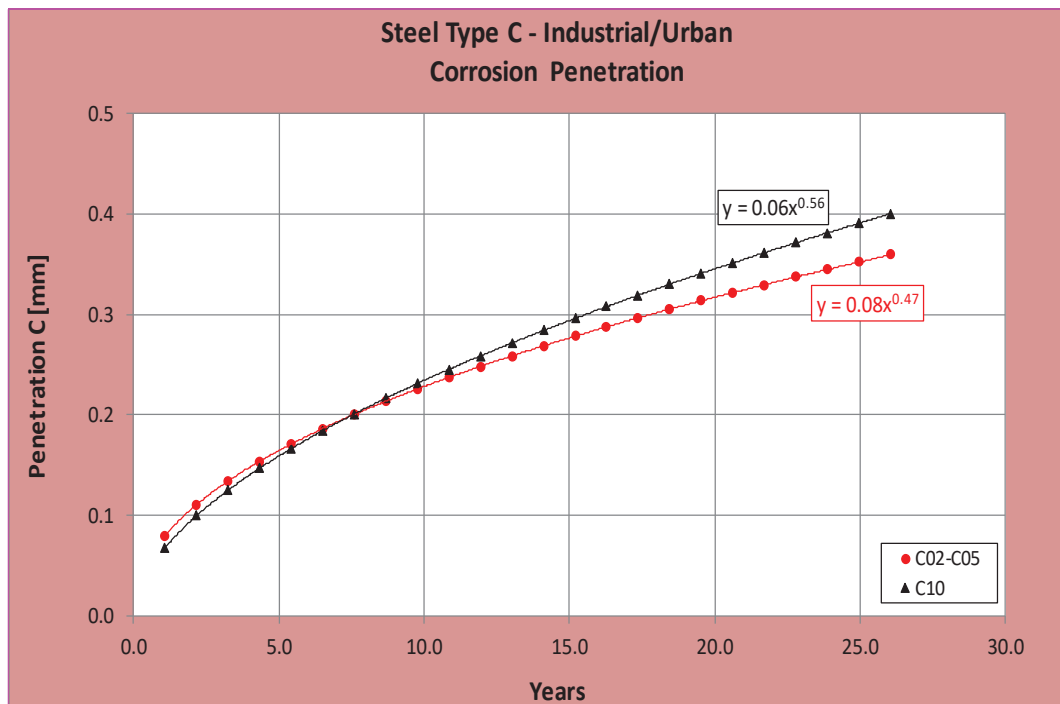


Figure 6.9: Corrosion penetration vs. time - steel Type C - Industrial/Urban environment

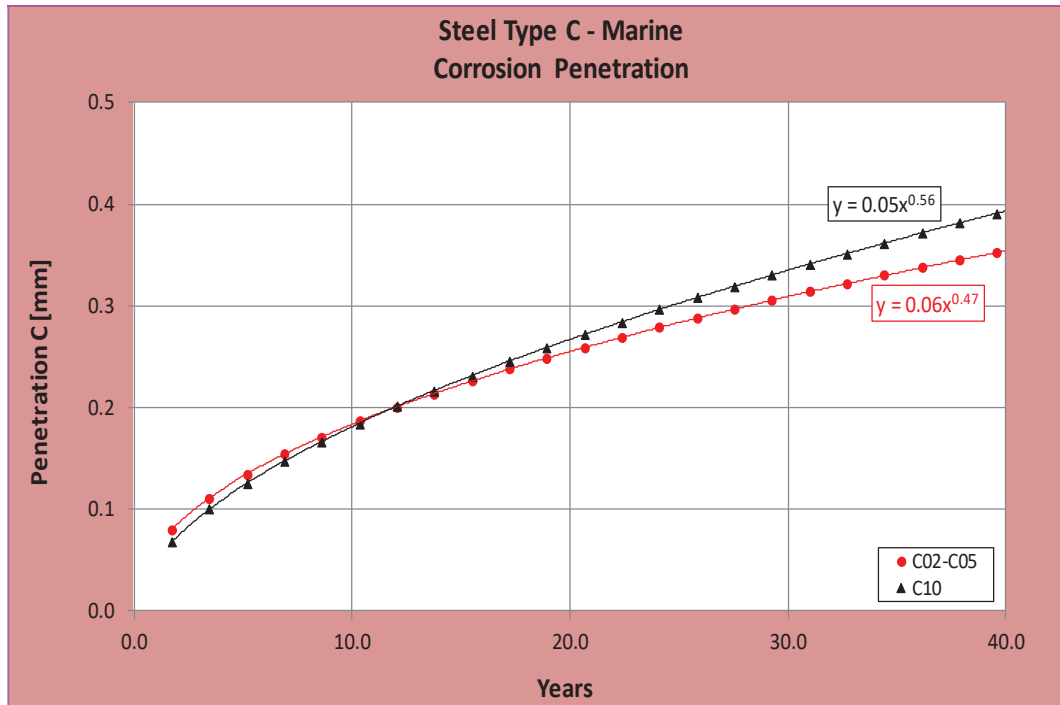


Figure 6.10: Corrosion penetration vs. time - steel Type C - Marine environment

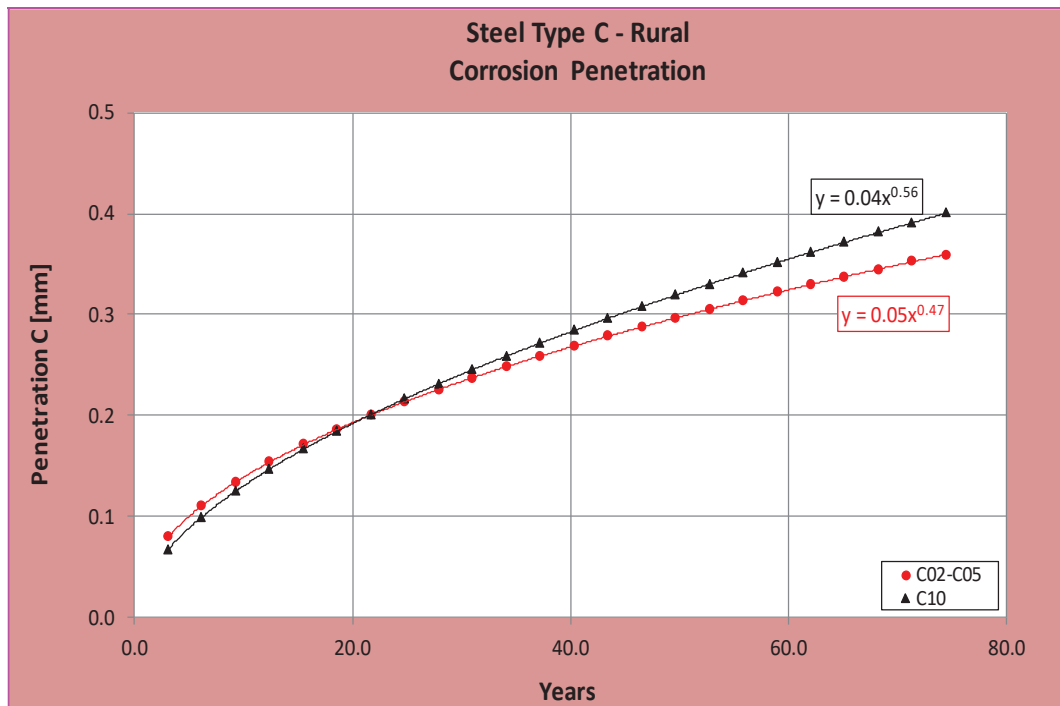


Figure 6.11: Corrosion penetration vs. time - steel Type C - Rural environment

The steel washing alternative produced lower corrosion penetration rates than the no washing alternative, for all cases analyzed herein, as presented in Figures 6.6 to 6.11. Regardless the type of steel, Type A or Type C, the corrosion penetration is always lower for the washing scenario. The corrosion values for washing and no washing alternatives are similar at the beginning of the corrosion process, but as the process develops in time, the steel washing alternative produces lower corrosion penetration rates than the no washing alternative. This behavior is analyzed in detail in chapter 7.

6.4 Sensitivity Analysis between Control Test Data and ACT Data

Weight change data (actually weight increment) corresponding to control test coupons should present similar values to those coupons from Group A10 during their first 10 weeks of ACT. Since both groups of coupons were never washed, their weight increment should be similar. A review of those values showed that the weight increment for coupons from Group A10, during their first 10 weeks, had a lower weight increment than the control test coupons. The differences in weight increment are presented in Table 6.11.

Table 6.11: Weight increment data from control test and Group A10

Weeks	Weight Increment [mg/mm ²]	
	Control Test - Type A 10 weeks	Group A10 first 10 weeks
0	0.00	0.00
2	0.16	0.21
4	0.44	0.39
6	0.97	0.58
8	1.22	0.80
10	1.94	0.85

Given the considerable difference in data values after week 4, it was necessary to perform the correlation analysis presented in section 6.3 using data from Group A10 coupons. Data from Group A10, provided the weight increment for the coupons each week, but no information was obtained in relation to the actual corrosion penetration. In order to

estimate the magnitude of corrosion penetration experienced by coupons from Group A10 an indirect method had to be used. This was done by using the ratio of corrosion penetration to weight increment from the control test data, as shown in Table 6.12.

Table 6.12: Ratio of corrosion penetration to weight increment for control test data

Control Test			
(1)	(2)	(3)	(4)
Week	Weight Increment [mg/mm ²]	Corrosion Penet. [mm]	RATIO (3)/(2)
0	0.00	0.00	0.00
2	0.16	0.07	0.42
4	0.44	0.11	0.25
6	0.97	0.18	0.19
8	1.22	0.25	0.20
10	1.94	0.31	0.16

Applying the ratios obtained from the control test data (Table 6.12) to the weight increment values of coupons from Group A10, at the same week of analysis, the corresponding corrosion penetration values could be estimated. The penetration values obtained with this procedure are presented in table 6.13. The weight increment versus the corrosion penetration values from Group A10, are plotted in Figure 6.12.

Table 6.13: Corrosion penetration from weight increment for Group A10

Group A10 - First 10 weeks			
(1)	(2)	(3)	(2)*(3)
Week	Weight Increment [mg/mm ²]	RATIO	Corrosion Penet. [mm]
0	0.00	0.00	0.00
2	0.21	0.42	0.09
4	0.39	0.25	0.10
6	0.58	0.19	0.11
8	0.80	0.20	0.16
10	0.85	0.16	0.13

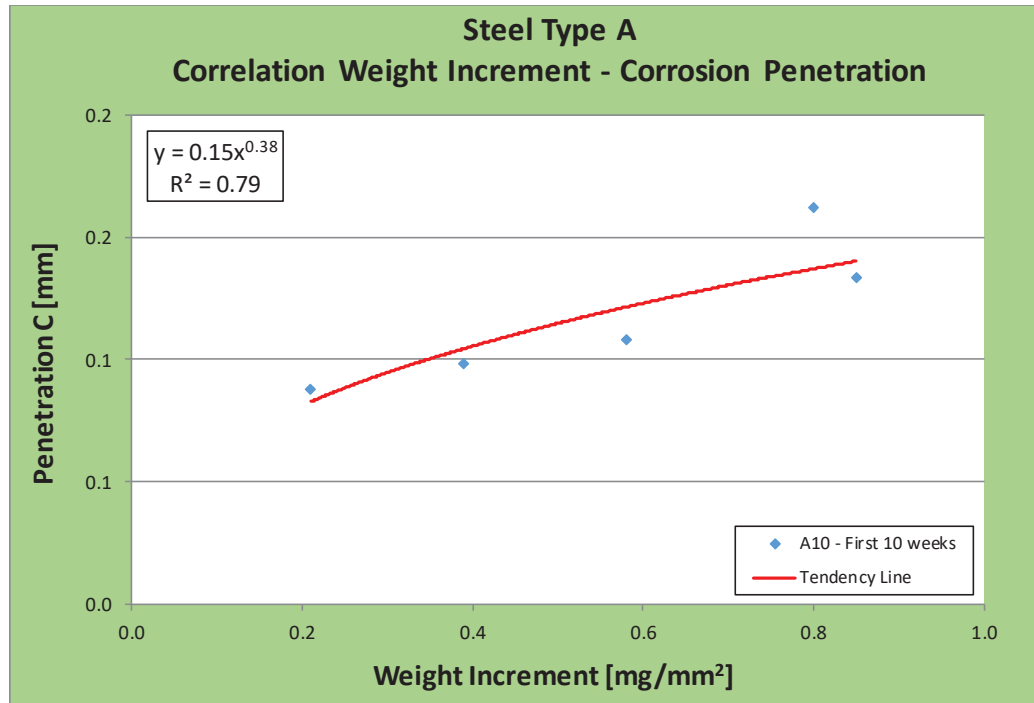


Figure 6.12: Correlation weight increment-corrosion penetration for steel Type A

The expression correlating the weight increment with the corrosion penetration for steel Type A, using data corresponding to the first 10 weeks of Group A10, is presented in Equation 6.6.

$$C_A = 0.15 W_A^{0.38} \quad \text{Equation 6.6}$$

where:

- C_A = corrosion penetration for steel Type A [mm]
- W_A = weight increment for steel Type A using Group A10 coupons [mg/mm²]
- A = exposed area = 8871 mm²
- γ = specific weight = 7.85 mg/mm³

Equation 6.6 was applied to the weight increment from Groups A02-A05 and Group A10 during the 24 weeks the ACT lasted, resulting in the corresponding values for corrosion

penetration C [mm]. The evaluated corrosion penetration values are presented in Table 6.14.

Table 6.14: Corrosion penetration values from Group A10

Week	Weight Increment [mg/mm ²]		Corrosion Penetration [mm]	
	A02-A05	A10	A02-A05 (*)	A10 (*)
0	0.000	0.000	0.000	0.000
1	0.171	0.106	0.077	0.064
2	0.282	0.207	0.093	0.082
3	0.377	0.306	0.104	0.096
4	0.464	0.404	0.112	0.106
5	0.545	0.502	0.119	0.115
6	0.621	0.598	0.125	0.123
7	0.694	0.694	0.131	0.131
8	0.764	0.790	0.135	0.137
9	0.832	0.885	0.140	0.143
10	0.897	0.980	0.144	0.149
11	0.961	1.075	0.148	0.154
12	1.023	1.169	0.151	0.159
13	1.084	1.263	0.155	0.164
14	1.143	1.357	0.158	0.168
15	1.202	1.450	0.161	0.173
16	1.259	1.543	0.164	0.177
17	1.315	1.637	0.166	0.181
18	1.370	1.729	0.169	0.185
19	1.425	1.822	0.172	0.188
20	1.478	1.915	0.174	0.192
21	1.531	2.007	0.176	0.195
22	1.583	2.099	0.179	0.199
23	1.635	2.191	0.181	0.202
24	1.686	2.283	0.183	0.205

(*) Using Equation 6.6

Solving for t from the power function given by Equation 6.4 and using the parameters A and B determined by Kayser (1988), the corresponding number of years for the actual (real) environment were evaluated for each value of corrosion penetration from Groups A02-A05 and Group A10 determined in Table 6.14. The evaluated number of years at real environments versus corrosion penetration are presented in Table 6.15 and plotted in Figure 6.13.

Table 6.15: Correlating penetration from Group A10 with years at real environments

Corrosion Penetration C [mm]	Steel Type A - Carbon Steel			
	Time for Group A10 Weeks	Time at Real Environments		
		Industrial/Urban Years	Marine Years	Rural Years
0.00	0	0.0	0.0	0.0
0.09	2	1.2	1.3	4.3
0.10	4	1.4	1.5	5.1
0.11	6	1.7	1.7	5.9
0.16	8	3.3	2.9	11.1
0.13	10	2.4	2.2	8.2

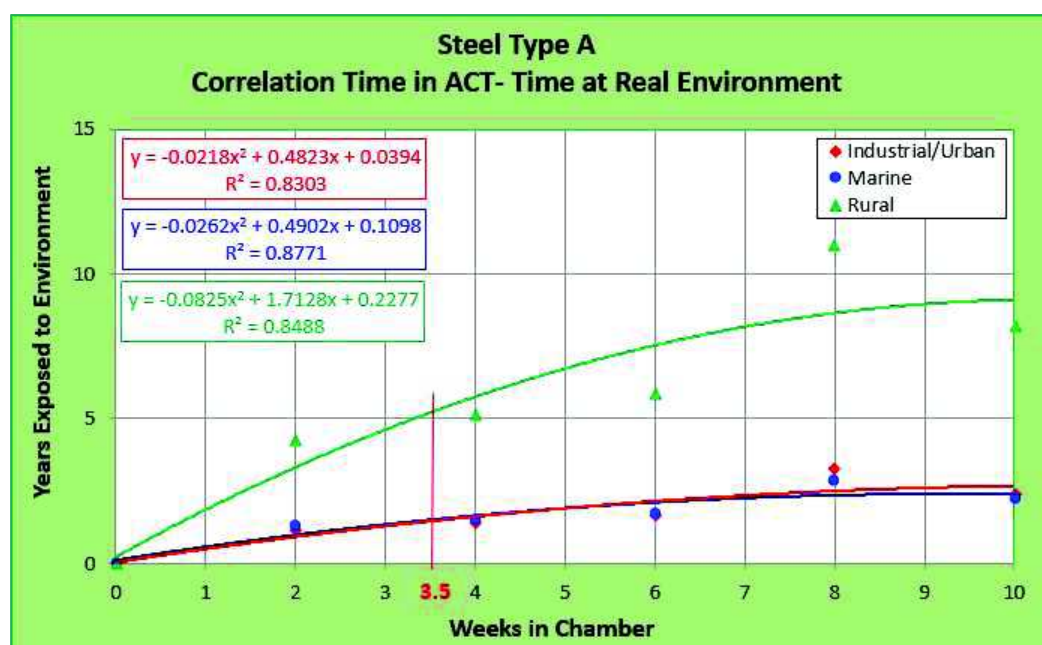


Figure 6.13: Correlating weeks in the ACT with years at real environments – Type A

The curves depicted in Figure 6.13 were used to determine the equivalent number of years corresponding to the washing frequency of 3.5 weeks, and the results are presented in Table 6.16 for each of the three different environments.

Table 6.16: Correlating years at real environments for 3.5 weeks at ACT – Steel Type A

Steel Type A - Years at Real Environments			
Weeks at ACT	Industrial/Urban	Marine	Rural
3.5	1.46	1.50	5.21

With the equivalence between weeks in the ACT and years of exposure in the actual (real) environments, the corresponding number of years versus corrosion penetration at each environment were found, for the 24 weeks the ACT lasted, and the results are presented in Table 6.17.

Table 6.17: Corrosion penetration C for steel type A versus time measured in weeks at ACT and years at real environments

ACT	Corrosion Penetration C [mm]		Industrial/ urban environment	Marine environment	Rural environment
	A02-A05	A10	Years	Years	Years
0	0.00	0.000	0.00	0.00	0.00
1	0.077	0.064	0.42	0.43	1.49
2	0.093	0.082	0.83	0.86	2.98
3	0.104	0.096	1.25	1.29	4.47
4	0.112	0.106	1.67	1.72	5.96
5	0.119	0.115	2.09	2.15	7.45
6	0.125	0.123	2.50	2.58	8.93
7	0.131	0.131	2.92	3.01	10.42
8	0.135	0.137	3.34	3.44	11.91
9	0.140	0.143	3.76	3.87	13.40
10	0.144	0.149	4.17	4.30	14.89
11	0.148	0.154	4.59	4.73	16.38
12	0.151	0.159	5.01	5.16	17.87
13	0.155	0.164	5.42	5.59	19.36
14	0.158	0.168	5.84	6.02	20.85
15	0.161	0.173	6.26	6.45	22.34
16	0.164	0.177	6.68	6.88	23.83
17	0.166	0.181	7.09	7.31	25.31
18	0.169	0.185	7.51	7.74	26.80
19	0.172	0.188	7.93	8.17	28.29
20	0.174	0.192	8.35	8.60	29.78
21	0.176	0.195	8.76	9.03	31.27
22	0.179	0.199	9.18	9.46	32.76
23	0.181	0.202	9.60	9.89	34.25
24	0.183	0.205	10.01	10.32	35.74

From Table 6.17 the values of corrosion penetration C [mm] for steel Type A as a function of the number of years exposed to Industrial/urban environment are plotted in Figure 6.14

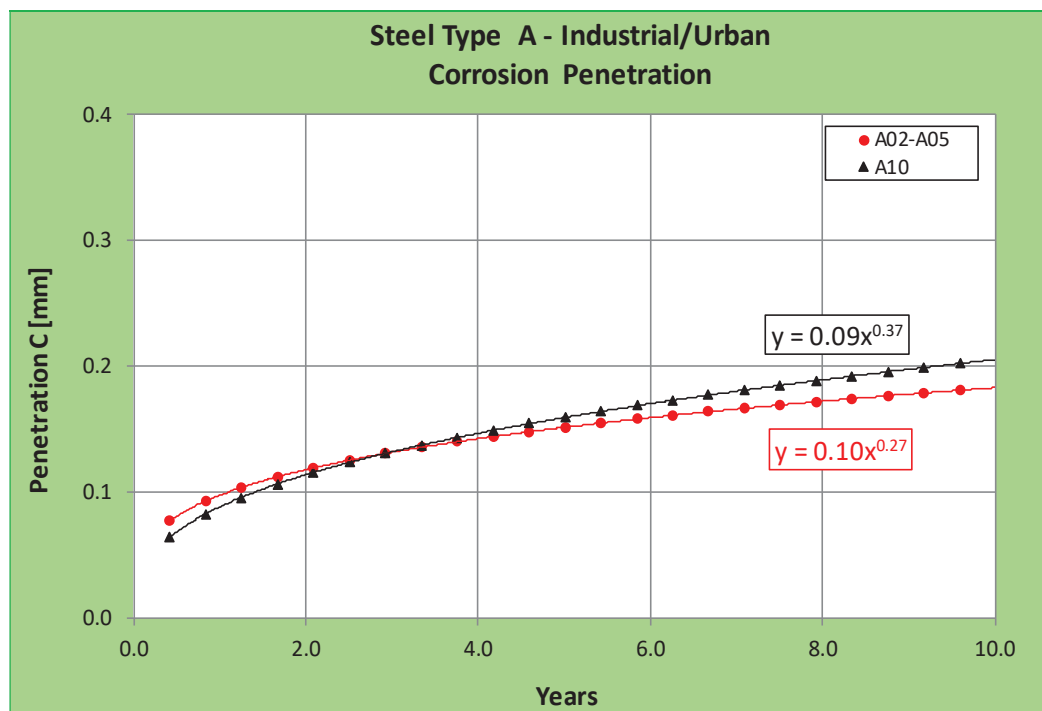


Figure 6.14: Corrosion penetration vs time – steel Type A – Industrial/urban environment

The corrosion penetration values for steel Type A was evaluated from data corresponding to Group A10 coupons, during their first 10 weeks of ACT. Corrosion penetration estimated using data from Group A10 resulted in lower values than those obtained when data from the control test coupons were used. This is evident when comparing the plots in Figures 6.6 and 6.14, which correspond to the same Industrial/urban environment.

The differences in corrosion rates obtained from control test data and Group A10 data could be explained by the fact that both tests were not performed at the same time, but instead at different times. As the misting system received maintenance periodically, it is possible that the system sprayed different amounts of the salt solution in both cases, due

to periodic clogging of the nozzles. Another source of variability could be the change of position inside the chamber for the sets of coupons. Without another source of analysis to define which corrosion rates are more reliable, the most conservative values were assumed for further use. Since the higher rates of corrosion penetration were obtained from the control test data, resulting in more conservative conditions, these results were assumed as the values to be used in the rest of the study.

The sensitivity analysis performed for steel Type A was also applied to coupons from steel Type C. The values of corrosion penetration C [mm] for steel Type C (obtained from Group C10 data) as a function of the number of years exposed to Industrial/urban environment are plotted in Figure 6.15. The same pattern previously observed for steel Type A is observed for steel Type C, the corrosion rates obtained from control test data produced higher corrosion rates than those obtained from Group 10 data. This is again evident when comparing the plots in Figures 6.9 and 6.15, which correspond to the same Industrial/urban environment. Hence as before, the more conservative control group samples were used for further analysis.

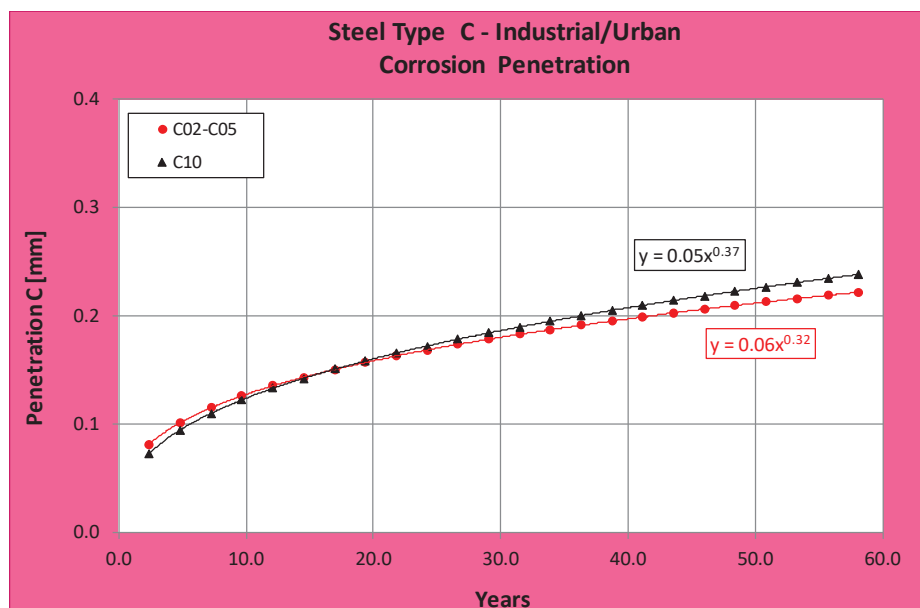


Figure 6.15: Corrosion penetration vs time – steel Type C – Industrial/urban environment

CHAPTER 7. STRUCTURAL ANALYSIS, DESIGN, AND LOAD RATING

7.1 Introduction

The structural capacity degradation of typical steel girder highway bridges due to atmospheric corrosion attack is presented in this chapter. The study used the deterioration models presented in chapter 3 and corrosion penetration values obtained in chapter 6 for different steel types and environments. The most critical corrosion rates, those obtained from control test data, were employed since they provided the most conservative results. Typical steel girder highway bridges were considered with variations of the span length, number of spans, steel types, environment types, maintenance alternatives, and bridge structure age. The emphasis was focused on the parametric analyses of several corroded steel girder bridges under two alternatives: first, when steel bridge girder washing was performed according to the frequency determined on chapter 6, and second, when no bridge girder washing was performed. The reduction of structural capacity was observed for both alternatives throughout the structure service life, which was estimated to be 100 years. The structural capacity degradation was measured through the evaluation of moment and shear capacity for the steel girders and the measure of the corresponding bridge load rating. The maximum elastic deflection of girders was also estimated as a measure of the structural serviceability reduction.

The structural analysis and design, and load rating were based on the adherence to the AASHTO LRFD Bridge Design Specifications (AASHTO, 2012), and the AASHTO Manual for Bridge Evaluation (AASHTO, 2011). A commercial software package was used to conduct the structural analyses of typical highway steel girder bridges. Several

spreadsheets were used to process the corresponding data and determine the targeted parameters. As a result, curves for the bridges structural capacity and serviceability degradation, and the corresponding drop of load rating factors, were obtained during the bridge structures service lives.

7.2 Bridge Load and Resistant Models

The major loads a typical steel highway bridge experiences during its service life are dead load, live load, dynamic load, environmental loads, and other special loads. Those loads are modeled and combined according to the AASHTO LRFD Bridge Design Specifications (AASHTO, 2012). For short to medium span bridges (up to 200 ft.), as those considered in this research, only dead load, live load, and dynamic loads are of particular interest (Barker, 2007). Therefore, dead load, live load, and dynamic loads were considered simultaneously in order to produce the most critical stresses on the structural elements.

7.2.1 Dead Load

The dead load DL represents the self-weight of structural and nonstructural elements permanently connected to the bridge. In this category are considered the weight of deck slab, wearing surface, sidewalks, barriers, girders, diaphragms, stiffeners, etc. The typical statistical parameters for steel and concrete unit weights are presented in Table 7.1

Tabla 7.1: Typical values for materials weight

Material	Weight
Reinforced concrete	150 lb/ft ³
Structural steel	490 lb/ft ³

7.2.2 Live Load

The live load LL represents the forces produced by moving vehicles on the bridge deck. The live load is affected by several parameters such as: span length, truck weight, axle loads and configuration, number of vehicles, transverse position of vehicle, traffic volume, girder spacing, and stiffness of deck and girders (Tantawi, 1986; Czarnecki, 2006). The live load is a very uncertain variable, and it is specified by means of a “notional” load model since they do not represent any particular truck (AASHTO, 2012). According to the AASHTO LRFD Bridge Design Specifications (AASHTO, 2012) the vehicular live loading, designated as HL-93, consist of a combination of three loads: the design truck, the design tandem, and the design lane load. The three live load combinations proposed by the code are presented in Figure 7.1

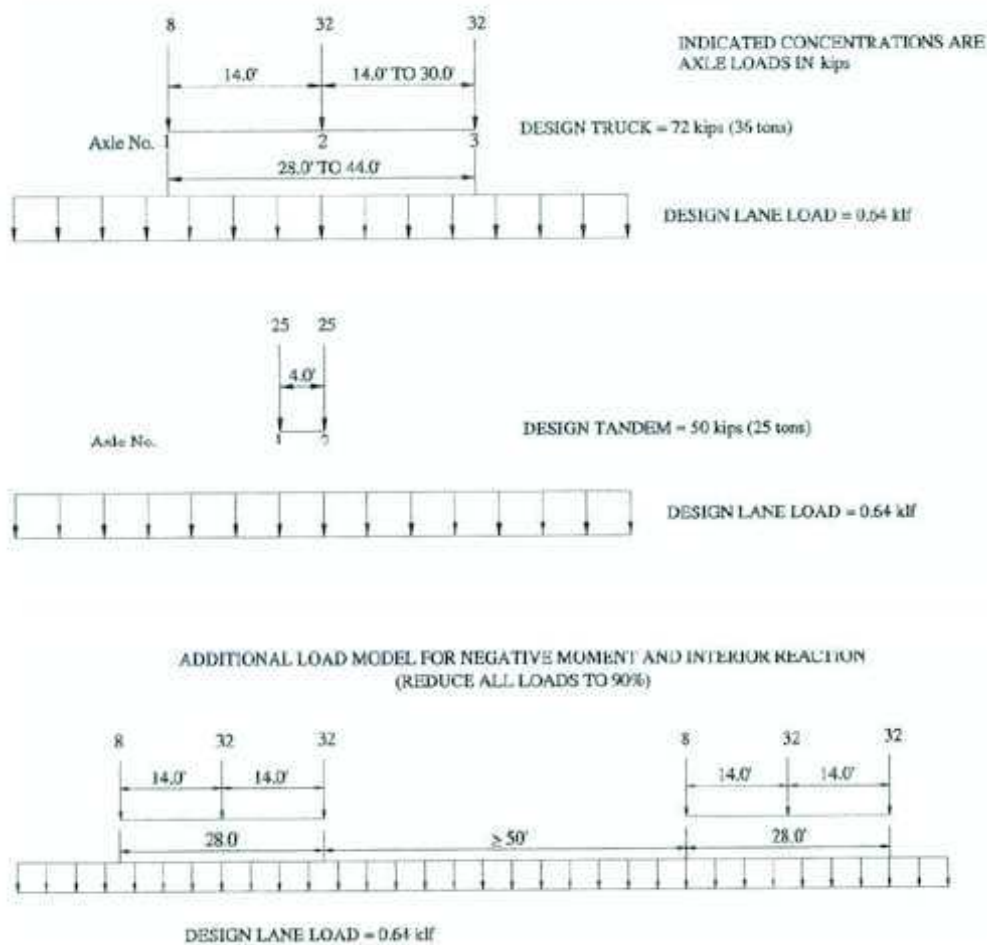


Figure 7.1: AASHTO LRFD design live load (HL-93) (AASHTO, 2011)

7.2.3 Dynamic Load

The dynamic load IL represents the effect of impact produced by a truck when passing over the deck. The dynamic load can be considered as a fraction of the live load, expressed by the dynamic load allowance (IM). The IM can be assumed as an increment of the wheel load to account for the wheel impact from passing vehicles over the deck. The dynamic load is affected by three factors: the surface condition (bumps, potholes), the dynamic characteristics of the bridge (mass and stiffness), and the dynamic characteristics of the vehicle (suspension, shock absorbers) (Tantawi, 1986; AASHTO,

2012). Table 7.2 presents the dynamic load allowance percentages. The dynamic load allowance is specified by the AASHTO LRFD Bridge Design Specifications (AASHTO, 2012) as 0.33 of the design truck or design tandem effect, and zero for the design lane load for conventional maximum loading conditions. Different dynamic load allowances are used for fatigue and deck joints.

Tabla 7.2: Dynamic load allowance (AASHTO, 2012)

Component	IM
Deck Joints—All Limit States	75%
All Other Components:	
• Fatigue and Fracture Limit State	15%
• All Other Limit States	33%

7.2.4 Bridge Resistance Model

The load carrying capacity of a steel girder highway bridge depends upon its geometry and the structural capacity of its components and connections. For a composite steel girder bridge, its resistance capacity is a function of material strength, section geometry, and dimensions. The geometry includes the bridge configuration, which is represented by the span length, number of girders, girder spacing, and position of diaphragms (Czarnecki, 2006; Laumet, 2006).

7.3 Structural Analysis and Design According to AASHTO LRFD

All the structural analysis and design of bridges developed in this research are based on the AASHTO LRFD Bridge Design Specifications (AASHTO, 2012). The Specifications provide the necessary formulation and requirements for application of limit states for each structural member.

Based on the specifications given by the AASHTO LRFD code, analytical models were created to analyze several typical steel girder highway bridges. The models included the following factors for an appropriate analysis and design: structural capacity, load combinations, and evaluation of maximum stresses and deformations. A parametric structural analysis was performed, based on the typical steel bridges designed, focusing on the progressive corrosion of steel girders. Simple supported and two-span continuous I-girder bridges were analyzed and load rating was performed for different ages throughout the expected bridge service life.

7.3.1 Representative I-Girder Steel Bridges Considered

Most bridges can be divided into two main parts: superstructure and substructure. The substructure supports the superstructure and transfers loads to the foundation. The superstructure, on the other hand, is the part of the bridge which provides support for the traffic. The superstructure of a steel girder bridge is composed of the deck, girders, diaphragms, and stiffeners as structural elements. Also the superstructure could include some nonstructural elements such as wearing surface, barriers, sidewalks, stay-in-place forms, signs, etc. In this research typical steel girder superstructures were considered for analysis and design. The analysis and design of the substructure was not considered herein, since the parametric analysis of corroded girders does not affect substantially these parts of a bridge. Consequently, only code expressions and requirements related to the superstructure analysis and design are presented in this chapter.

To appreciate the structural capacity degradation of steel girder bridges due to atmospheric corrosion, typical highway bridge configurations were considered. A typical bridge section was assumed to be similar to that described in the document “AASHTO Steel Bridge Design Handbook Vol. 21- Design Example 2A: Two-Span Continuous Straight Composite Steel I-Girder Bridge” (Barth, 2012). Figure 7.2 shows the typical cross section for the steel girder bridges considered. The section is considered as a representative of steel highway bridges in the USA, wide enough for two lanes.

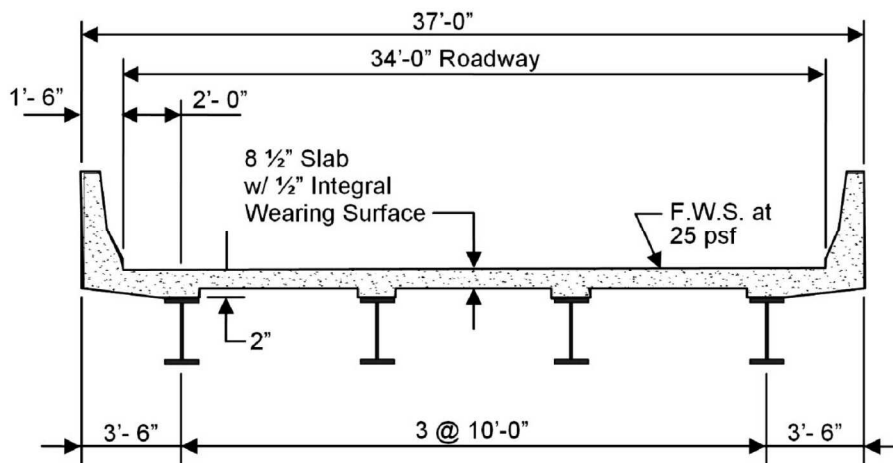


Figure 7.2: Typical bridge cross section (Barth, 2012)

For the bridge section it is assumed that an 8.5 in. thick reinforced concrete deck is used, including a 0.5 in. integral wearing surface, with concrete barriers to each edge. Also, for design a 25 lb/ft² future wearing surface is considered over the entire roadway. The roadway width is 34 ft. and the entire deck is 37 ft. wide. The deck is supported by four plate girders. Each girder is in contact to the deck through a haunch 2 in. thick. The girders are spaced at 10 ft. with 3.5 ft. overhang at each side of the deck. The girders were designed assuming composite action with the concrete deck. The composite section is modeled by considering that there is a complete connection from the girders to the concrete deck, with zero relative displacement between them. The analysis and design followed the specifications from the AASHTO LRFD Bridge Design Specifications (AASHTO, 2012).

Simply supported and two-span continuous I-girder bridges were considered, with span lengths of 70 ft., 90 ft., 110 ft., and 130 ft., as shown in Figure 7.3. The typical one span bridge is supported at one extreme by a pinned support which only allows section rotations in the three main directions (X-,Y-,Z-direction), while at the other end there is a roller support which allows section rotations (X-,Y-,Z-direction) and free longitudinal displacements (X-direction). The typical two-span bridge has two equal spans and it is supported at one end by a pinned support which only allows section rotations in the three

main directions (X-,Y-,Z-direction), while at the bent and in the other end there are roller supports which allow section rotations (X-,Y-,Z-direction) and free longitudinal displacements (X-direction).

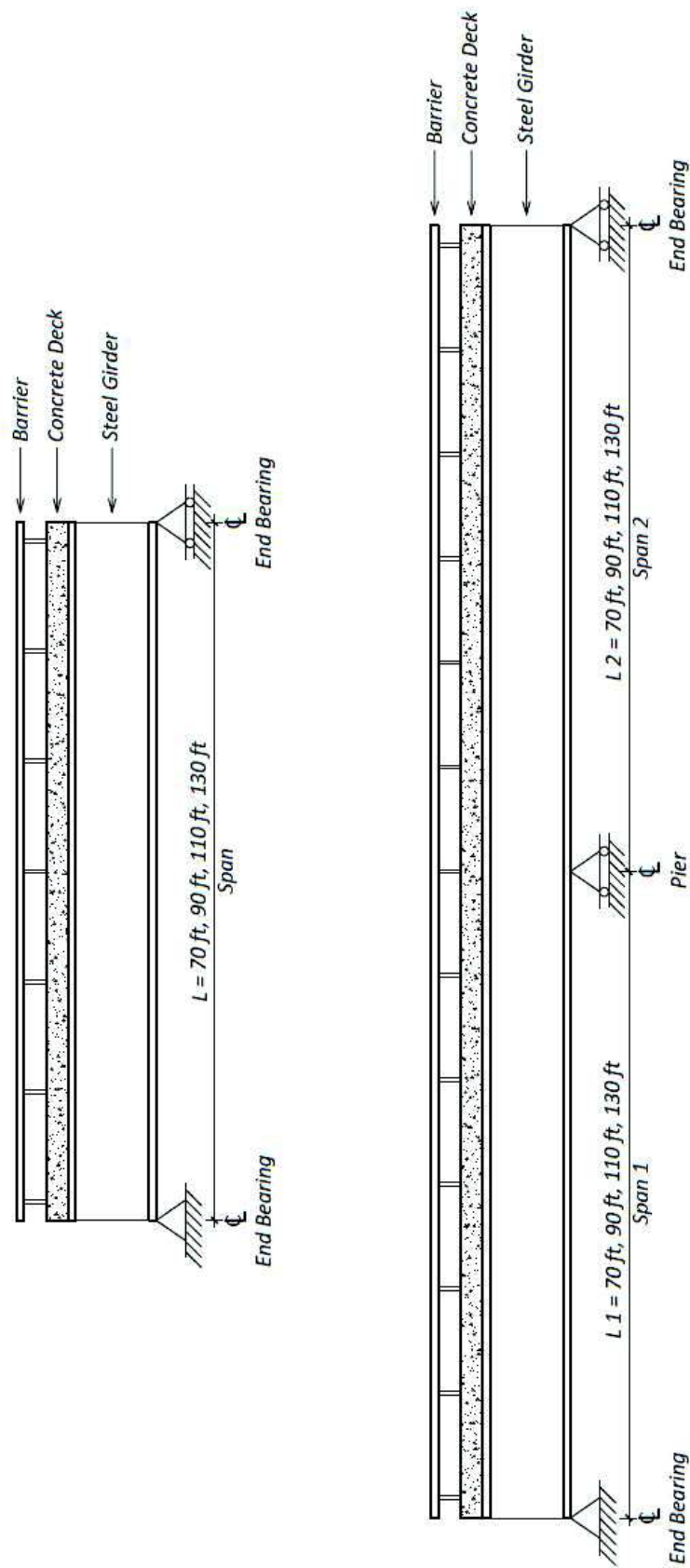


Figure 7.3: Sketch of longitudinal view for typical one-span and two-span bridges

7.3.2 Design Parameters and Loading Considerations

Table 7.3 shows the most important design parameters assumed for the structural analysis and design of the steel girder bridges considered herein.

Table 7.3: Material properties assumed for composite steel girder bridges

PROPERTY		VALUE	
Concrete			
Modulus of Elasticity	E	3,600	ksi
Modulus of Poisson	ν	0.20	
Shear Modulus	G	1,500	ksi
Compressive Strength	f'_c	4.0	ksi
Structural Steel			
Modulus of Elasticity	E	29,000	ksi
Modulus of Poisson	ν	0.30	
Shear Modulus	G	11,154	ksi
Yield Stress	F_y	50	ksi
Tensile Stress	F_u	65	ksi
Reinforcing Steel			
Modulus of Elasticity	E	29,000	ksi
Yield Stress	F_y	60	ksi

The dead load DL is classified into three categories: the dead load corresponding to structural ($DC1$) and nonstructural components ($DC2$) and the dead load due to wearing surfaces (DW). The composite girder behavior is considered by analyzing different stages of loading and different resistant sections. Since not all of the dead load acts at the same time over the composite section, the dead loading effect is divided into three stages. First, the dead load corresponding to the steel girders' self-weight and the fresh concrete weight immediately after casting, identified as $DC1$, which is resisted only by the steel section, without composite behavior. Secondly, the dead loading on the long-term composite section, named $DC2$, after the concrete has achieved its full design resistance, supporting the steel girder self-weight, the concrete deck, and all nonstructural elements

placed on the deck. Finally, the dead load corresponding to the future wearing surface, named DW , which is resisted also by the long-term composite section.

The live load LL , represented by the three live load combinations, is analyzed assuming the possibility that one or two lanes are loaded. The structural analysis focused on finding the most critical situation from both cases. The live loads are resisted by the composite section (Barth, 2012). Table 7.4 presents the factors to affect the live load LL , based on the number of loaded lanes. Since the deck width is enough for two lanes, a factor of 1.0 was considered.

Tabla 7.4: Multiple presence factors, m (AASHTO, 2012)

I Number of Loaded Lanes	Multiple Presence Factors, m
1	1.20
2	1.00
3	0.85
>3	0.65

7.3.3 Load and Resistance Factor Design (AASHTO LRFD)

The Load and Resistance Factor Design (LRFD) is a modern structural design method based on the strength of materials, which includes the variability of material resistance as well as the expected load effects, and that provides a level of safety based on the probability of failure (Barker, 2007; AASHTO LRFD, 2012). Some important characteristics from the code specifications are presented in the following:

- The variability of material resistance is taken into account by the resistance factor ϕ , which is usually less than one. The resistance factor ϕ is related to the influence of material properties, equations that predict strength, workmanship, quality control, and the consequence of a failure.

- The variability of load effects is included by the load factor γ , which is usually greater than one. The load factor γ is related to the uncertainties of load magnitude, loads position, and possible load combinations.
- Structural ductility, redundancy, and operational classification are included in the method by the load modifier factor η . While ductility and redundancy are directly related to material strength, operational classification is related to the consequences of closing the bridge.
- Probability theory has been applied to the election of resistance factors and load factors. Statistical analysis has been performed to define values of material weights and truck loads.

The basic design expression given by the AASHTO LRFD, which must be accomplished by each component and connection, is presented in Equation 7.1 (AASHTO LRFD, 2012).

$$\sum \eta_i \gamma_i Q_i \leq \phi R_n = R_r \quad \text{Equation 7.1}$$

where:

Q_i	=	the force effect
R_n	=	the nominal resistance
R_r	=	the factored resistance
ϕ	=	the resistance factor
γ_i	=	the load factor
η_i	=	the load modifier factor.

7.3.4 Limit States

“Limit State is a condition beyond which the bridge or component ceases to satisfy the provisions for which it was designed” (AASHTO LRFD, 2012). The limit states define the several ways a structure could fail to accomplish to AASHTO LRFD requirements. The several state limits are appropriate to analyze the different bridge components, under

different load conditions and expected failure. All structures and their members should verify two conditions: the structural safety against collapse and its adequate serviceability. There are four groups of different limit states to verify those two mentioned conditions: Strength (I-V), Service (I-IV), Extreme Event (I - II) and Fatigue (I – II). However, for typical short to medium span bridges, the analysis of Strength I limit state for safety from collapse is enough, since this limit state governs the design in most cases. Strength I limit state is expressed by Equation 7.2. In Equation 7.2 the coefficients 1.25, 1.50, and 1.75 are the load factors according to the AASHTO LRFD, to consider the load uncertainties.

$$1.25DD + 1.50DW + 1.75LL(1 + IL) \leq \phi R_n \quad \text{Equation 7.2}$$

where:

DD	=	dead load effect of self-weight of elements permanently attached to the bridge
DW	=	dead load effect due to wearing surface
LL	=	live load effect due to moving vehicles
IL	=	dynamic load factor
ϕ	=	resistance factor ($\phi = 1.00$ for flexure and shear limit states in compact sections)
R_n	=	nominal moment or shear capacity

The analysis of deflection limit state on composite steel girders is optional according to the AASHTO LRFD, because its violation is not expected to produce a structural failure. This limit is related to the maximum elastic deflection due to live load and could be considered as the span/800 for vehicular bridges (AASHTO LRFD, 2012).

7.3.5 Design for Flexural Capacity

The provisions for I-girder flexural design are given by the AASHTO LRFD Bridge Design Specifications (AASHTO, 2012), section 6.10 or Appendix A6. Steel girders connected to concrete deck through shear connectors that prove an adequate composite

behavior should be designed according to the provisions of AASHTO LRFD Article 6.10.10. The elastic stresses at any location on the composite section should be evaluated as the sum of three stresses caused by loads acting separately on these three different sections: 1) steel girder section, 2) short-term composite section, and 3) long-term composite section.

The flexural stresses for sections under positive flexure are evaluated based on a composite section that includes the steel section and the transformed area of the effective width of concrete deck. Concrete in tension is not considered effective in the resistant capacity – AASHTO LRFD Article 6.10.1.1.1b. The flexural stresses for sections under negative flexure are evaluated based on a composite section, for both short-term and long-term moments, that includes the steel section and the longitudinal reinforcement within the effective width of concrete deck – AASHTO LRFD Article 6.10.1.1.1c.

For a simply supported bridge, the desirable type of bending failure at ultimate capacity is steel yielding at midspan, where the maximum positive moment occurs. This is a type of ductile failure with pronounced deformations that provide forewarning of any impending failure. In composite I-girder sections, a ductile failure is produced when the structural steel starts to yield, before the concrete from the deck begins to crush. Also it is assumed that slippage of shear connectors is not possible, assuring a perfect composite action. Additionally, for a two-span continuous composite bridge it is possible to fail due to buckling of its lower flange at sections in regions of negative moment near the pier support. The slenderness of the bottom flange should be adequate to avoid this type of undesirable failure.

The flexural design procedure for composite I-girders is not presented in this research. Section 6.10 and Appendix A6 of the AASHTO LRFD provides all necessary information for a complete design. Also, adequate examples of flexural design for composite I-girders are available in the works from Czarnecki (2006), Barth (2012), and Barker and Puckett (2007).

7.3.6 Design for Shear Capacity

The design of a typical composite steel girder highway bridge included verification of adequate shear capacity. The I-girder nominal shear capacity was evaluated and compared with the acting shear stresses from the Strength I limit state. The critical sections for shear stresses occur near the supports at the abutments for one-span bridges, and at the pier for two-span bridges. The shear design considered always compact sections and it was assumed that the entire shear capacity was provided by the I-girder web. The nominal shear resistance according to AASHTO LRFD (AASHTO, 2012) is presented in equations 7.3 to 7.5.

$$V_u = \phi_v V_n \quad \text{Equation 7.3}$$

where:

- ϕ_v = resistance factor for shear
- V_n = nominal shear resistance [kip]
- V_u = shear at the web section under consideration due to factored loads [kip]

The nominal shear resistance of unstiffened webs shall be taken as:

$$V_n = V_{cr} = C V_p \quad \text{Equation 7.4}$$

in which:

$$V_p = 0.58 F_{yw} D t_w \quad \text{Equation 7.5}$$

where:

- C = ratio of the shear-buckling resistance to the shear yield strength
- V_{cr} = shear-buckling resistance [kip]
- V_n = nominal shear resistance [kip]
- V_p = plastic shear force [kip]
- F_{yw} = specified minimum yield strength of a web [kip]

D = web depth [in.]
 t_w = web thickness [in.]

The shear carrying capacity was checked during all design process, but actually it did not govern, since flexural requirements were more critical.

7.3.7 Elastic Deflections

According to AASHTO LRFD (AASHTO, 2012) bridges should be designed with the expressed condition “to avoid undesirable structural or psychological effects due to their deformations (AASHTO, 2012).” The code specifies the evaluation of elastic deflections based on the live load portion from Service I limit state, including the dynamic load allowance effects. Although the Specifications indicates that deflection limit state is an optional requirement related to serviceability, when applied, the deflection is limited to 1/800 of the span length for steel girders from vehicular bridges. The span length to estimate the elastic deflection should be the free distance between centers of support (INDOT, 2013). The estimated elastic deflection should be taken as the larger value resulting from the application of:

- the design truck alone, or
- 25 percent of the design truck taken together with the design lane load.

The elastic deflection on composite steel I-girder bridges is affected by bridge configuration, superstructure details, loading cases, and boundary conditions. Therefore, a reliable estimation of elastic deformation should be achieved when all these factors are included in the structural analysis.

7.3.8 Steel Highway Bridge Design using a FE Package

Steel I-girder bridges are the most common and effective solution for short to medium span bridges (Caltrans, 2015). The superstructure design according to AASHTO LRFD

(AASHTO, 2012) requires accomplishing several relationships from the bridge geometry, girder geometry, deck and girder materials, loading systems, etc. The procedure requires the assumption of specific values for member dimensions, bridge elements disposition, and material properties. Therefore, the analysis and design of one steel girder bridge is time consuming when all requirements are checked properly. For a wide variety of steel highway bridges, eight typical models were identified to be analyzed in this research. One and two-span, 70, 90, 110 and 130 feet span-length bridges were selected to be analyzed under the corrosion model identified in this study.

As an alternative to time consuming hand calculations, the use of commercial software packages has proven to be accurate, convenient, and extremely fast in verifying all code requirements. This approach allows to the designer to perform several run analyses for the same bridge model, while searching for the most effective bridge configuration and appropriate member dimensions. CSiBridge (Computers & Structures, Inc., 2011) is a versatile, integrated, and powerful tool for the analysis and design of steel girder bridges, developed by the same creators of SAP2000 - Computers & Structures, Inc. The package uses the finite element method to model the bridge elements and solve the several stress-strain relationships established for the model. The steel girder bridge analysis and design using CSiBridge is based on the application of load patterns, load cases, load combinations, and design requests, according to the desired code (Computers & Structures, Inc., 2011).

To verify the suitability of using the CSiBridge package for analyzing and designing a steel girder bridge, a comparative analysis was performed between the use of CSiBridge and the results from a hand solution. A step by step, hand solution, was selected from the document “AASHTO Steel Bridge Design Handbook Vol. 21- Design Example 2A: Two-Span Continuous Straight Composite Steel I-Girder Bridge” (Barth, 2012). This is an official document from AASHTO, where a detailed solution for a typical two-span (90 ft. – 90 ft.) continuous steel girder bridge is analyzed and designed according to the AASHTO LRFD code. The bridge section is composed of four plate girders spaced at

10.0 ft. and 3.5 ft. overhangs. The concrete deck is 34.0 ft. and it is centered over the four girders. The reinforced concrete deck is 8.5 inches thick, including a 0.5 inches integral wearing surface (Barth, 2012). The details for the bridge cross section were presented in Figure 7.2 and the steel girder configuration is shown in Figure 7.4.

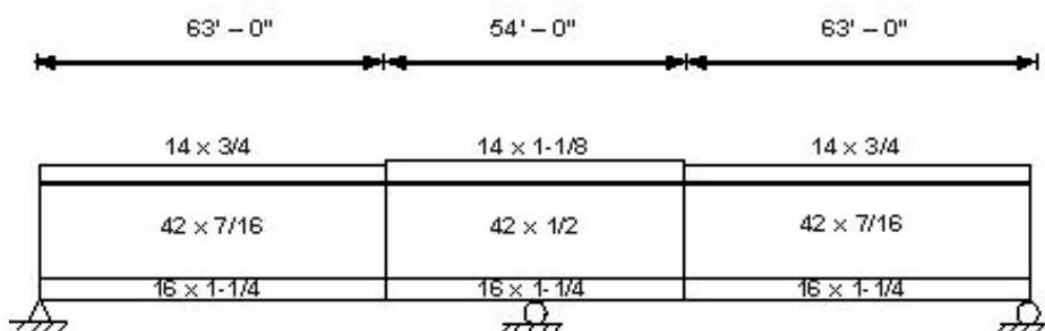


Figure 7.4: Sketch of typical steel girder elevation (Barth, 2012)

The maximum dead and live load moment values from the example by Barth (2012) and the corresponding values obtained applying CSiBridge are presented in Tables 7.5 and 7.6. For the same bridge analysis, the obtained results from CSiBridge show adequate accuracy in comparison to hand solution values reported by Barth (2012).

Tabla 7.5: Dead load moment values for CSiBridge and hand solution and analysis

<u>DEAD LOAD</u>						
EXTERIOR GIRDER						
	M(+) [kip-ft]			M(-) [kip-ft]		
	CSiBridge	AASHTO	%	CSiBridge	AASHTO	%
DC1	721	738	-2.4%	1319	1334	-1.1%
DC2	150	147	2.0%	271	265	2.2%
DW	118	120	-1.7%	212	217	-2.4%
INTERIOR GIRDER						
	M(+) [kip-ft]			M(-) [kip-ft]		
	CSiBridge	AASHTO	%	CSiBridge	AASHTO	%
DC1	641	632	1.4%	1128	1143	-1.3%
DC2	129	126	2.3%	222	227	-2.3%
DW	105	103	1.9%	191	186	2.6%

where:

- DC1 : Girders self-weight, weight of concrete slab (including the haunch and overhang taper), stay-in-place forms, cross diaphragms, and stiffeners
 DC2 : Self weight from barriers
 DW : Weight of future wearing surface

Tabla 7.6: Live load moment values for hand solution and CSiBridge analysis

<u>LIVE LOAD</u>							
	M(+) [kip-ft]				M(-) [kip-ft]		
	CSiBridge	AASHTO	%		CSiBridge	AASHTO	%
Exterior Girder	1646	1661	-0.9%	Exterior Girder	1690	1737	-2.8%
Interior Girder	1410	1423	-0.9%	Interior Girder	1448	1489	-2.8%

7.3.9 Analysis and Design of Typical Steel Girder Bridge

Based on the design parameters, the bridge configuration previously established in this chapter, and following the AASHTO LRFD Bridge Design Specifications (AASHTO, 2012), eight typical steel girder highway bridges, of one and two-span were analyzed and designed using the CSiBridge FE package. The design sought the most efficient sections, represented by the less girder depth, while trying to keep a constant web depth and thickness. The one-span bridges were designed with a constant section for the entire span length. For the two-span bridges, two or three different sections were used as needed accordingly to the load demands. In this case, web depth and thickness were maintained constant while increasing the flanges sections. In all cases the girder flexural capacity controlled the design, since the web depth and thickness were held constant over the entire span length after designing the critical section for shear. The changes in flange width and thickness produced important changes in the girder flexural capacity, but minimum changes in the shear capacity. As a practical rule, a minimum flange-plate size of 12" x 3/4" and a minimum web thickness of 1/2" with 1/16" increments were considered for the typical designs (INDOT, 2013; Caltrans, 2015). Sketches for the corresponding designs are presented in Figures 7.5 to 7.12

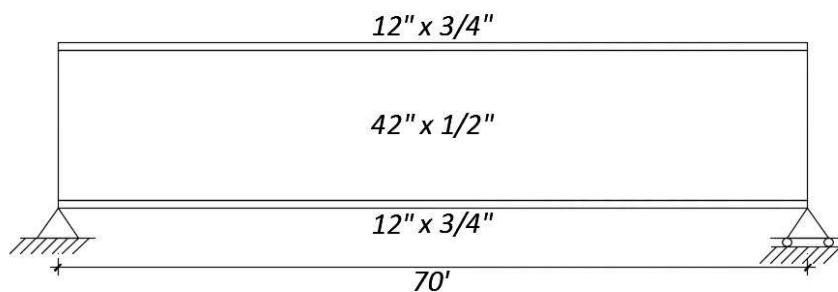


Figure 7.5: Sketch of the typical 70' one-span composite steel I-girder bridge

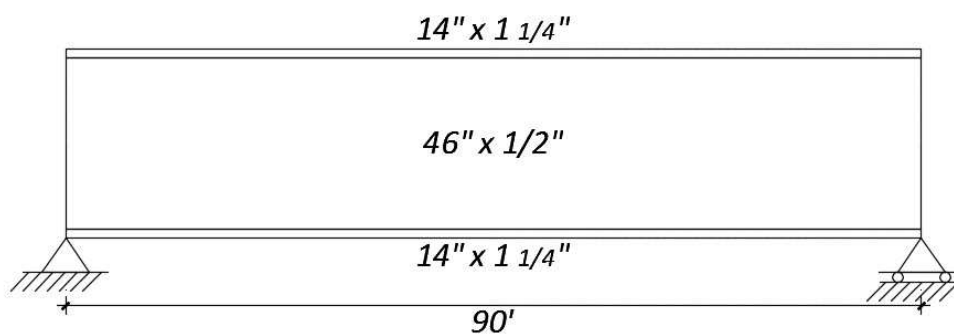


Figure 7.6: Sketch of the typical 90' one-span composite steel I-girder bridge

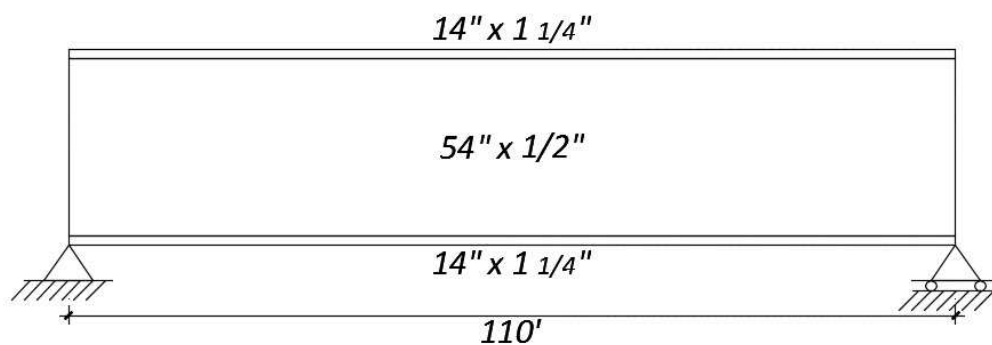


Figure 7.7: Sketch of the typical 110' one-span composite steel I-girder bridge

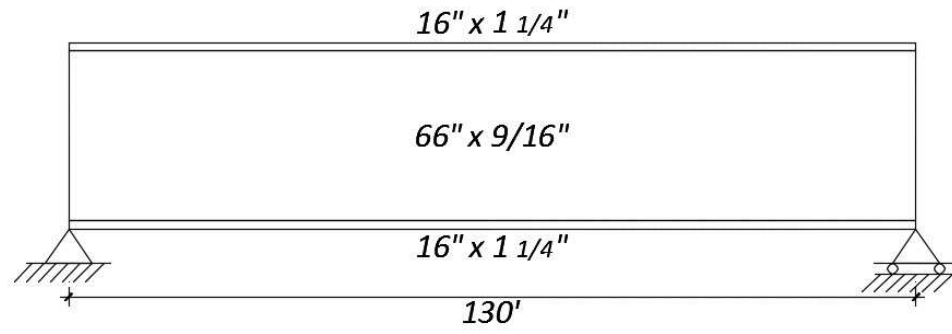


Figure 7.8: Sketch of the typical 130' one-span composite steel I-girder bridge

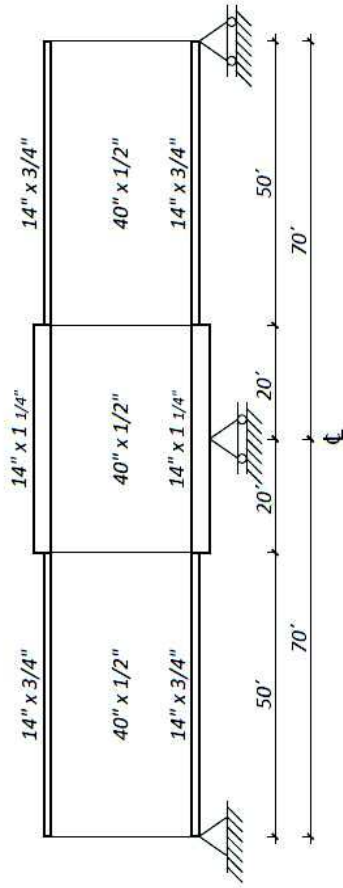


Figure 7.9: Sketch of the typical 70'-70' two-span composite steel I-girder bridge

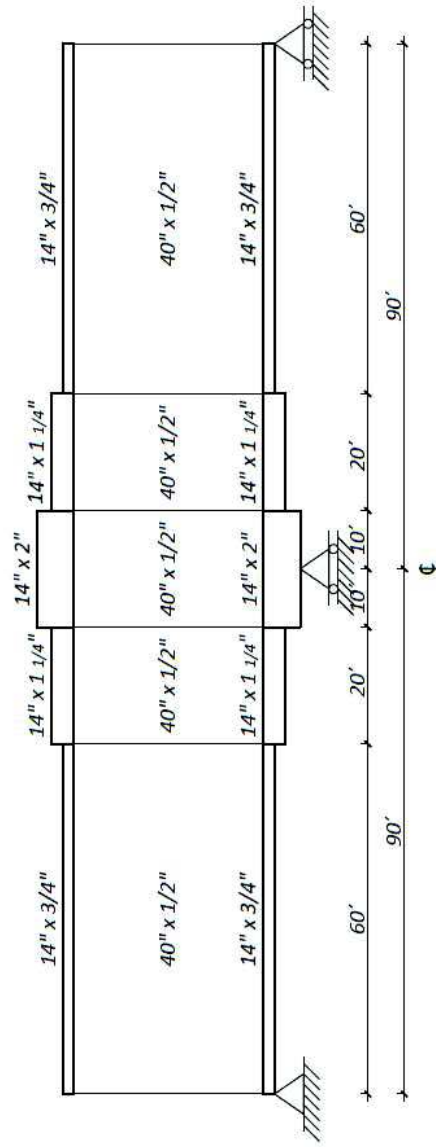


Figure 7.10: Sketch of the typical 90'-90' two-span composite steel I-girder bridge

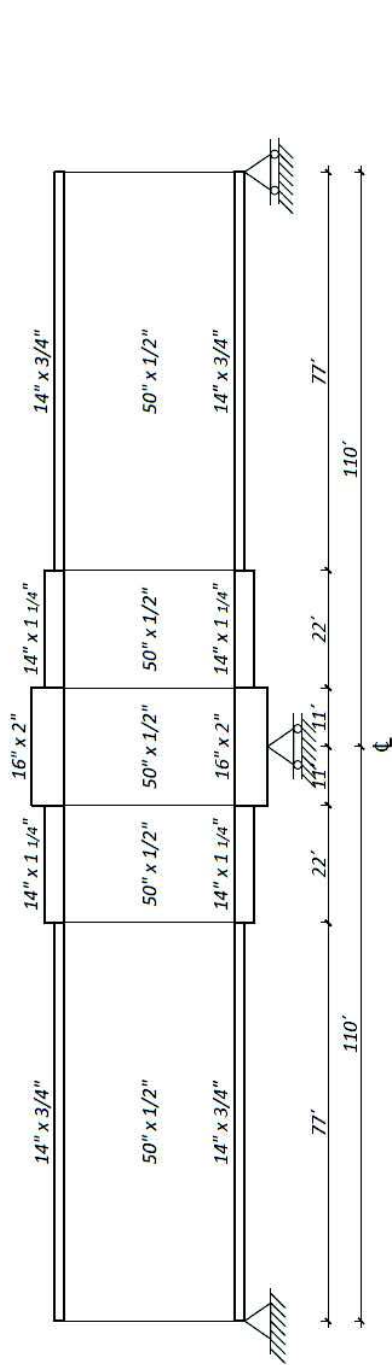


Figure 7.11: Sketch of the typical 110'-110' two-span composite steel I-girder bridge

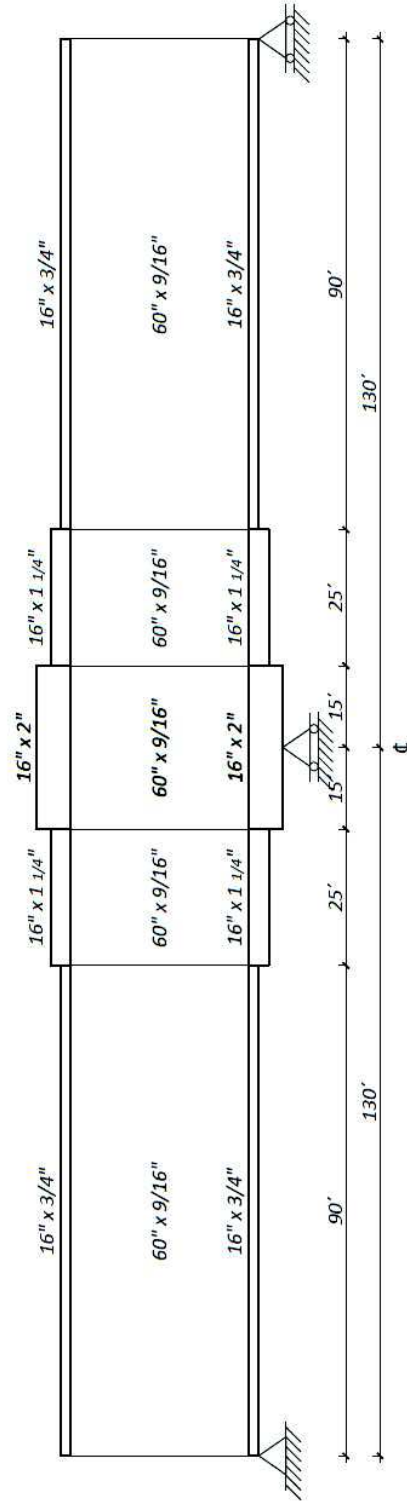


Figure 7.12: Sketch of the typical 130'-130' two-span composite steel I-girder bridge

The eight typical steel girder bridges showed a span-to-depth ratio lower than the limit required by AASHTO Specifications. The web slenderness limit depth-to-thickness were also below the specifications limits for all bridge models. Consequently, all the typical bridge designs did not require end bearing or intermediate stiffeners. The bridge designs included cross-frame diaphragms spaced a maximum of 25 ft. All bridge deflections were equal or shorter than the span/800 limit recommended by the LRFD Design Specification.

Table 7.7 shows the corresponding Demand/Capacity ratios for maximum positive and negative bending moments, and maximum shear force. The ratios of maximum elastic live load deflection to admissible deflection are also presented in Table 7.7.

Table 7.7: Maximum Demand/Capacity ratios for stresses and deflections

Bridge	D/C M(+)	D/C M(-)	D/C V(+/-)	$\Delta_{max}/\Delta_{adm}$
1 x 70'	0.62		0.47	0.88
1 x 90'	0.64		0.63	0.89
1 x 110'	0.72		0.80	0.98
1 x 130'	0.70		0.80	0.88
2 x 70'	0.50	0.86	0.46	0.70
2 x 90'	0.76	0.89	0.62	1.00
2 x 110'	0.78	0.90	0.79	1.00
2 x 130'	0.77	0.89	0.74	0.94

It can be seen in Table 7.7 that the controlling Demand/Capacity ratios for bending moment, shear, and deflection were equal or below 0.90, although the deflection value was allowed to be somewhat higher but always less than or equal to 1.0. This is a good design practice to obtain maximum stresses below the admissible values, providing to the structure with a margin for extra capacity. Since deflections are not strictly required by the code, the Maximum/Admissible ratios for elastic deflections were restricted to values equal or lower to 1.0. Consequently, the design results obtained from CSiBridge package are accepted as adequate to be used in a parametric analysis for structural capacity degradation due to atmospheric corrosion.

7.4 Steel Bridge Load Rating According to AASHTO MBE

Bridge load rating analysis is performed to determine the safe live load capacity of a bridge under the conditions presented at the moment of rating. Load rating is a procedure to estimate the actual capacity of the bridge for safety considerations. As a federal requirement all states should perform load rating of their bridge inventory. The AASHTO Manual for Bridge Evaluation (MBE) (AASHTO, 2011) is the official document published by the AASHTO for current specifications on bridge load rating. According to the AASHTO MBE, bridges should be rated for design loads and legal loads. The design load rating is performed to be reported to the National Bridge Inventory (NBI). The legal load rating indicates whether a bridge should be posted or strengthened (AASHTO, 2011). Bridges are posted when the structural capacity has decreased beyond the prescribed limits.

The bridge structural capacity can decrease as the result of many factors, such as collision damage, corrosion, modification of the section, or additional dead load. When the section capacity decrease is due to atmospheric corrosion attack, the corrosion penetration reduces the section thicknesses, and hence reduces the bridge structural capacity. As a means to estimate the actual reduction of a bridge structural capacity, a load rating analysis was performed for a series of steel girder bridges. A parametric analysis of load rating for a series of steel girder bridges, varying some selected parameters, was performed in order to appreciate the influence of steel washing as an effective bridge maintenance activity. In this section are presented the details for the bridge load rating procedure on the selected bridges.

7.4.1 Load and Resistance Factor Rating (LRFR)

The Load and Resistance Factor Rating (LRFR) is a methodology developed to provide uniform reliability in bridge load ratings, load postings, and permit decisions (AASHTO, 2011). There are different live load models and evaluation criteria that can be used when evaluating a bridge condition by load rating. The live load models are comprised by the

design live load, legal loads, and permit loads. A bridge load rating can be performed for different purposes. Bridge load rating are required to provide information to the National Bridge Inventory (NBI), to estimate the safety live load a bridge resists, or supporting a bridge rehabilitation decision. The load rating methodology is constituted by three different procedures which have to be done in a sequential manner: 1) design load rating, 2) legal load rating, and 3) permit load rating.

Load rating is an engineering process to determine the live load capacity of a bridge. This capacity is expressed by a rating factor (RF), which is the ratio of a vehicular live load effect (moment or shear), when the bridge is under certain limit state, to the corresponding nominal bridge capacity. The load rating analysis offers an evaluation of the adequacy or inadequacy of a structural element to support the load (stresses) produced by the passage of a particular truck load. A rating factor greater than 1.0 indicates the element/structure is capable of supporting the stresses produced by the considered live load; otherwise it fails and some actions are required. For moment and shear capacity the most relevant analysis is the Strength I limit state. Therefore, the load rating analysis is performed on bridges considering this limit state, and the results are the rating factor for moment capacity (RF_m) and for shear capacity (RF_v). A detailed flow chart is provided by AASHTO (2012), showing the different steps followed when performing a bridge load rating, as it is presented in Figure 7.13.

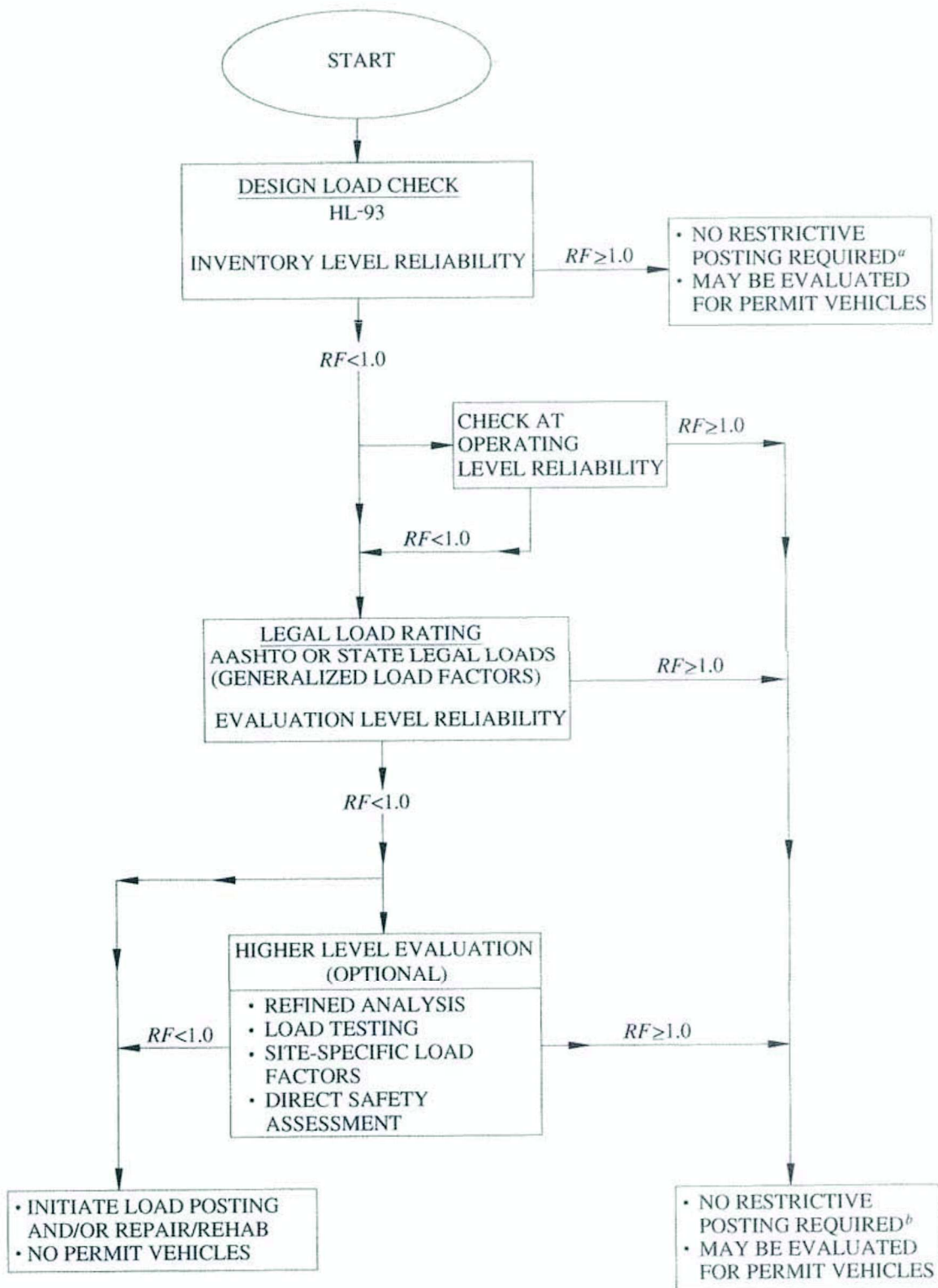


Figure 7.13: Load and resistance factor rating flow chart (AASHTO, 2011)

7.4.2 General Load-Rating Equation

The general AASHTO equation for the rating factor, RF, to be used in determining the load rating of a bridge member or connection under the effect of a single force, such as axial force, flexural moment, or shear force, is presented in Equation 7.6, and complemented by related Equations 7.7 to 7.9

$$RF = \frac{C - \gamma_{DC}(DC) - \gamma_{DW}(DW) \pm \gamma_P P}{\gamma_{LL}(LL + I)} \quad \text{Equation 7.6}$$

For the strength limit states:

$$C = \phi_c \phi_s \phi R_n \quad \text{Equation 7.7}$$

Where the following lower limit shall apply:

$$\phi_c \phi_s \geq 0.85 \quad \text{Equation 7.8}$$

For the service limit states:

$$C = f_R \quad \text{Equation 7.9}$$

where:

RF	=	Rating factor
C	=	Capacity
f_R	=	Allowable stress specified in the LRFD Specifications
R_n	=	Nominal member resistance (as inspected)
DC	=	Dead-load effect due to structural components and attachments
DW	=	Dead-load effect due to wearing surface and utilities
P	=	Permanent loads other than dead loads
LL	=	Live-load effect
IM	=	Dynamic load allowance
γ_{DC}	=	LRFD load factor for structural components and attachments
γ_{DW}	=	LRFD load factor for wearing surfaces and utilities

γ_P	=	LRFD load factor for permanent loads other than dead loads = 1.0
γ_{LL}	=	Evaluation live-load factor
ϕ_c	=	Condition factor
ϕ_s	=	System factor
ϕ	=	LRFD resistance factor

When the permanent loads other than dead loads, P , are not considered, the general equation is reduced to the Equation 7.10

$$RF = \frac{C - \gamma_{DC}(DC) - \gamma_{DW}(DW)}{\gamma_{LL}(LL + IM)} \quad \text{Equation 7.10}$$

Equation 7.10 was the expression used in this research to evaluate the load rating factor for the series of selected bridges. The load rating was performed to each applicable limit state and load effect, being the lowest value the controlling rating factor (AASHTO, 2011). According to AASHTO MBE (AASHTO, 2011) “The condition factor ϕ_c provides a reduction to account for the increased uncertainty in the resistance of deteriorated members and the likely increased future deterioration of these members during the period between inspection cycles. The condition factors are presented in AASHTO Table 6A.4.2.3-1. The system factors ϕ_s are multipliers applied to the nominal resistance to reflect the level of redundancy of the complete superstructure system. The system factors are presented in AASHTO Table 6A.4.2.4-1.” The resistant factor ϕ for bending and shear effects were taken as 1.0. The variability of load effects is included by the load factor γ , which is related to the uncertainties of load magnitude, loads position, and possible load combinations. As a limit state involves the effect of different load types and each load is estimated with different uncertainty, the total load effect is the sum of each load affected by its corresponding load factor. The load factors for load rating are presented in Table 6A.4.2.2-1 from the AASHTO MBE (2011).

7.4.3 Levels of Evaluation

The AASHTO MBE (2011) specifies three levels of live load rating, which have to be performed in a sequential manner, based on the owner needs. The first stage is the design-load rating, followed by the legal-load rating, and ending with the permit-load rating. The permit-load rating checks the safety and serviceability performance of a bridge under the passage of a special truck, exceeding the legal weight limitations. This is a very specialized bridge consideration that is not applicable to all bridges, and therefore, permit-load rating was not considered in this research. Therefore, only design-load and legal-load rating were performed in this study to all the considered bridge models.

7.4.3.1 Design-load rating

Design-load rating is the first level of evaluation of bridges and it is based on the HL-93 loading and the requirements from LRFD design standards. The assessment uses the actual section dimensions and material properties, as recorded during the most recent field inspection. This evaluation is a measure of performance of existing bridges to current LRFD bridge design standards. The live load rating at this stage can be performed at the same design level of reliability, known as Inventory level, for new bridges according to AASHTO LRFD (2012). Also the bridges can be assessed at a lower level of reliability equivalent to the Operating level, based on past load-rating practice. The design-load rating calculates Inventory and Operating rating factors for the LRFD-design live load HL-93. Strength I and Serviceability II limit states should be verified. The design live load HL-93 was presented in Figure 7.1.

7.4.3.2 Legal-load rating

Bridges without enough structural capacity under the design-load rating ($RF < 1.0$) should be analyzed for legal loads in order to establish the need for load posting or bridge repair or rehabilitation. Legal loads consist of:

- The AASHTO family of three legal loads (Type 3, Type 3S2 and Type 3-3) and lane type load, presented in Figure 7.14. The AASHTO legal vehicles and lane type load are used in load rating bridges for routine commercial traffic.
- The four specialized hauling vehicles (SHVs) presented in Figure 7.15, or the Notional rating load (NRL) which envelopes the SHVs configuration and is shown in Figure 7.16.
- Any specialized legal loads developed by individual states that are appropriate for use within their state and under their jurisdiction.

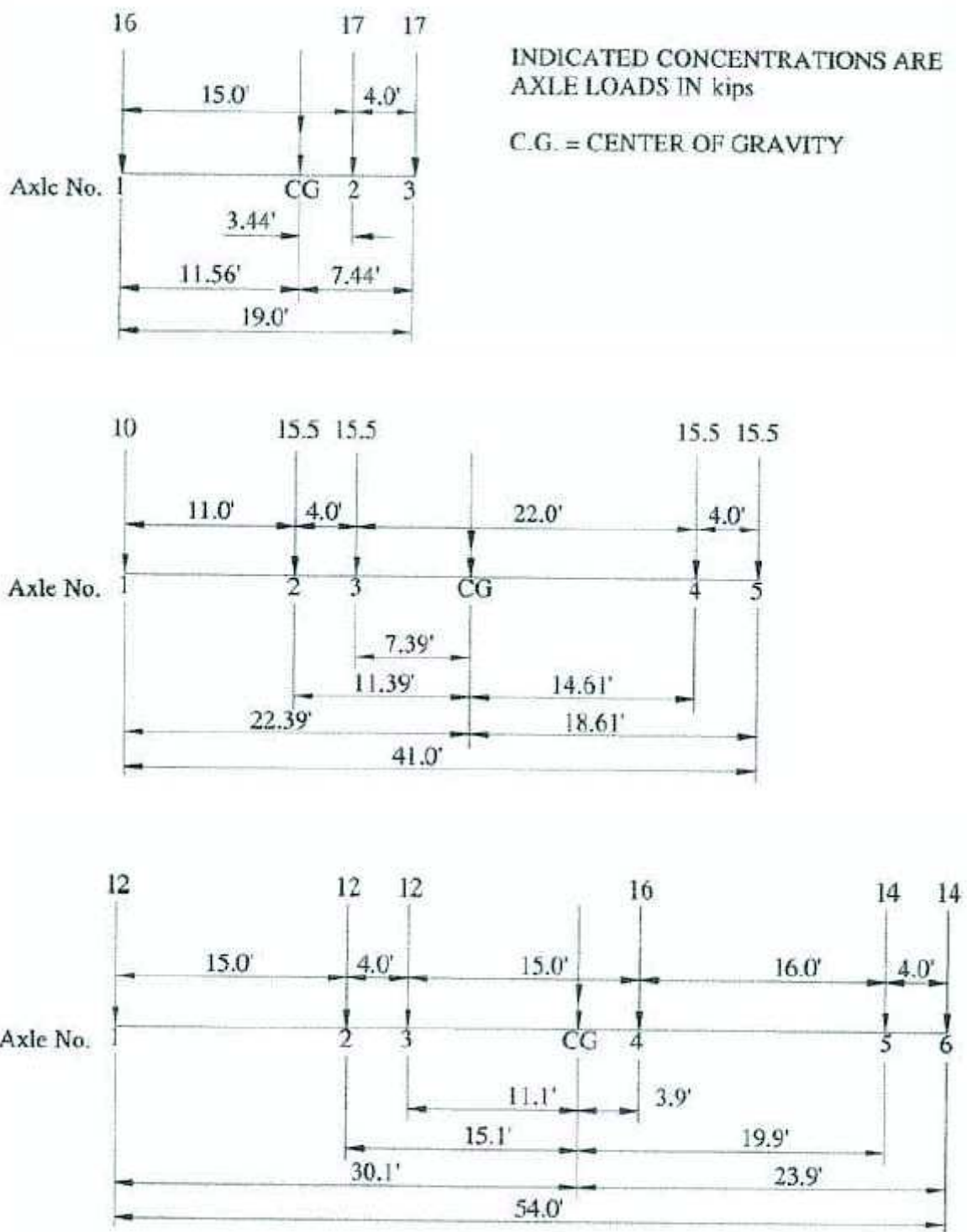


Figure 7.14: AASHTO legal trucks (AASHTO, 2011)

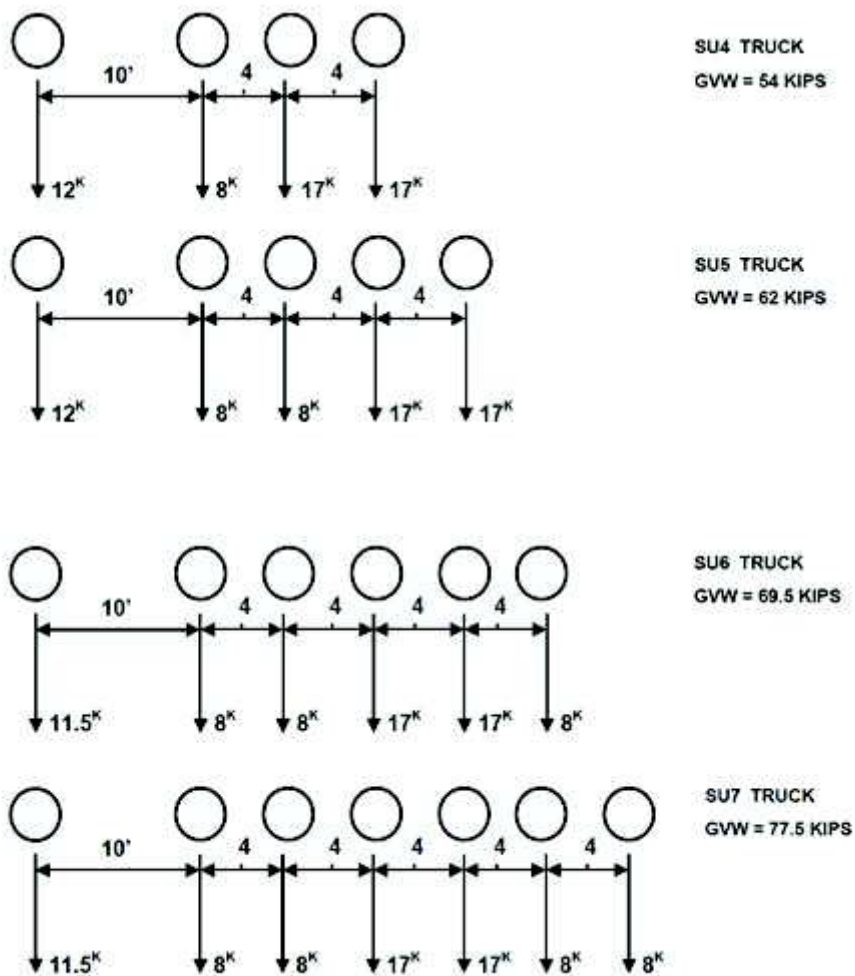


Figure 7.15: Bridge posting loads for single-unit SHVs (AASHTO, 2011)

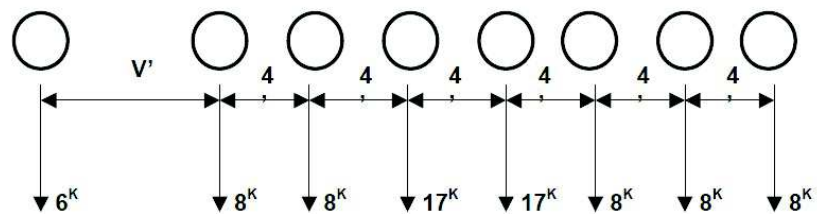


Figure 7.16: Notional rating load (AASHTO, 2011)

Strength I and Serviceability II limit states should be verified for legal-load rating. The live-load factors for legal-load rating at the Strength I limit state are a function of the average daily truck traffic (ADTT). An ADTT = 1000 was assumed for the typical selected bridges. Tables 7.8 and 7.9 show the corresponding factors. Higher or lower traffic volumes than the assumed ADTT of 1,000 would obviously produce somewhat different results.

Tabla 7.8: Generalized live load factors for commercial routine vehicles - Evaluation for strength I limit state (AASHTO, 2011)

Traffic Volume (One direction)	Load Factor for Type 3, Type 3S2, Type 3-3 and Lane Loads
Unknown	1.80
$ADTT \geq 5000$	1.80
$ADTT = 1000$	1.65
$ADTT \leq 100$	1.40

Tabla 7.9: Generalized live load factors for specialized hauling vehicles - Evaluation for strength I limit state (AASHTO, 2011)

Traffic Volume (One direction)	Load Factor for NRL, SU4, SU5, SU6, and SU7
Unknown	1.60
$ADTT \geq 5000$	1.60
$ADTT = 1000$	1.40
$ADTT \leq 100$	1.15

Linear interpolation is permitted for other ADTT.

7.4.4 Load Rating for Representative Bridges Considered

Steel I-girder bridges were evaluated for load rating using the three levels, inventory, operating, and legal, and following the procedure specified by the AASHTO MBE (2011). The four one-span and four two-span bridges presented in Figures 7.5 to 7.12

were assumed to experience structural degradation due to the effects of atmospheric corrosion attack. More specifically, the corrosion penetration and development was assumed to follow the corrosion models defined in Section 3.5, and the section reduction was evaluated throughout the bridge service life. The structural degradation over the bridge service life is evidenced by the reduction of thickness of the cross section, and the corresponding reduction in section properties such as the moment of inertia and radius of gyration.

To achieve wide evidence on the effect of corrosion, some bridge characteristics were varied. The typical eight composite steel bridges were analyzed considering two types of structural steel for the girders: uncoated carbon steel and uncoated weathering steel. Three typical local environments for highway bridges were considered: industrial/urban, marine, and rural. The bridges were analyzed under the two maintenance alternatives: periodic washing steel girder and no washing. Therefore, the eight typical composite steel bridges, analyzed for two structural steel types, three local environments, and two maintenance alternatives, resulted in $8 \times 2 \times 3 \times 2 = 96$ bridge cases under study. Additionally, the structural capacity degradation on the steel girders due to atmospheric corrosion was examined at five different periods over the 100 years bridge service life. Hence, each bridge case was load rated at ages 0, 20, 40, 60, 80, and 100 years of exposure. Consequently, the total parametric study resulted in 576 load rated analysis.

Given the large number of bridge cases to be analyzed and rated, a code system was implemented in order to identify each bridge case with a short nomenclature. Each bridge case was labeled by a 5-character code, a number followed by four capital letters. The first character is a number 1 or 2, indicating the bridge is one-span or two-span. The second character is a letter A, B, C, or D, corresponding to the span length of 70, 90, 110, or 130 feet respectively. The third character is a letter S or T, indicating the structural steel correspond to carbon steel or weathering steel. The fourth character is a letter I, M, or R, corresponding to the local environments Industrial/Urban, Marine, or Rural, respectively. The final character is a letter W or N, corresponding to the two maintenance

alternatives considered in the study, steel washing or no washing respectively. Based on that codification system, the 110'-110' two-span bridge, with uncoated carbon steel girders, exposed to industrial/urban environment, and under the steel no-washing maintenance alternative, was identified by the bridge code 2CSIN. This code system was used to identify each bridge in all generated graphs.

Each load rating analysis included the three evaluation levels mentioned previously: inventory, operating, and legal. No permit load rating was considered. The CSiBridge FE package was useful to automatize the structural analysis and load rating according to the AASHTO LRFD and AASHTO MBE, respectively. The structural analyses using CSiBridge provided the maximum values for bending moments, shear forces, and elastic deflections. The maximum values $M_{max}(+)$, $M_{max}(-)$, $V_{max}(+)$, $V_{max}(-)$, and Δ_{max} were incorporated into Excel spreadsheets designed to calculate the bending rating factor RF_m and the shear rating factor RF_v . Also, the ratio $\Delta_{max}/\Delta_{adm}$ corresponding to the maximum elastic deflection to the admissible deflection was evaluated.

Plots are used to compare bridge cases for the three levels of evaluation. The plots present the load rating factor corresponding to the bending and shear effects, for the inventory, operating, and legal loads, evaluated at ages 0, 20, 40, 60, 80, and 100 years. The plots show the rating value of 1.0 as a red line, which specifies the limit value for each rating factor. The critical case was when the legal load plot passes below the rating limit value of 1.0. In that case, the MBE code requires the bridge should be posted or programmed for repair or rehabilitation. As a typical example, the graphs shown in Figure 7.17 illustrate the load rating factors RF_m and RF_v for the bridge case 2CSIN.

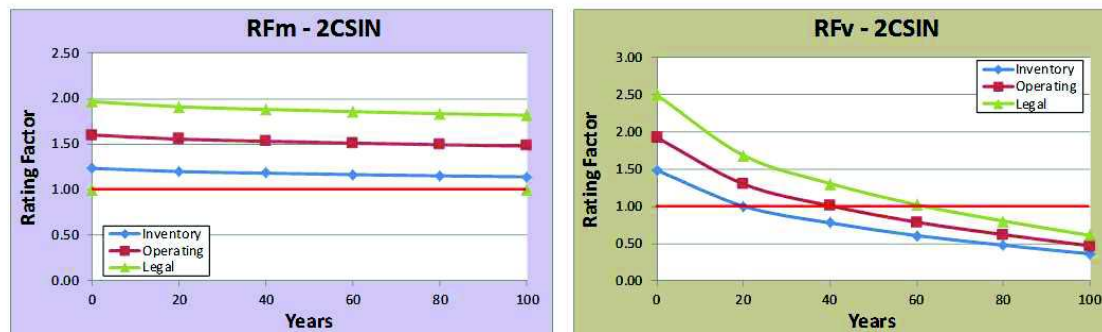


Figure 7.17: RFm and RFv versus time for bridge case 2CSIN

The plots corresponding to the load rating for all bridge cases and for the three levels of evaluation are presented in Appendix J. The results of these plots are discussed below.

The load rating process itself is not presented in this work. Detailed hand calculations of load rating for several bridges can be found in the AASHTO MBE (2011) Appendix A - Illustrative Examples.

7.5 Results and Discussion

Steel I-girder bridges were studied under the attack of atmospheric corrosion. The corrosion penetration rates over the bridge service life were estimated by extrapolation of values obtained through an accelerated corrosion process in the laboratory. The corrosion penetration was evaluated for different local environments, types of structural steel, and maintenance alternatives. Eight typical one-span and two-span composite steel I-girder highway bridges were designed according to AASHTO LRFD (2012). The typical bridges were then load rated according to AASHTO MBE (2011) at different ages, to analyze their structural capacity degradation due to the attack of atmospheric corrosion. Several bridge parameters were selected as variables in this study in order to achieve a more general pattern on the corrosion process of steel I-girder bridges. The study focused on the effect of steel washing as an effective bridge maintenance activity to reduce the atmospheric corrosion rates on steel girders.

The load rating analysis followed the requirements stipulated in the AASHTO MBE (2011), using the time dependent corrosion penetration rates, corrosion section model, typical steel highway bridges configuration, and structural parameters previously defined for this research. The basic procedure was to evaluate: 1) the thickness reduction for web and bottom flange of girder sections at selected ages (0, 20, 40, 60, 80, and 100 years), 2) the bridge section properties at selected ages, 3) the structural capacity for bending and shear effects at each selected age, and 4) the corresponding rating factors RF_m and RF_v at those selected ages. According to the AASHTO MBE (2011) a bridge should be posted when the maximum effect due to legal load exceeds the safe load capacity of a bridge member ($RF < 1.0$). In that case the bridge is allowed to service only to a maximum live load corresponding to the legal load times the legal rating factor (posting), otherwise the bridge should be closed for rehabilitation/repair. Legal loads to be analyzed were presented in the previous section. Posting a bridge can create serious restrictions and limit the passage of truck traffic.

The parametric load rating analysis on the selected bridge cases included the following variables: number of spans (one or two), span length (70, 90, 110, and 130 feet), steel type (carbon steel or weathering steel), local environment (Industrial/urban, Marine, and Rural), and maintenance alternative (steel washing or no washing). These variables were applied to the typical eight bridge models selected. The data obtained from the load rating analyses were processed and evaluated using spreadsheets from Microsoft Excel. This tool was used to process the abundant data from each bridge analysis at each defined age, such as: 1) section properties, 2) maximum moment and shear effects, and maximum elastic deflections due to dead load DC1, DC2, and DW, 3) maximum moment and shear effects, and maximum elastic deflections due to live load LL+IM for operating loads, inventory loads, and legal loads, and 4) nominal moment and shear capacity, and permissible elastic deflections. The final results were the values of rating factors for bending and shear effects RF_m and RF_v respectively, for each load level (inventory, operating, and legal) and at each selected age. After all calculations were completed, the

results were processed and summarized in a series of plots, which are shown in Appendix J. Some trends and interpretations for the results are summarized below.

7.5.1 Effect of Stress Type

The reduction of moment and shear capacities due to atmospheric corrosion attack was observed in all of the load rating analyses. In general, it was found that the bridge bending capacity reduces at a low rate during its service life. In contrast, the bridge shear capacity was found to reduce faster over time. The design conditions of the typical bridge sections utilized elements that were compact sections, with slenderness ratios lower than the maximum values prescribed by the AASHTO LRFD Specifications. The selected bridge cases were analyzed at different ages of their service lives, showing incremental progress of the corrosion penetration with time, and consequently, a reduction on the thicknesses of the section. The corrosion process changed the initial condition of some elements, as the slenderness ratios of web and flanges. Three important facts on the steel girders design and the atmospheric corrosion attack were: 1) the web thickness was always thinner than the flanges thickness, 2) the section deterioration model considered corrosion on both web faces, and 3) the section deterioration model considered flange corrosion only on the top faces of the bottom flange. The assumed corrosion behavior reduced dramatically the section shear capacity, mainly provided by the web area. On the other hand, the bottom flange thickness reduced considerably less than that of the web. As a consequence, the section moment capacity, which is mainly generated by the flanges area, was reduced at a lower rate.

Figure 7.18 presents the RF_m and RF_v factors due to bending and shear stresses respectively, for the three levels of evaluation: inventory, operating, and legal, and for the two steel types considered. In Figure 7.18 (left) the results are presented for the rating analysis for the bridge case 1ASIN (one-span, 70' span length, carbon steel type, industrial/urban local environment, and no washing alternative), while in Figure 7.18 (right) the corresponding results are shown for bridge 1ASIW, which is equivalent to the

previous bridge case, but for the steel washing alternative. Figure 7.18 (left and right) illustrate how quickly the RFv (solid line) decrease with time in comparison to RFm (dotted line) reduction. The RFv reduction for the three levels of evaluation show a similar pattern, with the three curves quite parallel. As indicated, the RFm reduces at a lower rate but they also present a similar pattern, with the three curves almost parallel.

In Figure 7.19 (left) the load rating results for the bridge case 2CTMN (two-span, 110'-110' span length, weathering steel, marine local environment, and no washing alternative) are shown. Figure 7.19 (right) meanwhile shows the results for bridge case 2CTMW, which is the same as the previous bridge but for the steel washing alternative. The two bridge cases presented in Figure 7.19 included different parameters than those presented in Figure 7.18, but still demonstrate the same pattern, with RFv (solid line) reducing more rapidly with time than RFm (dotted line), and with rating curves almost parallel as noted in Figure 7.18. The parallel pattern for RFm and RFv curves was marked by the difference on the bridge structural capacity at age zero. This pattern was the same for both one-span and two-span bridge cases.

In the four cases presented in Figures 7.18 and 7.19, it can be seen that the rating factors for inventory level were the lowest, followed by the operating rating factors, and lastly by the legal rating factors, which were the highest values. This pattern remained the same in all the analyzed cases, as expected, since the inventory level was the most demanding evaluation, followed for the operating level, and ending with the legal level as the least demanding. Based on this general pattern, the rest of analyses were performed only focusing on the RFm and RFv factors for legal-load level, since this is the trigger level for posting or closing a bridge for repair/rehabilitation. The bending capacity reduced at a very low rate, and consequently the RFm parameter never reached the limit value of 1.0 during the entire bridge service life. At the other hand, the shear capacity drooped at a deep ratio, and hence the RFv parameter reached the limit of 1.0 for several bridge cases. Therefore, the shear capacity degradation, expressed by the drop of the RFv parameter, is analyzed in more detail in the next sections.

Figures 7.18 and 7.19 showed that the steel washing alternative (1ASIW and 2CTMW) generated higher rating factors due to both bending and shear stresses than the no washing alternatives (1ASIN and 2CTMN). A similar trend was also observed for all other bridge cases studied. Therefore, the steel washing alternative reduces the rates of capacity degradation due to atmospheric corrosion.

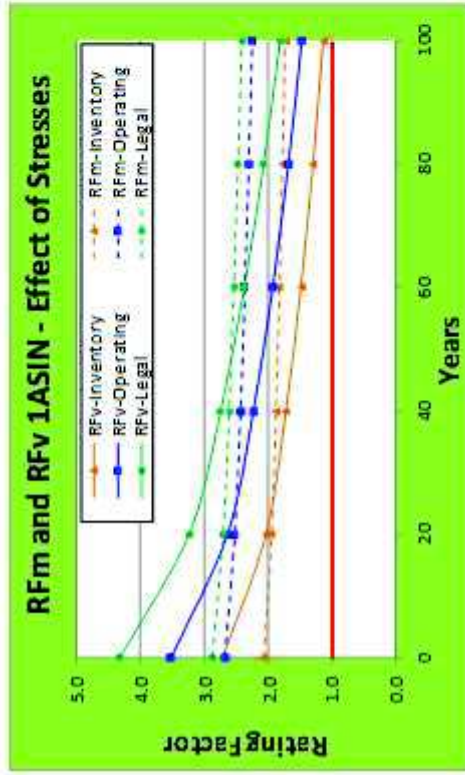
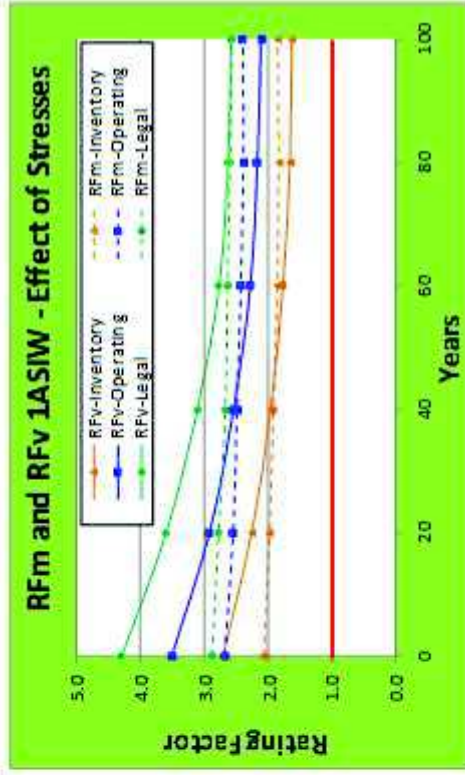


Figure 7.18: RFm and RFv variation on time (inventory, operating, legal) – Cases 1ASIN and 1ASIW

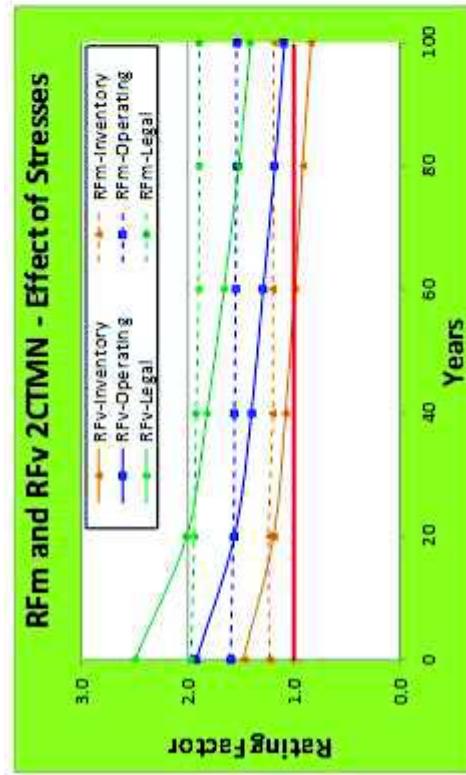
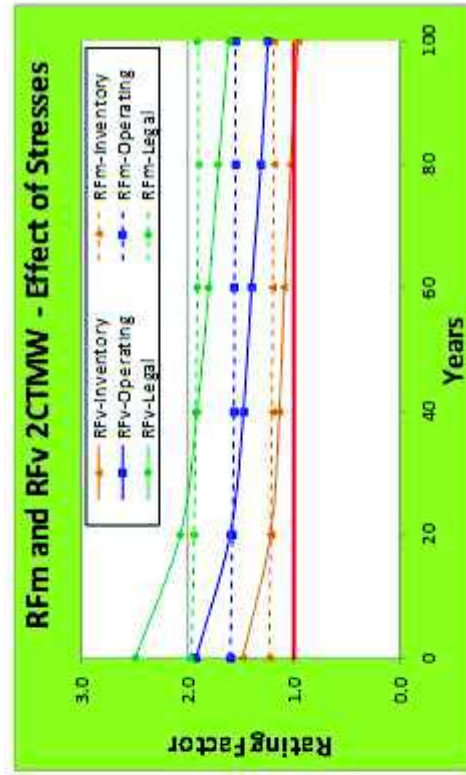


Figure 7.19: RFm and RFv variation on time (inventory, operating, legal) – Cases 2CTMN and 2CTMW

7.5.2 Effect of Local Environment

A general pattern for all bridge cases analyzed in this study showed that local industrial/urban environment always produced the higher structural capacity degradation for both bending and shear effects due to atmospheric corrosion attack. The local marine environment resulted in the second most aggressive local environment for both bending and shear effects. The local rural environment was the least aggressive condition for all analyzed cases.

Figure 7.20 shows the plots for RFv factors for two sets of bridge cases from weathering steel and for legal load level. One set conformed to the three bridge cases (1AT_N, solid lines) corresponding to bridge cases of one-span, 70' span length, weathering steel type, no washing alternative, and exposed to the three possible environments: industrial/urban, marine, or rural. The second set of bridge cases correspond to the same three previous bridge cases indicated, but for the steel washing alternative (1AT_W, dotted lines). The plots show a general pattern for the six considered cases, with industrial/marine as the most aggressive environment, followed by the marine environment, and the rural environment as the less aggressive local environment.

Figure 7.21 shows the plots for RFv factors for two more sets of bridge from cases from carbon steel and for legal load level. One set consisted by the three bridge cases (2BT_N, solid lines) corresponding to bridge cases of two-span, 90' equal span length, weathering steel type, no washing alternative, and exposed to the three possible environments: industrial/urban, marine, or rural. The second set of bridge cases correspond to the same three previous bridge cases indicated, but for the steel washing alternative (2BT_W, dotted lines). The plots show the same general pattern as in Figure 7.20, with industrial/urban as the most aggressive environment, followed by the marine environment, and the rural environment as the less aggressive environment.

Figures 7.20 and 7.21 show that steel washing alternative always resulted in higher rating factors than the no washing alternative for all bridge cases analyzed. For both types of steel, carbon and weathering steel, the washing alternative always produced lower corrosion degradation, which is expressed by higher rating factors RFv than the no washing alternative. Therefore, the steel washing alternative reduces the rates on structural capacity degradation due to atmospheric corrosion.

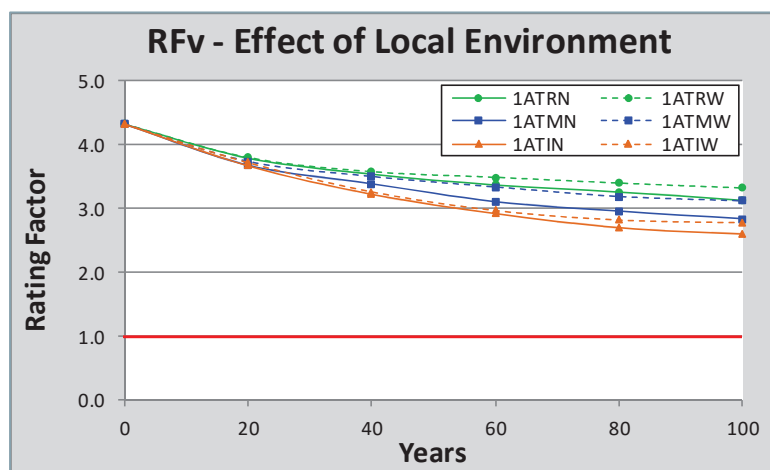


Figure 7.20: RFv versus time for bridge cases 1AT_N/W and for the three local environments

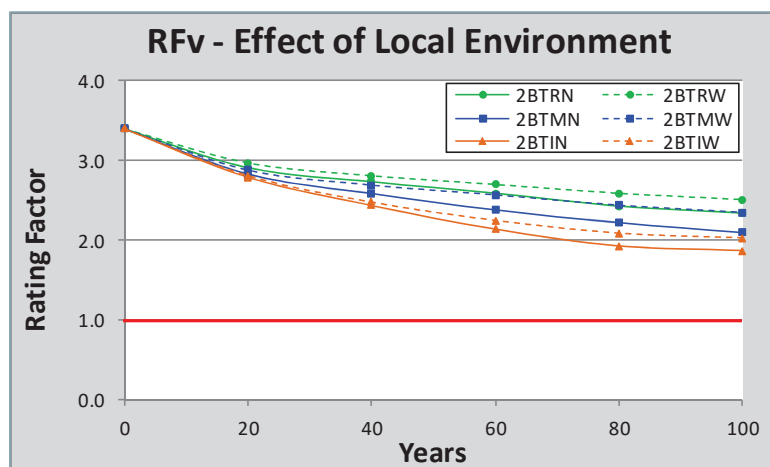


Figure 7.21: RFv versus time for bridge cases 2BT_N/W and for the three local environments

7.5.3 Effect of Number of Spans

The number of spans showed no influence when comparing the rating factor RF_v for bridge cases of one-span and two-span, carbon and weathering steel, exposed to atmospheric corrosion, and at legal load level. In general, the structural capacity degradation for a bridge of one or two-spans was very similar for the span lengths investigated. Two sets, of four bridge cases each, were selected to show the influence of number of spans in the structural capacity degradation due to corrosion. One set was constituted by bridge cases with a one-span configuration, no washing alternative, and varying the other parameters such as: span length, steel types, and local environment (only industrial/urban and marine). The bridge cases selected were 1ASIN, 1BTMN, 1CSIN, and 1DTMN. The second set of bridge cases were similar to the first set, but for the two equal spans configuration. Hence, the second set included the bridge cases 2ASIN, 2BTMN, 2CSIN, and 2DTMN. Both set of four pairs were evaluated to the legal load level.

Figure 7.22 shows the plots for the rating factors RF_v corresponding to the two sets of selected bridge cases for the no washing alternative. It can be observed in Figure 7.22 that the structural capacity degradation due to shear, expressed as the RF_v variation, follows a pattern very similar for each pair of bridge case, for one-span (solid lines) and two-span (dotted lines) cases. The difference between each pair of curves, for one and two spans cases is minimal, and it is due to the initial structural capacity, at age zero. When the initial structural capacity is similar for the same bridge of one or two spans, the corresponding two curves for rating factor RF_v are almost coincident.

In Figure 7.23 the shear rating factors RF_v for the same two sets of bridge cases previously analyzed are shown, but in this case for the steel washing alternative. Again, the pattern observed in Figure 7.22 is repeated in Figure 7.23, in that the structural capacity degradation follows a similar pattern for the one-span and two-span configurations. From Figures 7.22 and 7.23 can be concluded that the number of spans have no influence in the structural capacity degradation pattern for the range of typical

spans investigated. The parallel pattern for RFv curves corresponding to one-span and two-span bridge cases is marked by the difference on the initial structural capacity at age zero.

Lastly, and most significant, it can be noted that by comparing Figures 7.22 and 7.23 it can be observed that the bridge cases for the steel washing alternative consistently produced rating factors RFv higher than the no washing alternative. A detailed analysis for bridge cases 1CSIN and 2CSIN shows that both cases have almost the same trace, which means both deteriorate at the same rate during their service life. This is so because both cases had the same initial structural capacity. In the same way, the other pair of cases (1ASIN-2ASIN, 1BTMN-2BTMN, and 1DTMN-2DTMN) show a trace almost parallel, which is explained by the difference in their initial structural capacity at year zero -the beginning of their service life. In other words, if each pair of cases had had the same initial structural capacity, their structural capacity degradation would have been almost similar throughout their entire service life. Therefore, it appears that regular washing of the steel structure reduces the rates of capacity degradation due to atmospheric corrosion, regardless the number of spans.

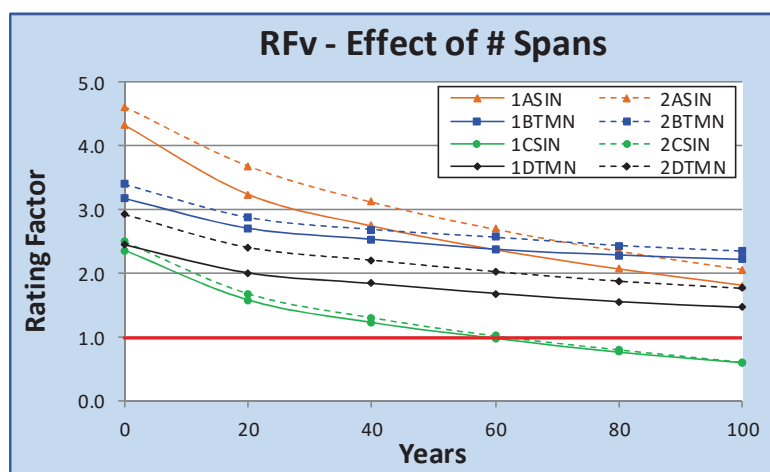


Figure 7.22: RFv for one-span and two-span configurations and no washing alternative

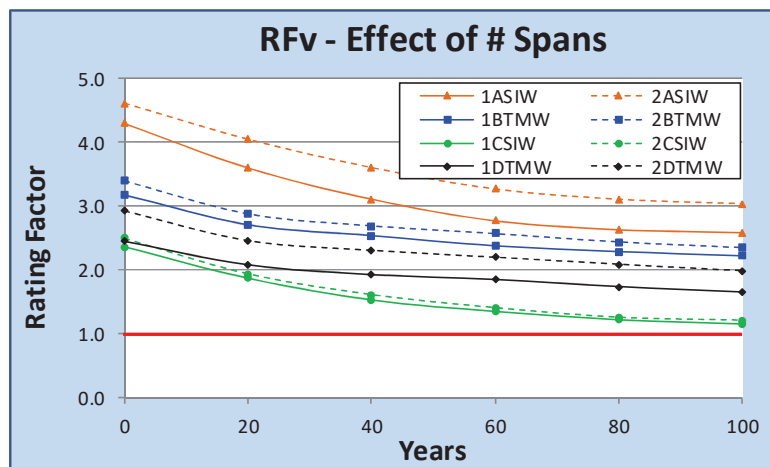


Figure 7.23: RFv for one-span and two-span configurations and steel washing alternative

7.5.4 Effect of Span Length

Minimal effects on RFv were observed when the span length was varied for one and two span bridges, while holding the other bridge parameters constant. Two sets, of four bridge cases each, were selected to show the influence of span length in the structural capacity degradation due to corrosion. One set was constituted by bridge cases with a one-span configuration, carbon steel type, exposed to industrial/urban environment, no washing alternative, and varying the span length, to 70, 90, 110, and 130 feet, corresponding to cases 1ASIN, 1BSIN, 1CSIN, and 1DSIN. The second set of bridge cases were similar to the first set, but for the washing alternative. Hence, the second set included the bridge cases 1ASIW, 1BSIW, 1CSIW, and 1DSIW.

Figure 7.24 shows the plots for the rating factors RFv corresponding to the two sets of bridge cases indicated. In Figure 7.24 can be seen that the structural capacity degradation due to shear, expressed as the RFv variation, follows a pattern very similar for the four bridge cases corresponding to the no washing alternative (solid lines). The difference between the four corresponding curves is marked by the initial structural capacity at age zero. The RFv curves for the second set of bridge cases presented in Figure 7.24, and corresponding to the washing alternative, showed also a similar pattern between them.

Two more sets of bridge cases were analyzed, consisting of the same sets previously studied, but for the two-span configuration. Figure 7.25 shows the plots for the two sets of bridge cases for the two-span configuration. Again, the same pattern identified in Figure 7.24 is repeated for the bridge cases presented in Figure 7.25. The four curves corresponding to the no washing alternative (solid lines) were almost parallel to each other. The four curves for the steel washing alternative (dotted lines) in Figure 7.25 also followed the same pattern between them. From Figures 7.24 and 7.25 it can be concluded that the span length has no influence in the rates of structural capacity degradation since the curves are mostly parallel to each other. However, the shift in the parallel pattern for RFv curves corresponds to different span length cases and reflects the difference in the initial structural capacity at age zero. That pattern is valid for both one-span and two-span configurations. Both set of four pairs were evaluated to the legal load level.

In both Figure 7.24 and Figure 7.25 it can be observed that the steel washing alternative always produced rating factors RFv higher than the no washing alternatives. Therefore, the steel washing alternative reduces the rates on capacity degradation due to atmospheric corrosion.

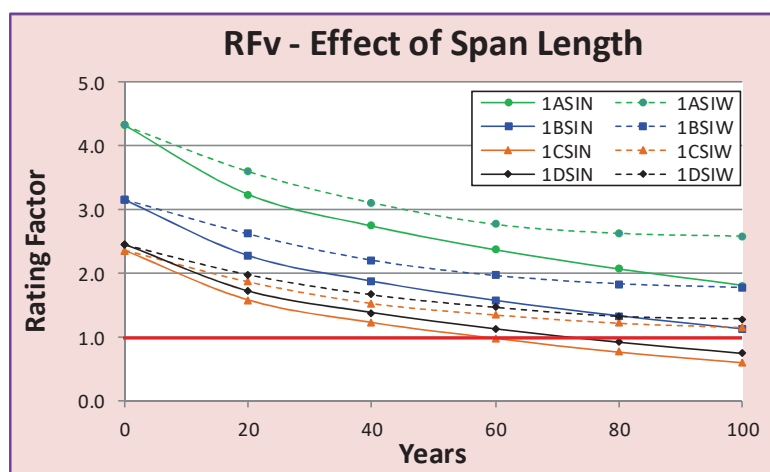


Figure 7.24: RFv vs. time for bridge cases of one-span (70', 90', 110', and 130')

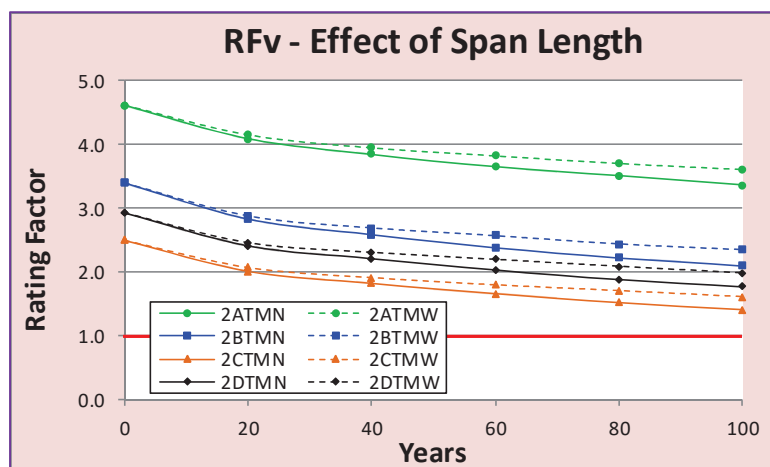


Figure 7.25: RFv vs. time for bridge cases of two-span (70', 90', 110', and 130')

7.5.5 Effect of Steel Type

The steel type showed a marked influence in the structural capacity degradation of bridges exposed to atmospheric corrosion. In general, for all of the considered bridge cases, carbon steel girders showed a higher rate of corrosion than weathering steel girders. Consequently, a more significant shear capacity degradation, expressed by the decrement of rating factors RFv, was found on carbon steel girder bridges in comparison to weathering steel girder bridges. Two identically designed bridges, one built with carbon steel and the other with weathering steel behave differently when exposed to atmospheric corrosion attack. Data obtained in this research confirmed that weathering steel showed more resistant capacity to corrosion than carbon steel.

Four pairs of bridge cases were selected for the analysis on the influence of steel type on the structural capacity degradation due to atmospheric corrosion attack. One pair of bridges consisted of the one-span, 70 feet span length, exposed to industrial/urban environment, and no washing alternative, for both carbon and weathering steel. The other three pairs were similar to the first pair described, but for 90, 110, and 130 feet span lengths. The rating factor RFv curves for the four pairs of bridge cases are presented in Figure 7.26, where the cases for the carbon steel showed the same pattern between them, with a trace of one curve almost parallel to all other curves. The weathering steel cases

also has a very similar pattern between them. Clearly, from Figure 7.26 it is observed that a bridge case corresponding to carbon steel girders (solid line) exhibited lower rating factors RF_v , than the same bridge case with weathering steel girders (dotted line).

An additional four pairs of bridge cases were selected to study the effect of steel type on the structural capacity degradation due to atmospheric corrosion attack for the two-span configuration. The same four pairs of bridge cases previously presented but for the steel washing alternative are shown in Figure 7.27, with the cases for carbon steel in solid lines and weathering steel in dotted lines. It can be seen that a bridge case corresponding to carbon steel girders (solid line) presented lower rating factors RF_v than the same bridge case with weathering steel girders (dotted line). From Figures 7.26 and 7.27 can be concluded that weathering steel offers better resistance to atmospheric corrosion attack over the entire bridge service life than plain carbon steel. Both set of four pairs were evaluated to the legal load level.

As before, it can be observed when compared Figure 7.26 and Figure 7.27 that the bridge cases for the steel washing alternative produced greater rating factors RF_v than the no washing alternatives. Therefore, it can be concluded that the steel washing alternative reduces the rates of capacity degradation due to atmospheric corrosion.

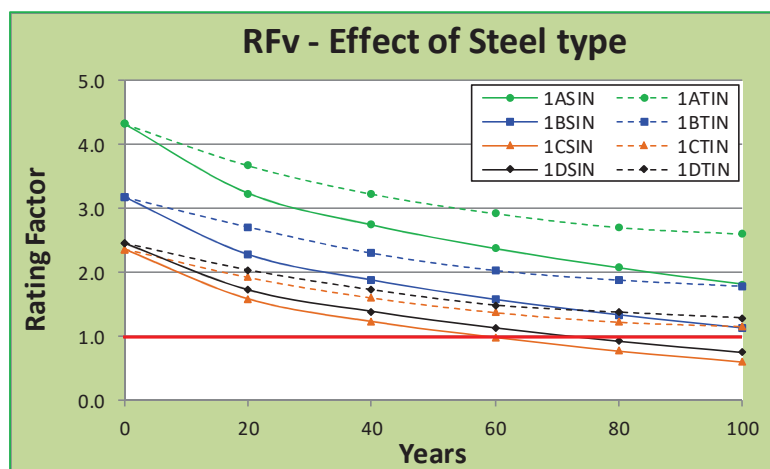


Figure 7.26: RFv versus time for bridge cases 1_SIN and 1_TIN

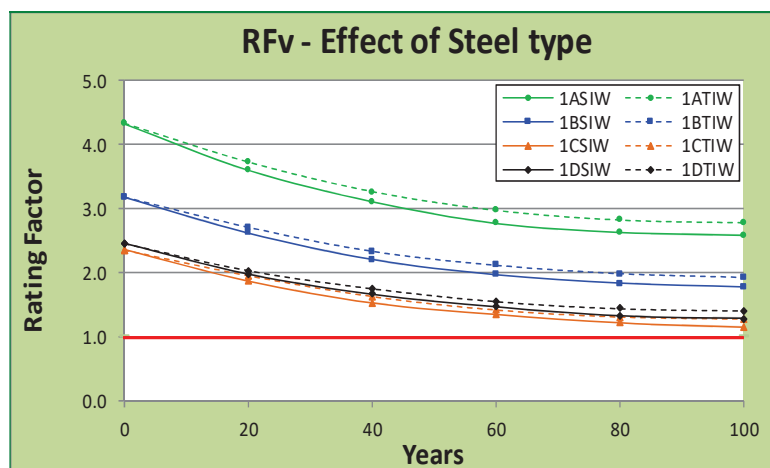


Figure 7.27: RFv versus time for bridge cases 1_SIW and 1_TIW

7.5.6 Effect on Live-Load Deflections

The limits for live-load elastic deflections are optional, according to the AASHTO LRFD (2012), unless required according to the bridge's owner considerations. As another reference for structural capacity degradation, the elastic deflections were calculated for all bridge cases considered in this study. Therefore, the structural analysis of the corroded steel girder bridges during their service lives included the evaluation of live-load deflections. The AASHTO LRFD (2012) Specifications prescribe that live-load

deflections should be limited to $L/800$ for vehicular bridges, where L is the span length. This limit is intended to ensure reduced vibrations on the structure, avoiding unpleasant sensations for vehicle users (not for pedestrians). The live-load for deflection evaluation was previously described. For the selected bridge cases, the design truck alone always produced the maximum deflections. The results in this study showed that the structural capacity degradation on the analyzed bridge cases also produced a corresponding increase of live-load deflections. This is a consequence of the girders cross section reduction, and the corresponding change in elastic section properties.

Figure 7.28 (left) shows the live-load elastic deflections for two sets of bridge cases. One set consisted of the four bridges 1_SIN, one-span, 70, 90, 110 or 130 feet span length, girders from carbon steel type, exposed to industrial/urban environment, and no washing alternative (solid line). The other set of bridges was similar to the first set, but for the steel washing alternative 1_SIW (dotted line). Both sets of curves illustrate the increment of elastic deflections due to live-load over the entire bridge service life. All four curves corresponding to the same set of bridges are quite similar, with a difference marked by their initial deflection at age zero. Hence, the rates for the increments of deflections over time are similar for all bridges belonging to the same set, regardless the span length. In Figure 7.28 (right) the deflection curves corresponding to bridge cases 1CSIN/W and 1DSIN/W in an enlarged scale are shown, illustrating in more detail the increment of live-load deflections over time.

Figure 7.29 (left) presents the live-load deflections for two sets of bridge cases for the two-span configuration. The bridge cases 2_SIN for 70, 90, 110, and 130 feet span length (solid line) and the set of bridge cases 2_SIW, similar to the previously indicated bridges but for the steel washing option (dotted line) are shown in the plot. Figure 7.29 (left) shows the two sets have the same pattern found in Figure 7.28 (left). The elastic live-load deflections increase over time and the deflection curves from the same set of curves are similar. As before, Figure 7.29 (right) illustrates the curves corresponding to

bridge cases 2CSIN/W and 2DSIN/W in an enlarged scale, where more detail of the increment of live-load deflections over time can be observed.

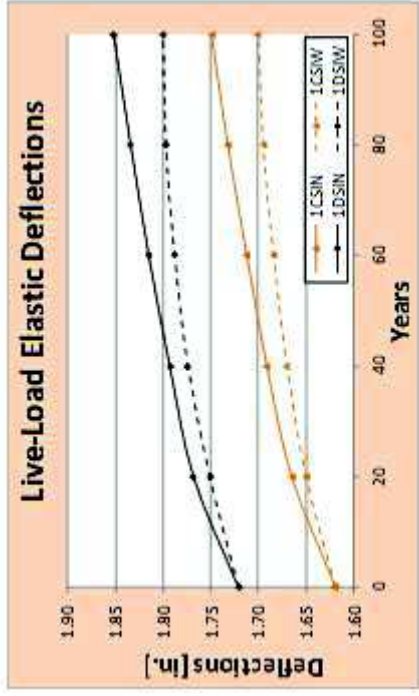
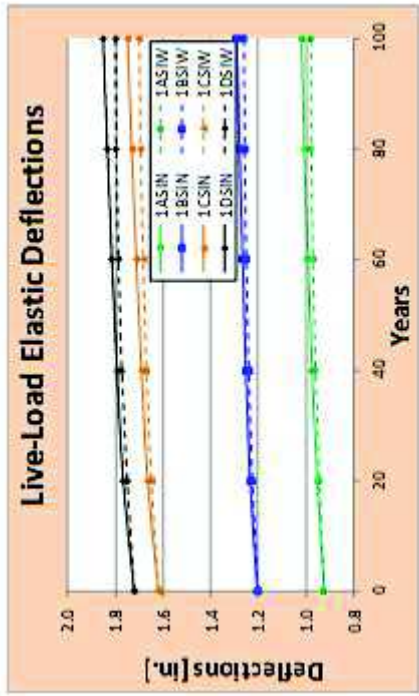


Figure 7.28: Live-load elastic deflections versus time for cases 1_SIN and 1_SIW

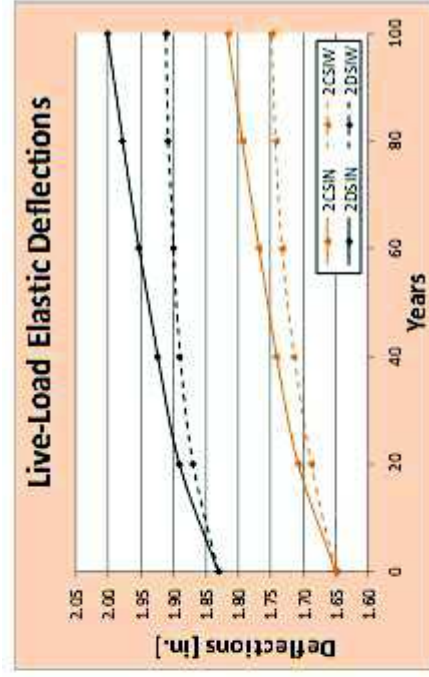
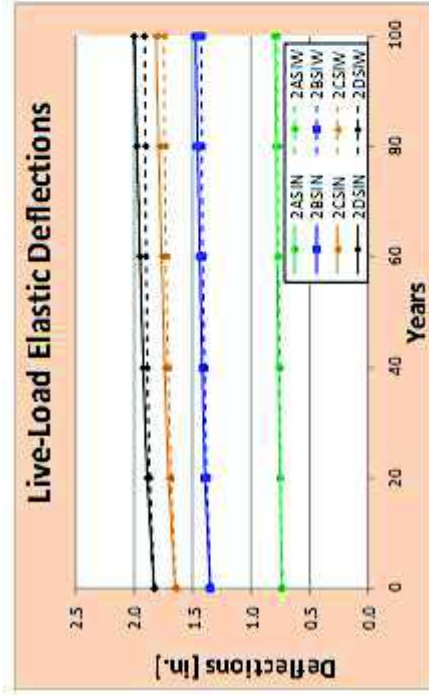


Figure 7.29: Live-load elastic deflections versus time for bridge 2_SIN and 2_SIW

7.5.7 Effect of Maintenance Alternative

The maintenance alternative has a notable effect on the structural capacity degradation of steel girder bridges exposed to atmospheric corrosion attack. From the analysis of all 96 bridge cases, the steel washing alternative always resulted in higher rating factors RF_v than those corresponding to the no washing alternative. From the facts found in this research it can be concluded that the steel washing alternative reduces the penetration corrosion rates on the steel girders, and therefore, reduces the structural capacity degradation of steel girders in comparison to the no washing alternative.

Figure 7.30 presents the rating factors RF_v corresponding to bridge cases 1CSIN/W (left) and 2CSIN/W (right). The bridge cases 1CSIN and 2CSIN, for the no washing alternative (solid line), always resulted in lower RF_v values than the corresponding steel washing alternatives 1CSIW and 2CSIW (dotted line). In Figure 7.30 (left) can be noticed that the 1CSIN bridge reached the legal rating limit of 1.0 at approximate 58 years of service bridge. Therefore, at age 58 the 1CSIN bridge should be posted or rehabilitation - repair work should be initiated. In the same Figure 7.30 (left) is plotted the rating factor RF_v for bridge case 1CSIW, and can be noticed that the legal rating factor did not reach the limit of 1.0 during the entire bridge service life. Consequently, the bridge case 1CSIW did not required to be posted or closed for rehabilitation/repair due to atmospheric corrosion attack during its service life.

In Figure 7.30 (right) are plotted the rating factors RF_v for the bridge cases 2CSIN and 2CSIW, which are similar to the bridge cases plotted at the left, but for the 2-span configuration. The pattern for bridge cases 2CSIN and 2CSIW were similar to their equivalent one-span bridge cases. Figure 7.30 (right) shows that bridge 2CSIN reached the legal rating limit of 1.0 at approximate 61 years of service life. Then, at age 61 the bridge case 2CSIN should be posted or closed for rehabilitation/repair. Figure 7.30 (right) also shows the rating factor RF_v for bridge case 2CSIW, which did not reach the

legal rating limit of 1.0 during the entire service life. As a consequence, bridge 2CSIW did not need to be posted or closed.

Figure 7.31 presents the rating factors RF_v corresponding to bridge cases 1DSIN/W (left) and 2DSIN/W (right). The bridge case 1DSIN and 2DSIN, for the no washing alternative (solid line), always resulted in lower RF_v values than the corresponding steel washing alternatives 1DSIW and 2DSIW (dotted line). In Figure 7.31 (left) it can be noticed that the 1DSIN bridge reached the legal rating limit of 1.0 at approximate 70 years of service bridge. Therefore, at age 70 the 1DSIN bridge should be posted or rehabilitation - repair work initiated. In the same Figure 7.31 (left) is plotted the rating factor RF_v for bridge case 1DSIW, and can be noticed that the legal rating factor did not reach the limit of 1.0 during the entire bridge service life. Consequently, the bridge case 1DSIW did not required to be posted or closed for rehabilitation/repair due to atmospheric corrosion attack during its entire service life.

In Figure 7.31 (right) are plotted the rating factors RF_v for the bridge cases 2DSIN and 2DSIW, which are similar to the bridge cases plotted at the left, but for the 2-span configuration. The pattern for bridge cases 2DSIN and 2DSIW were similar to their equivalent one-span bridge cases. Figure 7.31 (right) shows that bridge 2DSIN reached the legal rating limit of 1.0 at approximate 92 years of service life. Then, at age 92 the bridge case 2DSIN should be posted or closed for rehabilitation/repair. Figure 7.31 (right) also shows the rating factor RF_v for bridge case 2DSIW, which did not reach the legal rating limit of 1.0 during the entire service life. As a consequence, bridge 2DSIW did not need to be posted or closed.

Figures 7.30 and 7.31 show typical plots related to RF_v factors for similar bridge cases for both alternatives: steel washing and no washing. In those figures it can be observed that for all bridge cases the steel washing alternative produced rating factors RF_v higher than the no washing alternative. This pattern remained the same for all the bridge cases

considered in this study. Therefore, the steel washing alternative on steel highway bridges reduces the rates on capacity degradation due to atmospheric corrosion attack.

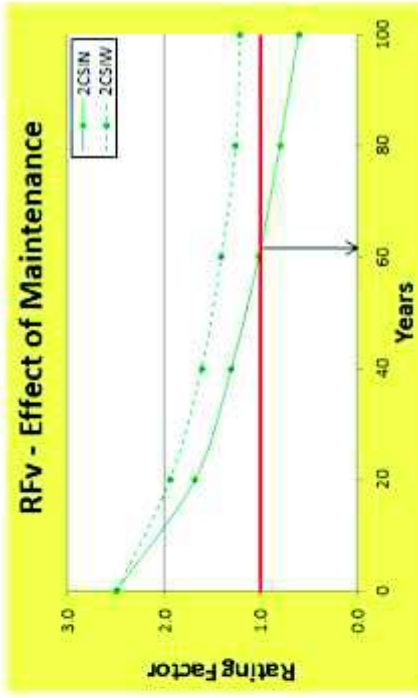


Figure 7.30: RFv versus time for bridge cases 1CSIN/W and 2CSIN/W

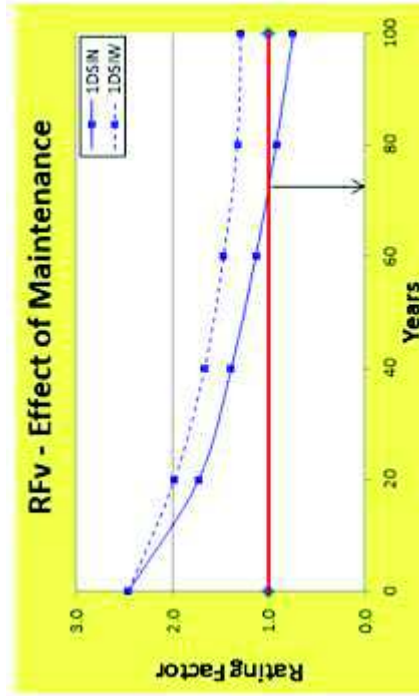
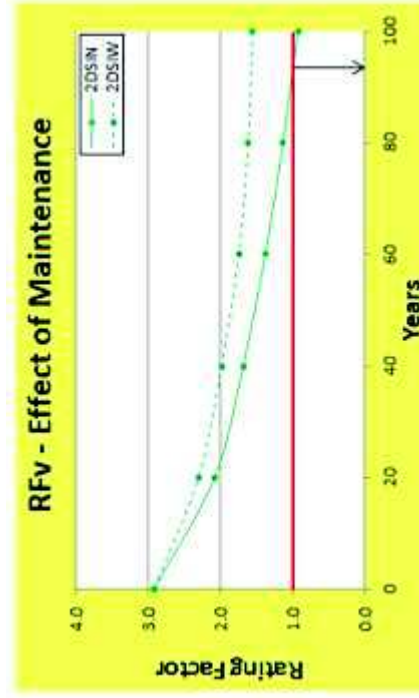
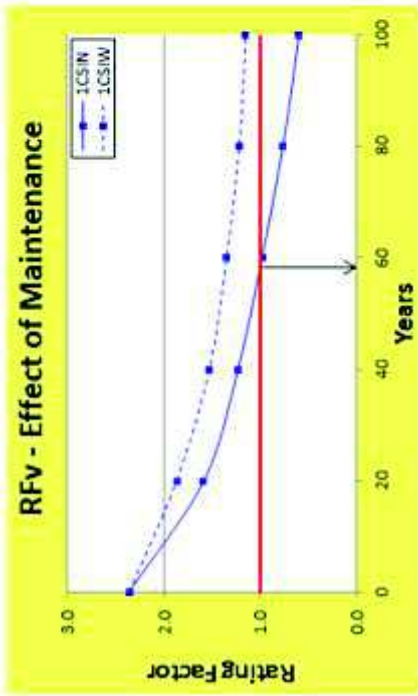


Figure 7.31: RFv versus time for bridge cases 1DSIN/W and 2DSIN/W

In this chapter have been analyzed the effects of all different variables considered in the parametric study. It was analyzed the structural capacity degradation of steel girder highway bridges due to atmospheric corrosion attack. The analyses considered both no washing and steel bridge washing alternatives. The vast data acquired in this research supports the statement that steel washing is an effective bridge maintenance activity, reducing the structural capacity degradation of steel girder highway bridges. The steel washing alternative resulted in a better option by reducing the rate of structural capacity degradation when compared to the no washing option for all variables included in this parametric study.

CHAPTER 8. ECONOMIC EVALUATION OF CORRODED STEEL BRIDGES

8.1 Introduction

Economic evaluation of steel bridges is an analysis of future-value cash-flows, representing all expenditures required to operate a bridge under the expected conditions of serviceability. For the case of corroded steel bridges, the analysis should deal with appropriate measures, and their respective costs, to control or fix the corrosion problem with the aim of achieving the expected bridge service life.

“The cost of keeping a bridge in a safe and good condition is not a one-time expenditure based on the initial cost of construction” (Bowman and Moran, 2015). The cost of operating a bridge in good condition requires a long-term investment during the entire expected service life (Hema et al., 2004). Due to normal exposure and operation, all bridges experience a deterioration process. As a consequence, all bridge members experience physical and mechanical changes over their service life, thereby resulting in a decline in the bridge service condition and a corresponding reduction in structural capacity (Abed-Al-Rahim and Johnston, 1995). One of the most dangerous changes for steel bridge members is the loss of section due to corrosion attack. Knowledge of the section loss rate of the steel bridge members is critical to reliably predict the bridge service life.

To achieve the expected bridge service life, all elements of the structure should receive appropriate maintenance, rehabilitation, and repairs, which can be provided applying different strategies. The strategy selection is based on the transportation agencies' expectations on bridge service life, the costs of possible strategies, and the available

resources to be used (Hawk, 2003). Bridge maintenance activities are performed based on their effectiveness to reduce deterioration and according to the availability of enough funds. DOT's authorities are aware of the benefits of most strategic bridge maintenance activities, and the convenient frequency to apply them.

Several studies have proved that scheduled preventive bridge maintenance activities are more efficient and cost-effective than reactionary maintenance activities (NYSDOT, 2008; FHWA, 2011; Yanev, 2011). The expected benefit from performing bridge maintenance activities is the service life extension, and as a consequence, delaying a major bridge rehabilitation or even a bridge replacement. In order to select the best bridge maintenance strategy among all available options, DOTs agencies are prone to use a cost-benefit analysis, based on a Life-Cycle Cost Analysis.

8.2 Life Cycle Cost Analysis

Life-Cycle Cost Analysis (LCCA) is a decision making tool oriented to show the benefits from different alternatives to achieve the same expected results (Azizinamini et al., 2013). When performing a LCCA, cash flows from past, present or future interventions must be evaluated and compared. A widely accepted method is evaluating the Present Value (PV), which represents the value of any cash flow expressed as a value corresponding to the present time. The LCCA procedure for bridge maintenance requires the assumption of some values and factors, such as the costs of maintenance activities, possible rehabilitation costs, bridge replacement cost, the expected bridge service life, and the cost of funds expressed as a discount rate.

A LCCA is performed typically in the following sequential steps:

- Identify alternatives
- Define time for analysis, normally the bridge service life
- Define costs components for each alternative
- Evaluate PV for each alternative

- Compare PV from different alternatives and make a final decision

8.2.1 Bridge Service Life

Bridge service life is understood as the expected time span a bridge can perform properly under the expected service conditions before major rehabilitation/replacement is required. The bridge owner can implement several policies to pursue the expected bridge service life. Those policies are based on the owner's criteria, the knowledge of appropriate bridge conservation measures, and most importantly, the available resources to implement the selected measures to keep the bridge in good conditions over the entire service life. Most of the references from specialized literature consider the bridge service life to be from 75 to 100 years (So, 2012; Azizinamini, 2013). In this research a bridge service life of 100 years was assumed for all analyses.

8.2.2 Cost of Bridge Maintenance Activities, Rehabilitation, and Replacement

The LCCA procedure requires several inputs to perform it appropriately. Cost of alternatives to be compared are of the most essential, to achieve reliable results from a LCCA. The main source to obtain accurate bridge maintenance, rehabilitation or replacement costs is the historical data recorded for the maintenance unit of each agency.

There are several studies related to bridge maintenance activities. Some of those studies provide unit costs for the most common bridge maintenance activities. Although, there are few studies regarding bridge superstructure washing, and only very few of them provide some data about unit costs.

Several unit costs related to bridge maintenance activities and major bridge rehabilitation were collected and presented in the studies conducted by Sobanjo (2001) and Hearn (2012). In this work were considered unit costs for steel bridge superstructure washing and rehabilitate steel girder, as presented in Table 8.1.

Table 8.1: Unit costs for bridge maintenance activities (Sobanjo, 2001; Hearn, 2012)

ACTIVITY	UNIT COST (\$/LF)
Wash steel girder (no corroded)	10.00
Overcoating/Re-coating	52.00
Rehabilitate steel girder	6000.00

8.2.3 Discount Rate

A discount rate, r , to relate future and present costs has to be used when utilizing financial math forecasting. Most of federal, state and local governments use a discount rate of 4% for infrastructure projects based on the recommendation given by the federal government for long-term discount rates (Chandler, 2004). INDOT also recommends a discount rate of 4% (INDOT, 2013).

8.2.4 Present Value

Some basic financial expressions to evaluate the PV for one-time and annual expenditures are provided in the following (Hawk, 2003):

$$\text{One-time future event: } PV = \frac{FV_n}{(1+r)^n} \quad \text{Equation 8.1}$$

$$\text{Equal annual events: } PV = \frac{C [1-(1+r)^{-n}]}{r} \quad \text{Equation 8.2}$$

where:

- PV = present value of the expenditure
- FV_n = future value of an expenditure made at time n
- r = discount rate
- n = # of periods (generally years) between the present and future time
- C = value of uniform periodic resource flows

Therefore, the benefit of considering certain maintenance activities can be determined by comparing the PV of all the costs for the proposed maintenance activities against the PV of the alternative that does not consider performing any maintenance activity. If the PV of all the costs of the maintenance activities exceeds the PV of the alternative of not performing any maintenance, then performing those maintenance activities may not be worth pursuing and should likely be rejected. However, when the PV of the maintenance activities is less than when no maintenance is performed, and sometimes far less than the PV of the alternative of not performing maintenance, then the maintenance activities are undoubtedly worth pursuing.

8.2.5 Bridge Load Rating

Bridge load rating was performed to determine the safe live load capacity that a bridge can resist under the actual conditions of the structure. In Chapter 7 a parametric analysis was applied to several composite steel girder highway bridge models, to determine the live load capacity at three different levels: Inventory level, Operating level, and Legal level. Each rating level has specific applications and consequences when the minimum target is achieved. Inventory Level is the most demanding analysis, followed by Operating level, and ending with the Legal level as the least demanding. The load rating at those different levels were performed at different ages (0, 20, 40, 60, 80, and 100 years of service) in order to determine the capacity degradation of the structure due to the attack of atmospheric corrosion throughout the structure's service life. The parametric analysis also included wash/no-wash alternatives: either performing steel girder washing as a maintenance activity or performing no steel girder washing.

The study of typical steel highway bridge models under those two alternatives highlighted the effect of steel girder washing in reducing the rate of capacity degradation under corrosion attack. The results showed in Chapter 7 support the statement that steel girder washing is an effective bridge maintenance activity, to reduce atmospheric corrosion, when performed regularly during the bridge service life.

Tables 8.2 show the ages, from the 96 bridge models considered in the evaluation, when the bridge members reached their limits ($RF_v = 1.0$) at any of the three rating levels. Therefore, those bridge cases with no age shown in Tables 8.2 to 8.4 correspond to cases in which the load rating limit of $RF_v = 1.00$ was not reached for that specific load level during the entire bridge service life.. Tables 8.2 to 8.4 show that a bridge under a steel girder washing program always resulted in a less corroded situation than the same bridge without girder washing.

Another source to understand the structural capacity degradation is relating the load rating factor with the demand/capacity ratio of the structure. When a bridge case reaches the limit rating factor of $RF_v = 1.00$ at the Inventory level, the demand/capacity ratio for shear is near to 1.00; when $RF_v = 1.0$ at the Operating level, the demand/capacity ratio for shear is near to 1.15; and when $RF_v = 1.0$ at the Legal level, the demand/capacity ratio for shear is close to 1.30. That means that the structure is overstressed by 15% when reaching the load rating limit at Operating level, and overstressed by 30% at the limit for load Legal level.

Table 8.2: Bridge's service age (years) when reaching Rfv=1.0 - Industrial/urban

Bridge	Inventory	Operating	Legal
1BSIN	58	90	-
1CSIN	18	38	58
1CSIW	30	70	-
1CTIN	38	70	-
1CTIW	40	80	-
1DSIN	22	45	70
1DSIW	40	90	-
1DTIN	45	95	-
1DTIW	48	-	-
2BSIN	60	85	-
2CSIN	18	38	58
2CSIW	32	75	-
2CTIN	40	80	-
2CTIW	42	100	-
2DSIN	40	60	90
2DSIW	72	-	-
2DTIN	70	-	-
2DTIW	95	-	-

Table 8.3: : Bridge's service age (years) when reaching Rfv=1.0 - Marine

Bridge	Inventory	Operating	Legal
1BSMN	60	88	-
1CSMN	18	38	58
1CSMW	35	90	-
1CTMN	48	100	-
1CTMW	60	-	-
1DSMN	22	45	70
1DSMW	45	-	-
1DTMN	65	-	-
1DTMW	95	-	-
2BSMN	60	88	-
2CSMN	18	38	58
2CSMW	42	-	-
2CTMN	60	-	-
2CTMW	90	-	-
2DSMN	40	-	-

Table 8.4: Bridge's service age (years) when reaching RFv=1.0 - Rural

Bridge	Inventory	Operating	Legal
1CSRN	58	-	-
1CTRN	75	-	-
1DSRN	70	-	-
2CSRN	60	-	-
2CTRN	80	-	-

8.3 Economic Analysis for Bridge Maintenance Activities

An economic analysis was performed using Life Cycle Cost Analysis (LCCA) to study two alternatives for a bridge exposed to atmospheric corrosion attack: (a) no bridge maintenance activity was performed until the structure required rehabilitation/repair due to shear capacity degradation when reaching the load rating limit for legal load (RFv = 1.00), and (b) the bridge superstructure was maintained with a steel girder washing program, with a specific frequency, to reduce the shear capacity degradation of steel girders until reaching the load rating limit for legal load. The methodology to evaluate the load safety capacity of bridges followed the design and evaluation requirements of AASHTO LRFD (2012) and AASHTO MBE (2011) respectively.

The costs of the two options were evaluated using the method of Present Value (PV), for a bridge span life of 100 years, and a discount rate of 4%. For simplicity, the LCCA only focused on the expenditures related to bridge rehabilitation/replacement and maintenance activities. The initial cost due to construction, the costs of bridge operations, as well as other costs that are common to both alternatives, were not considered in the LCCA.

8.3.1 Effect of Steel Girder Washing Activity for Uncoated Carbon Steel

The effect of steel girder washing, as an effective bridge maintenance activity to reduce the rate of atmospheric corrosion, is evaluated by an economic analysis. The bridge model corresponding to one-span, 110 feet span-length, with uncoated carbon steel type, exposed to Industrial/Urban local environment, was studied under two alternatives. One

alternative was to analyze the bridge case when no maintenance activities are performed during the entire service life, identifying this case with the code 1CSIN. The analysis for the second alternative consisted of the same bridge case subjected to a scheduled maintenance program, and it was identified with the code 1CSIW.

The steel washing activity was applied according with the frequency evaluated in Chapter 6 for uncoated carbon steel type when exposed to Industrial/Urban local environment. Table 6.7 indicates that steel girder washing activity should be performed regularly each 1.6 years for uncoated carbon steel exposed to Industrial/Urban environment. For practical aspects the steel washing frequency can be rounded each two years to perform it always during the summer season. For this study the original 1.6 years frequency was used. Following the conclusions obtained from the parametric analysis in Chapter 7, the analysis was performed for both alternatives until the legal load limit for shear capacity was reached. At that limit, a decision for the structure must be made: specifically whether or not to post the bridge with a reduced load limit or close the bridge for significant rehabilitation work that will improve the structural rating factor.

For the bridge model 1CSIN (no washing alternative), the age to reach the load rating limit for shear capacity is 58 years of service, as observed from the plot in Figure 8.1 and Table 8.2. Consequently, rehabilitation/replacement of the uncoated steel girders will be required at that age.

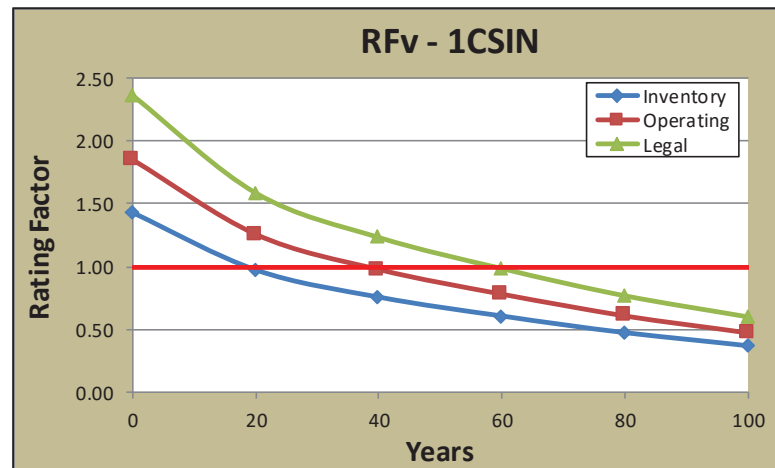


Figure 8.1: Load rating factor for shear capacity - bridge case 1CSIN, uncoated steel

From Table 8.1 a cost of \$6000.00/LF needs to be allocated for rehabilitation of corroded steel girders. Applying a one-time future event at year 58, considering a discount rate of $r=4\%$, and using Equation 8.1, a total PV of \$616.9/LF was obtained. Figure 8.2 represents the analysis for this alternative considering girders major rehabilitation at year 58.

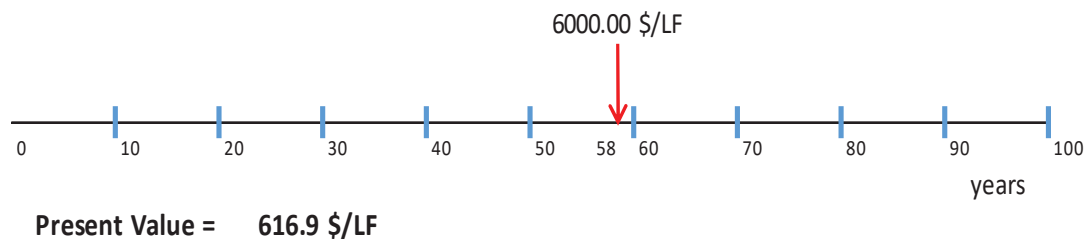


Figure 8.2: LCCA for bridge 1CSIN uncoated steel - alternative with no maintenance

As a second alternative, the bridge previously evaluated was analyzed under a maintenance program. The bridge model identified as 1CSIW (washing alternative) was regularly maintained, applying a steel girder washing program with a frequency of 1.6 years (see Table 6.7). In this case the bridge never reached the Legal load rating limit ($RFv = 1.00$) during its entire service life, as depicted in the plot in Figure 8.3

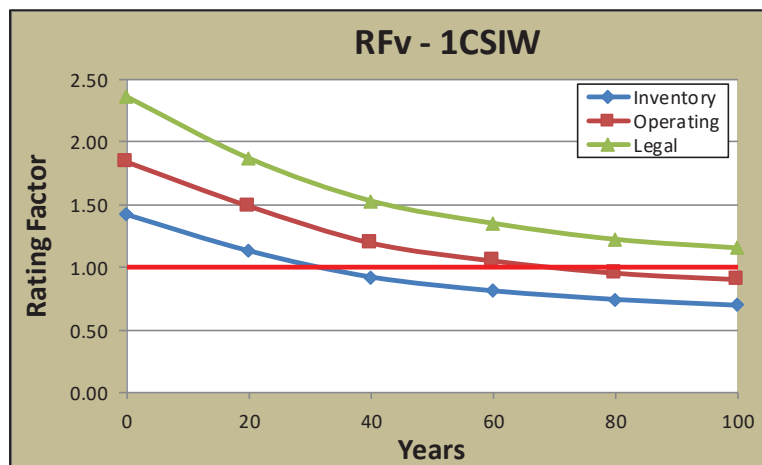


Figure 8.3: Load rating factor for shear capacity - bridge case 1CSIW, uncoated steel

Therefore, for this second alternative the LCCA for bridge case 1CSIW considered only the cost corresponding to steel girder washing each 1.6 years. From Table 8.1 a cost of \$10.00/LF needs to be allocated to perform this maintenance program each 1.6 years. Since the frequency is not annual, the equal annual event expression (Equation 8.2) cannot be used but the one-time event (Equation 8.1) was applied each 1.6 years, until the 100 years of service life, to evaluate the PV for this alternative. The PV for this alternative is sketched and evaluated in Figure 8.4.

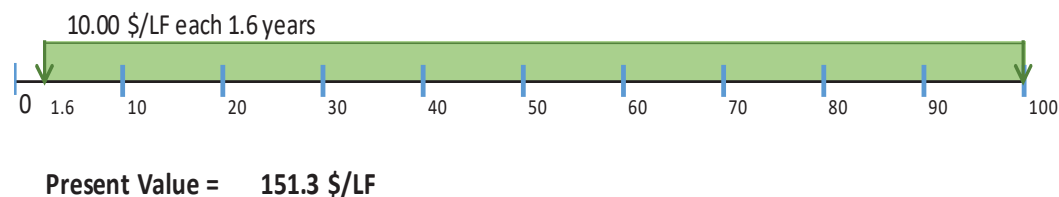


Figure 8.4: LCCA for bridge 1CSIW uncoated steel - alternative with maintenance

The PV for the first alternative, when no maintenance activity is considered, was \$616.9/LF. The PV for the second alternative, when steel girder washing is applied regularly each 1.6 years, resulted on \$151.3/LF. Therefore, close to 300% of the PV is saved when the bridge is treated under a maintenance program, performing steel girder washing activity with a frequency of 1.6 years.

In the same manner, other bridge models were also analyzed, which are presented in Table 8.5. There is a small difference, for the age when reaching the load rating limit $RF_v = 1.0$ for the one-span and two-span cases from similar bridges, as it is observed in Table 8.5. This is because shear is the governing effect and the values of shear demand and shear capacity are closely similar in both cases. Also, the Industrial/urban and Marine environments have similar corrosion penetration ratios as showed in Table 6.7, therefore, the age when reaching the load rating limit are similar for both environments.

Table 8.5: Bridge models reaching legal load rating limit $RF_v = 1.00$

BRIDGE	# spans	Span Length	Steel Type	Environment	Maintenance Alternative	Age for $RF_v = 1.00$
2CSIN	2	110'	Carbon uncoated	Industrial	No washing	61 years
1CSMN	1	110'	Carbon uncoated	Marine	No washing	58 years
2CSMN	2	110'	Carbon uncoated	Marine	No washing	61 years

The bridge cases presented in Table 8.5 had close service age when reaching the Legal load rating limit for shear capacity. Therefore, those models with no maintenance activity had similar PV. The 1CSMN case had also a PV of \$616.9/LF, while the cases 2CSIN and 2CSMN had a PV of \$548.4/LF. The bridge cases corresponding to the same models from Table 8.5, but for the steel girder washing alternative: 2CSIW, 1CSMW, and 2CSMW, did not reach the load rating limit $RF_v=1.00$ during their entire service lives. Consequently, the bridge models under maintenance activity 2CSIW, 1CSMW, and 2CSMW had the same PV of \$151.3/LF as evaluated for bridge 1CSIW.

8.3.2 Effect of Steel Girder Washing Activity for Coated Carbon Steel

The analysis presented in the previous section was based on the use of uncoated carbon steel as a structural material for bridges. Since this material is not used in the USA for bridge structures, the previous analysis was not realistic but only useful to show the application of the proposed methodology. A more realistic situation is the use of coated carbon steel as the structural material for bridge construction. Therefore, the effect of

bridge washing on extending the service life of coated carbon steel girders is analyzed in this section.

In Chapter 5 was studied the behavior of coated steel coupons made from carbon steel under an accelerated corrosion process at the laboratory. From the results obtained in the accelerated corrosion test for coated carbon steel, no damage was presented to the three-coat paint system during the entire test. It was concluded that no appropriate conditions were achieved during the accelerated corrosion test to replicate the damage to the coat system due to atmospheric corrosion attack. Consequently, there is no data available from the tests for the age when the coating system stops protecting the steel element due to atmospheric corrosion attack.

As an alternative, to estimate the age a typical three-coat paint system stops working properly as a steel protective system, some data were obtained from the specialized literature. The estimated service life for a three-coat steel paint system according to various research studies are shown in Table 8.6.

Table 8.6: Three-coat paint system service life

Researcher	Three-coat System Service Life (years)
Chang (1999) - INDOT	30
Dadson (2001)	15 - 17
American Iron and Steel Institute (2007)	25
Kogler (2012) - FHWA	
- Aggressive environment	15 - 20
- Moderate environment	25

Based on the data presented in Table 8.6, it can be assumed that an average service life of 25 years is reasonable for a typical three-coat steel paint system. As a consequence, a coated carbon steel element exposed to atmospheric corrosion will start its deterioration process after the first 25 years of service. The structural capacity of a bridge model with a

three-coat protection system, is expected to remain without degradation by the first 25 years of service life. After 25 years of service life, the coating system is expected to fail and structural capacity degradation can develop, assuming that no additional coating is applied to the bridge. The degradation model will follow the same pattern presented in section 8.3.1. Therefore, for bridge model 1CSIN, protected with a three-coat system, the load rating limit for shear capacity will be reached at approximately $25 + 58 = 83$ years. Under these assumptions, the LCCA for bridge 1CSIN, for coated steel, is presented in Figure 8.5. The PV for this bridge case resulted in \$231.4/LF

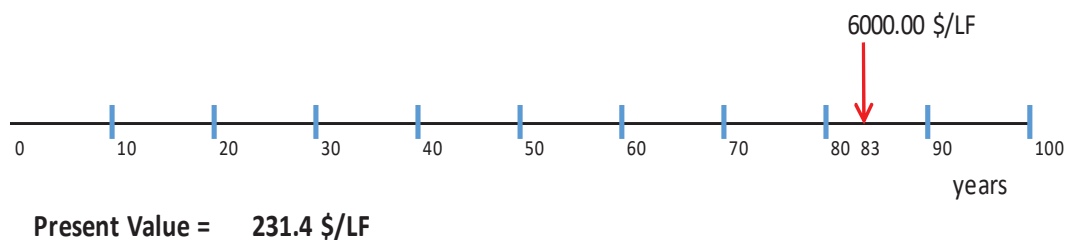


Figure 8.5: LCCA for bridge 1CSIN coated steel - alternative with no maintenance

The LCCA for bridge 1CSIW, corresponding to the coated carbon steel, and under steel girder washing program alternative, is sketched in Figure 8.6. For bridge model 1CSIW with coated steel, the maintenance program will start after the three-coat paint system reached its service life. Thus, after 25 years of bridge 1CSIW's construction, when the coat service life has finished, it is required to perform steel girder washing as a bridge maintenance activity. The PV for this bridge case resulted in \$57.1/LF.

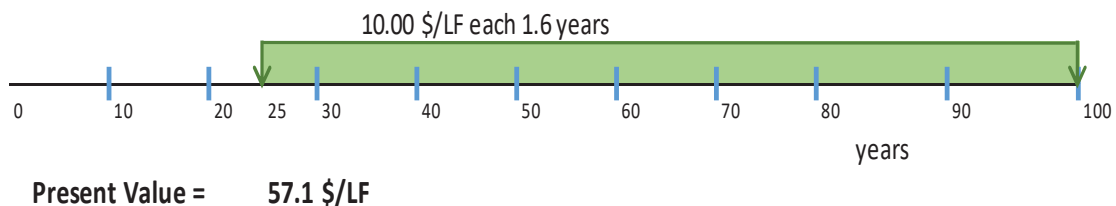


Figure 8.6: LCCA for bridge 1CSIW coated steel - alternative with maintenance

For bridge case 1CSIN made from coated steel, corresponding to the no maintenance alternative, its PV resulted on \$231.4/LF. For the bridge case 1CSIW made from coated steel, when steel girder washing is applied regularly each 1.6 years, resulted on a PV of \$57.1/LF. Therefore, close to 300% of the PV is saved when the coated steel girder highway bridge is treated under a maintenance program, performing steel girder washing activity with a frequency of 1.6 years, starting the program at age 25 of service life.

Following the same procedure presented in Section 8.3.1, the bridge models presented in Table 8.5 (2CSIN, 1CSMN, 2CSMN) but made from coated carbon steel, were analyzed until the Legal load rating limit for shear capacity was reached. The bridge case 1CSMN, with protection coating system, had a similar service life of 83 years as bridge 1CSIN case, and also a PV of \$231.4/LF. Bridge cases 2CSIN and 2CSMN, with protection coating system, had service life of approximately $25 + 61 = 86$ years and a PV of \$205.7/LF. At the other hand, the three cases (2CSIW, 1CSMW, 2CSMW) subjected to a maintenance program of steel girder washing performed each 1.6 years and starting after the first 25 years of service life (after the coating system has deteriorated) did not reach the load rating limit $RF_v = 1.0$ during their entire service life, having all of them a PV of \$57.1/LF.

In Table 8.7 are summarized the results for the bridge cases analyzed, for uncoated and coated carbon steel, with and without steel girder washing as a regular maintenance program. The no maintenance program included a steel girder rehabilitation of deteriorated girders after reaching their service life. The maintenance program consisted in regular steel girder washing each 1.6 years, starting at year zero for uncoated girders and after the first 25 years of service life for coated girders. As presented in Table 8.5, the bridge cases under maintenance program reached the 100 years of service life without rehabilitation/replacement.

Table 8.7: Summary of PV for bridge cases of carbon steel, uncoated and coated

Uncoated Girders

Without Maintenance

Case	SL (years)	PV (\$/LF)
1CSIN	58	616.9
2CSIN	61	548.4
1CSMN	58	616.9
2CSMN	61	548.4

With Maintenance

Case	SL (years)	PV (\$/LF)
1CSIW	>100	151.3
2CSIW	>100	151.3
1CSMW	>100	151.3
2CSMW	>100	151.3

Coated Girders

Without Maintenance

Case	SL (years)	PV (\$/LF)
1CSIN	83	231.4
2CSIN	86	205.4
1CSMN	83	231.4
2CSMN	86	205.4

With Maintenance

Case	SL (years)	PV (\$/LF)
1CSIW	>100	57.1
2CSIW	>100	57.1
1CSMW	>100	57.1
2CSMW	>100	57.1

SL: Service Life PV: Present Value

8.3.3 Effect of Washing on Coated and Re-coated Carbon Steel Members

Extending the bridge service life by performing steel girder washing as a unique requirement can be considered not enough realistic. Therefore, another economic analysis is presented, similar to that from the previous section, but including the benefit of steel washing on extending the service life of the coating and re-coating protection system. In this research was not obtained data referring the coating service life extension can be obtained by performing steel washing. From the specialized literature it was found that steel washing can extend from 5 to 10 years the service life of a coating system. This is a field for more research.

A three-coat paint system is supposed to last 25 years, as referenced in Table 8.6. Then, it can be assumed that steel washing will extend the coating service life in 10 more years. Therefore, at the age of 35 years the coating condition is expected to be at the end of its service life and an adequate treatment will be required. This is a common situation for real steel bridges, and a practical solution is to re-coat the steel members. Considering

that the service life of a re-coating system is 15 years in average, it can be accepted that frequently washing a re-coated member can extend its service life in 5 more years, resulting in 20 years the re-coating service life. Then, at the age of 55 years the coating + recoating system the service life is expected to be finished if no more recoating is scheduled. Thus, at the age of 55 years of service life it is expected to start the corrosion degradation for these steel members. The steel washing should be applied regularly each 1.6 years as indicated before, since the year zero until reaching the expected 100 years of the bridge service life.

A LCCA was applied to the bridge case 1CSIW, with coated and re-coated carbon steel girders, with a regular steel washing program each 1.6 years, following the scheme detailed in this section. The details of this LCCA are represented in Figure 8.7. The unit cost were presented in Table 8.1. The cost of steel washing regularly each 1.6 years during the entire bridge service life had a PV of \$151.3/LF. Additionally, the present value for recoating the girders at year 35 had a PV of \$13.2/LF, resulting in a total PV of \$164.5/LF for this alternative. This was a PV higher than the \$57.1/LF but more realistic and still it was lower than the PV of \$231.4/LF for the no maintenance case, found in section 8.3.2. As mentioned, this was a more conservative and realistic alternative and still it was more cost-effective than the no washing alternative.

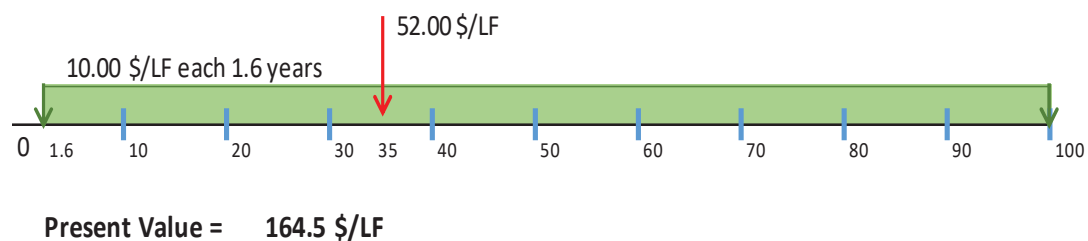


Figure 8.7: LCCA for bridge 1CSIN coated steel - alternative with washing and re-coating

8.3.4 Effect of Steel Washing Activity for Uncoated and Coated Weathering Steel

The load rating analyses performed to bridge cases from uncoated weathering steel are presented in detail in Appendix J. From a review of all the plots corresponding to the bridge cases from weathering steel can be observed that none of them reached the rating limit of $RF_v = 1.0$. This was the trigger limit to take some action on a deteriorated bridge, such as posting the bridge with a lower load capacity or close it for major rehabilitation. As a consequence, the methodology applied to the previous cases to show the benefit of steel washing is not possible to apply to uncoated weathering steel bridges. Thus, another approach should be applied to analyze the effect of bridge washing on uncoated weathering steel members.

From the plots in Appendix J is shown clearly the benefit of steel washing alternative over the no maintenance alternative. In all analyzed cases for uncoated weathering steel, the no washing cases deteriorated at a higher rate than the washing alternative. The plots corresponding to bridge cases 1CTIN/W, 2CTIN/W, 1DTMN/W, and 2DTMN/W, corresponding to both alternatives washing and no washing, are presented in Figures 8.8 to 8.11.

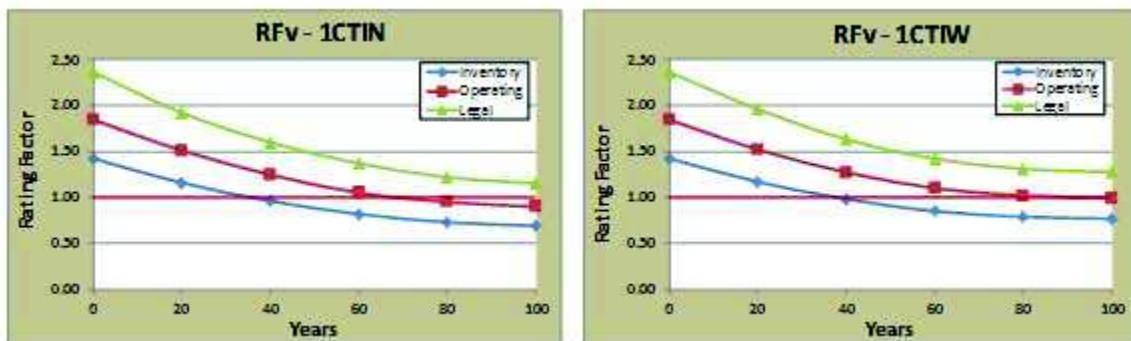


Figure 8.8: 1-Span x 110' – Weathering steel – Industrial – No washing/Washing

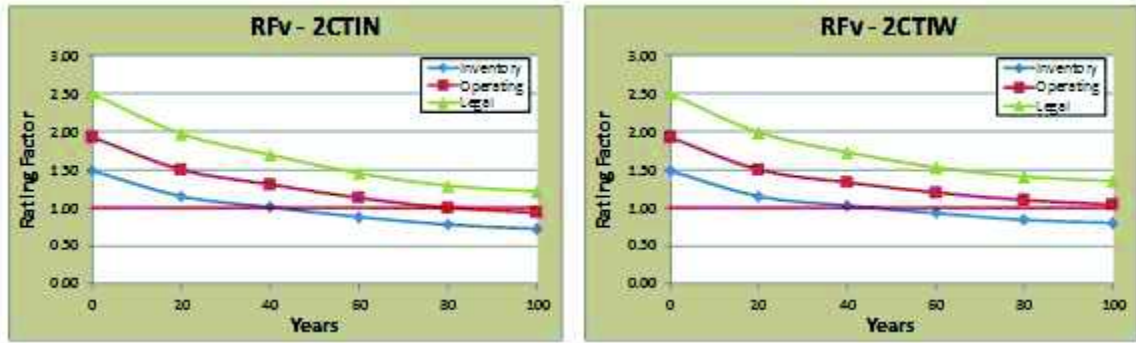


Figure 8.9: 2-Span x 110' – Weathering steel – Industrial – No washing/Washing

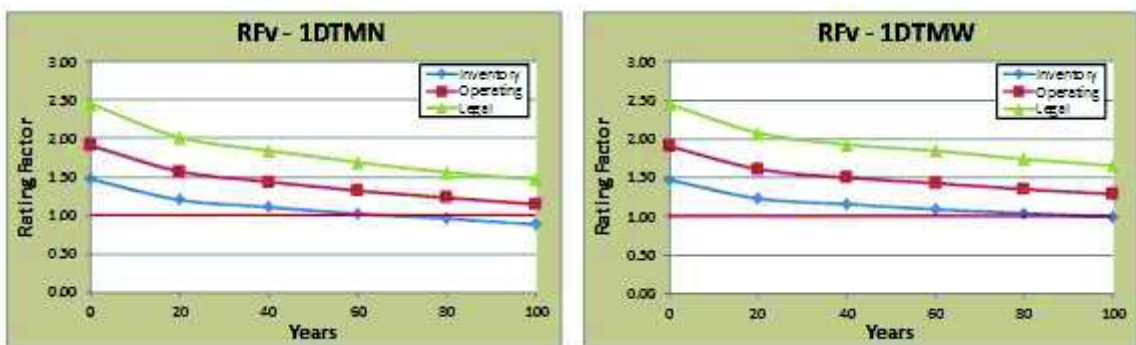


Figure 8.10: 1-Span x 130' – Weathering steel – Marine – No washing/Washing

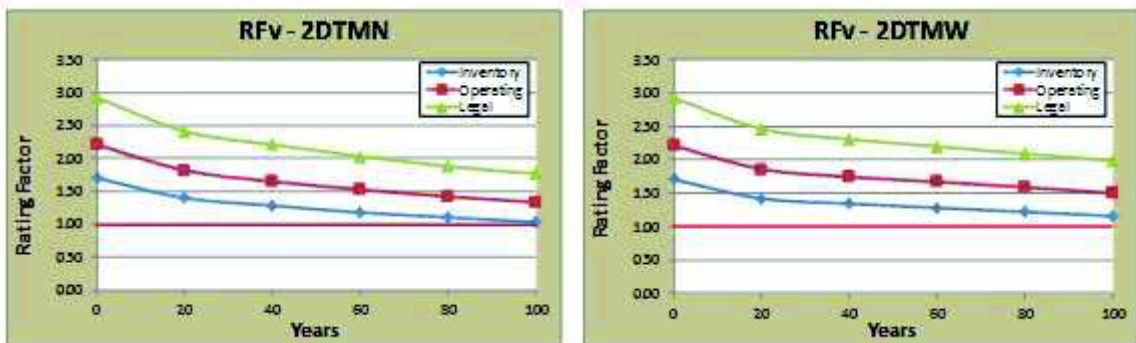


Figure 8.11: 2-Span x 130' – Weathering steel – Marine – No washing/Washing

From the four bridge cases and their both alternatives (no washing and washing) showed in Figures 8.8 to 8.11 can be noticed the benefit that steel washing produces in reducing the structural capacity degradation of steel girders. This is depicted in all plots, where the rating factors are always higher for the washing alternative than the no washing, regardless the load level considered (Inventory, Operating, or Legal).

Additionally, when considering a bridge case from coated weathering steel, the same criteria from section 8.3.3 can be followed. In section 8.3.3 it was assumed that washing carbon steel girders protected with an initial coat and recoated after 35 years is more cost-effective than the no washing alternative. Hence, it can be considered that the coating system for weathering steel will have the same service life of 35 years that had the coat for a carbon steel member. Also, it can be accepted that a re-coating system for weathering steel will last the same 20 years it lasted for a carbon steel member. Therefore, after 55 years of service life, the coating system of a weathering steel member will be ended and structural deterioration will develop. Then, maintaining under a regular washing program a weathering steel member, initially coated and recoated only once after 35 years of service life, will allow it to reach its service life with lower capacity degradation than the no washing alternative. When exposed to Industrial/urban environment, weathering steel should be washed regularly each 3.8 years, as found in section 6.3.2 and presented in Table 6.8.

8.4 Results from LCCA

From the PV obtained for the bridge cases considered herein, it can be concluded that periodic washing of steel highway bridge girders is a cost-effective bridge maintenance option to reduce the structural capacity degradation due to atmospheric corrosion. The conclusions are valid for bridges made from uncoated and coated carbon and weathering steel.

The presented analyses focused on those bridges that reached the load rating limit for shear capacity when submitted to Legal loads during their service lives. The analysis for Legal load level is the less demanding condition, as prescribed by the AASHTO MBE (2011). Therefore, for a more demanding condition, the load rating limit will be reached at an early age, and consequently the Present Value (PV) will be higher than those estimated for Legal loads.

The unit costs considered in this research were obtained from a specialized source, but always those values are accepted with precaution. Special attention should be given to rehabilitation/replacement costs, which actually reflects the bridge owner costs with some approximation. Rehabilitation and replacement and major works unit costs do not reflect the user costs, which are quite specific for each case, difficult to estimate, and often are not considered. Consequently, the rehabilitation/replacement activities could represent higher costs than those reflected by unit cost found in the specialized literature.

CHAPTER 9. SUMMARY, CONCLUSIONS AND RECOMMENDATIONS

9.1 Summary

The objective of this research was to understand, model, and assess the structural capacity degradation of typical steel girder highway bridges due to atmospheric corrosion, so that regular high-pressure superstructure washing and spot painting could be evaluated as effective maintenance activities to reduce the corrosion process. The study was limited to consider the effect of uniform (general) corrosion as the only factor for structural degradation of the steel highway bridge girders.

Data collected by Albrecht and Naeemi (1984) and the methodology from Kayser (1988) were used to model atmospheric corrosion rates at different environments and to model the corrosion process on steel girders. Although there is a lack of conclusive evidence, superstructure bridge washing is widely considered by bridge inspectors, engineers, and maintenance crews as an efficient alternative to reduce atmospheric corrosion on steel girder bridges and extend the bridge service life.

An Accelerated Corrosion Test (ACT) was developed to simulate the effect of atmospheric corrosion on steel coupons under a washing program. An ACT is accepted as a useful tool to analyze the corrosion of metal elements in a shorter period of time and in a simplified manner. A relationship was developed to extrapolate the results from the ACT during a short period of time to real problems of longer periods of time, such as the bridge service life.

The ACT rapidly produced corrosion effects over the uncoated coupons of carbon and weathering steel (steel Types A and C), but did not produce any appreciable damage to coated carbon steel (steel Type B). During the ACT the corrosion rates for uncoated steel coupons, under a regular washing program, always resulted lower than the corrosion rates for unwashed coupons from the same steel, carbon or weathering. Scribed coated steel coupons were also tested using the ACT, and it was found that the rate of rust creepage area increased when a damaged coated coupon was subjected to frequent washing actions.

A parametric analysis of corroded steel girder bridges was considered. Eight typical steel highway bridges were designed and analyzed under atmospheric corrosion attack. The analyses were performed with variation of the bridge span length, number of spans, steel types, environment types, maintenance alternatives, and age of structure. The emphasis was focused on the parametric analyses of corroded steel girder bridges under two alternatives: (a) when steel bridge girder washing is performed according to a particular frequency, and (b) when no bridge washing is performed to the girders. The reduction of structural capacity was observed for both alternatives along the structure service life, estimated on 100 years. Eight typical composite steel bridges were analyzed for two structural steel types, three local environments, and two maintenance alternatives, resulting in $8 \times 2 \times 3 \times 2 = 96$ bridge cases under study. Each bridge case was load rated at ages 0, 20, 40, 60, 80, and 100 years of atmospheric exposure, therefore, the total parametric study resulted in 576 load rated analysis scenarios. The structural capacity degradation was measured through the evaluation of moment and shear capacity for the steel girders and the measure of the corresponding bridge load rating. The maximum elastic deflection of girders was also estimated as a measure of the structural serviceability reduction. Shear was the governing effect for all bridge cases considered under atmospheric corrosion attack.

Finally, an economic analysis was performed using the Life Cycle Cost Analysis (LCCA) to study the wash/no-wash alternatives for a bridge exposed to atmospheric corrosion attack. Specifically, for the considered alternatives: (a) no bridge maintenance activity is

performed until the bridge structure required rehabilitation/repair due to shear capacity degradation, when reaching the load rating limit for legal load ($RF_v = 1.00$); and (b) when the bridge superstructure was maintained with a steel girder washing program, with a specific frequency, to reduce the shear capacity degradation of steel girders until reaching the load rating limit for legal load.

9.2 Conclusions

Bridges are fundamental elements of a highway system, representing an important investment and a strategic link that facilitates the transport of persons and goods. The cost to rehabilitate or replace a highway bridge represents an important, and often significant, expenditure for the owner, who needs to evaluate the correct time to assume that cost. Consequently, prolonging the service lives of highway bridges by requiring only short interruptions is an effective way to provide optimal service for the users and to make more efficient use of the owner's scarce resources.

An ACT following the ASTM B117 standard test resulted in an effective procedure to reproduce atmospheric corrosion on small uncoated steel coupons in a shorter period of time and in a simplified manner. The implemented ACT failed to reproduce atmospheric corrosion on coated steel coupons, probably due to the absence of UV light emission during the test, which can lead to the deterioration in the effectiveness of the coating materials.

From the ACT implemented in this research, uncoated steel coupons from carbon and weathering steel, regularly washed, presented lower rates of corrosion than the coupons that were not washed. Based upon a correlation developed between corrosion initiated using the ACT and corrosion for actual in-situ environments, different curves were constructed to estimate corrosion penetration for each type of uncoated steel, and for each local environment, versus the service age of the steel bridge. In all these curves, the steel washing alternative provided lower corrosion rates than the no washing alternative. As expected, corrosion rates were found larger for carbon steel than for weathering steel.

Correlation between the ACT and corrosion penetration at real environments was used to determine the optimum average frequency a steel girder bridge should be washed. It was found that uncoated carbon steel girders should be washed each 1.6, 1.7, and 5.7 years, when exposed to Industrial/Urban, Marine, and Rural environments, respectively. Uncoated weathering steel girders should be washed each 3.8, 6.0, and 10.9 years, when exposed to Industrial/Urban, Marine, and Rural environments, respectively.

It was found from the parametric structural analysis of the 96 typical steel bridges, for the six different service ages along the 100-years structure service life, that the steel washing alternative reduces the rates of capacity degradation due to atmospheric corrosion, regardless of the:

- type of stress - bending or shear.
- local environment - Industrial/Urban, Marine, or Rural.
- number of bridge spans - one or two.
- span length - 70, 90, 110, or 130 feet.
- steel type -uncoated carbon steel or uncoated weathering steel.

It was also observed that the steel washing alternatives always produced lower live-load deflections than the no washing alternatives. This observation confirms that the steel washing alternative reduces the structural capacity degradation on steel girder bridges due to atmospheric corrosion attack.

Some differences were found for corrosion penetration rates from two sources, the Control Test coupons and Group 10 coupons. Due to the several factors affecting the accelerated corrosion test procedure, it was decided to proceed the structural capacity analysis using data from Control Test. The selected data for corrosion rates provided a more conservative analysis, since the higher corrosion rates were employed. A more deep analysis can be performed using the complete original data presented in the corresponding appendices.

The parametric load rating analysis showed that the bridge shear capacity was reduced at a higher rate than the bending capacity. The structural capacity was measured through the rating factors for bending (RF_m) and shear (RF_v). As a result, the shear rating limit of RF_v = 1.00 was reached at early ages than the bending rating limit of RF_m = 1.0 in all bridge cases. The reason for this behavior is believed to be the result of corrosion on both faces of the web, making it a critical slender element, since the girder shear capacity is provided entirely by the web section. The load rating analysis also confirmed that steel girder washing is an effective maintenance alternative to reduce the atmospheric corrosion attack, in comparison to the no washing alternative.

The economic analysis, using the LCCA method, also demonstrated that it is more cost-effective to perform steel girder washing as a scheduled maintenance activity in contrast to the no washing alternative for uncoated or coated carbon steel. The no-washing case typically resulted in reaching the Legal load rating limit of RF_v = 1.00 sooner during their service lives than for cases with regular bridge washing, and consequently they had to be closed sooner for girder rehabilitation/replacement. The economic evaluation for a closed bridge for girder rehabilitation/replacement resulted in a Present Value (PV) higher than the PV corresponding to the alternative when the bridge is maintained using a regular steel girder washing program. For uncoated and coated weathering steel the benefit of a regular washing program was determined by the analysis of structural capacity degradation. The structural capacity degradation was measured by the load rating factor for shear capacity RF_v, which always resulted higher for the washing alternative than the no washing.

The structural capacity degradation considered in this research was based only on the atmospheric corrosion attack. Therefore, some other negative effects from natural or human origin that can cause deterioration of steel highway bridge girders were not considered in this study. The models created for corrosion penetration, and for corrosion propagation in the girder section, should be considered as a rough approximation to actual behavior on steel girder bridges.

Coated steel girders with spot damages should be repaired applying spot painting as soon as possible. It is recommended to follow recommendations from the paint producer. The damaged spot must be cleaned properly before painting application.

Performing steel washing on spot damages was found counterproductive, according to results obtained in this research. Therefore, the solution for this type of problems is not washing but spot painting as soon as possible.

In general, Industrial/urban and marine environments were always more aggressive than rural environment. For rural environment the analyzed bridge cases never reached the load rating limit of $RF_v = 1.0$. For Industrial/urban and Marine environments, some bridge cases did not reach the load rating limit of $RF_v = 1.0$ due to their larger initial structural capacity than those that reached the rating limit.

Based on the models assumed in this research, under the limited data available for the estimation of actual atmospheric corrosion rates, accepting the several assumptions proposed throughout the study, and following the methodology proposed herein, it was found that regular, periodic washing of the steel highway bridge girders resulted in an effective bridge maintenance activity that extended the service life of the girders. The results from this research showed that steel girder washing reduced the rate of shear structural capacity degradation of steel highway bridges exposed to atmospheric corrosion attack in comparison to the alternative of not washing the steel girders.

9.3 Recommendations

Further research on corrosion penetration under actual environmental conditions would be useful. The corrosion models used in this research are based on data obtained from some particular locations, and consequently, a generalization of those results to be applied in any other location will include some type of deviation and uncertainty. Also, the limitations of the accelerated corrosion testing should be explored further to address more realistic modeling of the actual environment.

Data from actual steel girder bridges should be recorded with an appropriate methodology, following the same protocols at different agencies. Special consideration should be given to the record of: corrosion penetration rates on steel girders at different ages of service, unit costs of steel girder washing, steel girder washing procedures, and how frequent is performed the steel girder washing.

The methodology presented should be improved in order to evaluate more precisely the effectiveness of steel girder washing as a preventive maintenance activity and determine the adequate frequency of washing. This methodology could be considered as a better alternative, over the informal and intuitive procedures currently used, to decide the implementation of this maintenance activity.

Appropriate procedures at the laboratory should be developed to study the effect of atmospheric corrosion on coated steel elements and the benefit of regular steel washing as an effective maintenance activity to reduce the corrosion rates.

LIST OF REFERENCES

LIST OF REFERENCES

- AASHTO (2011). "The Manual for Bridge Evaluation." American Association of State Highway and Transportation Officials.
- AASHTO (2012). "AASHTO LRFD Bridge Design Specifications." American Association of State Highway and Transportation Officials.
- Abed-Al-Rahim, I., Johnston, D., (1995). "Bridge Element Deterioration Rates." Transportation Research Record 1490. TRB, National Research Council, Washington, D.C.,
- AISC, (2015). "About the Steel Day Facility Tours: Steel Mills." American Institute of Steel Construction. Steelday. <https://www.aisc.org/content.aspx?id=23272> [Accessed January 16, 2015]
- AISI (1985). Steel Product Manual—Plates, American Iron and Steel Institute, Washington, DC.
- Albrecht, P. and Naeemi, A. (1984). "Performance of Weathering Steel in Bridges." National Cooperative Highway Research Program. NCHRP Report 272. Transportation Research Board
- Albrecht, P., Hall, T., (2003). "Atmospheric Corrosion Resistance of Structural Steels." American Society of Civil Engineers. Journal of Materials in Civil Engineering. Vol. 15, No. 1.
- Appleman, B., Weaver, R., Bruno, J., (1995). "Maintenance Coating of Weathering Steel: Field Evaluation and Guidelines." Research and Development, Turner-Fairbank Highway Research Center. Report No. FHWA-RD-92-055.
- ASTM (2008). "ASTM D1654-08 - Standard Test Method for Evaluation of Painted or Coated Specimens Subjected to Corrosive Environments." American Society for Testing and Materials

- ASTM (2010). “ASTM D7087-05a (2010) - Standard Test Method for an Imaging Technique to Measure Rust Creepage at Scribe on Coated Test Panels Subjected to Corrosive Environments.” American Society for Testing and Materials
ASTM (2011). “ASTM B117-11 - Standard Practice for Operating Salt Spray (Fog) Apparatus.” American Society for Testing and Materials
- ASTM (2011). “ASTM G1-03 (2011) - Standard Practice for Preparing, Cleaning, and Evaluating Corrosion Test Specimens.” American Society for Testing and Materials
- ASTM, (2012). “ASTM D610-08 (2012) - Standard Practice for Evaluating Degree of Rusting on Painted Steel Surfaces.” American Society for Testing and Materials
- AutoCAD 2016 (2016). “Autodesk Inc.”
- Azizinamini, A., Power, E., Meyers, G., Ozyildirim, H., Kline, E., Whitmore, D., and Mertz, D., (2013). “Design Guide for Bridges for Service Life.” Strategic Highway Research Program, Transportation Research Board, SHRP 2 Renewal Project R19A.
- Barker, R., and Puckett, J., (2007). “Design of Highway Bridges – An LRFD Approach.” John Wiley & Sons, Inc.
- Barth, K., (2012). “Steel Bridge Design Handbook. Design Example 2A: Two-Span Continuous Straight Composite Steel I-Girder Bridge.” Office of Bridge Technology Federal Highway Administration. Publication No. FHWA-IF-12-052 - Vol. 21.
- Berman, J., Roeder, C., Burgdorfer, R., (2013). “Determining the Cost/Benefit of Routine Maintenance Cleaning on Steel Bridges to Prevent Structural Deterioration.” Washington State Department of Transportation. WSDOT Research Report. Report No. WA-RD-11.1
- Bowman, M., and Moran, L., (2015). “Bridge Preservation Treatments and Best Practices.” Joint Transportation Research Program. SPR-3617. Purdue University, Indiana Department of Transportation, USDOT, FHWA.
- Bradford, S., (1998). “Practical Self-Study Guide to Corrosion Control.” CASTI Publishing Inc.
- Caltrans, (2015). “Bridge Design Practice – Chapter 9: Steel Plate Girders”
<http://www.dot.ca.gov/des/techpubs/manuals/bridge-design-practice/page/bdp-9.pdf>
[Accessed January 16, 2015]
- Cambier, S., (2014). “Atmospheric Corrosion of Coated Steel; Relationship between Laboratory and Field Testing.” PhD Dissertation in Civil Engineering. Ohio State University.

- Carlsson, B., Engstrom, G., Lejre, A., Johansson, M., Lahtinen, R., Strom, M., (2006). "Guideline for Selection of Accelerated Corrosion Test for Product Qualification." Nordic Innovation Centre. NORDTEST Technical Report TR-597.
- Chandler, R., (2004). "Life-Cycle Cost Model for Evaluating the Sustainability of Bridge Decks." Center for Sustainable Systems. University of Michigan. Report No. CSS04-06.
- Chang, L.-M., Zayed, T., Fricker, J. (1999). "Steel bridge protection policy – Volume IV: Life cycle cost analysis and maintenance plan." FHWA/IN/JTRP-98/21, Purdue University, Indiana Department of Transportation, USDOT, FHWA.
- Chong, S., and Yao, Y., (2007). "Selecting Overcoats for Bridges." Public Roads. Publication No. FHWA-HRT-07-006. Issue No. Vol. 71, No. 2
- Computers & Structures, Inc., (2011). "CSiBridge v15 - Bridge Superstructure Design." Computers & Structures, Inc. Structural and Earthquake Engineering Software.
- Corus Construction Center. "Corrosion Protection of Steel Bridges." Corus Construction Center. Brochure (2002).
- Crampton, D., Holloway, K., Fraczek, J., (2013). "Assessment of Weathering Steel Bridge Performance in Iowa and Development of Inspection and Maintenance Techniques." Wiss, Janney, Elstner Associates, Inc. Final Report SPR 90-00-RB17-012. WJE No. 2011.1671
- Cremer, (1996). "The Move to Cyclic Salt Spray Testing from Continuous Salt Spray." Anti-Corrosion Methods and Materials. Volume 43 – Number 3.
- Czarnecki, A., (2006). "System reliability Models for Evaluation of Corroded Steel Girder Bridges." PhD Dissertation in Civil Engineering. University of Michigan.
- Drazic, D., Vascic, V. (1989). "The Correlation between Accelerated Laboratory Corrosion Tests and Atmospheric Corrosion Station Tests on Steels." Corrosion Science, Vol. 29, No. 10,
- Eom, J., (2014). "Reliability Analysis Model for Deflection Limit State of Deteriorated Steel Girder Bridges." Journal of the Korea Institute for Structural Maintenance and Inspection Vol. 18, No. 2, March 2014.
- FHWA, (1989). "Uncoated Weathering Steel in Structures." Technical Advisory 5140.22. <https://www.fhwa.dot.gov/bridge/t514022.cfm> [Accessed Jan. 16, 2015].

- FHWA, (2011). "Bridge Preservation Guide – Maintaining a State of Good Repair Using Cost Effective Investment Strategies." FHWA Publication Number: FHWA-HIF-11042.
- FHWA, (2012). "Steel Bridge Design Handbook." US Department of Transportation.
- FHWA, (2015). USDOT. "Bridges and Structures – Bridges by Year Built 2013". Federal Highway Administration. US. Department of Transportation.
<http://www.fhwa.dot.gov/bridge/structyr.cfm> [Accessed Jan. 16, 2015].
- Fontana, M., (1986). "Corrosion Engineering." McGraw-Hill Book Company.
- Ford, K., Arman, M., Labi, S., Sinha, K., Thompson, P., Shirole, A., Li, Z., (2012). "Estimating Life Expectancies of Highway Assets – Volume 2: Final Report." National Cooperative Highway Research Program. NCHRP Report 713. Transportation Research Board.
- Golabi, K., Thompson, P., Hyman, W., (1993). "Pontis Technical Manual." Technical Report No. FHWA-SA-94-031. Optima Inc. and Cambridge Systematics, Inc.
- Guthrie, J., Battat, B., Grethlein, C., (2002). "Accelerated Corrosion Test." The AMPTIAC Quarterly, Volume 6, Number 3 11.
- Hara, S., Miura, M., Uchiumi, Y., Fujiwara, T., Yamamoto, M., (2005). "Suppression of Deicing Salt Corrosion of Weathering Steel Bridges by Washing." Corrosion Science 47.
- Hawk, H. (2003). "Bridge Life-Cycle Cost Analysis." National Cooperative Highway Research Program. NCHRP Report 483. Transportation Research Board.
- Hearn, G., (2012). "Deterioration and Cost Information for Bridge Management." Colorado Department of Transportation. DTD Applied Research and Innovation Branch. Report No. CDOT-2012-4. Final Report.
- Hema, J., Guthrie, W., Fonseca, F., (2004). "Concrete Bridge Deck Condition Assessment and Improvement Strategies." Utah Department of Transportation. Report UT-04-16
- Hopwood, T. and Meade, B., (1999). "Experimental Maintenance Painting by Overcoating on the I-64, I-71 and KY-22 Bridges." Research Report KTC-99-51. Kentucky Transportation Center. College of Engineering, University of Kentucky. Kentucky Transportation Cabinet.
- INDOT (2012). "Standard Specifications." Indiana Department of Transportation.

- INDOT (2013). "Design Manual." Indiana Department of Transportation.
- ITD, (2008). "Bridge Design LRFD Manual." Idaho Transportation Department
- Itoh, Y., Iwata, A., Kainuma, S., Kadota, Y., Kitagawa, T., (2006). "Accelerated Exposure Tests of Durability for Steel Bridges." Center for Integrated Research in Science and Engineering, Nagoya University, Japan
- Jones, D., (1996). "Principles and Prevention of Corrosion." Prentice Hall, Inc.
- Kayser, J. and Nowak, A., (1989). "Reliability of Corroded Steel Girder Bridges." Structural Safety, 6.
- Kayser, J., (1988). "The Effects of Corrosion on the Reliability of Steel Girder Bridges." PhD Dissertation in Civil Engineering. University of Michigan.
- Kepler, J.L., Darwin, D., Locke, C.E., (2000). "Evaluation of Corrosion Protection Methods for Reinforced Concrete Highway Structures". Kansas Department of Transportation, K-TRAN Project No. KU-99-6. University of Kansas Center research Inc.
- Kim, I., Itoh, Y., (2005). "Corrosion-Degradation Prediction of Steel Bridge Paintings." Proc. 8th Korea-Japan Joint Seminar on steel bridges, Nagoya, Japan, 2-3 August, 2005
- Koch, G., Brongers, M., Thompson, N., Virmani, P and Payerp, J., (2002). "Corrosion Costs and Preventive Strategies in the United States." FHWA-RD-01-156. U.S Department of Transportation. Federal Highway Administration
- Kogler, R., (2012). "Steel Bridge Design Handbook: Corrosion Protection of Steel Bridges." Publication No. FHWA-IF-12-052 - Vol. 19. U.S. Department of Transportation. Federal Highway Administration
- Komp, M., (1987). "Atmospheric Corrosion Ratings of Weathering Steels - Calculations and Significance", Mater. Perform. 26 (7).
- Kulicki, J., Prucz, Z., Sorgenfrei, D., Mertz, D., (1990). "Guidelines for Evaluating Corrosion Effects in Existing Steel Bridges." National Cooperative Highway Research Program. NCHRP Report 333. Transportation Research Board
- Landolfo, R., Cascini, L., and Portioli, F., (2010). "
- Lanterman, R., (2009). "Coating Condition Assessment of Portsmouth-Kittery Memorial Bridge." Project No. 13678-E. HDR Engineering, Inc. KTA-TATOR, Inc.

- Larrabee, C., and Coburn, S., (1962). "The Atmospheric Corrosion of Steels as Influenced by Changes in Chemical Composition." Proceedings, First International Congress on Metallic Corrosion, Butterworths.
- Laumet, P., (2006). "Reliability-Based Deterioration Model for Deflection Limit State in Steel Girder Bridges." PhD Dissertation in Civil Engineering. University of Michigan
- Lee, K., Cho, H., Cha, C., (2006). "Life-Cycle Cost-Effective Optimum Design of Steel Bridges Considering Environmental Stressors." *Engineering Structures* 28.
- Lin, C., Wang, C., (2005). "Correlation between Accelerated Corrosion tests and Atmospheric Corrosion Tests on Steel." *Journal of Applied Electrochemistry*, 35.
- McCrum, R., Arnold, C., and Dexter, R., (1985). "Effects of Corrosion on Unpainted Weathering Steel Bridges." Current Status Report. Michigan Transportation Commission. Research Project 78 G-241. Research Report No. R-1255.
- McCuen, R. H. and Albrecht, P., (1994) "Composite Modeling of Atmospheric Corrosion Penetration Data," Application of Accelerated Corrosion Tests to Service Life Prediction of Materials, ASTM STP 1194 Gustavo Cragolino and Narasi Sridhar, Eds., American Society for Testing and Materials.
- McCuen, R.H., and Albrecht, P. (1994). "Composite Modeling of Corrosion Penetration Data." Application of Accelerated Corrosion Tests to Service Life Prediction of Materials." American Society for Testing and Materials. ASTM STP 1194, Gustavo Cragolino, Ed.
- McDad, B., Laffrey, D., Dammann, M., Medlock, R., (2000). "Performance of Weathering Steel in TxDOT Bridges." Research Project Conducted for the Texas Department of Transportation. Project 0-1818
- MDOT, (2010). "Capital Preventive Maintenance Manual." Michigan Department of Transportation. Construction and Technology Division.
- Missouri Transportation Institute and Missouri Department of Transportation. Final Report TRyy0911.
- MnDOT, (2006). "Bridge Preservation, Improvement and Replacement Guidelines for Fiscal Year 2006 through 2008." Minnesota Department of Transportation. Engineering Services Division. <http://www.dot.state.mn.us/bridge/pdf/10b01.pdf> [Accessed Mar. 02, 2015]
- Modeling of Metal Structure Corrosion Damage: A State of the Art Report." Sustainability 2010, 2.

- Morcillo, M., de la Fuente, D., Diaz, I., and Cano, H., (2011). "Atmospheric corrosion of mild Steel." *Revista de Metalurgia*, 47 (5). Septiembre-Octubre.
- Myers, J., Zheng, W., Washer, G., (2010). "Structural Steel Coatings for Corrosion Mitigation." Missouri Department of Transportation Research, Development and Technology. Report No. OR11-006.
- Nickerson, R., (1995). "Performance of Weathering Steel in Highway Bridges – A Third Phase Report." American Iron and Steel Institute.
- NYS DOT, (2008). "Fundamentals of Bridge Maintenance and Inspection". New York State Department of Transportation. Office of Transportation Maintenance.
- Park, C., (1999). "Time dependent Reliability Models for Steel Girder Bridges." PhD Dissertation in Civil Engineering. University of Michigan
- Park, C., Nowak, A., Das, P., Flint, A., (1998). "Time-Varying Reliability Model of Steel Girder Bridges." *Proc. Institution of Civil Engineers, Structures and Buildings*, Thomas Telford Publishing, 128, Issue 4.
- Prucz, Z., and Kulicki, J., (1998). "Accounting for Effects of Corrosion Section Loss in Steel Bridges." *Transportation Research Record* 1624. Paper No. 98-0933.
- Purvis, R., (2003). "Bridge Deck Joint Performance - A Synthesis of Highway Practice." National Cooperative Highway Research Program. NCHRP Synthesis 319. Transportation research Board of the National Academies.
- Rahgozar, R. (2009). "Remaining Capacity Assessment of Corrosion Damaged Beams Using Minimum Curves." *Journal of Construction Steel research* 65, 2009. Elsevier Pub.
- Rea, F., (2014). "State of the Union Cleaning and Painting Steel Bridges." TSP2 Transportation System Preservation. Technical service program. Bridge Preservation. <https://www.pavementpreservation.org/wp-content/uploads/presentations/Rea%20SE%20Bridge%20Preservation%20Rea.pdf> [Accessed January 16, 2015]
- RIDOT, (2002). "Bridge Inspection/Washing Program - Bridge Drainage Program." Rhode Island Department of Transportation, Operations Division.
- Rossow, M. 2009. "Bridge Maintenance Training Reference Manual - Course No. S05-006." FHWA
- SAE (2003). "SAE J2334 - Laboratory Cyclic Corrosion Test." SAE International. Surface Vehicle Standard. Society of Automotive Engineers, Inc.

- Sinha, K., Labi, S., McCullough, B., Bhargava, A., Bai, Q., (2009). "Updating and Enhancing the Indiana Bridge Management System (IBMS)." Publication FHWA/IN/JTRP-2008/30. Joint Transportation Research Program, Indiana Department of Transportation and Purdue University, West Lafayette, Indiana.
- So, K., Cheung, M., Zhang, E., (2012). "Life-Cycle Management Strategy on Steel Girders in Bridges." Hindawi Publishing Corporation. *Advances in Civil Engineering*. Volume 2012, Article ID 643543
- Sobanjo, J., Thompson, P., (2001). "Development of Agency Maintenance, Repair & Rehabilitation (MR&R) Cost Data for Florida's Bridge Management System." Final Report. Contract No. BB-879. State Maintenance Office. Florida Department of Transportation.
- Spuler, T., Loehrer, R., and O'Suilleabhain, C., (2012). "Life-Cycle Considerations in the selection and Use of Bridge Expansion Joints." 18th Congress of IABSE, Seoul, 2012. International Association for Bridge and Structural Engineering
- Syed, S., (2006). "Atmospheric Corrosion of Materials." *Emirates Journal for Engineering Research*, 11 (1), 1-24.
- Tantawi, H., (1986). "Ultimate Strength of Highway Girder Bridges." PhD Dissertation in Civil Engineering. University of Michigan
- Townsend, H., and Zoccola, J., (1982). "Eight-Year Atmospheric Performance of Weathering Steel in Industrial, Rural, and Marine Environments." American Society for Testing and Materials. Special Technical Publication 767.
- Weyers, R., Prowell, B., Sprinkel, M., and Vorster, M., (1993). "Concrete Bridge Protection, Repair, and Rehabilitation Relative to Reinforcement Corrosion: A Methods Application Manual." SHRP-S-360, Strategic Highway Research Program, National Research Council. Washington, D.C.
- WisDOT, (2011). "Structures Inspection Manual." Wisconsin Department of Transportation. Part 2 – Bridges.
http://on.dot.wi.gov/dtid_bos/extranet/structures/maintenance/index.htm [Accessed Dec. 10, 2014]
- Yanev, B., Richards, G., (2011). "Bridge Maintenance in New York City. Network- and Project-Level Interaction." *Transportation Research Record: Journal of the Transportation Research Board*, No. 2220. Transportation Research Board of the National Academies, Washington, D.C.

Zaffetti, R., (2010). "Deterioration Factors at Girder Ends." Connecticut Department of Transportation. Presentation at the Northeast Bridge Preservation Partnership Meeting Hartford, CT.

APPENDICES

Appendix A Corrosion Penetration Data

Data from Albrecht and Naeemi (1984) study, for carbon and weathering steels are presented in Tables A.1 to A.3. The maximum time the steel coupons were exposed to atmospheric corrosion at each location are indicated. The study reported the parameter A in [μm] units, while B is a unitless parameter.

Table A.1: Parameters A and B – Industrial environment. Albrecht and Naeemi (1984)

INDUSTRIAL ENVIRONMENT					
Location	CARBON		WEATHERING A588		Max. Expos. [years]
	A [μm]	B	A	B	
Bayonne, N.J.	139.0	0.869			3
Pittsburg, Pa.	68.5	0.665			10
Bethlehem, Pa.	74.8	0.339	47.2	0.258	8
Newark, N.J.	50.4	0.346	36.1	0.273	8
Tinsley, U.K.			71.2	0.709	5
Middlesbrough, U.K.			59.1	0.585	5
Portishead, U.K.			42.0	0.527	5
Teesside, U.K.			65.3	0.646	5
Battersea, U.K.			57.2	0.693	5
Mullheim/Ruhr, F.R.G.	68.4	0.748	27.2	0.848	8

Table A.2: Parameters A and B – Marine environment. Albrecht and Naeemi (1984)

MARINE ENVIRONMENT					
Location	CARBON		WEATHERING A588		Max. Expos. [years]
	A [μm]	B	A	B	
Block Island, R.I.	149.8	0.755			3.3
Kure Beach, N.C.	71.9	0.522			3.5
Kure Beach 2, N.C.	31.7	1.459	28	0.621	8
Kure Beach 3, N.C.	43.5	0.656			7.5
Eastney, U.K.			42.9	0.511	5
Rye, U.K.			49.3	0.585	5
Cuxhaven, F.R.G.	56.2	0.547	40.4	0.512	8

Table A.3: Parameters A and B – Rural environment. Albrecht and Naeemi (1984)

RURAL ENVIRONMENT					
Location	CARBON		WEATHERING A588		Max. Expos. [years]
	A [μm]	B	A	B	
Saylorsburg, Pa.	31.9	0.697	27.1	0.481	8
Loudwater, U.K.			50.7	0.494	5
Silverdale, U.K.			38.4	0.471	5
Brixham, U.K.			28.6	0.574	5
Olpe, F.R.G.	36.1	0.602	21.8	0.468	8

Figures A.1 to A.4 show the corrosion penetration values based on mean parameters A and B estimated by Kayser (1988). Actual data collected by Albrecht and Naeemi (1984) is presented in solid lines, while extrapolated values to 50 years evaluated by Kayser (1988) are presented in dotted lines. The plots are presented in linear scales and log-log scales, for both carbon and weathering steel.

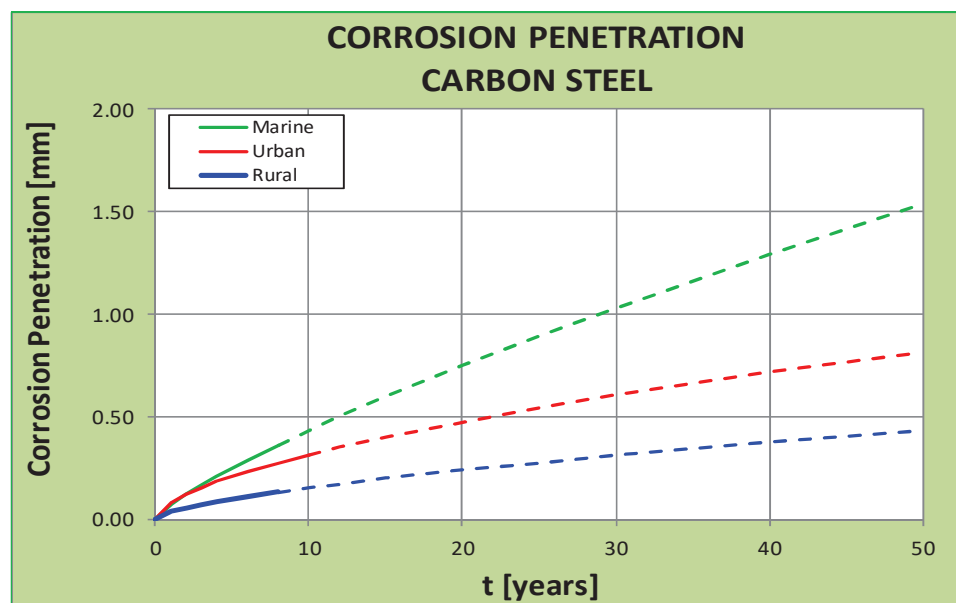


Figure A.1: Corrosion penetration for carbon steel - Linear axis

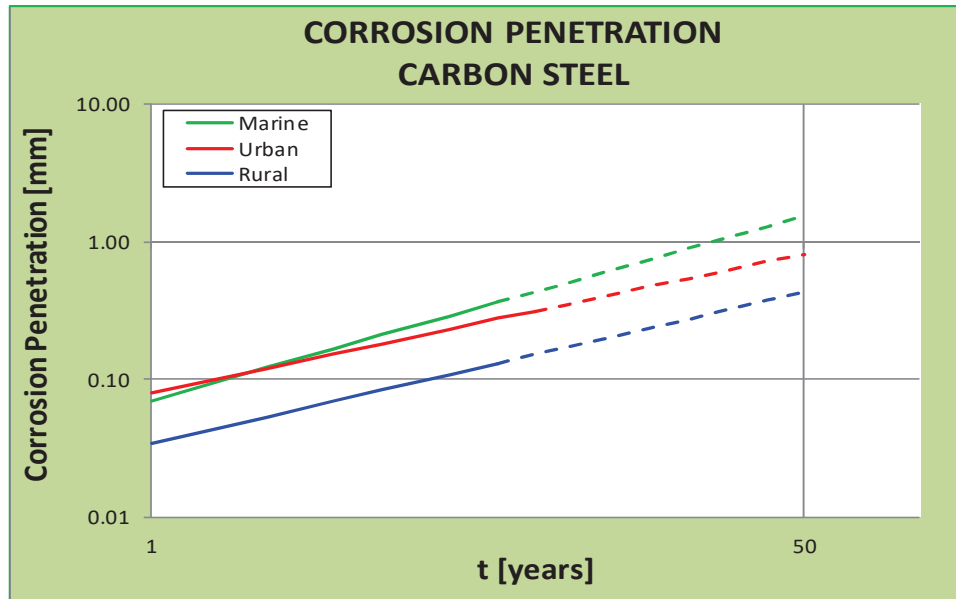


Figure A.2: Corrosion penetration for carbon steel – Log-Log axis

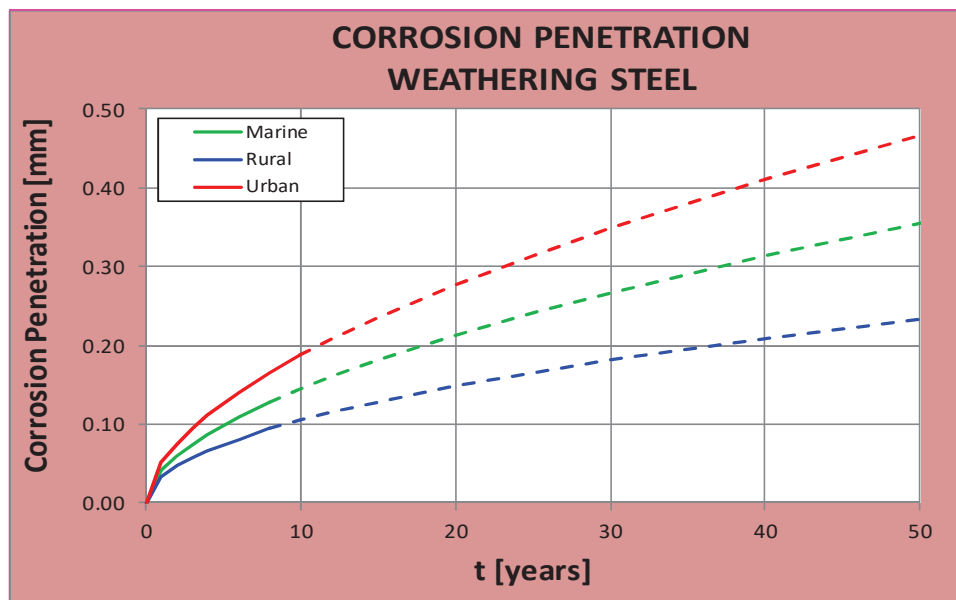


Figure A.3: Corrosion penetration for weathering steel - Linear axis

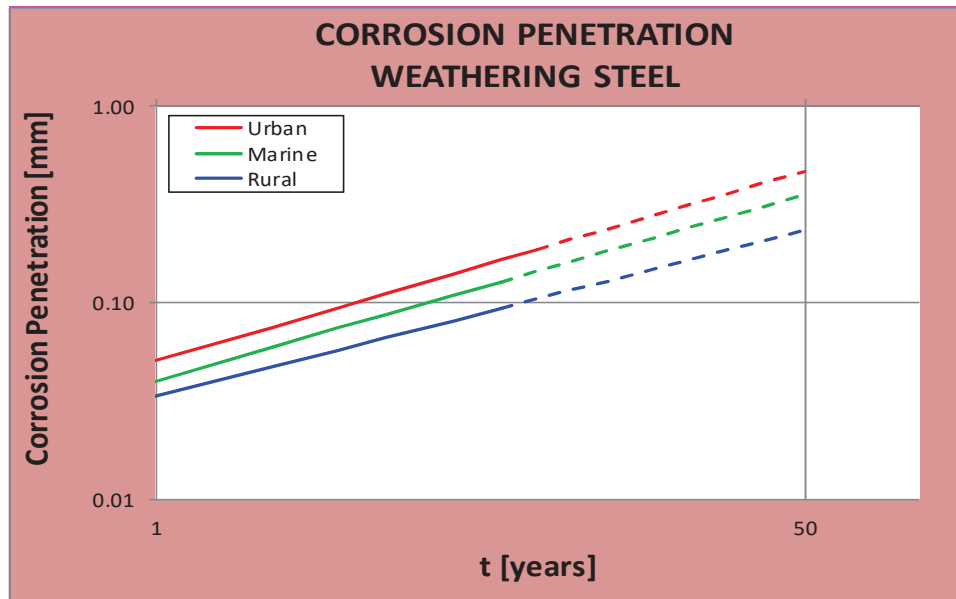
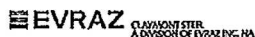


Figure A.4: Corrosion penetration for weathering steel – Log-Log axis

Appendix B Product Certificate

1. Material Test Report for Carbon Steel GR50 from EVRAZ, INC.
2. Report of Test and Analyses for Weathering Steel GR50W from ARCELORMITTAL STEEL USA
3. Certificate of Analysis for Sodium Chloride from MORTON SALT, INC.



Material Test Report

B/L: 294450

09/01/2011

4001 Philadelphia Pike, Claymont DE 19703

Sold To: STUPP BRIDGE COMPANY

3800 WEBER ROAD, ST. LOUIS, MO 63125

Order 226925-02 Customer PO 00430-02

Specifications:

ASTM A709/A709M-10 Grade 50(345) Type 2 Fully Killed Fine Grain Practice Non-Fracture Critical (T) Zone 2

AASHTO M270/M270-10 Grade 345(50) Fine Grain Practice Non-Fracture Critical (T) Zone 2

Products Shipped for Order 226925-02 (sorted by Serial)

Serial	Heat-Slab Orig	R/R	Plate Size in Inches	Plate Size in MM	Lbs	Kg
A81839-1	9C247D-905 USA	19.7	0.5000 x 95.0000 x 485.0000	12.70 x 2413.00 x 12319.00	6,533	2,940
A81839-2	9C247D-905 USA	19.7	0.5000 x 95.0000 x 485.0000	12.70 x 2413.00 x 12319.00	6,533	2,940

Shipment Summary of Order 226925-02: 2 pieces 13,066 lbs (5,900 kg)

Chemical Analysis for Order 226925-02 (sorted by Heat)

Heat	C	Mn	P	S	Si	Cu	NI	Cr	Mo	Sn
9C247D	0.08	1.36	0.012	0.012	0.19	0.030	0.010	0.030	0.004	0.006
	Al	V	Nb/Cb	N	Ascl	Ti	B			
	0.048	0.09	0.00	0.004	0.000	0.004	0.0001			

Tensile Tests for Order 226925-02 (sorted by Heat)

Serial	Heat-Slab	Gauge		Tensile		Yield		Elongation		RA %	Head Tail	Dir	Norm	S/R	Test ID
		Inches	MM	KSI	MPA	KSI	MPA	%	In.						
A80602-1	9C247D-301	0.3750	9.53	81	561	75	520	22	2	50		Tran			299078
A80657-1	9C247D-304	0.6250	15.88	67	459	52	356	42	2	50		Tran			299016

Impact Tests for Order 226925-02 (sorted by Heat)

Serial	Heat-Slab	Gauge		Temp		Ft-Lbs			Joules			Head Tail	Dir	Norm	Stress Rel	Test ID
		Inches	MM	°F	°C	1	2	3	1	2	3					
A81985-1	9C247D-903	0.6250	15.88	10	-12	227	235	232	308	319	315		Long			112921

Impact Tests for Order 226925-02 Supplemental Information (sorted by Heat)

Serial	Heat-Slab	Gauge		M11 Lat Exp			Shear %			Size	Loc	Head Tail	Dir	Norm	Stress Rel	Test ID
		Inches	MM	1	2	3	1	2	3							
A81985-1	9C247D-903	0.6250	15.88							Full	Std		Long			112921

Other Information for Order 226925-02

Material is 100% melted and manufactured in the USA.

Order 226926-02 Customer PO 00427-02

Specifications:

ASTM A709/A709M-10 Grade 50(345) Type 2 Fully Killed Fine Grain Practice Non-Fracture Critical (T) Zone 2

AASHTO M270/M270-10 Grade 345(50) Fine Grain Practice Non-Fracture Critical (T) Zone 2

Products Shipped for Order 226926-02 (sorted by Serial)

Serial	Heat-Slab Orig	R/R	Plate Size in Inches	Plate Size in MM	Lbs	Kg
A81823-1	9C247D-805 USA	19.7	0.5000 x 98.0000 x 615.0000	12.70 x 2489.20 x 15621.00	8,546	3,846

Shipment Summary of Order 226926-02: 1 piece 8,546 lbs (3,846 kg)

Notary Public: Alice Martin

Unless otherwise specified, Mercury, radium or alpha source materials have not been used.

certify the above results to be correct as contained in the records of the corporation.

Chief Metallurgist, David J. Cernava

D. J. Cernava

Revision:

Page 12 of 14

Figure B.1: Material test report for carbon steel GR50 from EVRAZ, INC.

F4859700
REV. J (4-08)

ARCELORMITTAL STEEL USA
QUALITY DEPARTMENT
REPORT OF TESTS AND ANALYSES

BURNS HARBOR PLATE

SHIPMENT NO. 803-15B74	DATE SHIPPED 11-19-12	CAR OR VEHICLE NO. CSS-CHGD-CSXT-GUTHRLMIC 036351
----------------------------------	---------------------------------	---

PAGE **2**

SOLD TO STUPP BROS INC DIV OF STUPP BROS CO 3800 WEBER RD ST LOUIS MO 63125	SHIP TO STUPP BROS INC STUPP BRIDGE CO DIV THEIR SIDING 445 CENTURY ST BOWLING GREEN KY 42101
---	--

NOTE	SERIAL NUMBER	PAT. NO.	HEAT NUMBER	NO. PCS	SIZE AND QUANTITY				WEIGHT	YIELD POINT	TENSILE STRENGTH	ELONG.		RED %
					THICKNESS	WIDTH OR DIA	LENGTH	INCHES				INCHES	INCHES	
QUALITY STEEL MELTED & MANUFACTURED IN THE U. S. A. PLATES - ASTM A709-11 GR 50WT2 KLD FINE GRAIN PRAC TYPE B, CH-V A673 FREQ (H) L 15/10 FTLBS AT +40F MFST - MFST MILL SERIAL# MFST TUCKER COUNTY WEST VIRGINIA MFST PPI 0046265- 0001 LIFT MAX 10 TON-SIZES SEP UNLDG OH-PLATE HOOK-MAGNET LOAD MAX 180000 # LOAD OV 120 IN WIDE-OK POST LOAD LOAD MAX 185000 # CO# 00465-01 GH 818-2495E <div style="display: flex; justify-content: space-between;"> 813X74420 1 1/2 96 610 8304 59100 85700 8 20 </div> PLATES - ASTM A709-11 GR 50WT2 KLD FINE GRAIN PRAC TYPE B, CH-V A673 FREQ (H) L 15/10 FTLBS AT +40F MFST - MFST MILL SERIAL# MFST WAYNE COUNTY WV MFST PPI 0046704- 0001 LIFT MAX 10 TON-SIZES SEP UNLDG OH-PLATE HOOK-MAGNET LOAD MAX 180000 # LOAD OV 120 IN WIDE-OK POST LOAD LOAD MAX 185000 # CO# 00468-01 GH 818-2517C <div style="display: flex; justify-content: space-between;"> 821Z01570 2 5/8 83.5 440.5 13040 64600 91700 8 21 </div>														

NOTE	O-QUENCH TEMPERATURE	T-TEMPER TEMPERATURE	N-NORMALIZE TEMPERATURE

SERIAL NUMBER	PAT. NO.	HEAT NUMBER	HARD	BEND	CHARPY IMPACT													
					THICKNESS	TYPE	SIZE	DR.	TEST TEMPR	ENERGY FT			SHEAR (KJ)			LAT. EXP		
INCHES	INCHES	INCHES	INCHES	INCHES	F	1	2	3	1	2	3	1	2	3	1	2	3	
813X74420					.500	V	FULL	L	+40	30	37	24						
821Z01570					.625	V	FULL	L	+40	56	63	47						

SUBSCRIBED AND SWORN TO BEFORE ME
 THIS 20 DAY OF NOVEMBER 2012
 NOTARY PUBLIC DOMINA J. POMERO
 PORTER COUNTY INDIANA
 MY COMMISSION EXPIRES: MAY 17, 2014

HEAT NUMBER	CHEMICAL ANALYSIS														MCQUAD	GRAN	SIZE
	C	Mn	P	S	Si	Cu	Ni	Cr	Mo	V	Ti	Al	B	Cb			
813X74420	.14	1.15	.018	.004	.396	.286	.17	.59	.007	.041		.033	.0003	.003			
821Z01570	.14	1.13	.012	.003	.398	.280	.19	.59	.005	.043		.034	.0003	.003			

I CERTIFY THAT THE ABOVE RESULTS ARE A TRUE AND CORRECT COPY OF ACTUAL RESULTS CONTAINED IN RECORDS MAINTAINED BY ARCELORMITTAL STEEL USA AND ARE IN FULL COMPLIANCE WITH THE REQUIREMENTS OF THE SPECIFICATION CITED ABOVE. THIS TEST REPORT CANNOT BE ALTERED AND MUST BE TRANSMITTED INTACT WITH ANY SUBSEQUENT THIRD PARTY TEST REPORTS, IF REQUIRED.

QUALITY MANAGER David G. Elwood PER [Signature]

Figure B.2: Report of test and analyses for weathering steel GR50W from ARCELORMITTAL STEEL USA

MORTON SALT
Morton Salt, Inc.

Certificate of Analysis

F112840000G 50Lb Culinox 999 Paper

Pvg Norwood Chemical
8080 Hubbard St
Detroit MI 48228-2331
USA

DISTRIBUTED BY
PVG NORWOOD CHEMICALS, INC.
10500 Harper Avenue
Detroit, MI 48213
(313) 925-0300

14-MAY-2014
HITTMAN
Judy Eames
Quality Control
330/9252015

Page 1/1

Manufacturer:	Morton Salt, Inc.	Morton Batch No.:	R114129020
Morton Order No.:	5100483590	Manufact. Date:	09-MAY-2014
Cost, Order No.:	182773		
Delivery / Item No.:	5200947366 / 000020		
Quantity:	392 BAG	Shipping date:	14-MAY-2014

General information:

This product meets the tolerances for Food Grade Salt as published in the Food Chemical Codex latest edition. It has been manufactured in compliance with all applicable parts of the Good Manufacturing Practice Regulations for foods as set forth in 21 CFR Part 110 and Canadian Food and Drugs Act and Regulations. Product does not contain any of the nine major food allergens or sulfate > 10ppm. Product does not contain genetically modified organisms and is not of animal origin. Salt is chemically stable and does not deteriorate over time.

Parameter	Result
Arsenic	< 1.0 ppm
Calcium & Magnesium as Calcium	8 ppm
Copper	0.53 ppm
Iron - Free	0.3 ppm
Heavy Metals as Lead	< 2.0 ppm
Insoluble Matter (ppm)	4 ppm
Moisture - Surface	0.010 %
Sodium Chloride	99.99 %
Sulfate	0.009 %
Bulk Density (lb/ft ³)	77.0 lb/ft ³
US #100 (150µm) Retained	2 %
US #20 (850µm) Retained	0 %
US #30 (600µm) Retained	1 %
US #40 (425µm) Retained	23 %
US #50 (300µm) Retained	54 %
US #70 (212µm) Retained	18 %
US FAN	1 %
Cumulative Passing US # 70	3 %

Shipping Plant: 151 Industrial Ave., Pittman, Or, 97137-1503

P.O. # 060914 CL
CODE/PART
NUMBER
715

Electronically released by Judy Eames quality on 11-MAY-2014

This certificate does not release the purchaser from examining the product upon delivery and gives no assurance of suitability of the product for any particular purpose.

Figure B.3: Certificate of analysis for sodium chloride from MORTON SALT, INC.

Appendix C Identification of Coupons for ACT

The coupon identification system is presented herein. Steel Type A involves uncoated carbon steel, and it is comprised by Groups A01 to A10. Steel Type B involves coated carbon steel, and it is comprised by Groups B01 to B10. Steel Type C involves uncoated weathering steel, and it is comprised by Groups C01 to C10. Steel Type D involves coated carbon steel with a scratch mark, and it is comprised by Groups D01 to D07.

Table C.1: Identification of steel coupons from steel types A, B, C, and D

STEEL TYPE A			STEEL TYPE B		
Group	No.	Coupon	Group	No.	Coupon
A01	A01	A01-a	B01	B01	B01-a
	A02	A01-b		B02	B01-b
	A03	A01-c		B03	B01-c
	A04	A01-d		B04	B01-d
A02	A05	A02-a	B02	B05	B02-a
	A06	A02-b		B06	B02-b
	A07	A02-c		B07	B02-c
	A08	A02-d		B08	B02-d
A03	A09	A03-a	B03	B09	B03-a
	A10	A03-b		B10	B03-b
	A11	A03-c		B11	B03-c
	A12	A03-d		B12	B03-d
A04	A13	A04-a	B04	B13	B04-a
	A14	A04-b		B14	B04-b
	A15	A04-c		B15	B04-c
	A16	A04-d		B16	B04-d
A05	A17	A05-a	B05	B17	B05-a
	A18	A05-b		B18	B05-b
	A19	A05-c		B19	B05-c
	A20	A05-d		B20	B05-d
A06	A21	A06-a	B06	B21	B06-a
	A22	A06-b		B22	B06-b
	A23	A06-c		B23	B06-c
	A24	A06-d		B24	B06-d
A07	A25	A07-a	B07	B25	B07-a
	A26	A07-b		B26	B07-b
	A27	A07-c		B27	B07-c
	A28	A07-d		B28	B07-d
A08	A29	A08-a	B08	B29	B08-a
	A30	A08-b		B30	B08-b
	A31	A08-c		B31	B08-c
	A32	A08-d		B32	B08-d
A09	A33	A09-a	B09	B33	B09-a
	A34	A09-b		B34	B09-b
	A35	A09-c		B35	B09-c
	A36	A09-d		B36	B09-d
A10	A37	A10-a	B10	B37	B10-a
	A38	A10-b		B38	B10-b
	A39	A10-c		B39	B10-c
	A40	A10-d		B40	B10-d

Table C.1: Continued

STEEL TYPE C			STEEL TYPE D				
Group	No.	Coupon	Group	No.	Coupon	Initial	
C01	C01	C01-a	D01	D01	D01-a	B03	
	C02	C01-b		D02	D01-b	B04	
	C03	C01-c		D03	D01-c	B07	
	C04	C01-d	D02	D04	D02-a	B08	
C02	C05	C02-a		D05	D02-b	B11	
	C06	C02-b		D06	D02-c	B12	
	C07	C02-c	D03	D07	D03-a	B15	
	C08	C02-d		D08	D03-b	B16	
C03	C09	C03-a	D09	D03-c	B19		
	C10	C03-b	D04	D10	D04-a	B20	
	C11	C03-c		D11	D04-b	B23	
	C12	C03-d		D12	D04-c	B24	
C04	C13	C04-a	D05	D13	D05-a	B27	
	C14	C04-b		D14	D05-b	B28	
	C15	C04-c		D15	D05-c	B31	
	C16	C04-d	D06	D16	D06-a	B35	
C05	C17	C05-a		D17	D06-b	B36	
	C18	C05-b		D07	D18	D07-a	B39
	C19	C05-c			D19	D07-b	B40
	C20	C05-d					
C06	C21	C06-a					
	C22	C06-b					
	C23	C06-c					
	C24	C06-d					
C07	C25	C07-a					
	C26	C07-b					
	C27	C07-c					
	C28	C07-d					
C08	C29	C08-a					
	C30	C08-b					
	C31	C08-c					
	C32	C08-d					
C09	C33	C09-a					
	C34	C09-b					
	C35	C09-c					
	C36	C09-d					
C10	C37	C10-a					
	C38	C10-b					
	C39	C10-c					
	C40	C10-d					

Coupon B32 was damaged during manipulation

Tablas and graphs were identified with specific color for each steel type:

steel type A: GREEN

steel type B: BLUE

steel type C: RED

steel type D: ORANGE

Appendix D Weight Change During ACT

The weight change for each steel coupon is presented in this Appendix, in tabulated and graphical manner. Weight changes for coupons from steel Types A, B, and C are presented week by week for the 24 weeks the ACT lasted. For coupons from steel Type D the data are presented for the 10 weeks they were under the ACT. The data are presented for each steel type and for each group, every week a group was subjected to washing.

Table D.1: Weight change during ACT for coupons from steel Type A

Group A01	WEIGHT (gr.)			
	A01-a	A01-b	A01-c	A01-d
Week				
00	1,152.75	1,155.89	1,152.52	1,146.31
01	1,153.68	1,156.94	1,153.45	1,147.25
02	1,154.72	1,157.89	1,154.57	1,148.15
03	1,155.31	1,158.61	1,155.16	1,148.93
04	1,156.44	1,160.04	1,156.23	1,149.96
05	1,157.15	1,160.75	1,157.05	1,150.52
06	1,157.60	1,161.03	1,157.12	1,151.09
07	1,158.77	1,162.29	1,158.63	1,152.32
08	1,159.53	1,163.14	1,160.04	1,153.50
09	1,159.96	1,163.70	1,160.93	1,154.01
10	1,161.63	1,165.39	1,162.37	1,155.65
11	1,162.73	1,166.43	1,163.38	1,157.21
12	1,163.09	1,166.62	1,163.17	1,157.63
13	1,164.55	1,168.99	1,164.37	1,159.32
14	1,165.66	1,169.35	1,164.74	1,159.98
15	1,166.34	1,169.53	1,165.15	1,160.97
16	1,166.21	1,168.92	1,164.72	1,161.09
17	1,167.81	1,170.31	1,166.16	1,162.43
18	1,168.46	1,170.35	1,166.80	1,161.79
19	1,171.24	1,172.90	1,169.28	1,164.69
20	1,172.21	1,173.48	1,170.05	1,165.92
21	1,173.52	1,174.90	1,171.23	1,167.79
22	1,174.34	1,175.81	1,171.93	1,168.12
23	1,173.02	1,174.52	1,170.73	1,166.88
24	1,176.81	1,177.81	1,173.80	1,169.43

Group A02	WEIGHT (gr.)			
	A02-a	A02-b	A02-c	A02-d
Week				
00	1,158.58	1,161.09	1,145.72	1,140.45
02	1,160.43	1,162.99	1,147.80	1,142.49
04	1,162.51	1,165.15	1,149.25	1,144.25
06	1,163.92	1,166.34	1,150.10	1,145.29
08	1,165.81	1,168.52	1,152.32	1,147.39
10	1,167.01	1,169.74	1,153.59	1,148.26
12	1,167.83	1,170.52	1,154.66	1,149.23
14	1,169.42	1,172.41	1,156.17	1,151.14
16	1,169.19	1,171.92	1,155.59	1,151.15
18	1,170.06	1,172.67	1,156.40	1,151.74
20	1,172.51	1,174.76	1,158.36	1,154.03
22	1,175.46	1,176.22	1,159.87	1,155.27
24	1,178.30	1,177.40	1,161.54	1,156.56

Group A03	WEIGHT (gr.)			
	A03-a	A03-b	A03-c	A03-d
Week				
00	1,171.93	1,153.70	1,137.44	1,160.18
03	1,174.70	1,156.47	1,140.40	1,162.87
06	1,177.65	1,159.77	1,143.60	1,165.52
09	1,178.26	1,160.31	1,144.15	1,166.47
12	1,180.12	1,161.71	1,145.10	1,167.82
15	1,181.55	1,163.37	1,145.97	1,169.81
18	1,180.32	1,162.93	1,144.94	1,169.35
21	1,182.21	1,164.51	1,146.99	1,171.58
24	1,183.96	1,166.33	1,148.56	1,174.65

Table D.1: Continued

Group A04		WEIGHT (gr.)			
Week	A04-a	A04-b	A04-c	A04-d	
00	1,287.46	1,184.34	1,141.08	1,139.69	
04	1,291.47	1,188.28	1,145.83	1,144.25	
08	1,294.62	1,191.63	1,149.31	1,146.97	
12	1,295.33	1,192.84	1,151.38	1,148.81	
16	1,296.97	1,194.13	1,153.46	1,151.19	
20	1,298.91	1,195.91	1,156.12	1,153.32	
24	1,301.25	1,198.61	1,159.73	1,157.33	

Group A05		WEIGHT (gr.)			
Week	A05-a	A05-b	A05-c	A05-d	
00	1,154.30	1,259.49	1,143.78	1,164.80	
05	1,159.24	1,264.79	1,149.42	1,170.12	
10	1,162.84	1,268.58	1,153.91	1,174.41	
15	1,165.00	1,271.94	1,158.28	1,178.22	
20	1,165.75	1,273.08	1,159.43	1,179.54	

Group A06		WEIGHT (gr.)			
Week	A06-a	A06-b	A06-c	A06-d	
00	1,149.84	1,127.47	1,152.23	1,151.98	
06	1,156.63	1,134.42	1,158.83	1,158.74	
12	1,158.26	1,136.72	1,160.74	1,160.19	
18	1,162.83	1,141.40	1,164.08	1,162.56	
24	1,163.41	1,141.39	1,164.69	1,164.65	

Group A07		WEIGHT (gr.)			
Week	A07-a	A07-b	A07-c	A07-d	
00	1,289.97	1,144.67	1,303.57	1,329.77	
07	1,296.10	1,151.44	1,309.78	1,336.08	
14	1,298.55	1,153.62	1,311.49	1,339.06	
21	1,299.01	1,153.31	1,311.11	1,339.86	

Group A08		WEIGHT (gr.)			
Week	A08-a	A08-b	A08-c	A08-d	
00	1,150.41	1,146.89	1,141.80	1,151.87	
08	1,156.71	1,153.18	1,147.93	1,158.01	
16	1,159.11	1,155.30	1,152.13	1,161.25	
24	1,161.45	1,157.89	1,155.33	1,163.39	

Group A09		WEIGHT (gr.)			
Week	A09-a	A09-b	A09-c	A09-d	
00	1,157.73	1,145.54	1,151.41	1,152.15	
09	1,165.32	1,152.98	1,158.90	1,159.91	
18	1,167.60	1,154.32	1,160.29	1,163.46	

Table D.1: Continued

Group A10	WEIGHT (gr.)			
	Week	A10-a	A10-b	A10-c
00	1,150.17	1,150.90	1,153.82	1,145.63
01	1,151.09	1,151.94	1,154.72	1,146.53
02	1,152.05	1,152.75	1,155.79	1,147.35
03	1,152.96	1,153.64	1,156.84	1,148.61
04	1,153.69	1,154.21	1,157.49	1,148.81
05	1,154.52	1,155.02	1,158.32	1,149.66
06	1,155.54	1,155.98	1,159.15	1,150.52
07	1,156.39	1,157.49	1,160.30	1,151.25
08	1,156.72	1,158.33	1,161.23	1,152.79
09	1,157.22	1,159.65	1,161.63	1,153.89
10	1,158.14	1,160.84	1,163.97	1,154.15
11	1,158.66	1,161.20	1,164.24	1,155.26
12	1,159.99	1,162.87	1,164.87	1,155.86
13	1,160.32	1,163.10	1,165.66	1,156.09
14	1,161.48	1,164.24	1,167.04	1,156.92
15	1,162.07	1,165.07	1,167.32	1,157.50
16	1,162.61	1,164.76	1,168.20	1,158.09
17	1,163.87	1,165.58	1,169.08	1,159.99
18	1,165.65	1,167.22	1,170.50	1,160.38
19	1,166.17	1,167.59	1,170.99	1,160.87
20	1,166.91	1,168.03	1,171.89	1,161.81
21	1,167.81	1,168.61	1,172.61	1,162.44
22	1,168.16	1,168.77	1,173.02	1,162.33
23	1,169.38	1,169.68	1,174.12	1,163.28
24	1,170.76	1,170.94	1,175.60	1,164.95

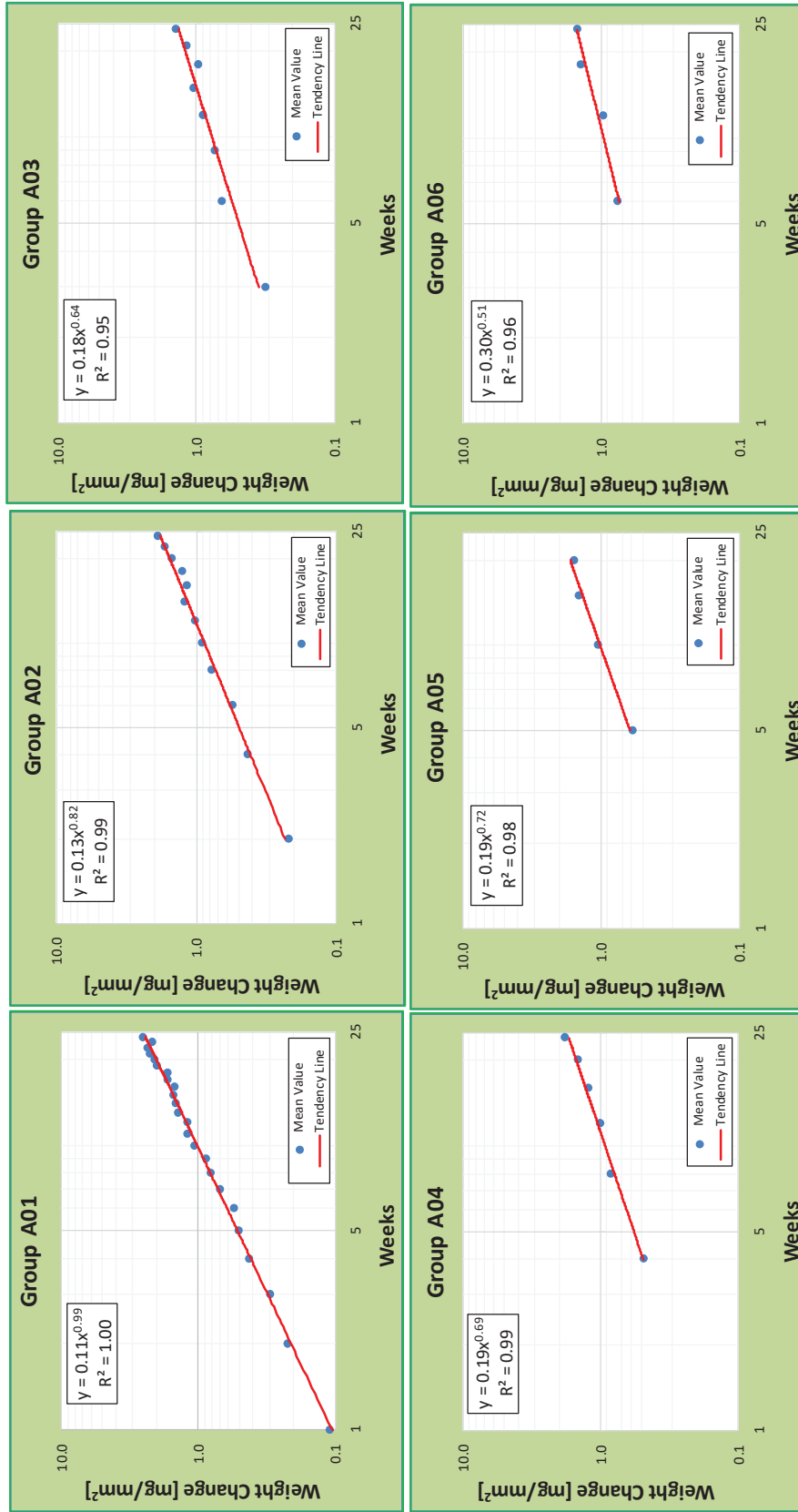


Figure D.1: Weight change versus time during ACT for coupons from steel Type A

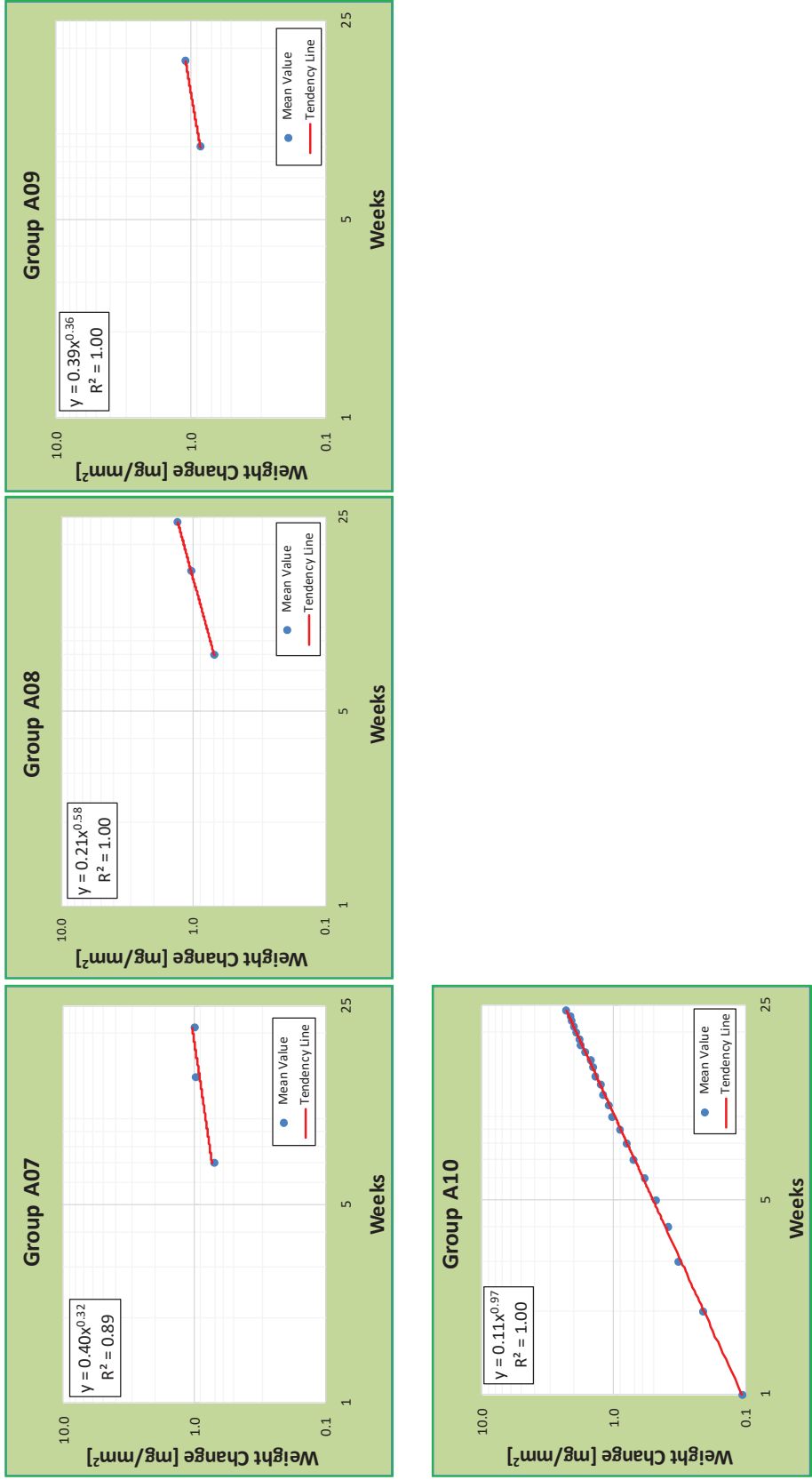


Figure D.1: Continued

Table D.2: Weight change during ACT for coupons from steel Type B

Group B01		WEIGHT (gr.)			
Week	B01-a	B01-b	B01-c	B01-d	
00	1,185.28	1,195.17	1,175.19	1,190.18	
01	1,185.25	1,195.19	1,175.23	1,190.15	
02	1,185.44	1,195.42	1,175.37	1,190.33	
03	1,185.49	1,195.46	1,175.41	1,190.40	
04	1,185.65	1,195.61	1,175.60	1,190.55	
05	1,185.57	1,195.55	1,175.49	1,190.48	
06	1,185.63	1,195.58	1,175.53	1,190.57	
07	1,185.54	1,195.51	1,175.51	1,190.50	
08	1,185.51	1,195.51	1,175.50	1,190.45	
09	1,185.38	1,195.29	1,175.38	1,190.22	
10	1,185.40	1,195.45	1,175.37	1,190.34	
11	1,185.64	1,195.70	1,175.70	1,190.53	
12	1,185.39	1,195.29	1,175.49	1,190.19	
13	1,185.14	1,195.12	1,175.12	1,190.04	
14	1,185.19	1,195.14	1,175.09	1,190.08	
15	1,185.25	1,195.20			
16	1,184.95	1,194.97			
17	1,185.10	1,194.97			
18	1,185.07	1,195.03			
19	1,185.10	1,195.02			
20	1,185.13	1,195.11			
21	1,185.14	1,195.10			
22	1,184.73	1,194.74			
23	1,185.02	1,194.90			
24	1,184.82	1,194.84			

Group B02		WEIGHT (gr.)			
Week	B02-a	B02-b	B02-c	B02-d	
00	1,204.53	1,196.12	1,188.62	1,187.04	
02	1,204.69	1,196.27	1,188.77	1,187.24	
04	1,204.91	1,196.51	1,189.01	1,187.49	
06	1,204.97	1,196.50	1,189.05	1,187.47	
08	1,204.77	1,196.40	1,188.91	1,187.33	
10	1,204.65	1,196.26	1,188.86	1,187.36	
12	1,204.59	1,196.17	1,188.77	1,187.25	
14	1,204.46	1,196.07	1,188.53	1,187.01	
16	1,204.16	1,195.81			
18	1,204.36	1,195.91			
20	1,204.46	1,196.02			
22	1,204.42	1,195.92			
24	1,204.31	1,195.78			

Group B03		WEIGHT (gr.)			
Week	B03-a	B03-b	B03-c	B03-d	
00	1,178.95	1,193.05	1,194.51	1,200.03	
03	1,179.21	1,193.33	1,194.79	1,200.34	
06	1,179.28	1,193.38	1,194.88	1,200.41	
09	1,179.10	1,193.07	1,194.63	1,200.15	
12	1,179.06	1,193.00	1,194.44	1,199.97	
15	1,178.91	1,192.96			
18	1,178.73	1,192.81			
21	1,178.90	1,192.91			
24	1,178.65	1,192.71			

Table D.2: Continued

Group B04		WEIGHT (gr.)			
Week	B04-a	B04-b	B04-c	B04-d	
00	1,198.52	1,191.53	1,205.14	1,216.70	
04	1,198.96	1,191.91	1,205.56	1,217.07	
08	1,198.83	1,191.79	1,205.43	1,216.95	
12	1,198.59	1,191.44	1,205.31	1,216.70	
16	1,198.23	1,191.30			
20	1,198.04	1,191.02			
24	1,197.71	1,190.85			

Group B05		WEIGHT (gr.)			
Week	B05-a	B05-b	B05-c	B05-d	
00	1,184.88	1,184.63	1,188.32	1,178.49	
05	1,185.25	1,184.93	1,188.68	1,178.88	
10	1,185.26	1,184.95	1,188.68	1,178.91	
15	1,184.87	1,184.59			
20	1,184.49	1,184.17			

Group B06		WEIGHT (gr.)			
Week	B06-a	B06-b	B06-c	B06-d	
00	1,200.20	1,182.55	1,203.75	1,204.98	
06	1,200.64	1,182.86	1,204.10	1,205.40	
12	1,200.38	1,182.61	1,203.86	1,205.12	
18	1,199.99	1,182.32			
24	1,199.63	1,181.98			

Group B07		WEIGHT (gr.)			
Week	B07-a	B07-b	B07-c	B07-d	
00	1,193.29	1,216.94	1,195.37	1,180.12	
07	1,193.45	1,217.10	1,195.42	1,180.32	
14	1,193.13	1,216.91	1,195.20	1,180.14	
21	1,192.80	1,216.58			

Group B08		WEIGHT (gr.)			
Week	B08-a	B08-b	B08-c	B08-d	
00	1,194.51	1,186.67	1,200.83	1,203.98	
08	1,194.73	1,186.94	1,201.13	1,204.29	
16	1,194.16	1,186.42			
24	1,193.66	1,186.04			

Group B09		WEIGHT (gr.)			
Week	B09-a	B09-b	B09-c	B09-d	
00	1,186.49	1,184.92	1,147.10	1,190.81	
09	1,186.55	1,185.04	1,147.43	1,190.99	
18	1,186.22	1,184.80			

Table D.2: Continued

Group B10	WEIGHT (gr.)			
Week	B10-a	B10-b	B10-c	B10-d
00	1,188.30	1,182.95	1,202.55	1,188.37
01	1,188.51	1,183.03	1,202.69	1,188.49
02	1,188.55	1,183.13	1,202.78	1,188.51
03	1,188.63	1,183.19	1,202.85	1,188.58
04	1,188.71	1,183.27	1,202.89	1,188.66
05	1,188.78	1,183.33	1,202.88	1,188.75
06	1,188.77	1,183.38	1,202.98	1,188.79
07	1,188.93	1,183.45	1,203.09	1,188.82
08	1,188.72	1,183.37	1,202.95	1,188.79
09	1,188.76	1,183.23	1,202.92	1,188.74
10	1,188.55	1,183.03	1,202.84	1,188.50
11	1,188.41	1,182.98	1,202.76	1,188.43
12	1,188.36	1,182.92	1,202.68	1,188.39
13	1,188.22	1,182.84	1,202.59	1,188.29
14	1,188.10	1,182.78	1,202.51	1,188.22
15	1,188.06	1,182.70		
16	1,187.93	1,182.67		
17	1,187.91	1,182.59		
18	1,187.83	1,182.55		
19	1,187.77	1,182.50		
20	1,187.69	1,182.49		
21	1,187.62	1,182.45		
22	1,187.51	1,182.37		
23	1,187.41	1,182.31		
e 24	1,187.33	1,182.26		

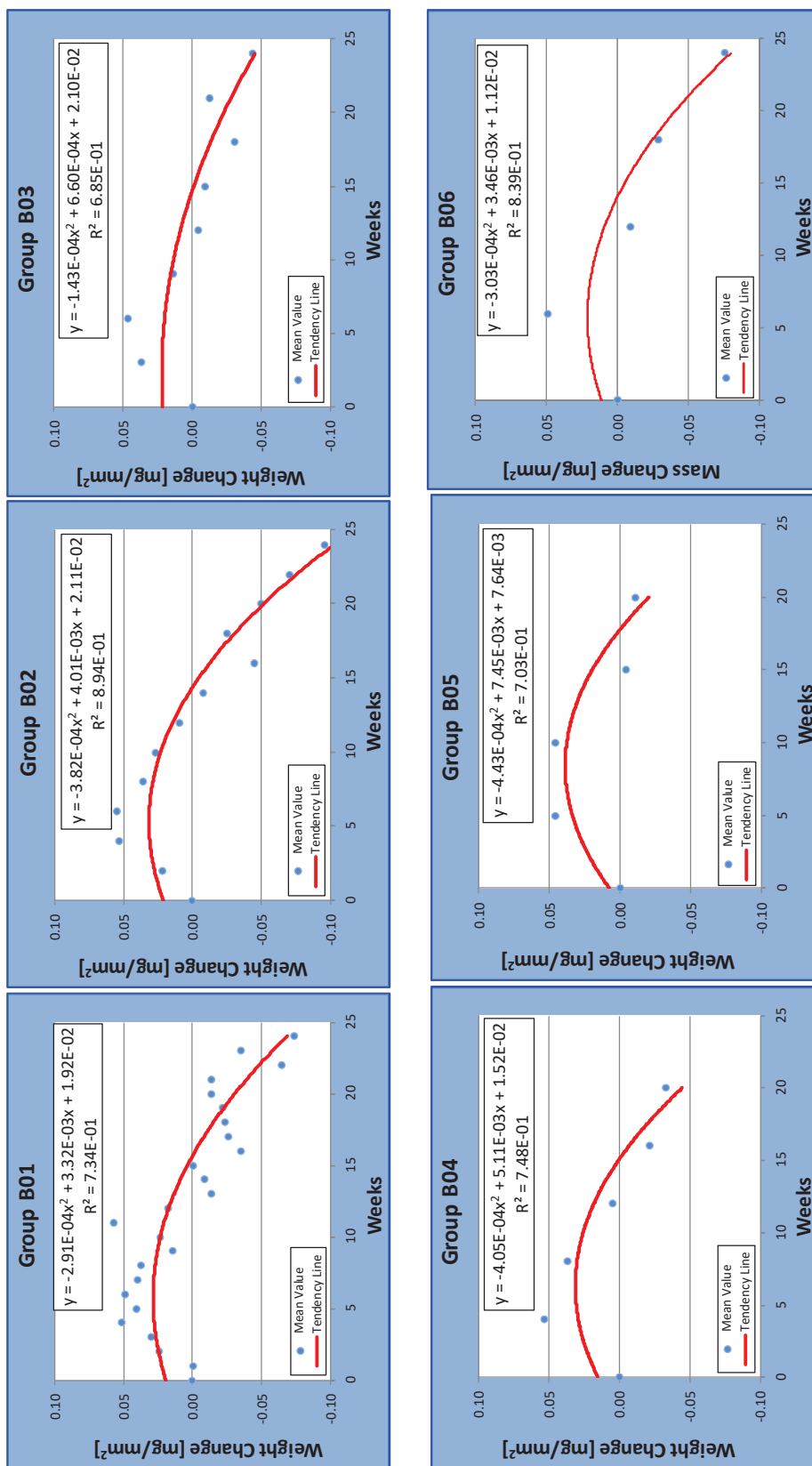


Figure D.2: Weight change versus time during ACT for coupons from steel Type B

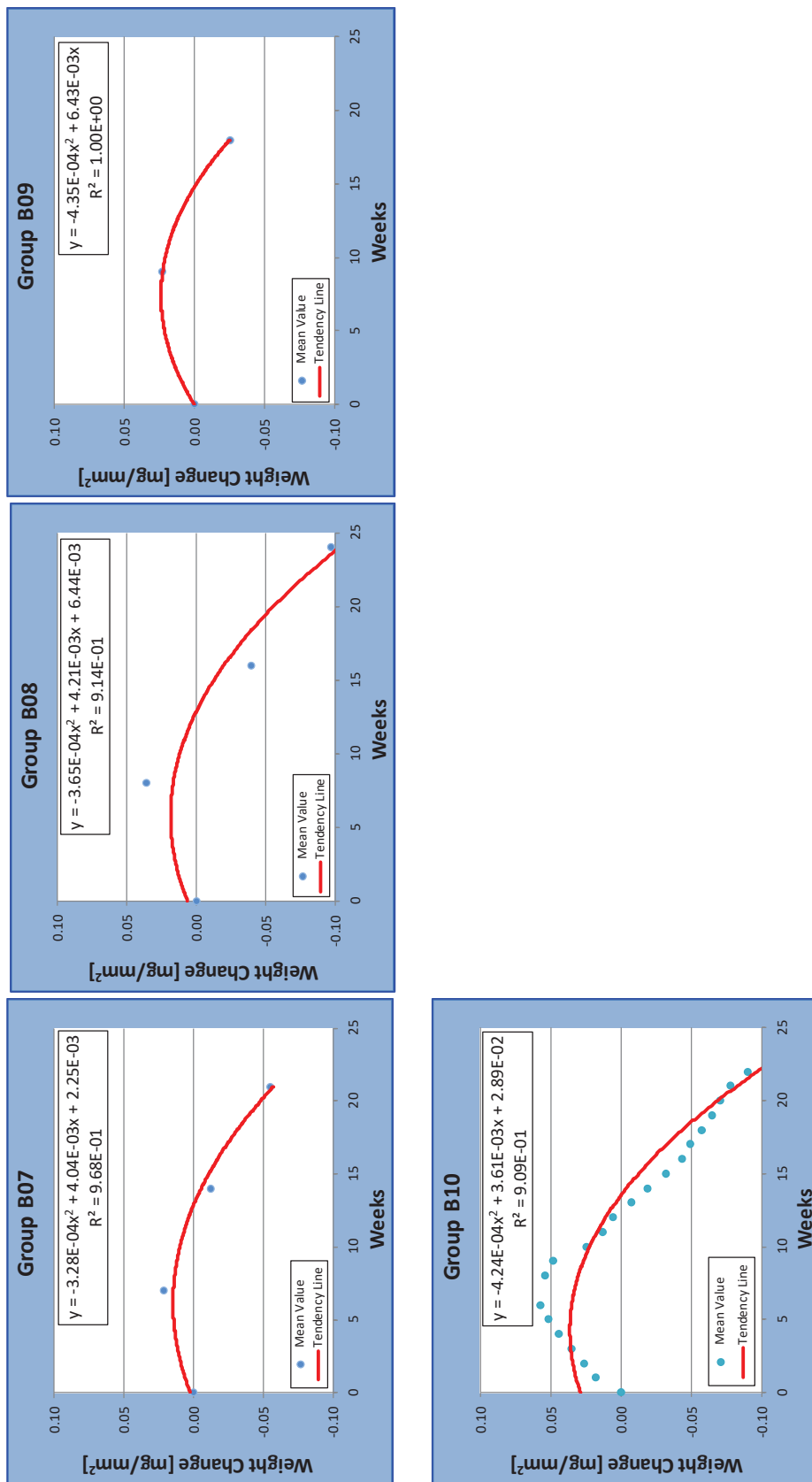


Figure D.2: Continued

Table D.3: Weight change during ACT for coupons from steel Type C

Group C01		WEIGHT (gr.)			
Week	C01-a	C01-b	C01-c	C01-d	
0	1,216.43	1,202.10	1,191.54	1,199.93	
1	1,217.95	1,203.50	1,192.90	1,201.14	
2	1,219.07	1,204.22	1,193.70	1,201.79	
3	1,220.33	1,205.69	1,194.96	1,203.45	
4	1,222.09	1,207.63	1,196.96	1,205.49	
5	1,223.32	1,208.34	1,197.69	1,206.12	
6	1,225.72	1,210.52	1,200.15	1,208.26	
7	1,227.78	1,212.77	1,201.52	1,210.29	
8	1,229.50	1,214.05	1,202.82	1,210.64	
9	1,231.13	1,215.52	1,204.83	1,212.62	
10	1,231.90	1,216.23	1,204.59	1,212.61	
11	1,234.02	1,218.35	1,207.32	1,214.83	
12	1,233.97	1,218.87	1,207.32	1,214.45	
13	1,234.53	1,219.64	1,209.22	1,216.89	
14	1,235.41	1,220.52	1,210.01	1,217.82	
15	1,236.74	1,222.24	1,211.45	1,219.56	
16	1,237.62	1,223.41	1,212.42	1,220.58	
17	1,236.72	1,223.03	1,211.66	1,220.37	
18	1,240.12	1,226.70	1,214.72	1,223.41	
19	1,242.73	1,229.29	1,217.13	1,226.04	
20	1,242.34	1,229.78	1,217.75	1,226.39	
21	1,242.91	1,230.73	1,218.38	1,227.08	
22	1,243.60	1,231.68	1,219.19	1,227.88	
23	1,244.14	1,232.16	1,219.67	1,228.18	
24	1,244.14	1,232.43	1,219.90	1,228.37	

Group C02		WEIGHT (gr.)			
Week	C02-a	C02-b	C02-c	C02-d	
0	1,220.58	1,200.73	1,193.26	1,163.79	
2	1,223.06	1,203.61	1,195.73	1,167.09	
4	1,225.81	1,206.13	1,198.51	1,169.87	
6	1,228.90	1,208.68	1,201.20	1,172.22	
8	1,231.71	1,211.25	1,203.83	1,174.90	
10	1,232.84	1,212.68	1,205.41	1,176.42	
12	1,234.02	1,214.29	1,207.20	1,178.64	
14	1,236.88	1,217.63	1,210.23	1,182.37	
16	1,238.62	1,220.04	1,212.73	1,185.15	
18	1,240.40	1,222.21	1,215.24	1,187.29	
20	1,242.22	1,225.41	1,217.86	1,190.12	
22	1,243.04	1,226.42	1,218.79	1,192.13	
24	1,241.89	1,226.02	1,215.32	1,189.58	

Group C03		WEIGHT (gr.)			
Week	C03-a	C03-b	C03-c	C03-d	
0	1,181.03	1,200.39	1,193.61	1,195.91	
3	1,184.73	1,204.35	1,197.57	1,199.60	
6	1,188.39	1,208.15	1,201.10	1,203.80	
9	1,192.02	1,211.93	1,205.05	1,207.74	
12	1,192.48	1,213.04	1,205.69	1,208.34	
15	1,196.83	1,218.50	1,210.83	1,213.64	
18	1,198.05	1,219.93	1,212.51	1,215.63	
21	1,200.19	1,221.94	1,214.78	1,218.12	
24	1,200.59	1,222.63	1,215.04	1,218.32	

Table D.3: Continued

Group C04		WEIGHT (gr.)			
Week	C04-a	C04-b	C04-c	C04-d	
0	1,171.65	1,205.89	1,192.79	1,164.92	
4	1,177.69	1,211.68	1,198.60	1,171.00	
8	1,180.78	1,215.38	1,202.43	1,174.88	
12	1,182.31	1,216.46	1,203.39	1,176.08	
16	1,186.71	1,220.86	1,207.15	1,181.99	
20	1,190.60	1,224.46	1,211.03	1,186.78	
24	1,194.19	1,227.38	1,215.32	1,190.44	

Group C05		WEIGHT (gr.)			
Week	C05-a	C05-b	C05-c	C05-d	
0	1,132.90	1,212.24	1,207.48	1,176.10	
5	1,139.69	1,219.13	1,214.28	1,182.91	
10	1,144.77	1,224.05	1,218.82	1,188.16	
15	1,151.14	1,229.96	1,224.65	1,195.19	
20	1,152.53	1,230.82	1,226.81	1,197.33	

Group C06		WEIGHT (gr.)			
Week	C06-a	C06-b	C06-c	C06-d	
0	1,132.99	1,195.75	1,192.89	1,200.17	
6	1,143.00	1,205.36			
12	1,145.83	1,207.92			
18	1,154.08	1,214.20			
24	1,161.40	1,220.25			

Group C07		WEIGHT (gr.)			
Week	C07-a	C07-b	C07-c	C07-d	
0	1,197.19	1,179.42	1,172.12	1,180.68	
7	1,207.52	1,189.17	1,181.52	1,189.81	
14	1,214.02	1,194.70	1,187.08	1,194.05	
21	1,218.20	1,199.42	1,193.98	1,198.97	

Group C08		WEIGHT (gr.)			
Week	C08-a	C08-b	C08-c	C08-d	
0	1,229.12	1,201.61	1,178.92	1,213.79	
8	1,241.96	1,212.11	1,190.58	1,225.62	
16	1,247.81	1,218.13	1,197.23	1,231.78	
24	1,252.53	1,222.77	1,202.15	1,236.03	

Group C09		WEIGHT (gr.)			
Week	C09-a	C09-b	C09-c	C09-d	
0	1,216.35	1,171.85	1,216.06	1,190.61	
9	1,227.74	1,182.56	1,227.64	1,201.52	
18	1,233.68	1,187.70	1,235.35	1,208.67	

Table D.3: Continued

Group C01	WEIGHT (gr.)			
	Week	C01-a	C01-b	C01-c
0	1,216.43	1,202.10	1,191.54	1,199.93
1	1,217.95	1,203.50	1,192.90	1,201.14
2	1,219.07	1,204.22	1,193.70	1,201.79
3	1,220.33	1,205.69	1,194.96	1,203.45
4	1,222.09	1,207.63	1,196.96	1,205.49
5	1,223.32	1,208.34	1,197.69	1,206.12
6	1,225.72	1,210.52	1,200.15	1,208.26
7	1,227.78	1,212.77	1,201.52	1,210.29
8	1,229.50	1,214.05	1,202.82	1,210.64
9	1,231.13	1,215.52	1,204.83	1,212.62
10	1,231.90	1,216.23	1,204.59	1,212.61
11	1,234.02	1,218.35	1,207.32	1,214.83
12	1,233.97	1,218.87	1,207.32	1,214.45
13	1,234.53	1,219.64	1,209.22	1,216.89
14	1,235.41	1,220.52	1,210.01	1,217.82
15	1,236.74	1,222.24	1,211.45	1,219.56
16	1,237.62	1,223.41	1,212.42	1,220.58
17	1,238.72	1,225.03	1,213.66	1,222.37
18	1,240.12	1,226.70	1,214.72	1,223.41
19	1,242.73	1,229.29	1,217.13	1,226.04
20	1,242.34	1,229.78	1,217.75	1,226.39
21	1,242.91	1,230.73	1,218.38	1,227.08
22	1,243.60	1,231.68	1,219.19	1,227.88
23	1,244.14	1,232.16	1,219.67	1,228.18
24	1,244.14	1,232.43	1,219.90	1,228.37

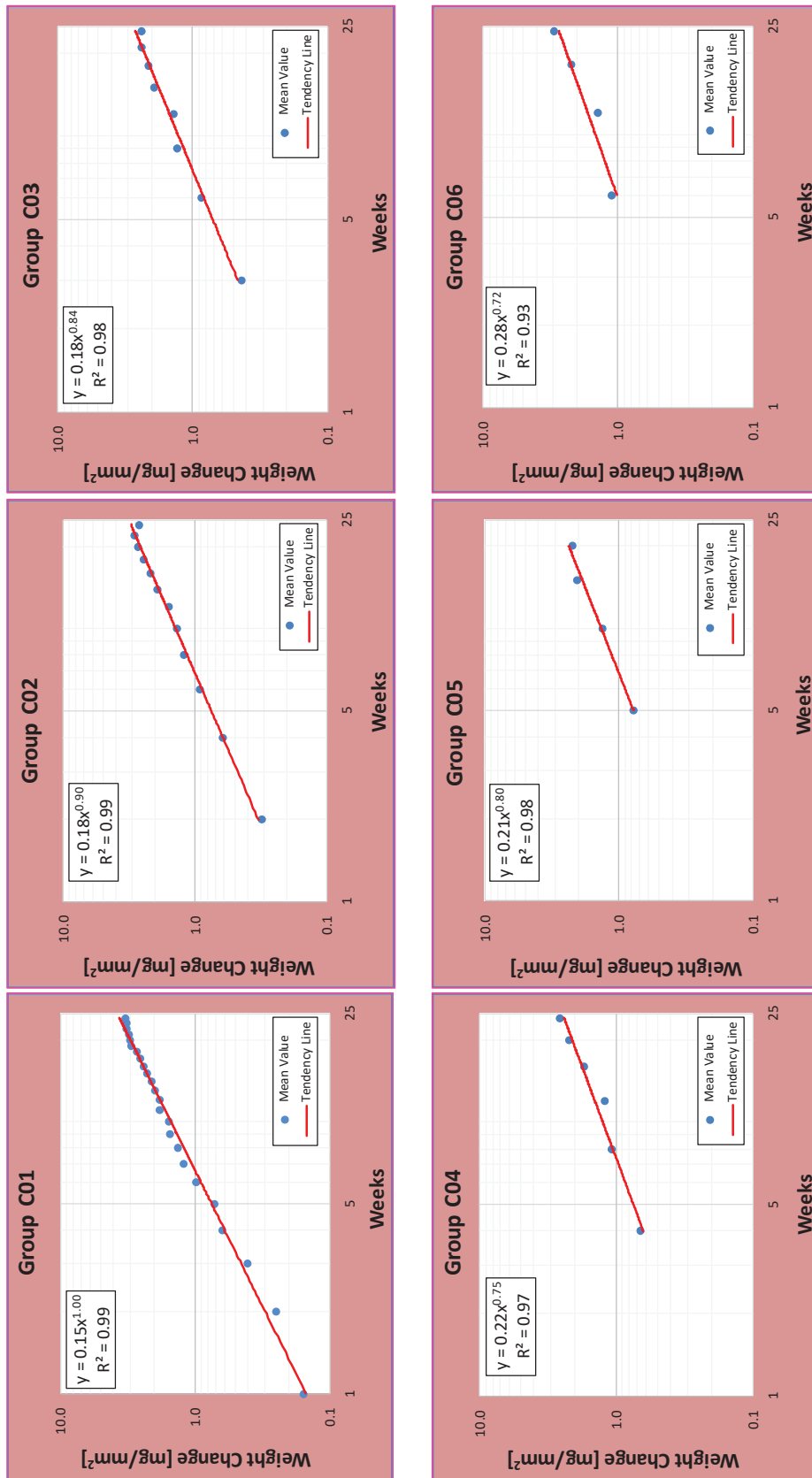


Figure D.3: Weight change versus time during ACT for coupons from steel Type C

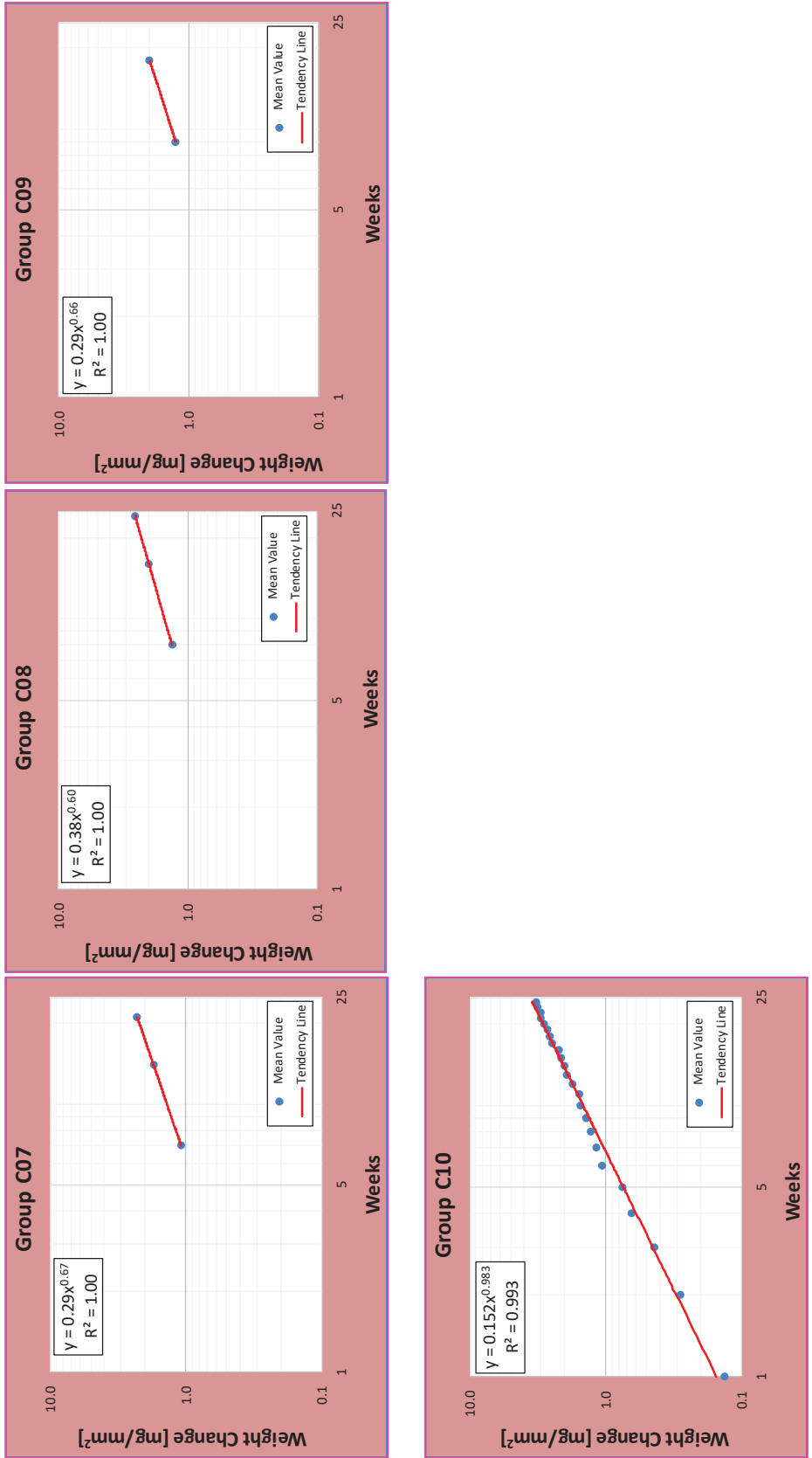


Figure D.3: Continued

Table D.4: Weight change during ACT for coupons from steel Type D

Group D01		WEIGHT (gr.)		
Week	D01-a	D01-b	D01-c	
00	1,174.72	1,189.63	1,188.10	
01	1,174.72	1,189.63	1,188.11	
02	1,174.75	1,189.63	1,188.16	
03	1,174.76	1,189.68	1,188.17	
04	1,174.81	1,189.70	1,188.25	
05	1,174.85	1,189.72	1,188.30	
06	1,174.92	1,189.74	1,188.32	
07	1,174.94	1,189.74	1,188.32	
08	1,174.95	1,189.74	1,188.38	
09	1,174.95	1,189.78	1,188.40	
10	1,174.99	1,189.80	1,188.40	

Group D02		WEIGHT (gr.)		
Week	D02-a	D02-b	D02-c	
00	1,186.65	1,194.06	1,199.59	
02	1,186.73	1,194.16	1,199.64	
04	1,186.77	1,194.25	1,199.69	
06	1,186.79	1,194.28	1,199.72	
08	1,186.80	1,194.30	1,199.82	
10	1,186.82	1,194.34	1,199.88	

Group D03		WEIGHT (gr.)		
Week	D03-a	D03-b	D03-c	
00	1,204.60	1,216.18	1,187.93	
03	1,204.74	1,216.28	1,188.09	
06	1,204.85	1,216.40	1,188.15	
09	1,204.97	1,216.49	1,188.26	

Group D04		WEIGHT (gr.)		
Week	D04-a	D04-b	D04-c	
00	1,178.22	1,203.21	1,204.53	
04	1,178.38	1,203.39	1,204.68	
08	1,178.45	1,203.43	1,204.77	

Group D06		WEIGHT (gr.)		
Week	D06-a	D06-b		
00	1,146.72	1,190.41		
01	1,146.73	1,190.42		
02	1,146.77	1,190.45		
03	1,146.80	1,190.49		
04	1,146.82	1,190.53		
05	1,146.85	1,190.59		
06	1,146.86	1,190.62		
07	1,146.90	1,190.63		
08	1,146.93	1,190.65		
09	1,146.94	1,190.67		
10	1,146.98	1,190.70		

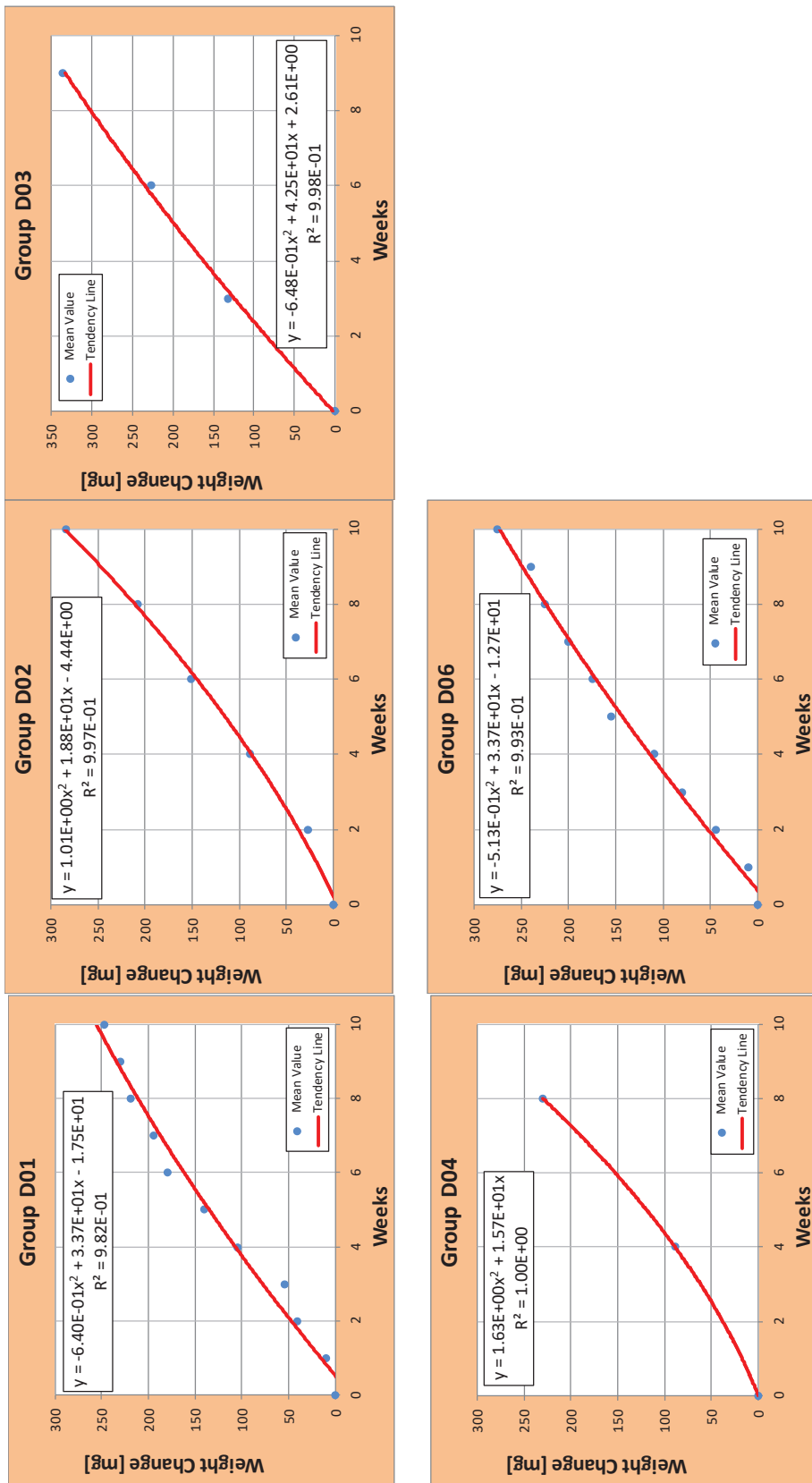


Figure D.4: Weight change versus time during ACT for coupons from steel Type D

Appendix E Initial Dimensions of Coupons

The initial dimensions of each steel coupon are presented. The area for both faces, the mean area and mean thickness are evaluated for each coupon. The data are presented in tables for each steel type and each group (01 to 10).

Table E.1: Initial dimensions of coupons from steel Type A

			STEEL TYPE A - INITIAL DIMENSIONS										
Group	No.	Code	Width 1 (Top) - [in]		Width 2 (Bottom) - [in]		Length 1 (Left) - [in]		Length 2 (Right) - [in]		Area Front	Area Back	Mean Area
			Front	Back	Front	Back	Front	Back	Front	Back	[in ²]	[in ²]	[in ²]
A01	A01	A01-a	2.983	2.994	2.980	3.021	6.025	6.042	6.022	6.027	18.0311	18.0765	18.0538
	A02	A01-b	3.033	3.019	3.037	2.997	5.990	5.985	5.999	5.994	18.1182	18.0914	18.1048
	A03	A01-c	3.006	3.042	2.957	2.966	6.002	6.009	6.014	6.023	18.1606	17.8238	17.9922
	A04	A01-d	2.975	2.986	2.993	3.023	6.009	6.021	6.008	6.009	17.9277	18.0736	18.0006
A02	A05	A02-a	2.959	2.977	2.981	3.018	6.088	6.054	6.084	6.053	18.0187	18.2025	18.1106
	A06	A02-b	3.036	3.003	2.999	2.983	6.023	6.028	6.019	6.019	18.1940	18.0028	18.0984
	A07	A02-c	2.986	2.998	2.988	3.018	6.001	6.010	6.004	6.003	17.9685	18.0285	17.9985
	A08	A02-d	2.985	3.005	2.960	3.008	5.987	5.981	5.982	5.980	17.9221	17.8473	17.8847
A03	A09	A03-a	2.983	3.020	2.985	3.006	6.108	6.071	6.119	6.109	18.2776	18.3145	18.2961
	A10	A03-b	3.054	3.000	3.002	2.992	6.046	6.011	6.033	6.018	18.2483	18.0584	18.1533
	A11	A03-c	3.035	2.994	3.010	2.987	5.942	5.988	5.916	5.945	17.9815	17.7826	17.8820
	A12	A03-d	2.978	3.039	2.997	3.012	6.034	6.045	6.026	6.066	18.1698	18.1652	18.1675
A04	A13	A04-a	3.248	3.214	3.450	3.408	6.023	6.053	6.012	6.058	19.5088	20.6940	20.1014
	A14	A04-b	2.986	2.999	2.992	3.036	6.196	6.161	6.171	6.129	18.4892	18.5361	18.5126
	A15	A04-c	3.014	2.974	3.006	2.987	5.982	5.979	5.968	5.969	17.9056	17.8846	17.8951
	A16	A04-d	2.977	2.994	2.970	3.006	5.998	6.003	5.994	5.991	17.9145	17.9056	17.9100
A05	A17	A05-a	2.982	2.998	2.987	3.033	6.025	6.041	6.023	6.032	18.0387	18.1428	18.0907
	A18	A05-b	3.133	3.144	3.304	3.337	6.056	6.049	6.061	6.038	18.9958	20.0874	19.5416
	A19	A05-c	2.999	2.982	3.001	2.968	6.013	6.006	6.023	6.009	17.9714	17.9548	17.9631
	A20	A05-d	3.005	3.074	3.005	3.047	5.979	5.977	5.990	5.990	18.1701	18.1257	18.1479
A06	A21	A06-a	2.993	3.001	2.973	3.012	6.000	6.007	5.998	5.998	17.9925	17.9490	17.9708
	A22	A06-b	2.888	2.934	2.979	3.048	5.973	5.971	5.959	5.958	17.3845	17.9559	17.6702
	A23	A06-c	2.983	2.975	3.024	2.985	6.043	6.033	6.068	6.028	17.9872	18.1712	18.0792
	A24	A06-d	2.986	3.008	2.982	3.024	6.000	6.010	5.994	5.999	17.9970	18.0075	18.0022
A07	A25	A07-a	3.250	3.216	3.413	3.391	6.024	6.065	6.023	6.074	19.5419	20.5770	20.0594
	A26	A07-b	2.962	2.906	3.052	2.986	5.975	5.970	5.993	5.982	17.5233	18.0763	17.7998
	A27	A07-c	3.270	3.288	3.399	3.441	6.083	6.028	6.063	6.038	19.8560	20.6927	20.2743
	A28	A07-d	3.449	3.404	3.237	3.184	6.219	6.218	6.228	6.172	21.3077	19.9051	20.6064
A08	A29	A08-a	2.991	3.005	2.979	3.033	6.000	6.008	5.995	5.998	18.0000	18.0255	18.0127
	A30	A08-b	2.991	3.008	2.961	3.018	5.992	6.000	5.984	5.988	17.9850	17.8951	17.9401
	A31	A08-c	2.993	3.005	2.951	2.998	6.035	5.998	5.997	5.953	18.0435	17.7726	17.9081
	A32	A08-d	3.007	2.990	3.020	2.982	5.980	5.987	5.998	5.995	17.9415	17.9955	17.9685
A09	A33	A09-a	2.993	3.000	2.983	3.026	5.989	6.004	5.993	6.002	17.9685	18.0195	17.9940
	A34	A09-b	2.982	2.999	2.953	3.002	6.023	6.030	6.016	6.019	18.0222	17.9171	17.9697
	A35	A09-c	2.991	3.004	2.974	3.004	6.003	6.015	5.994	6.001	18.0120	17.9265	17.9693
	A36	A09-d	2.983	2.989	2.985	3.016	6.030	6.051	6.022	6.037	18.0369	18.0915	18.0642
A10	A37	A10-a	3.048	2.975	2.992	2.957	5.985	5.983	5.975	5.973	18.0208	17.7697	17.8952
	A38	A10-b	2.979	3.028	2.984	2.996	6.007	6.002	6.013	6.017	18.0345	17.9849	18.0097
	A39	A10-c	2.970	3.004	2.976	3.010	6.085	6.050	6.046	6.007	18.1236	18.0373	18.0805
	A40	A10-d	2.937	2.978	2.993	3.070	5.988	5.995	5.972	5.980	17.7199	18.1162	17.9181

Table E.2: Initial dimensions of coupons from steel Type B

			STEEL TYPE B - INITIAL DIMENSIONS										
Group	No.	Code	Width 1 (Top) - [in]		Width 2 (Bottom) - [in]		Length 1 (Left) - [in]		Length 2 (Right) - [in]		Area Front	Area Back	Mean Area
			Front	Back	Front	Back	Front	Back	Front	Back	[in ²]	[in ²]	[in ²]
B01	B01	B01-a	2.985	2.991	3.018	3.002	6.047	5.970	6.052	5.967	17.9534	18.0886	18.0210
	B02	B01-b	3.036	3.014	3.003	3.008	6.066	5.984	6.057	5.990	18.2256	18.1036	18.1646
	B03	B01-c	3.008	2.984	2.986	2.986	6.016	5.868	6.098	5.952	17.8022	17.9907	17.8964
	B04	B01-d	3.025	3.006	3.006	3.002	6.072	5.985	6.051	5.968	18.1789	18.0525	18.1157
B02	B05	B02-a	3.090	3.019	3.042	3.022	6.084	5.944	6.053	5.930	18.3698	18.1662	18.2680
	B06	B02-b	3.041	3.006	3.012	3.006	6.057	5.995	6.061	5.986	18.2196	18.1247	18.1722
	B07	B02-c	3.006	2.999	2.991	2.988	5.987	5.996	6.078	6.095	17.9895	18.1956	18.0925
	B08	B02-d	2.989	3.018	2.975	2.999	6.100	5.949	6.058	5.904	18.0946	17.8652	17.9799
B03	B09	B03-a	3.029	3.002	2.996	2.980	5.987	5.852	6.089	5.957	17.8503	17.9967	17.9235
	B10	B03-b	3.006	3.001	2.988	2.988	6.051	6.039	6.107	6.079	18.1562	18.2059	18.1810
	B11	B03-c	3.012	2.996	2.985	2.986	6.049	6.022	6.092	6.087	18.1306	18.1802	18.1554
	B12	B03-d	3.060	3.019	3.021	3.019	6.057	5.942	6.017	5.958	18.2355	18.0823	18.1589
B04	B13	B04-a	3.042	3.004	3.012	3.003	6.072	5.977	6.036	5.947	18.2121	18.0194	18.1157
	B14	B04-b	3.032	3.016	3.008	3.008	6.064	5.986	6.024	5.943	18.2196	17.9984	18.1090
	B15	B04-c	3.087	3.014	3.053	3.022	6.090	5.953	6.047	5.917	18.3686	18.1703	18.2695
	B16	B04-d	3.074	3.018	3.030	3.018	6.067	6.072	6.039	6.052	18.4877	18.2816	18.3846
B05	B17	B05-a	2.984	2.963	3.008	2.998	6.111	5.956	6.079	5.948	17.9406	18.0585	17.9996
	B18	B05-b	2.970	2.988	2.918	2.971	6.073	5.993	6.068	5.992	17.9723	17.7553	17.8638
	B19	B05-c	3.026	3.000	2.998	2.989	6.052	5.885	6.108	5.956	17.9831	18.0568	18.0199
	B20	B05-d	3.002	2.991	2.977	2.979	6.033	5.876	6.106	5.939	17.8427	17.9350	17.8888
B06	B21	B06-a	3.041	3.066	2.966	2.997	6.064	6.031	6.028	5.990	18.4660	17.9158	18.1909
	B22	B06-b	2.946	2.976	2.936	2.962	6.050	5.993	6.064	5.990	17.8297	17.7736	17.8016
	B23	B06-c	3.085	3.004	3.029	3.021	6.039	6.030	5.986	6.082	18.3720	18.2529	18.3124
	B24	B06-d	3.097	3.017	3.036	3.026	6.095	5.970	6.062	5.958	18.4414	18.2163	18.3288
B07	B25	B07-a	3.009	3.001	3.029	3.013	6.021	5.938	6.064	5.981	17.9684	18.1940	18.0812
	B26	B07-b	3.041	2.998	3.106	3.023	5.999	6.039	6.024	6.027	18.1744	18.4651	18.3198
	B27	B07-c	3.037	2.978	3.073	2.998	6.033	5.947	6.075	5.998	18.0149	18.3238	18.1694
	B28	B07-d	3.007	3.007	2.989	2.984	5.947	5.930	6.152	6.010	17.8571	18.1609	18.0090
B08	B29	B08-a	3.014	3.003	3.035	3.024	6.044	5.960	6.061	5.982	18.0570	18.2421	18.1496
	B30	B08-b	3.012	2.994	2.997	2.992	6.049	5.900	6.098	5.953	17.9414	18.0434	17.9924
	B31	B08-c	3.080	3.005	3.030	3.017	6.058	6.093	5.966	6.025	18.4847	18.1274	18.3061
	B32	B08-d	3.069	3.008	3.033	3.021	6.044	6.046	5.995	6.013	18.3677	18.1741	18.2709
B09	B33	B09-a	3.036	3.027	3.014	3.006	6.063	5.975	6.034	5.952	18.2466	18.0389	18.1428
	B34	B09-b	3.040	3.014	3.007	3.004	6.061	5.980	6.024	5.948	18.2241	17.9909	18.1075
	B35	B09-c	2.930	2.974	2.806	2.894	5.898	5.952	5.924	5.968	17.4906	16.9461	17.2184
	B36	B09-d	2.991	2.968	3.007	2.989	6.118	5.956	6.110	5.939	17.9872	18.0615	18.0243
B10	B37	B10-a	2.986	2.987	3.010	2.997	6.098	5.969	6.094	5.942	18.0190	18.0751	18.0471
	B38	B10-b	3.009	2.994	2.994	2.985	6.078	5.926	6.099	5.969	18.0150	18.0386	18.0268
	B39	B10-c	3.108	3.031	3.052	3.028	6.075	5.971	6.020	5.926	18.4876	18.1579	18.3228
	B40	B10-d	3.043	2.969	3.020	2.984	6.061	5.909	6.100	5.959	17.9909	18.1006	18.0457

Table E.3: Initial dimensions of coupons from steel Type C

			STEEL TYPE C - INITIAL DIMENSIONS										
Group	No.	Code	Width 1 (Top) - [in]		Width 2 (Bottom) - [in]		Length 1 (Left) - [in]		Length 2 (Right) - [in]		Area Front	Area Back	Mean Area
			Front	Back	Front	Back	Front	Back	Front	Back	[in ²]	[in ²]	[in ²]
C01	1	C01-a	3.116	3.060	3.051	3.050	6.089	5.960	6.070	5.944	18.6037	18.3244	18.4640
	2	C01-b	3.144	3.032	3.085	3.010	5.996	6.009	5.976	5.993	18.5357	18.2378	18.3867
	3	C01-c	3.042	3.039	3.003	3.016	6.055	5.953	5.997	5.949	18.2552	17.9757	18.1155
	4	C01-d	2.996	2.997	3.036	3.029	6.038	5.971	6.054	5.995	17.9925	18.2693	18.1309
C02	5	C02-a	3.002	3.055	2.998	3.034	6.036	6.091	6.069	6.120	18.3633	18.3810	18.3722
	6	C02-b	3.048	3.048	3.028	3.010	6.042	5.986	6.078	5.987	18.3307	18.2121	18.2714
	7	C02-c	3.013	3.002	3.053	3.020	6.028	5.963	6.055	5.986	18.0315	18.2812	18.1564
	8	C02-d	2.942	2.942	2.944	2.893	5.986	6.007	6.065	6.076	17.6417	17.7168	17.6792
C03	9	C03-a	3.013	3.000	2.970	2.968	6.021	5.919	6.075	5.991	17.9488	17.9120	17.9304
	10	C03-b	3.011	2.993	2.978	2.968	6.044	6.082	6.074	6.132	18.2011	18.1442	18.1727
	11	C03-c	3.017	3.012	2.987	2.989	5.985	6.045	5.990	6.054	18.1322	17.9937	18.0630
	12	C03-d	3.042	2.987	3.082	3.011	6.018	5.974	6.052	5.996	18.0749	18.3521	18.2135
C04	13	C04-a	3.004	2.989	2.968	2.953	6.048	5.898	6.097	5.982	17.8981	17.8799	17.8890
	14	C04-b	3.006	3.032	2.910	2.988	6.052	5.988	6.046	5.981	18.1744	17.7338	17.9541
	15	C04-c	3.090	2.966	3.027	2.936	6.053	5.978	6.022	5.966	18.2149	17.8711	18.0430
	16	C04-d	2.920	3.019	2.833	2.943	6.064	5.995	6.047	5.983	17.9046	17.3713	17.6380
C05	17	C05-a	2.892	2.962	2.682	2.748	6.103	5.965	6.116	5.960	17.6615	16.3932	17.0273
	18	C05-b	3.106	3.044	3.057	3.036	6.093	5.957	6.038	5.901	18.5269	18.1861	18.3565
	19	C05-c	3.099	3.056	3.050	3.034	6.092	5.950	6.016	5.885	18.5296	18.1014	18.3155
	20	C05-d	3.002	2.999	2.965	2.957	5.971	5.895	6.077	5.983	17.8020	17.8548	17.8284
C06	21	C06-a	2.818	2.933	2.682	2.819	6.028	6.072	6.077	6.101	17.3968	16.7478	17.0723
	22	C06-b	2.932	3.023	3.008	3.078	6.092	5.936	6.103	5.944	17.9067	18.3295	18.1181
	23	C06-c	2.968	2.962	3.005	3.003	6.043	6.119	5.987	6.056	18.0302	18.0886	18.0594
	24	C06-d	3.047	3.039	3.011	3.001	6.076	5.993	6.087	5.997	18.3630	18.1623	18.2626
C07	25	C07-a	3.009	2.993	3.043	3.034	6.065	6.004	6.055	5.975	18.1095	18.2766	18.1931
	26	C07-b	2.991	3.005	2.969	2.971	6.009	5.871	6.093	5.975	17.8081	17.9210	17.8646
	27	C07-c	2.936	2.939	2.999	2.981	6.042	5.972	6.057	5.991	17.6456	18.0118	17.8287
	28	C07-d	3.012	3.016	2.982	2.980	6.007	5.850	6.105	5.954	17.8685	17.9739	17.9212
C08	29	C08-a	3.089	3.050	3.048	3.034	6.125	6.141	6.044	6.074	18.8252	18.4254	18.6253
	30	C08-b	3.074	2.999	3.005	3.001	6.072	6.031	6.002	6.083	18.3754	18.1456	18.2605
	31	C08-c	2.974	2.990	2.991	2.998	6.105	5.970	6.033	5.909	18.0038	17.8802	17.9420
	32	C08-d	3.079	3.045	3.034	3.033	6.081	6.172	6.005	6.033	18.7593	18.2586	18.5090
C09	33	C09-a	3.074	3.013	3.023	3.023	6.100	6.115	6.037	6.060	18.5882	18.2846	18.4364
	34	C09-b	2.948	2.962	2.963	2.976	6.056	5.923	6.128	5.974	17.6990	17.9684	17.8337
	35	C09-c	3.080	2.985	3.158	3.004	5.997	6.013	6.032	6.065	18.2102	18.6354	18.4228
	36	C09-d	2.985	3.015	3.021	3.029	6.050	5.994	6.053	6.005	18.0660	18.2377	18.1519
C10	37	C10-a	3.008	2.923	3.030	2.913	6.105	5.966	6.078	5.950	17.8983	17.8706	17.8844
	38	C10-b	3.070	3.025	3.019	3.006	6.006	5.980	6.019	5.947	18.2637	18.0238	18.1437
	39	C10-c	2.877	2.869	2.939	2.923	6.110	5.966	6.054	5.920	17.3472	17.5479	17.4475
	40	C10-d	2.978	2.978	3.018	2.990	6.072	5.981	5.940	5.879	17.9469	17.7521	17.8495

Appendix F Thickness Change During ACT

The thickness change for each steel coupon is presented in this Appendix, in tabulated and graphical manner. Weight changes for coupons from steel Types A, B, and C are presented week by week for the 24 weeks the ACT lasted. The data are presented for each steel type and for each group, every week a group was subjected to washing.

Table F.1: Thickness change during ACT for coupons from steel Type A

Group A01		THICKNESS (in.)			
Week	A01-a	A01-b	A01-c	A01-d	
0	0.5327	0.5328	0.5313	0.5320	
1	0.5408	0.5386	0.5397	0.5395	
2	0.5458	0.5419	0.5453	0.5436	
3	0.5501	0.5455	0.5496	0.5502	
4	0.5539	0.5483	0.5528	0.5501	
5	0.5583	0.5546	0.5576	0.5549	
6	0.5612	0.5579	0.5612	0.5588	
7	0.5649	0.5618	0.5628	0.5604	
8	0.5669	0.5659	0.5646	0.5622	
9	0.5692	0.5713	0.5703	0.5650	
10	0.5702	0.5752	0.5711	0.5681	
11	0.5720	0.5783	0.5733	0.5709	
12	0.5767	0.5843	0.5751	0.5744	
13	0.5791	0.5899	0.5773	0.5778	
14	0.5818	0.5903	0.5785	0.5774	
15	0.5833	0.5931	0.5804	0.5793	
16	0.5844	0.5951	0.5830	0.5805	
17	0.5868	0.5975	0.5865	0.5826	
18	0.5892	0.6017	0.5849	0.5826	
19	0.5905	0.6025	0.5877	0.5849	
20	0.5926	0.6032	0.5896	0.5855	
21	0.5955	0.6035	0.5919	0.5912	
22	0.5971	0.6047	0.5933	0.5939	
23	0.5985	0.6058	0.5948	0.5951	
24	0.5998	0.6070	0.5966	0.5973	

Group A02		THICKNESS (in.)			
Week	A02-a	A02-b	A02-c	A02-d	
0	0.5301	0.5426	0.5372	0.5359	
2	0.5436	0.5536	0.5504	0.5476	
4	0.5530	0.5680	0.5527	0.5554	
6	0.5684	0.5742	0.5613	0.5690	
8	0.5716	0.5866	0.5694	0.5779	
10	0.5777	0.5903	0.5734	0.5884	
12	0.5870	0.5972	0.5806	0.5932	
14	0.5936	0.5992	0.5861	0.5983	
16	0.5993	0.6036	0.5933	0.6039	
18	0.6034	0.6085	0.5969	0.6076	
20	0.6044	0.6107	0.6024	0.6106	
22	0.6066	0.6156	0.6058	0.6136	
24	0.6123	0.6179	0.6072	0.6145	

Group A03		THICKNESS (in.)			
Week	A03-a	A03-b	A03-c	A03-d	
0	0.5416	0.5323	0.5322	0.5397	
3	0.5563	0.5482	0.5463	0.5533	
6	0.5723	0.5536	0.5649	0.5621	
9	0.5759	0.5653	0.5697	0.5688	
12	0.5839	0.5704	0.5740	0.5761	
15	0.5887	0.5748	0.5772	0.5793	
18	0.5909	0.5803	0.5778	0.5850	
21	0.5960	0.5876	0.5808	0.5881	
24	0.6011	0.5921	0.5883	0.5934	

Table F.1: Continued

Group A04	THICKNESS (in.)			
	A04-a	A04-b	A04-c	A04-d
Week				
0	0.5318	0.5368	0.5336	0.5302
4	0.5559	0.5488	0.5517	0.5492
8	0.5741	0.5734	0.5706	0.5739
12	0.5783	0.5827	0.5778	0.5937
16	0.5886	0.5931	0.5900	0.6051
20	0.5926	0.5967	0.5961	0.6133
24	0.5971	0.5996	0.6075	0.6174

Group A05	THICKNESS (in.)			
	A05-a	A05-b	A05-c	A05-d
Week				
0	0.5335	0.5412	0.5313	0.5333
5	0.5575	0.5659	0.5688	0.5609
10	0.5738	0.5887	0.5819	0.5836
15	0.5842	0.5981	0.5893	0.5942
20	0.5917	0.6012	0.5916	0.5975

Group A06	THICKNESS (in.)			
	A06-a	A06-b	A06-c	A06-d
Week				
0	0.5378	0.5346	0.5327	0.5439
6	0.5695	0.5850	0.5672	0.5835
12	0.5862	0.5987	0.5829	0.5924
18	0.6027	0.6164	0.5959	0.5986
24	0.6236	0.6316	0.6083	0.6112

Group A07	THICKNESS (in.)			
	A07-a	A07-b	A07-c	A07-d
Week				
0	0.5402	0.5507	0.5427	0.5346
7	0.5664	0.5994	0.5750	0.5733
14	0.5740	0.6116	0.5878	0.5879
21	0.6047	0.6363	0.6090	0.6050

Group A08	THICKNESS (in.)			
	A08-a	A08-b	A08-c	A08-d
Week				
0	0.5347	0.5448	0.5435	0.5379
8	0.5685	0.5768	0.5819	0.5649
16	0.5788	0.5894	0.6109	0.5983
24	0.5856	0.5966	0.6198	0.6087

Group A09	THICKNESS (in.)			
	A09-a	A09-b	A09-c	A09-d
Week				
0	0.5364	0.5348	0.5360	0.5376
9	0.5789	0.5775	0.5677	0.5917
18	0.5965	0.5985	0.5793	0.6087

Table F.1: Continued

Group A10	THICKNESS (in.)			
Week	A10-a	A10-b	A10-c	A10-d
0	0.5346	0.5310	0.5313	0.5372
1	0.5418	0.5382	0.5377	0.5425
2	0.5481	0.5455	0.5464	0.5479
3	0.5523	0.5498	0.5497	0.5504
4	0.5559	0.5539	0.5529	0.5537
5	0.5593	0.5583	0.5572	0.5569
6	0.5635	0.5651	0.5621	0.5602
7	0.5681	0.5688	0.5652	0.5630
8	0.5700	0.5727	0.5688	0.5649
9	0.5730	0.5722	0.5702	0.5659
10	0.5749	0.5744	0.5709	0.5683
11	0.5762	0.5769	0.5749	0.5722
12	0.5785	0.5836	0.5858	0.5767
13	0.5845	0.5922	0.5824	0.5814
14	0.5870	0.5926	0.5874	0.5801
15	0.5906	0.5976	0.5906	0.5839
16	0.5931	0.6013	0.5965	0.5885
17	0.5962	0.6035	0.5985	0.5909
18	0.5996	0.6073	0.6025	0.5943
19	0.6013	0.6088	0.6053	0.5953
20	0.6051	0.6123	0.6082	0.5975
21	0.6084	0.6140	0.6117	0.5998
22	0.6100	0.6155	0.6133	0.6020
23	0.6129	0.6168	0.6156	0.6041
24	0.6144	0.6183	0.6186	0.6065

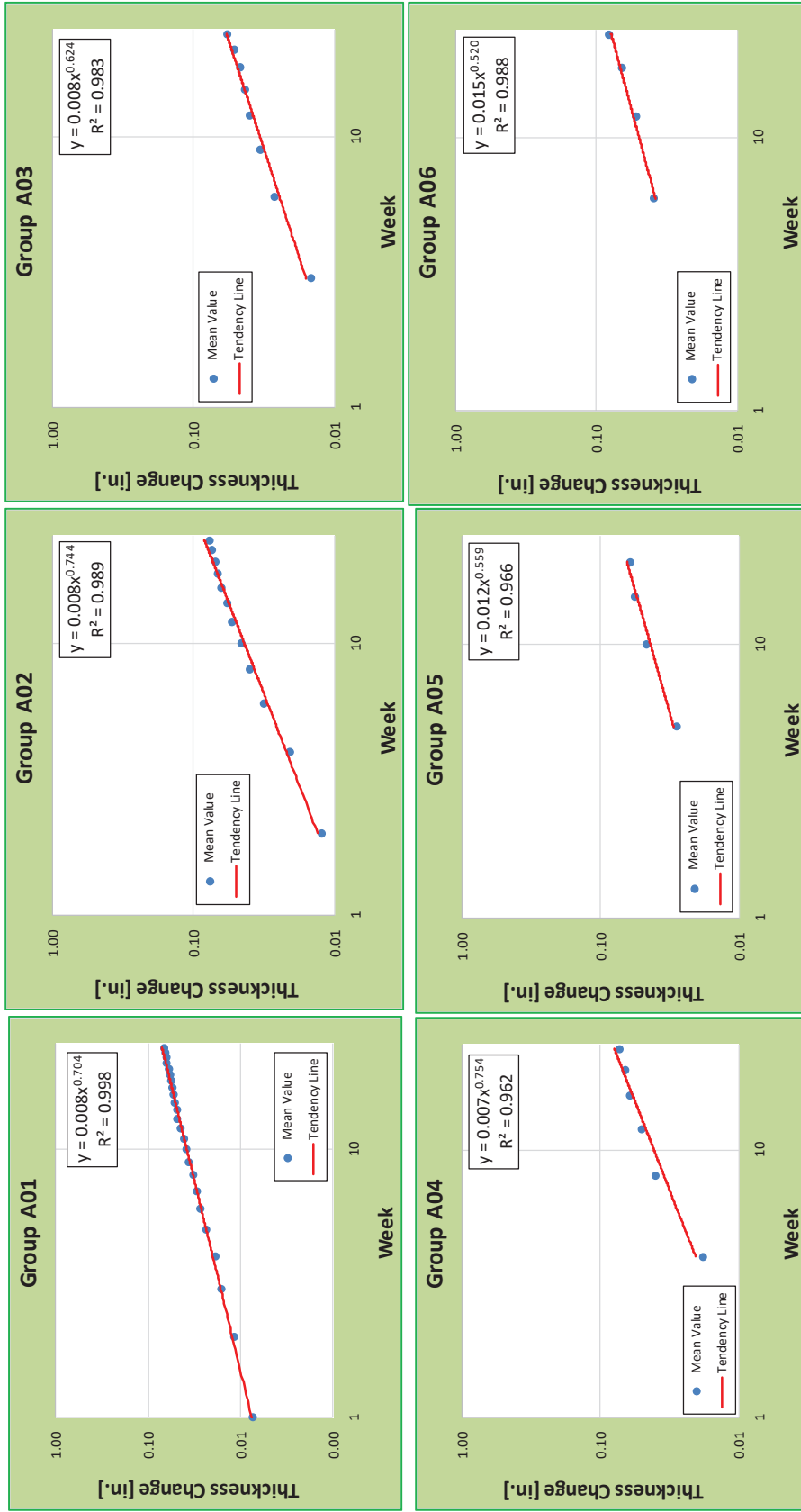


Figure F.1: Thickness change versus time during ACT for coupons from steel Type A

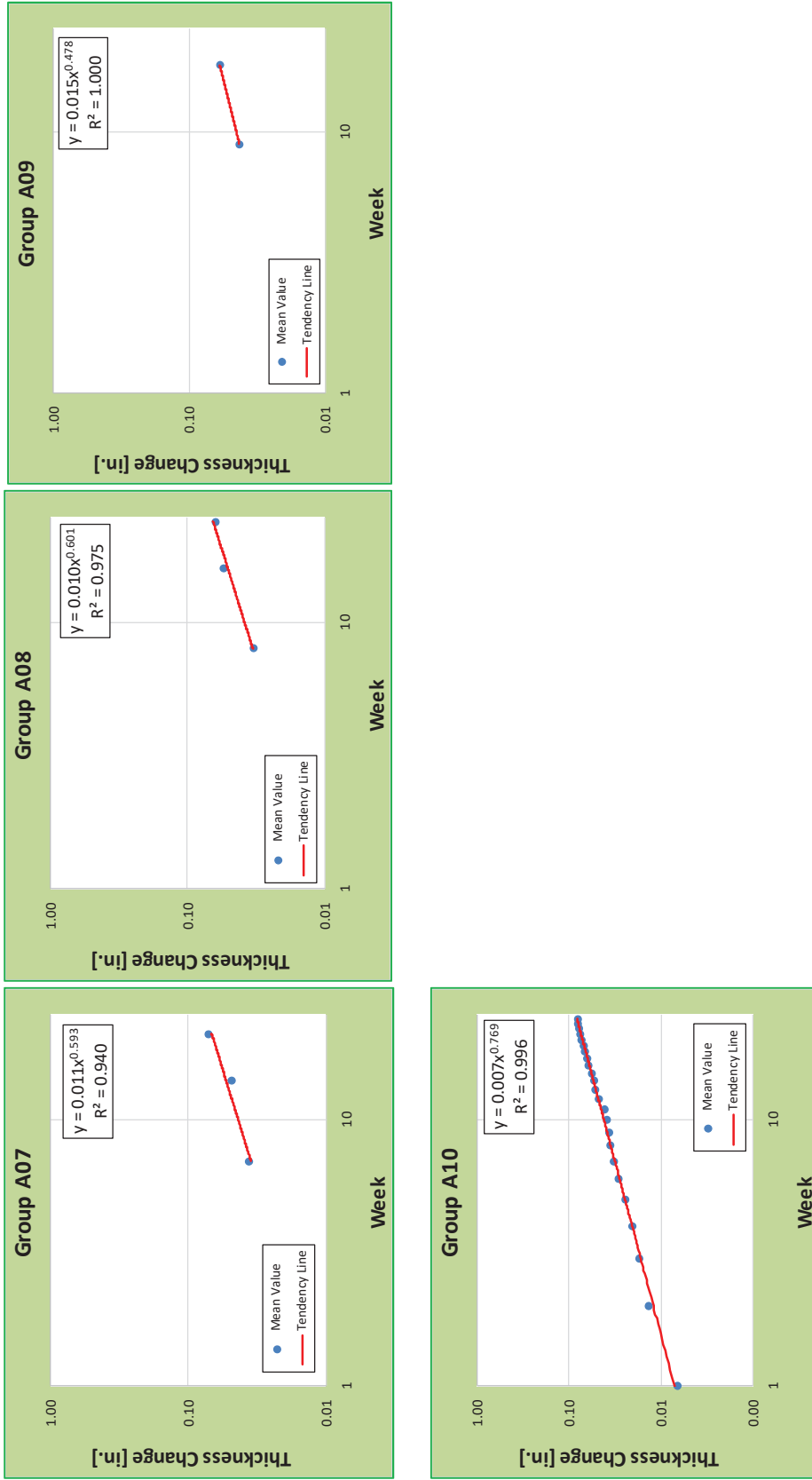


Figure F.1: Continued

Table F.2: Thickness change during ACT for coupons from steel Type B

Group B01	THICKNESS (in.)			
	B01-a	B01-b	B01-c	B01-d
WEEK				
0	0.5589	0.5669	0.5553	0.5616
1	0.5590	0.5672	0.5556	0.5622
2	0.5595	0.5674	0.5561	0.5624
3	0.5596	0.5676	0.5562	0.5628
4	0.5596	0.5677	0.5564	0.5624
5	0.5596	0.5676	0.5563	0.5620
6	0.5594	0.5675	0.5559	0.5617
7	0.5592	0.5674	0.5557	0.5615
8	0.5590	0.5672	0.5555	0.5614
9	0.5588	0.5669	0.5554	0.5612
10	0.5587	0.5665	0.5555	0.5611
11	0.5585	0.5667	0.5553	0.5611
12	0.5584	0.5665	0.5551	0.5610
13	0.5583	0.5663	0.5550	0.5610
14	0.5581	0.5663		
15	0.5580	0.5661		
16	0.5580	0.5661		
17	0.5579	0.5660		
18	0.5578	0.5659		
19	0.5579	0.5659		
20	0.5578	0.5658		
21	0.5577	0.5656		
22	0.5577	0.5656		
23	0.5576	0.5654		
24	0.5575	0.5655		

Group B02	THICKNESS (in.)			
	B02-a	B02-b	B02-c	B02-d
WEEK				
0	0.5587	0.5585	0.5568	0.5631
2	0.5600	0.5591	0.5577	0.5639
4	0.5600	0.5586	0.5568	0.5636
6	0.5585	0.5584	0.5565	0.5632
8	0.5577	0.5583	0.5563	0.5632
10	0.5574	0.5581	0.5564	0.5630
12	0.5573	0.5580	0.5561	0.5628
14	0.5571	0.5580		
16	0.5566	0.5578		
18	0.5566	0.5575		
20	0.5564	0.5570		
22	0.5561	0.5570		
24	0.5560	0.5567		

Group B03	THICKNESS (in.)			
	B03-a	B03-b	B03-c	B03-d
WEEK				
0	0.5650	0.5575	0.5610	0.5624
3	0.5653	0.5577	0.5611	0.5627
6	0.5646	0.5574	0.5608	0.5625
9	0.5643	0.5573	0.5607	0.5623
12	0.5642	0.5570	0.5606	0.5620
15	0.5640	0.5568		
18	0.5638	0.5563		
21	0.5632	0.5560		
24	0.5627	0.5555		

Table F.2: Continued

Group B04		THICKNESS (in.)			
WEEK	B04-a	B04-b	B04-c	B04-d	
0	0.5722	0.5603	0.5678	0.5659	
4	0.5725	0.5608	0.5678	0.5660	
8	0.5722	0.5606	0.5675	0.5656	
12	0.5720	0.5603	0.5672	0.5653	
16	0.5717	0.5600			
20	0.5714	0.5595			
24	0.5710	0.5591			

Group B05		THICKNESS (in.)			
WEEK	B05-a	B05-b	B05-c	B05-d	
0	0.5614	0.5677	0.5720	0.5666	
5	0.5616	0.5679	0.5727	0.5664	
10	0.5609	0.5675	0.5724	0.5659	
15	0.5605	0.5673			
20	0.5600	0.5669			

Group B06		THICKNESS (in.)			
WEEK	B06-a	B06-b	B06-c	B06-d	
0	0.5610	0.5714	0.5622	0.5642	
6	0.5616	0.5719	0.5626	0.5648	
12	0.5612	0.5714	0.5619	0.5640	
18	0.5605	0.5709			
24	0.5601	0.5702			

Group B07		THICKNESS (in.)			
WEEK	B07-a	B07-b	B07-c	B07-d	
0	0.5632	0.5693	0.5745	0.5638	
7	0.5632	0.5694	0.5746	0.5637	
14	0.5628	0.5690			
21	0.5622	0.5679			

Group B08		THICKNESS (in.)			
WEEK	B08-a	B08-b	B08-c	B08-d	
0	0.5658	0.5658	0.5637	0.5705	
8	0.5657	0.5658	0.5636	0.5701	
16	0.5652	0.5654			
24	0.5644	0.5646			

Group B09		THICKNESS (in.)			
WEEK	B09-a	B09-b	B09-c	B09-d	
0	0.5639	0.5674	0.5638	0.5668	
9	0.5636	0.5674	0.5638	0.5666	
18	0.5625	0.5663			

Table F.2: Continued

Group B10	THICKNESS (in.)			
	WEEK	B10-a	B10-b	B10-c
0	0.5659	0.5688	0.5680	0.5738
1	0.5666	0.5690	0.5683	0.5740
2	0.5671	0.5692	0.5684	0.5742
3	0.5677	0.5694	0.5685	0.5745
4	0.5676	0.5695	0.5685	0.5748
5	0.5673	0.5697	0.5683	0.5751
6	0.5670	0.5697	0.5680	0.5751
7	0.5669	0.5697	0.5677	0.5749
8	0.5668	0.5695	0.5677	0.5748
9	0.5666	0.5694	0.5676	0.5746
10	0.5665	0.5694	0.5674	0.5744
11	0.5661	0.5693	0.5672	0.5744
12	0.5659	0.5690	0.5670	0.5742
13	0.5658	0.5690	0.5668	0.5741
14	0.5655	0.5688		
15	0.5654	0.5687		
16	0.5652	0.5686		
17	0.5652	0.5685		
18	0.5650	0.5684		
19	0.5649	0.5681		
20	0.5647	0.5681		
21	0.5647	0.5679		
22	0.5644	0.5679		
23	0.5646	0.5677		
24	0.5643	0.5676		

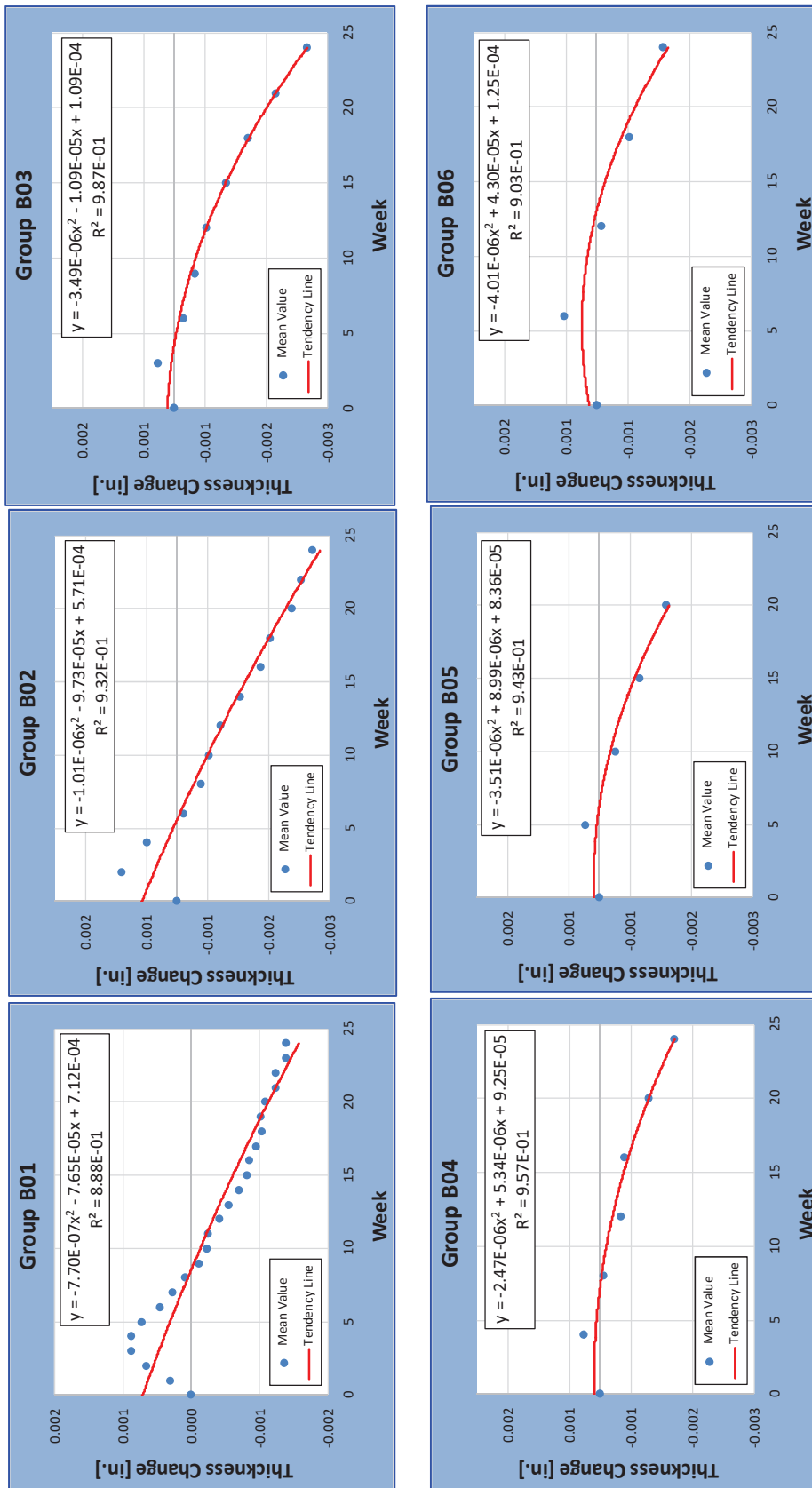


Figure F.2: Thickness change versus time during ACT for coupons from steel Type B

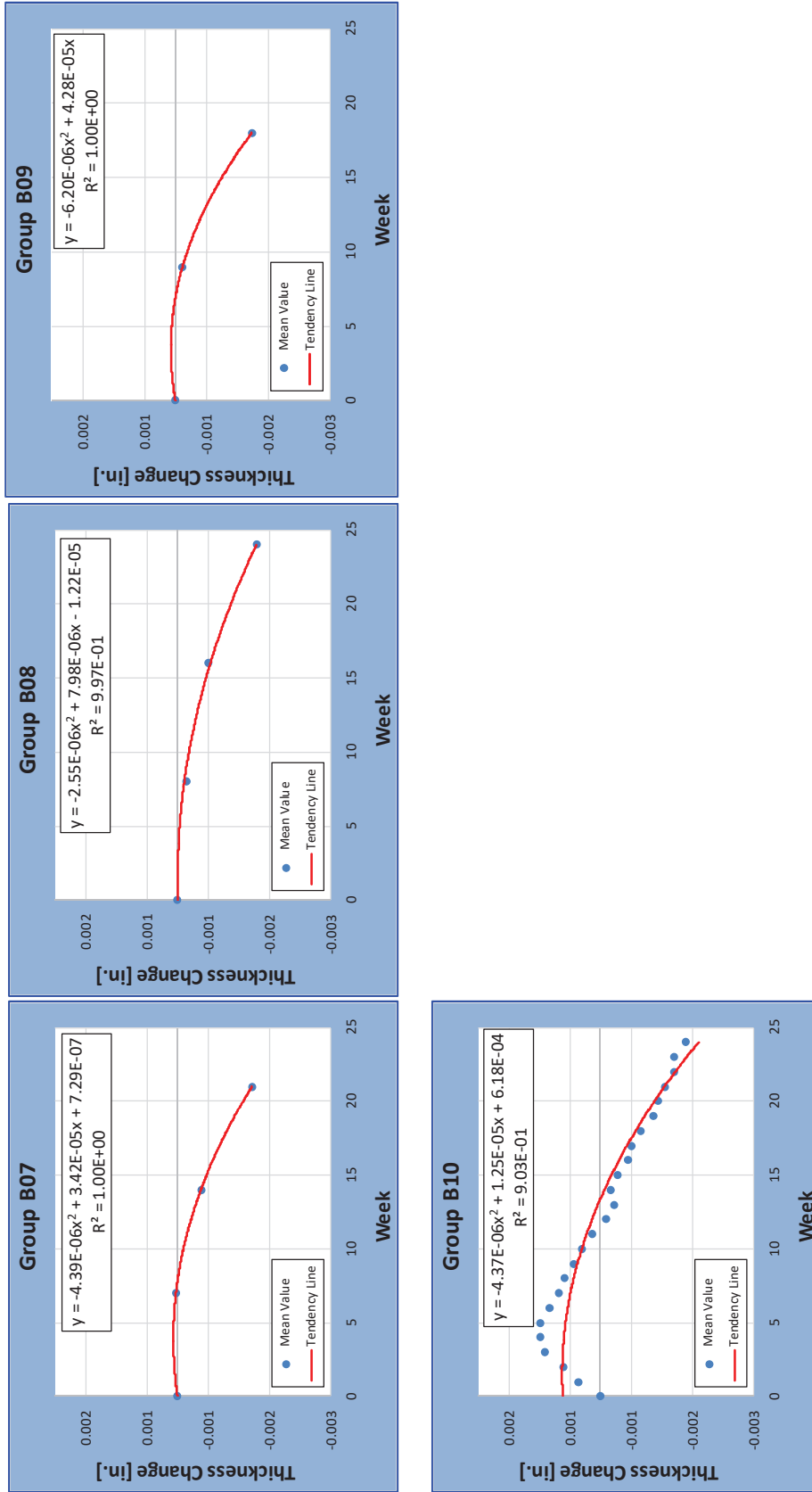


Figure F.2: Continued

Table F.3: Thickness change during ACT for coupons from steel Type C

Group C01		THICKNESS (in.)			
WEEK	C01-a	C01-b	C01-c	C01-d	
0	0.5761	0.5643	0.5700	0.5856	
1	0.5850	0.5711	0.5770	0.5931	
2	0.5884	0.5774	0.5829	0.5991	
3	0.5912	0.5806	0.5866	0.6069	
4	0.5941	0.5875	0.5906	0.6118	
5	0.6033	0.5940	0.5966	0.6154	
6	0.6099	0.5999	0.6071	0.6135	
7	0.6146	0.6053	0.6117	0.6225	
8	0.6184	0.6084	0.6148	0.6242	
9	0.6219	0.6101	0.6178	0.6274	
10	0.6231	0.6120	0.6217	0.6258	
11	0.6279	0.6148	0.6239	0.6270	
12	0.6312	0.6186	0.6307	0.6291	
13	0.6334	0.6228	0.6403	0.6306	
14	0.6378	0.6234	0.6433	0.6366	
15	0.6427	0.6274	0.6479	0.6398	
16	0.6472	0.6320	0.6568	0.6422	
17	0.6486	0.6310	0.6582	0.6443	
18	0.6505	0.6343	0.6623	0.6454	
19	0.6534	0.6366	0.6659	0.6470	
20	0.6551	0.6381	0.6679	0.6486	
21	0.6575	0.6413	0.6690	0.6494	
22	0.6597	0.6435	0.6711	0.6509	
23	0.6628	0.6451	0.6728	0.6526	
24	0.6652	0.6464	0.6743	0.6540	

Group C02		THICKNESS (in.)			
WEEK	C02-a	C02-b	C02-c	C02-d	
0	0.5767	0.5701	0.5695	0.5677	
2	0.5867	0.5856	0.5832	0.5860	
4	0.6020	0.5976	0.5977	0.6036	
6	0.6176	0.6120	0.6102	0.6153	
8	0.6223	0.6208	0.6213	0.6222	
10	0.6265	0.6261	0.6259	0.6291	
12	0.6338	0.6384	0.6358	0.6330	
14	0.6368	0.6462	0.6473	0.6389	
16	0.6412	0.6529	0.6544	0.6488	
18	0.6517	0.6622	0.6628	0.6538	
20	0.6545	0.6652	0.6680	0.6585	
22	0.6582	0.6677	0.6728	0.6624	
24	0.6627	0.6703	0.6764	0.6657	

Group C03		THICKNESS (in.)			
WEEK	C03-a	C03-b	C03-c	C03-d	
0	0.5714	0.5727	0.5707	0.5725	
3	0.5901	0.5942	0.5926	0.5942	
6	0.6202	0.6060	0.6096	0.6163	
9	0.6298	0.6285	0.6248	0.6247	
12	0.6414	0.6370	0.6334	0.6310	
15	0.6502	0.6438	0.6448	0.6399	
18	0.6606	0.6497	0.6586	0.6457	
21	0.6635	0.6528	0.6634	0.6494	
24	0.6678	0.6557	0.6689	0.6546	

Table F.3: Continued

Group C04		THICKNESS (in.)			
WEEK	C04-a	C04-b	C04-c	C04-d	
0	0.5640	0.5825	0.5786	0.5862	
4	0.5916	0.6123	0.6085	0.6088	
8	0.6072	0.6346	0.6279	0.6319	
12	0.6233	0.6499	0.6456	0.6474	
16	0.6354	0.6559	0.6537	0.6662	
20	0.6431	0.6614	0.6648	0.6757	
24	0.6497	0.6663	0.6726	0.6803	

Group C05		THICKNESS (in.)			
WEEK	C05-a	C05-b	C05-c	C05-d	
0	0.5785	0.5838	0.5897	0.5703	
5	0.6280	0.6219	0.6185	0.6215	
10	0.6475	0.6448	0.6390	0.6460	
15	0.6695	0.6651	0.6591	0.6681	
20	0.6805	0.6751	0.6708	0.6806	

Group C06		THICKNESS (in.)			
WEEK	C06-a	C06-b	C06-c	C06-d	
0	0.5676	0.5666	0.5654	0.5644	
6	0.6083	0.6129			
12	0.6278	0.6450			
18	0.6493	0.6669			
24	0.6623	0.6804			

Group C07		THICKNESS (in.)			
WEEK	C07-a	C07-b	C07-c	C07-d	
0	0.5705	0.5743	0.5736	0.5791	
7	0.6220	0.6292	0.6202	0.6196	
14	0.6533	0.6516	0.6549	0.6380	
21	0.6635	0.6593	0.6619	0.6520	

Group C08		THICKNESS (in.)			
WEEK	C08-a	C08-b	C08-c	C08-d	
0	0.5743	0.5741	0.5737	0.5749	
8	0.6370	0.6129	0.6240	0.6217	
16	0.6809	0.6405	0.6613	0.6487	
24	0.7044	0.6592	0.6855	0.6615	

Group C09		THICKNESS (in.)			
WEEK	C09-a	C09-b	C09-c	C09-d	
0	0.5737	0.5754	0.5750	0.5797	
9	0.6296	0.6269	0.6285	0.6282	
18	0.6551	0.6503	0.6647	0.6578	

Table F.3: Continued

Group C10	THICKNESS (in.)			
WEEK	C10-a	C10-b	C10-c	C10-d
0	0.5750	0.5634	0.5784	0.5790
1	0.5833	0.5720	0.5869	0.5899
2	0.5905	0.5807	0.5952	0.5973
3	0.5972	0.5895	0.6011	0.6049
4	0.6041	0.5967	0.6069	0.6096
5	0.6119	0.6028	0.6133	0.6165
6	0.6189	0.6093	0.6217	0.6242
7	0.6263	0.6159	0.6264	0.6349
8	0.6323	0.6238	0.6329	0.6457
9	0.6360	0.6233	0.6339	0.6479
10	0.6419	0.6284	0.6371	0.6479
11	0.6505	0.6315	0.6384	0.6580
12	0.6594	0.6352	0.6459	0.6647
13	0.6654	0.6388	0.6482	0.6748
14	0.6702	0.6406	0.6527	0.6755
15	0.6721	0.6425	0.6555	0.6807
16	0.6780	0.6450	0.6603	0.6881
17	0.6785	0.6481	0.6632	0.6915
18	0.6866	0.6499	0.6684	0.6996
19	0.6896	0.6544	0.6716	0.7034
20	0.6971	0.6557	0.6773	0.7119
21	0.6996	0.6623	0.6792	0.7155
22	0.7017	0.6666	0.6815	0.7184
23	0.7029	0.6692	0.6844	0.7193
24	0.7040	0.6726	0.6871	0.7210

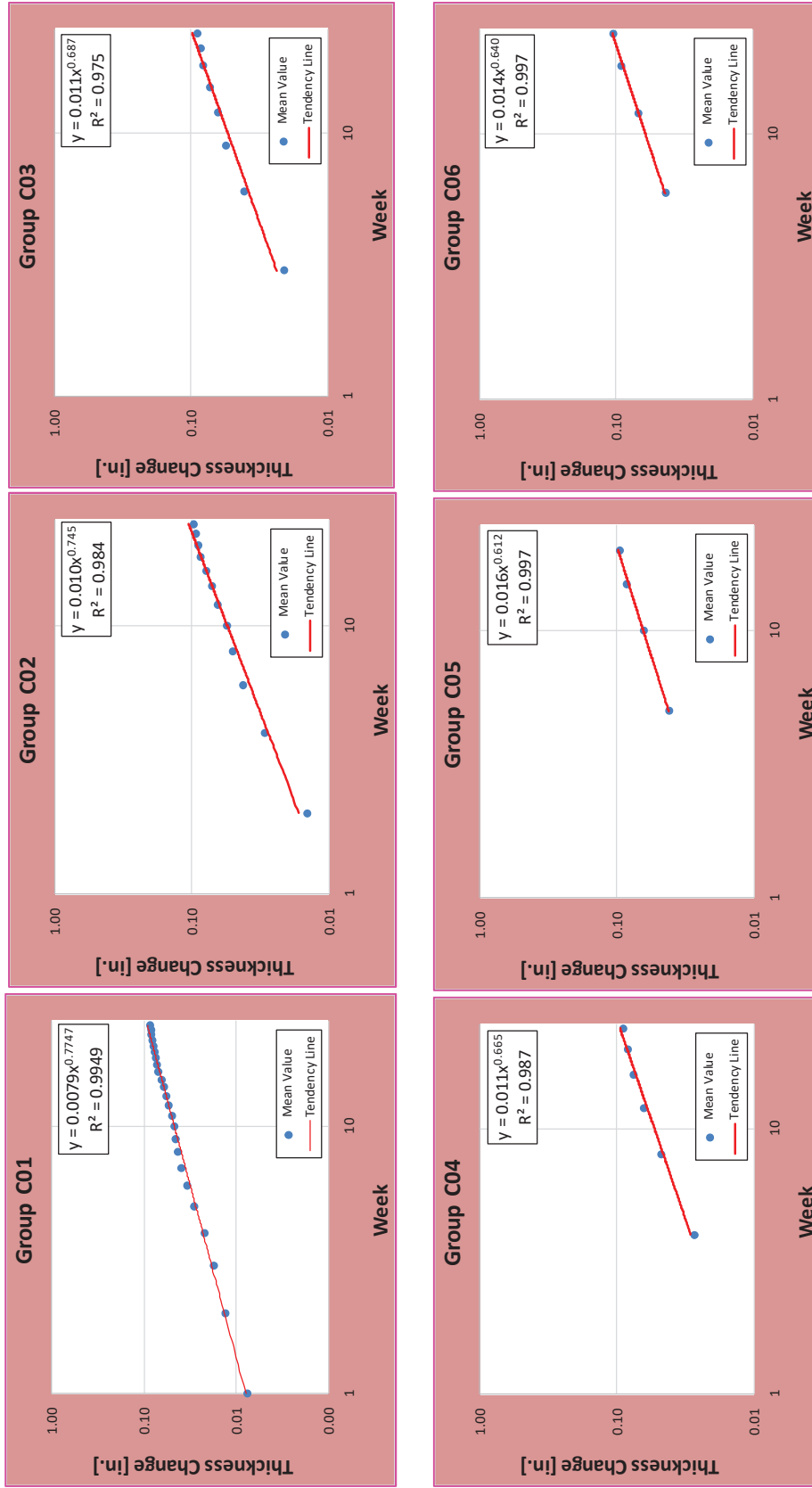


Figure F.3: Thickness change versus time during ACT for coupons from steel Type C

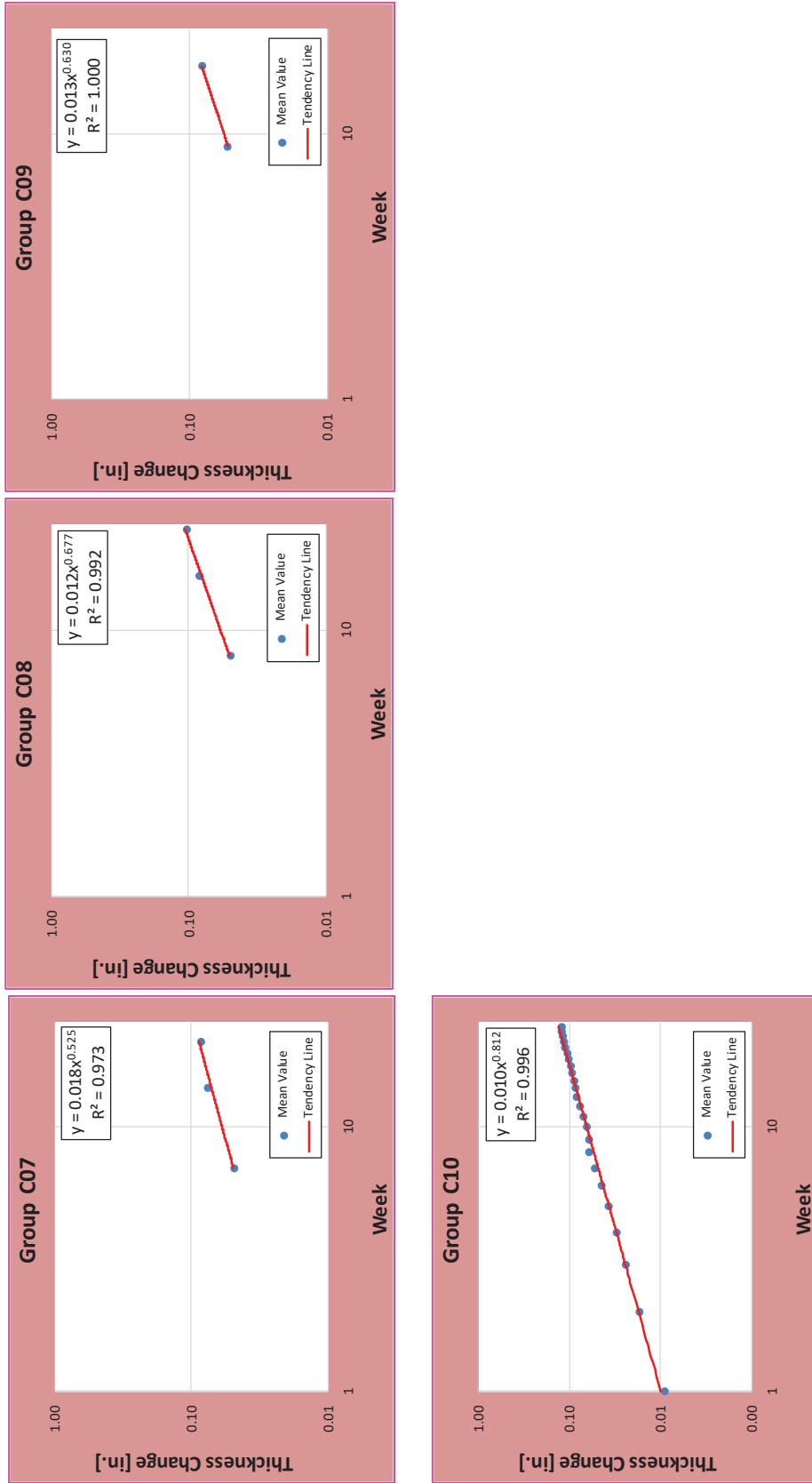


Figure F.3: Continued

Appendix G Photographs During ACT

The physical aspect changes during the ACT for an uncoated steel coupon is presented herein. A photography showing the aspect of coupon *A01-a* was taken every week for the 24 weeks the ACT lasted.

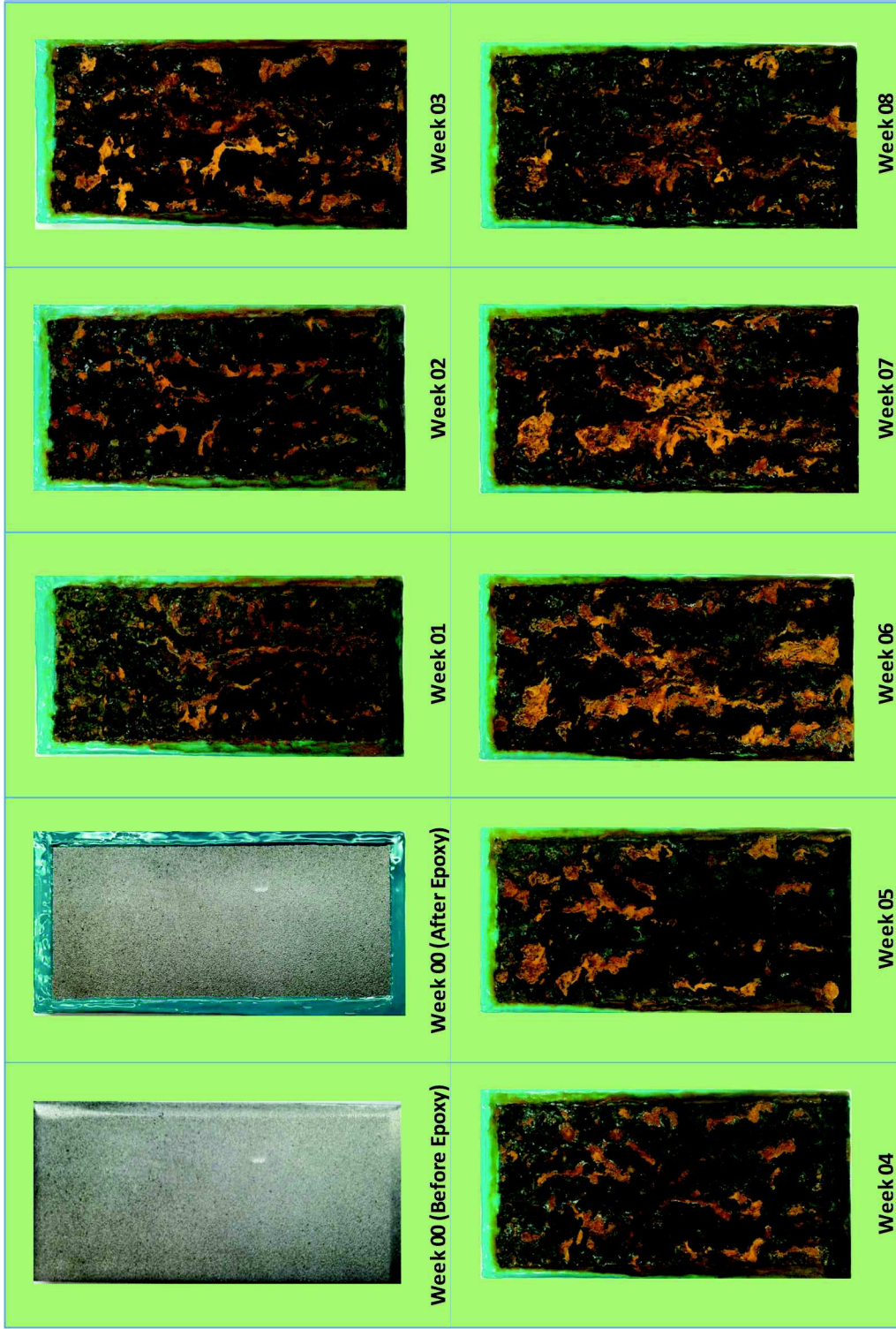


Figure G.1: Photographs showing physical aspect change during ACT - Coupon A01-a

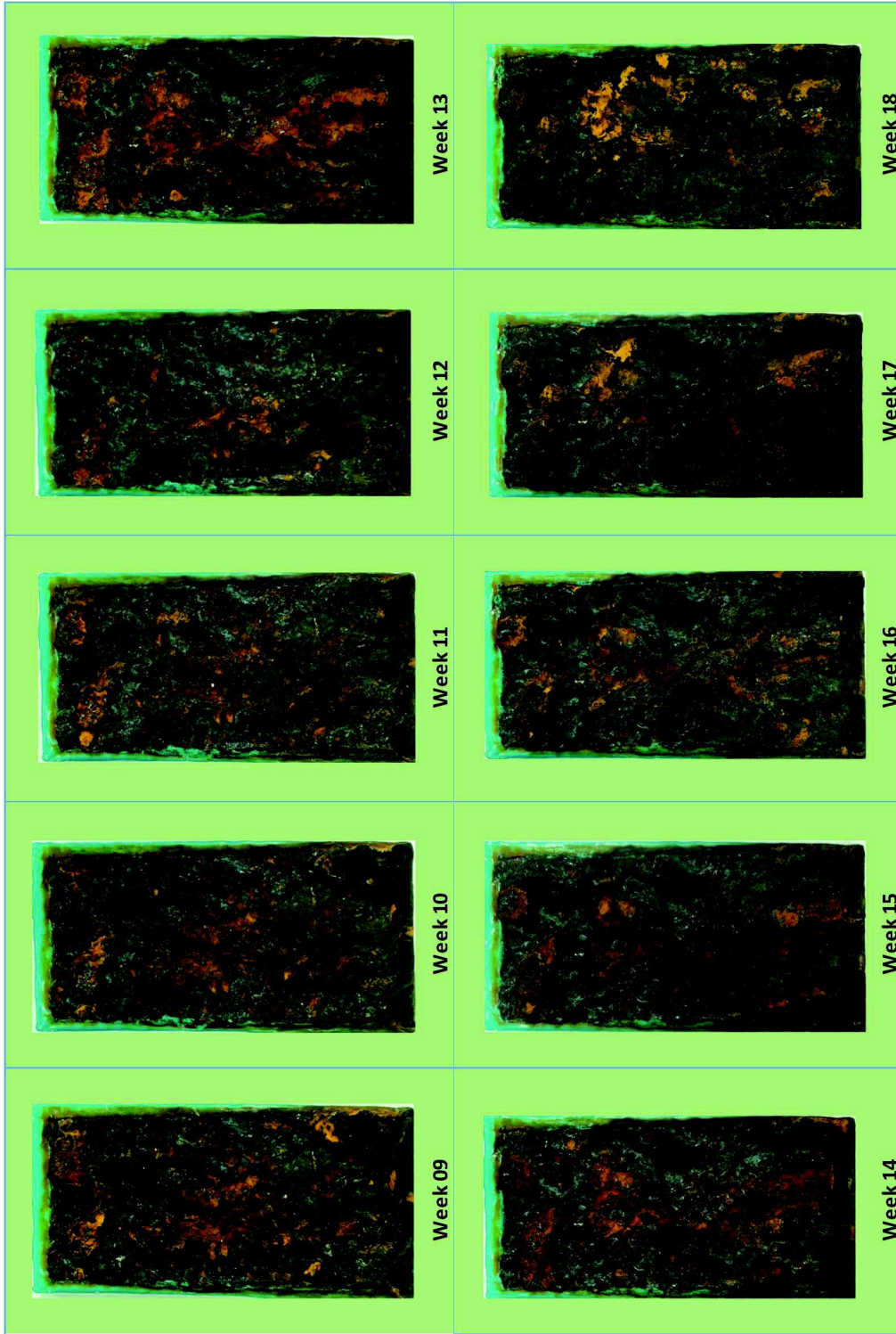


Figure G.1: Continued

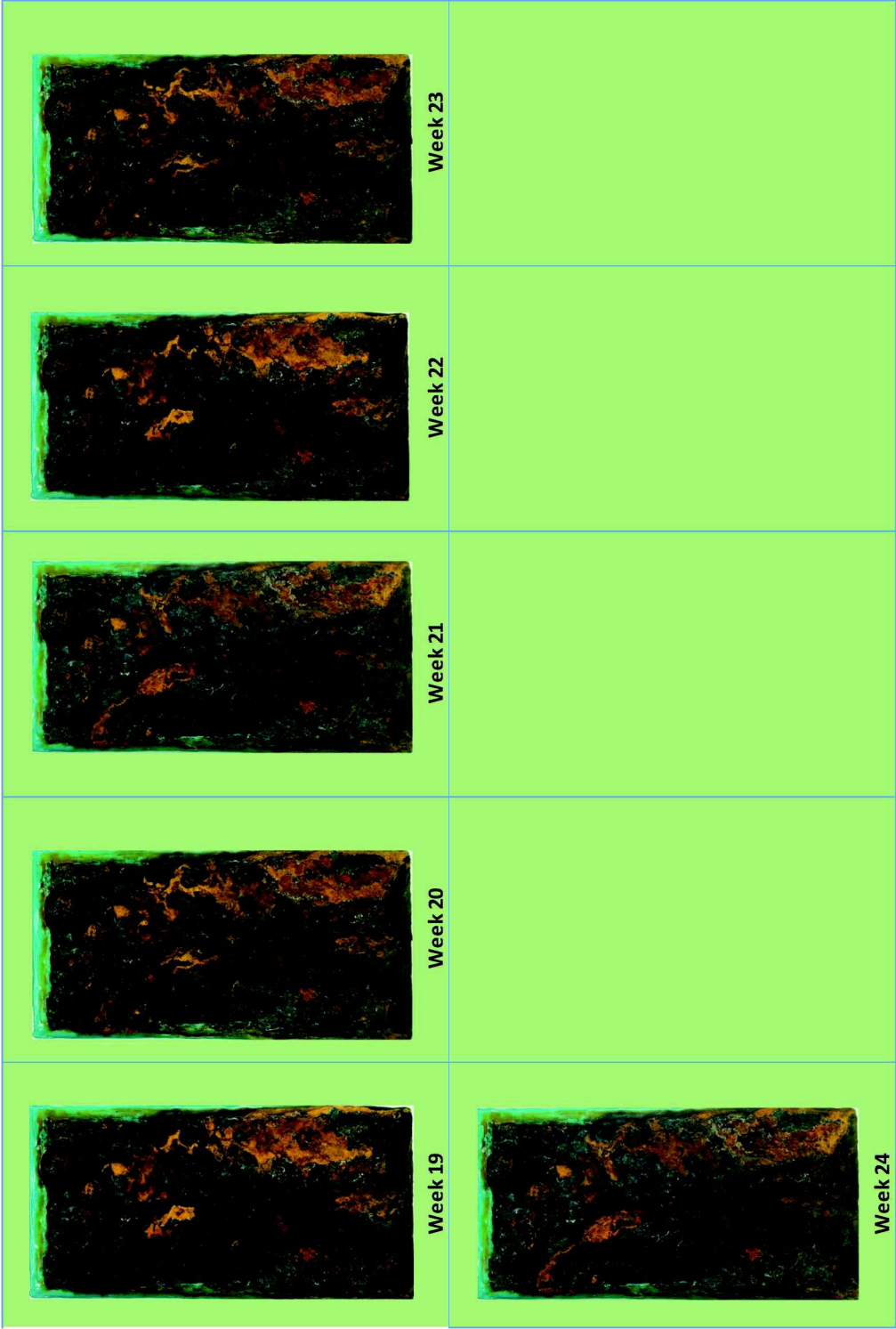


Figure G.1 : Continued

Appendix H Creepage Area Change of Scribed Coupons During ACT

Data corresponding to the change of creepage area from steel Type D coupons are presented herein. Photographs for coupons D01-a and D02-b show the increment of the NMC from week 0 to week 10. For all coupons from steel Type D are presented the increment of creepage area in tabulated and graphical manner.

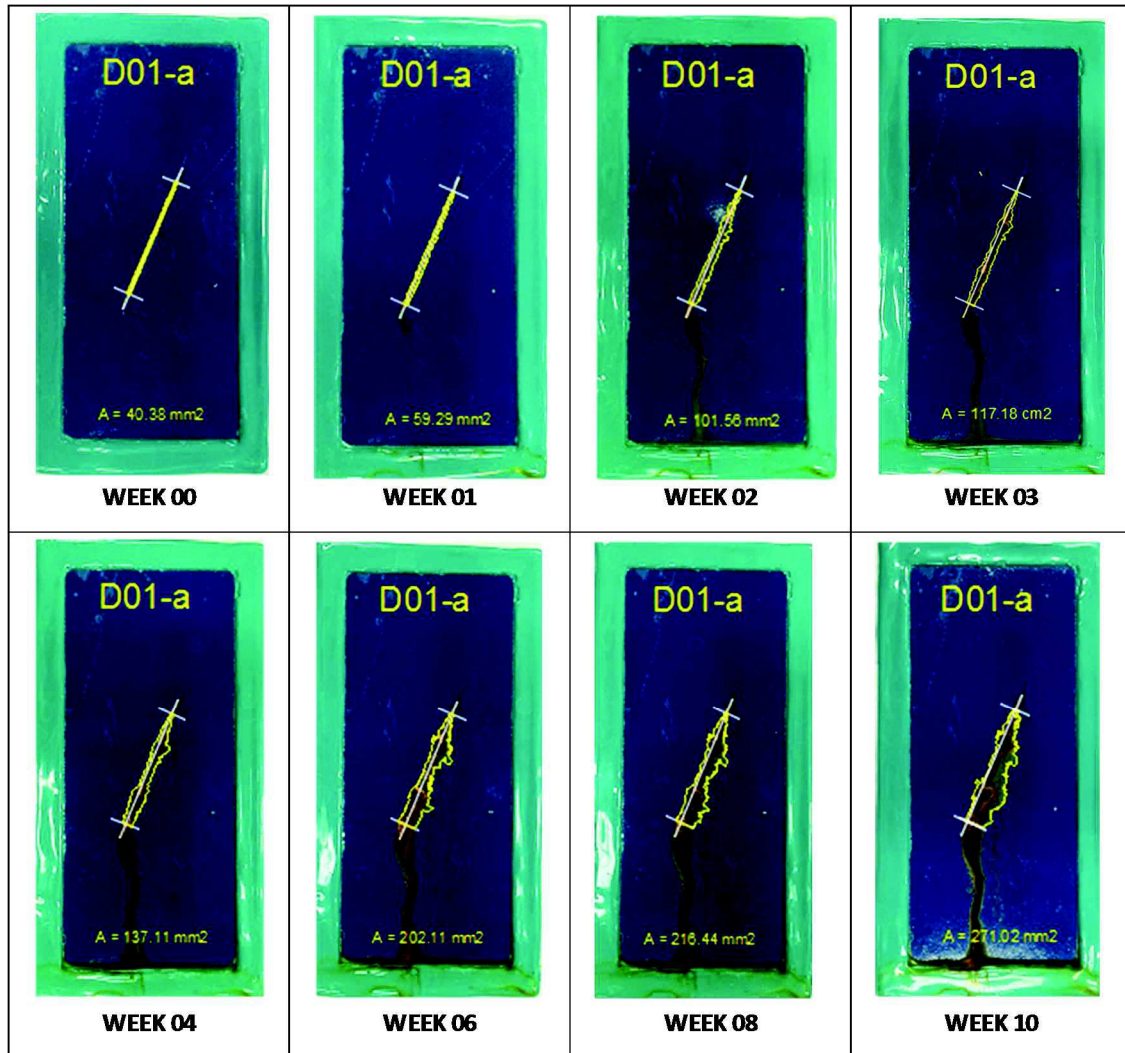


Figure H.1: Photographs of creepage area change during ACT - Coupon D01-a

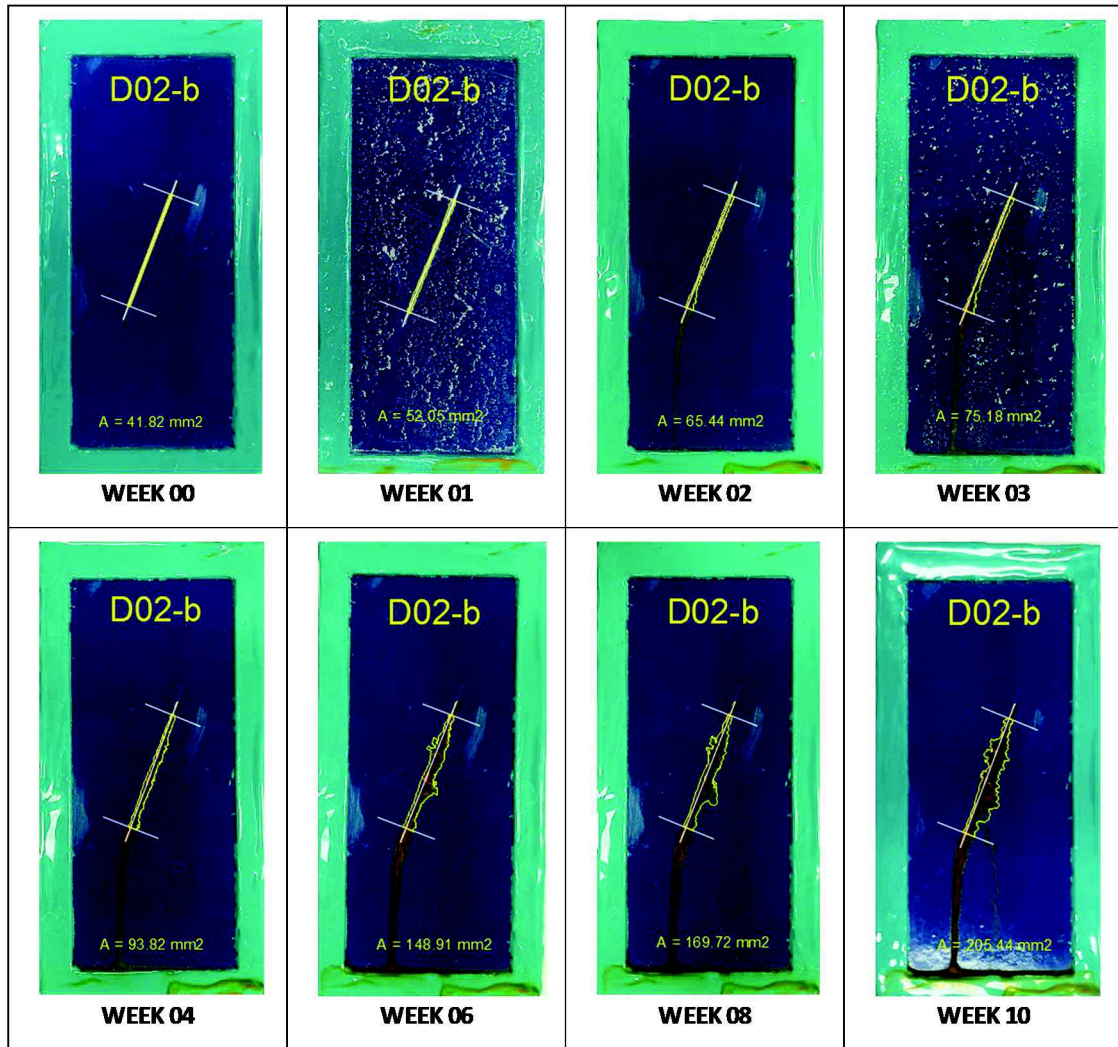


Figure H.2: Photographs of creep area change during ACT - Coupon D02-b

Table H.1: Creepage area change during ACT for coupons from steel Type D

Group D01	CREEPAGE AREA [mm ²]		
Week	D01-a	D01-b	D01-c
0	40.38	40.40	39.53
1	59.29	60.86	71.75
2	101.56	67.75	97.65
3	117.18	75.90	114.24
4	137.11	80.41	126.30
6	202.11	82.64	199.35
8	216.44	84.90	221.21
10	271.02	94.13	251.89

Group D02	CREEPAGE AREA [mm ²]		
Week	D02-a	D02-b	D02-c
0	40.79	41.82	41.25
1	53.03	52.05	51.26
2	54.50	65.44	60.72
3	62.31	75.18	66.83
4	78.63	93.82	73.60
6	103.36	148.91	102.37
8	104.30	169.72	104.82
10	136.20	205.44	139.35

Group D03	CREEPAGE AREA [mm ²]		
Week	D03-a	D03-b	D03-c
0	42.08	40.60	41.10
1	49.83	57.81	43.22
2	67.20	61.90	50.24
3	81.04	63.26	56.80
4	84.48	65.04	64.19
6	96.53	94.62	98.70
8	106.87	114.15	115.83
10	110.76	125.06	121.78

Group D04	CREEPAGE AREA [mm ²]		
Week	D04-a	D04-b	D04-c
0	41.28	41.67	41.68
1	42.08	50.60	44.35
2	44.13	95.71	58.05
3	60.37	106.56	76.67
4	77.30	121.57	82.70
6	85.98	161.64	91.15
8	98.51	206.79	98.81
10	108.03	237.29	115.95

Group D05	CREEPAGE AREA [mm ²]		
Week	D05-a	D05-b	D05-c
0	41.59	41.44	41.76
1	46.61	52.60	62.42
2	56.67	59.15	102.32
3	78.42	71.17	114.27
4	95.92	88.15	134.58

Group D06	CREEPAGE AREA [mm ²]	
Week	D06-a	D06-b
0	42.01	41.15
1	53.13	43.22
2	61.62	48.61
3	68.45	74.02
4	77.02	83.56
6	81.55	99.65
8	88.27	109.12
10	92.19	116.95

Group D07	CREEPAGE AREA [mm ²]	
Week	D07-a	D07-b
0	41.84	41.75
1	50.70	50.15
2	61.24	56.77
3	79.75	77.58
4	82.96	85.13

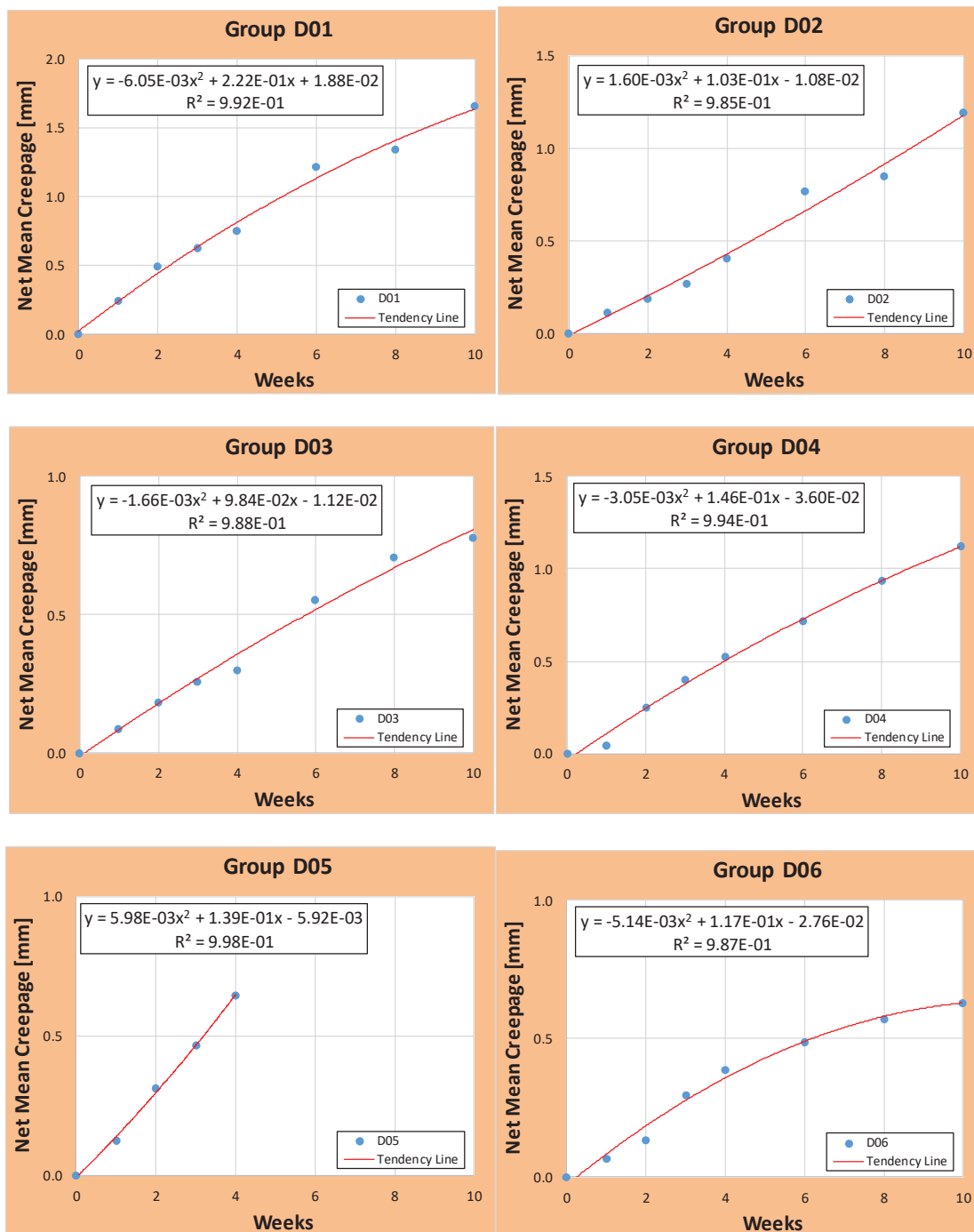


Figure H.3: Graphs for NMC change during ACT for coupons from steel Type D

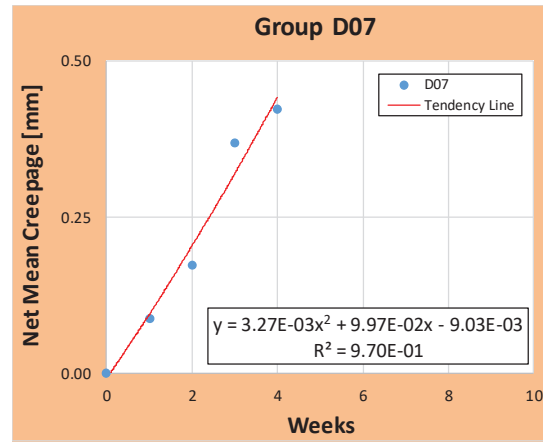


Figure H.3: Continued

Appendix I Control Test

Data corresponding to the coupons from Control Test are presented in this Appendix. The codification, and weight change is presented in tables. The physical changes due to the ACT from the beginning to the end of the test, and the final aspect after sandblasting, are documented by photographs at those different moments.

Table I.1: Identification for Control Test coupons, Groups X and W

Group	Plate	Coupon Code
X01	X01	X01-a
	X02	X01-b
	X03	X01-c
X02	X04	X02-a
	X05	X02-b
	X06	X02-c
X03	X07	X03-a
	X08	X03-b
	X09	X03-c
X04	X10	X04-a
	X11	X04-b
	X12	X04-c
X05	X13	X05-a
	X14	X05-b

Coupon X15 was damaged

Group	Plate	Coupon
W01	W01	W01-a
	W02	W01-b
	W03	W01-c
W02	W04	W02-a
	W05	W02-b
	W06	W02-c
W03	W07	W03-a
	W08	W03-b
	W09	W03-c
W04	W10	W04-a
	W11	W04-b
	W12	W04-c
W05	W13	W05-a
	W14	W05-b
	W15	W05-c

Table I.2: Weight change for Control Test, Groups X

Group	Plate	Coupon Code	Week Tested	WEIGHT (gr.)		
				Initial	Before*	After*
X01	X01	X01-a	2	1,148.33	1,149.70	1,143.50
	X02	X01-b		1,146.83	1,148.00	1,142.50
	X03	X01-c		1,285.27	1,287.10	1,280.10
X02	X04	X02-a	4	1,155.73	1,159.20	1,148.60
	X05	X02-b		1,159.49	1,164.00	1,150.70
	X06	X02-c		1,172.28	1,176.00	1,165.00
X03	X07	X03-a	6	1,152.54	1,161.10	1,139.80
	X08	X03-b		1,195.91	1,204.30	1,183.60
	X09	X03-c		1,181.44	1,190.20	1,168.90
X04	X10	X04-a	8	1,207.64	1,218.20	1,190.50
	X11	X04-b		1,166.36	1,178.00	1,148.20
	X12	X04-c		1,178.46	1,188.80	1,162.00
X05	X13	X05-a	10	1,183.35	1,200.90	1,161.60
	X14	X05-b		1,203.39	1,220.30	1,182.60

Coupon X15 was damaged

* Blasting

Table I.3: Weight change for Control Test, Groups W

Group	Plate	Coupon	Week Tested	WEIGHT (gr.)		
				Initial	Before*	After*
W01	W01	W01-a	2	1,159.93	1,161.20	1,155.00
	W02	W01-b		1,203.95	1,205.30	1,199.00
	W03	W01-c		1,172.29	1,173.60	1,167.50
W02	W04	W02-a	4	1,154.20	1,158.60	1,145.50
	W05	W02-b		1,171.85	1,175.60	1,163.40
	W06	W02-c		1,201.01	1,205.00	1,192.30
W03	W07	W03-a	6	1,167.63	1,174.40	1,156.20
	W08	W03-b		1,168.88	1,176.00	1,157.30
	W09	W03-c		1,155.24	1,161.80	1,144.50
W04	W10	W04-a	8	1,173.87	1,182.50	1,159.40
	W11	W04-b		1,166.07	1,176.60	1,149.70
	W12	W04-c		1,156.80	1,167.30	1,141.50
W05	W13	W05-a	10	1,153.10	1,167.80	1,133.80
	W14	W05-b		1,151.54	1,164.40	1,133.50
	W15	W05-c		1,154.81	1,167.00	1,137.50

* Blasting

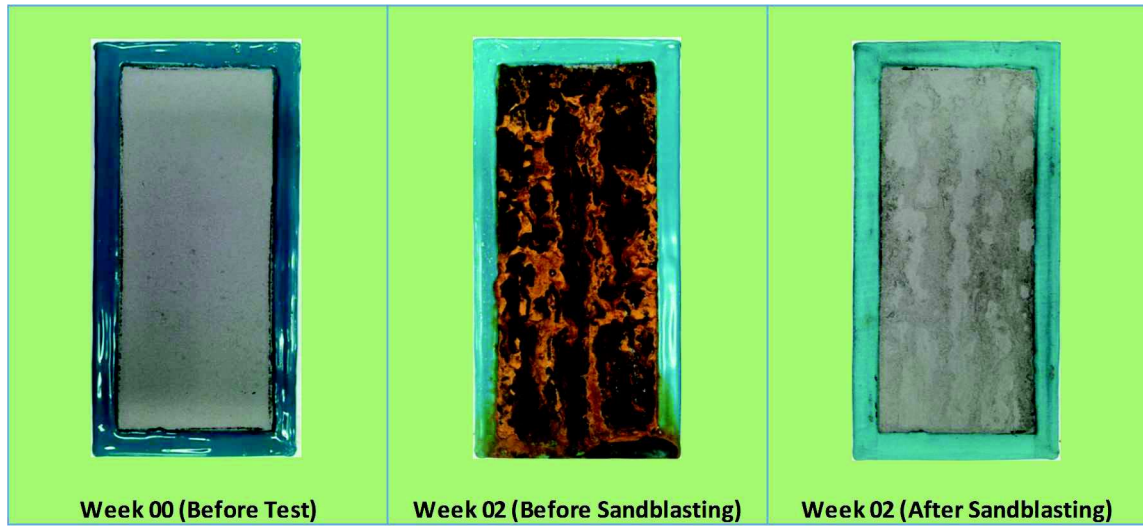


Figure I.1: Photographs from Control Test - coupon X01-a

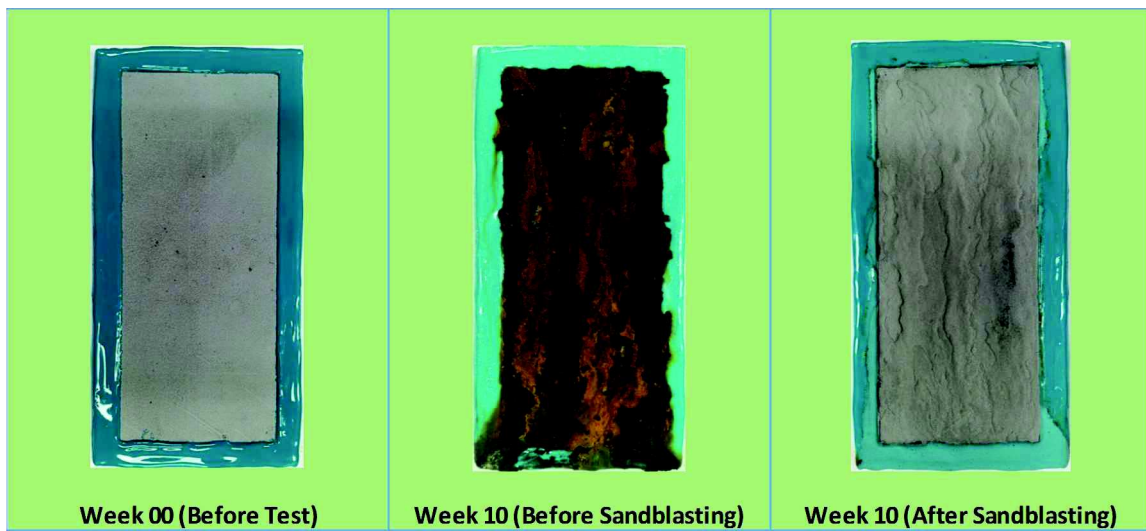
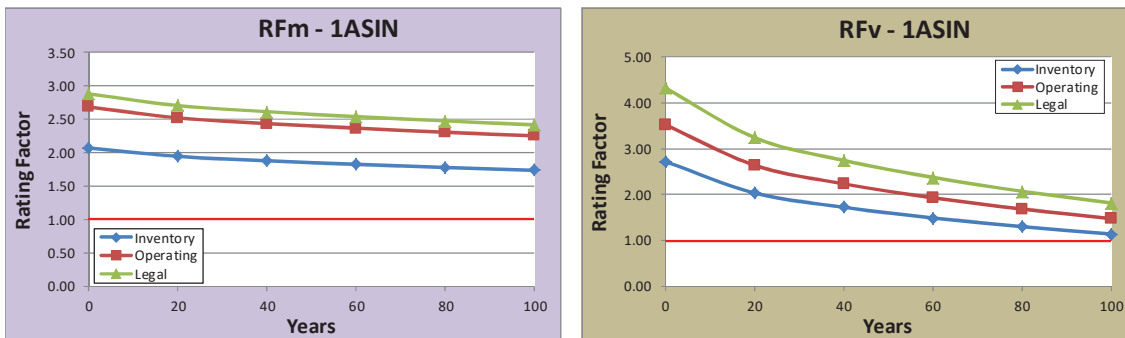


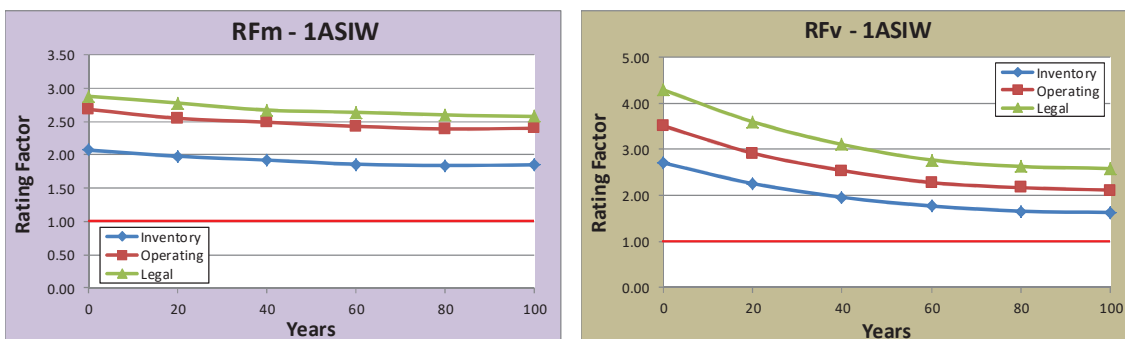
Figure I.2: Photographs from Control Test - coupon W05-a

Appendix J Rating Factors RF_m and RF_v

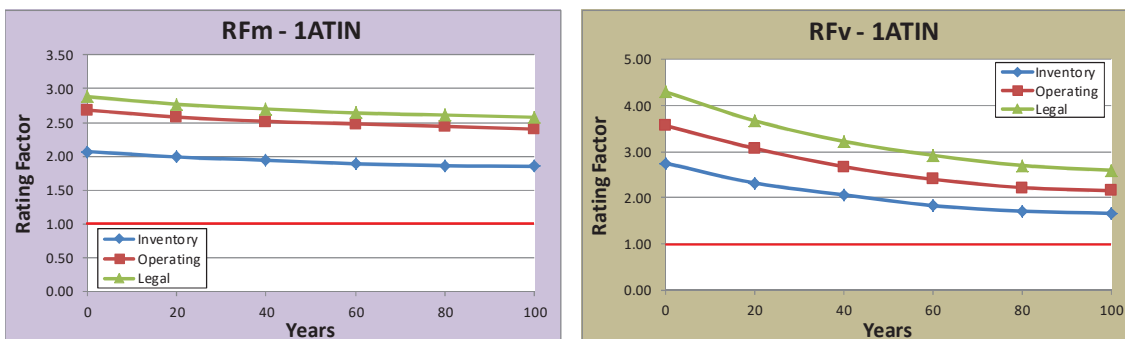
The load rating factors for bending capacity RF_m and shear capacity RF_v, corresponding to the 96 bridge cases considered in the parametric study for this research are presented from Figures J.1 to J.24. Both RF_m and RF_v values were calculated and plotted at ages 0, 20, 40, 60, 80, and 100 years of bridge service life. The factors RF_m and RF_v were evaluated for the load levels: Inventory, Operating, and Legal. For each rating plot the limit factor 1.0 is marked with a red line to emphasize the trigger age when some actions must be taken, according to the prescriptions given by the AASHTO MBE (AASHTO, 2011).



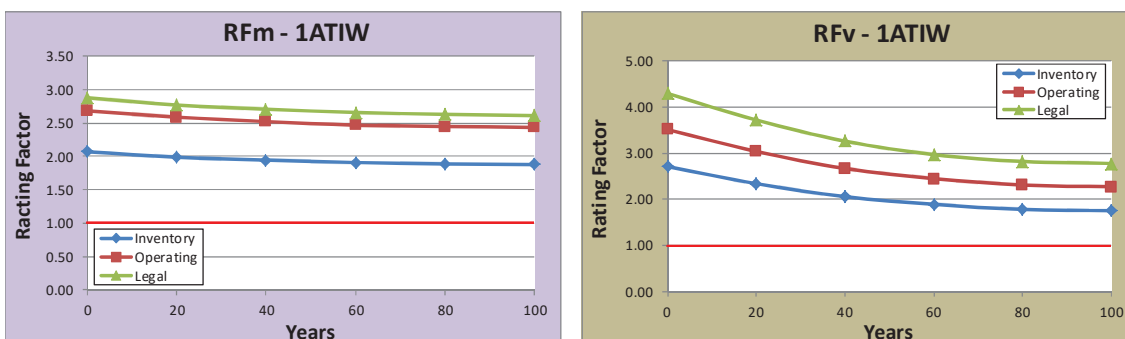
1-Span x 70' – Carbon steel – Industrial/urban – No washing



1-Span x 70' – Carbon steel – Industrial/urban – Steel washing

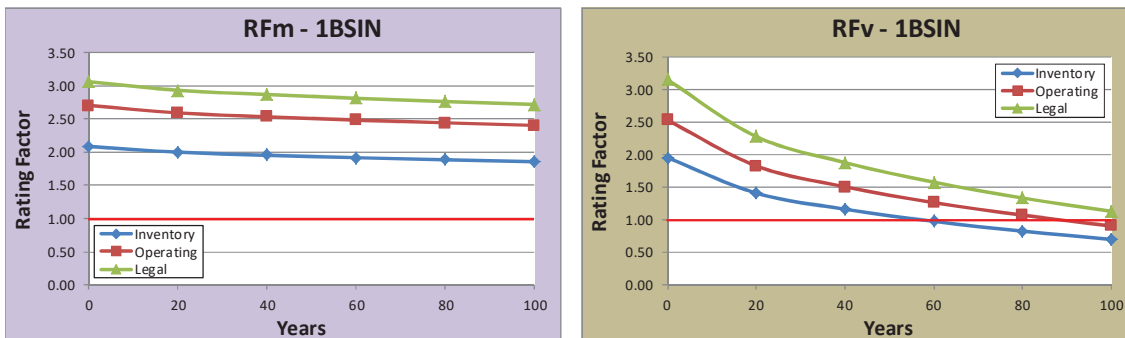


1-Span x 70' – Weathering steel – Industrial/urban – No washing

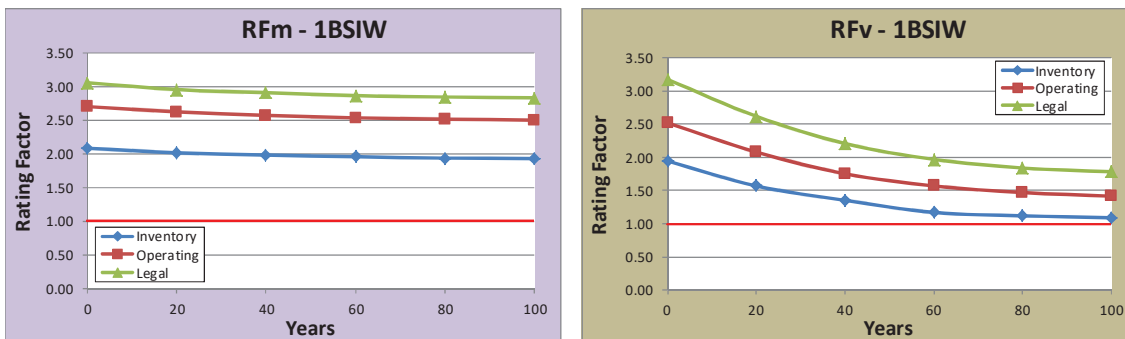


1-Span x 70' – Weathering steel – Industrial/urban – Steel washing

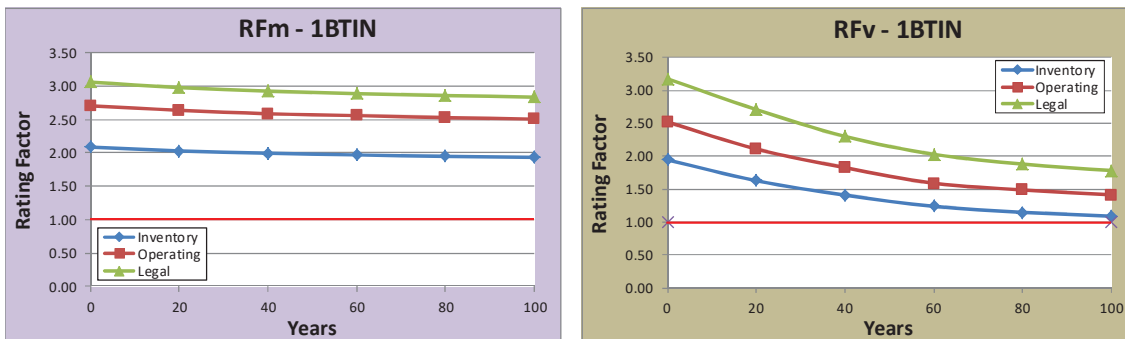
Figure J.1: RFm and RFv versus time for 1-Span x 70', Industrial/urban



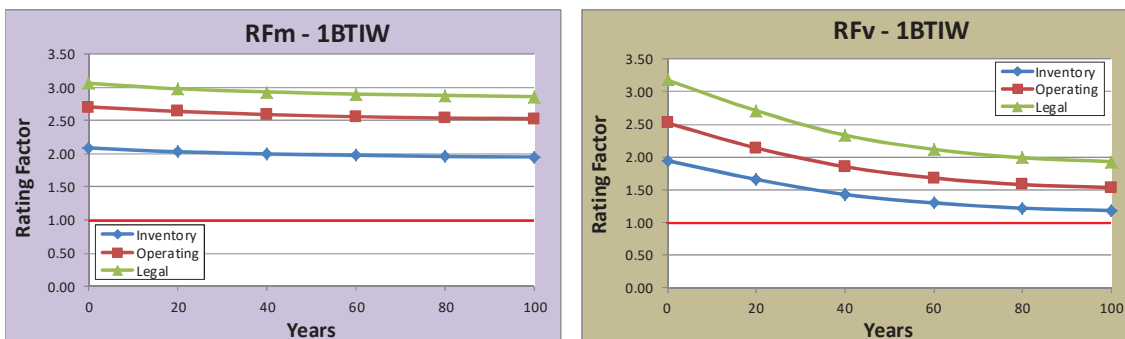
1-Span x 90' – Carbon steel – Industrial/urban – No washing



1-Span x 90' – Carbon steel – Industrial/urban – Steel washing

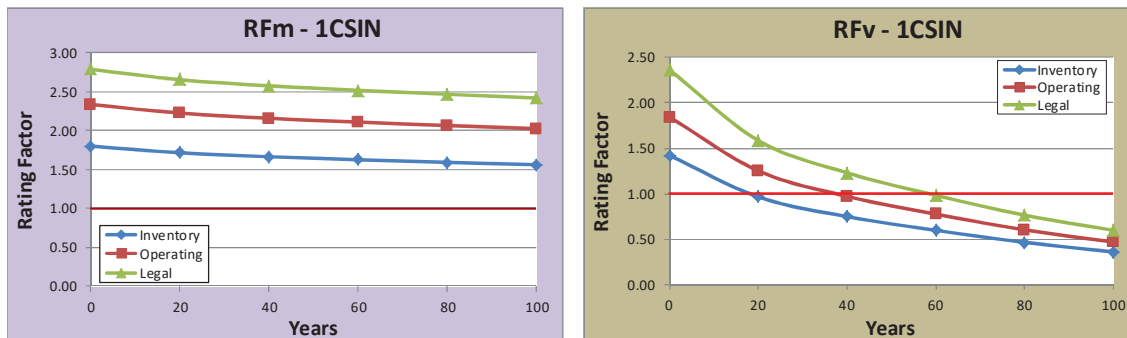


1-Span x 90' – Weathering steel – Industrial/urban – No washing

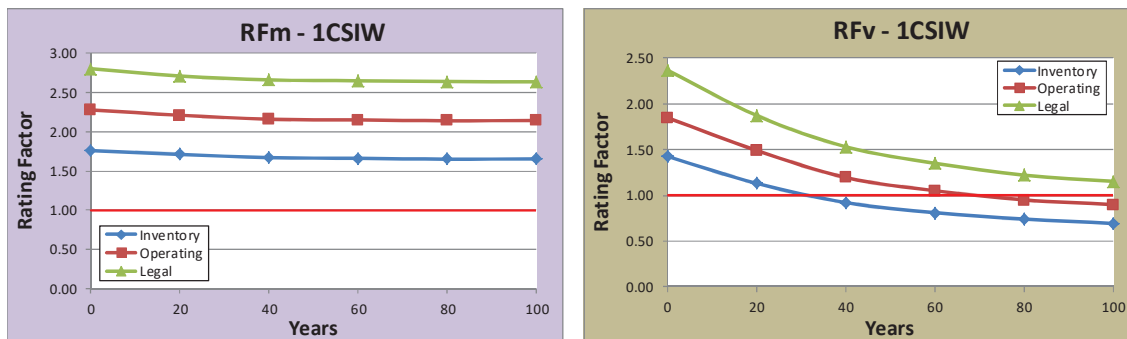


1-Span x 90' – Weathering steel – Industrial/urban – Steel washing

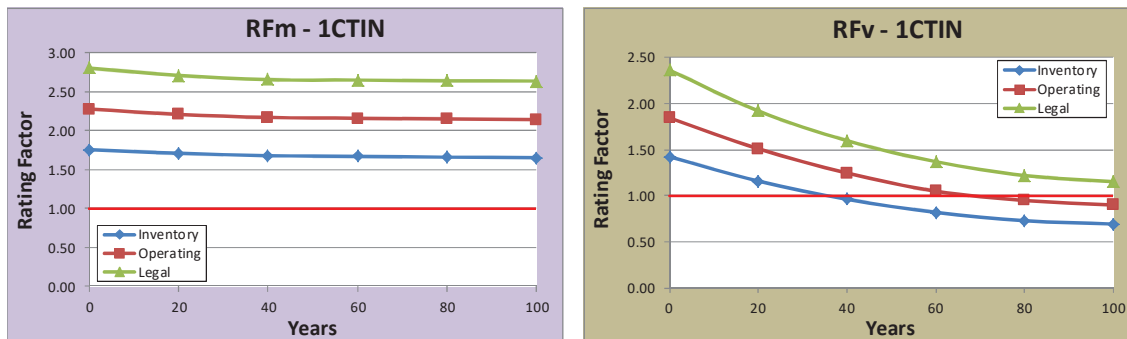
Figure J.2: RFm and RFv versus time for 1-Span x 90', Industrial/urban



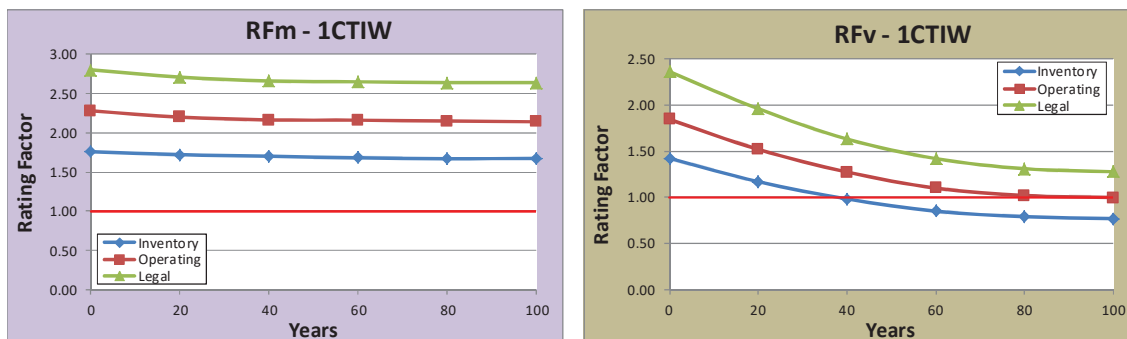
1-Span x 110' – Carbon steel – Industrial/urban – No washing



1-Span x 110' – Carbon steel – Industrial/urban – Steel washing

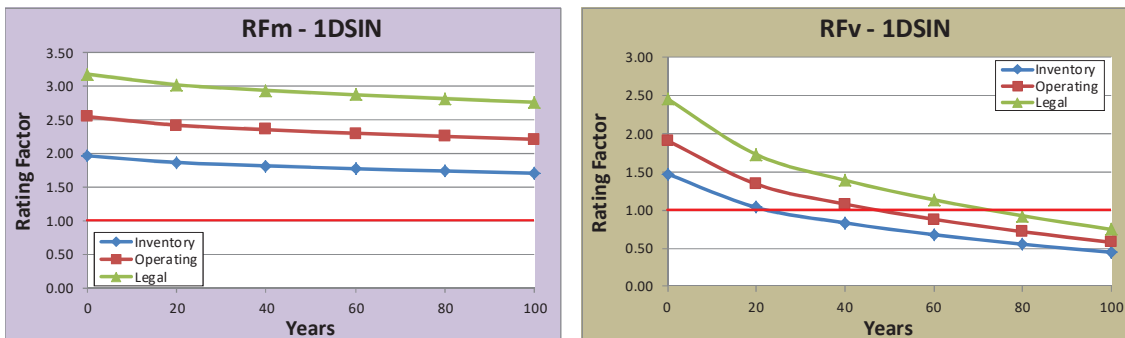


1-Span x 110' – Weathering steel – Industrial/urban – No washing

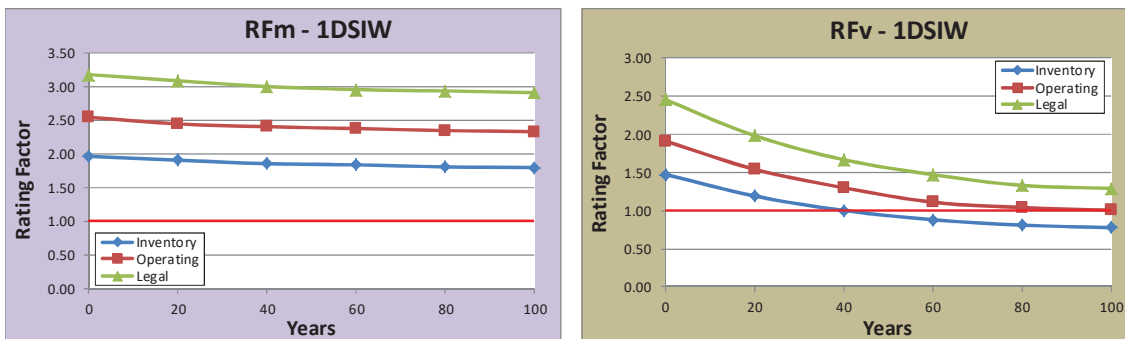


1-Span x 110' – Weathering steel – Industrial/urban – Steel washing

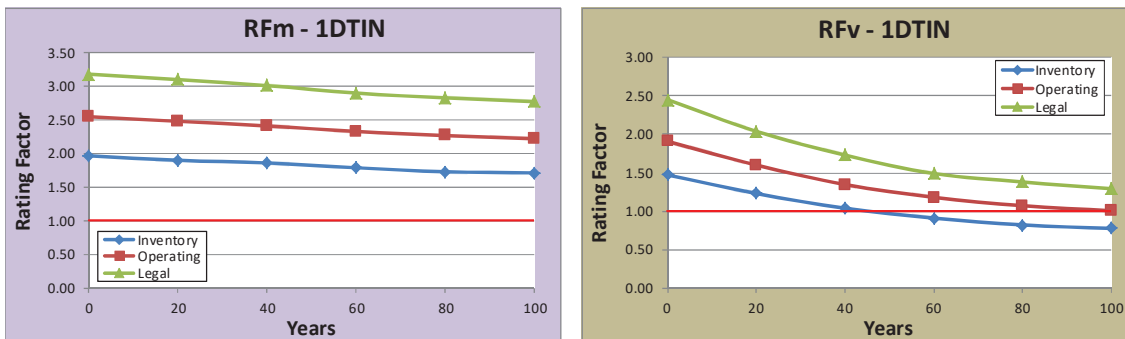
Figure J.3: RFm and RFv versus time for 1-Span x 110', Industrial/urban



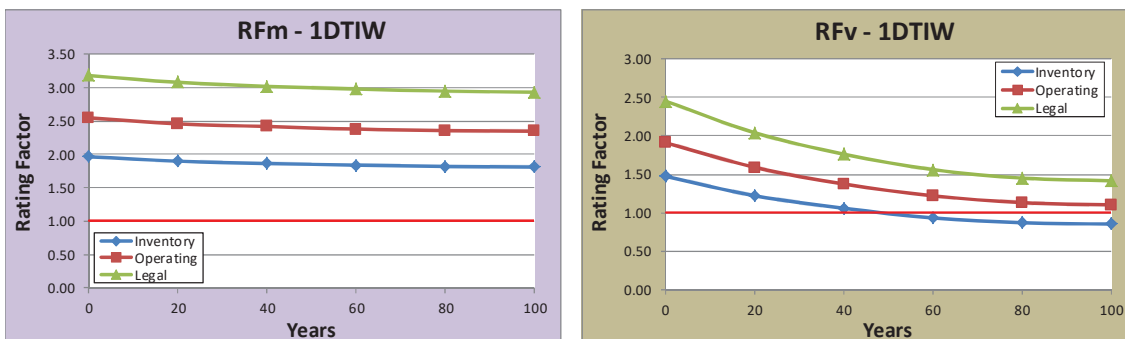
1-Span x 130' – Carbon steel – Industrial/urban – No washing



1-Span x 130' – Carbon steel – Industrial/urban – Steel washing

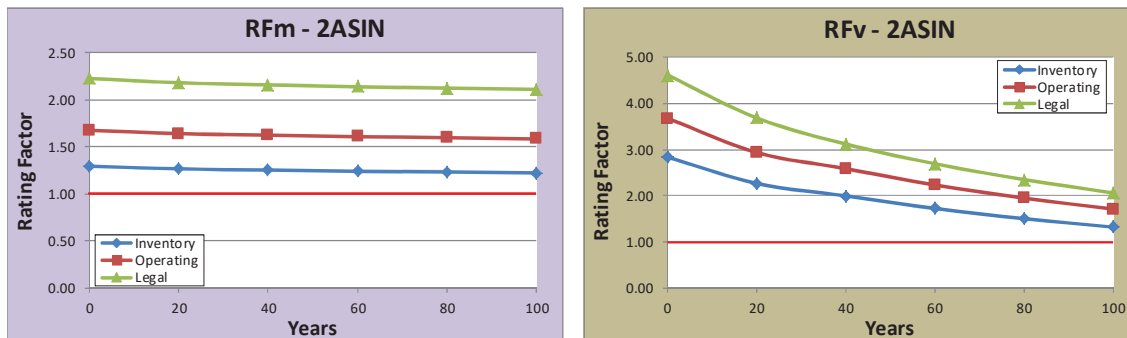


1-Span x 130' – Weathering steel – Industrial/urban – No washing

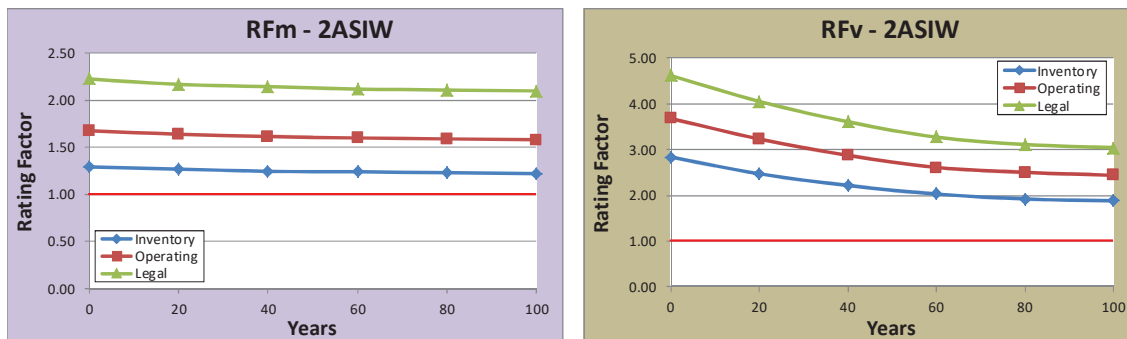


1-Span x 130' – Weathering steel – Industrial/urban – Steel washing

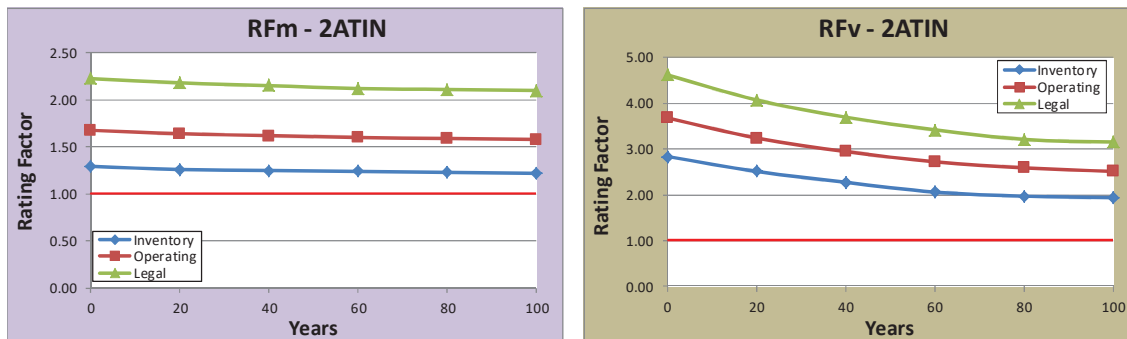
Figure J.4: RFm and RFv versus time for 1-Span x 130', Industrial/urban



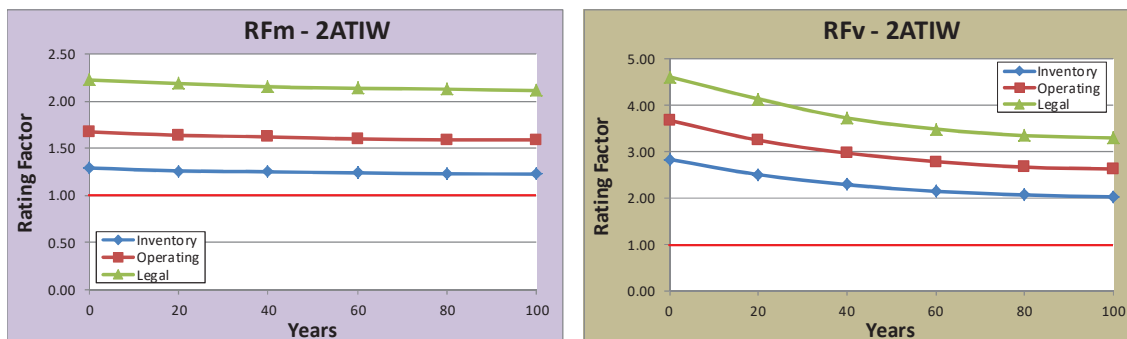
2-Span x 70' – Carbon steel – Industrial/urban – No washing



2-Span x 70' – Carbon steel – Industrial/urban – Steel washing



2-Span x 70' – Weathering steel – Industrial/urban – No washing



2-Span x 70' – Weathering steel – Industrial/urban – Steel washing

Figure J.5: RFm and RFv versus time for 2-Span x 70', Industrial/urban

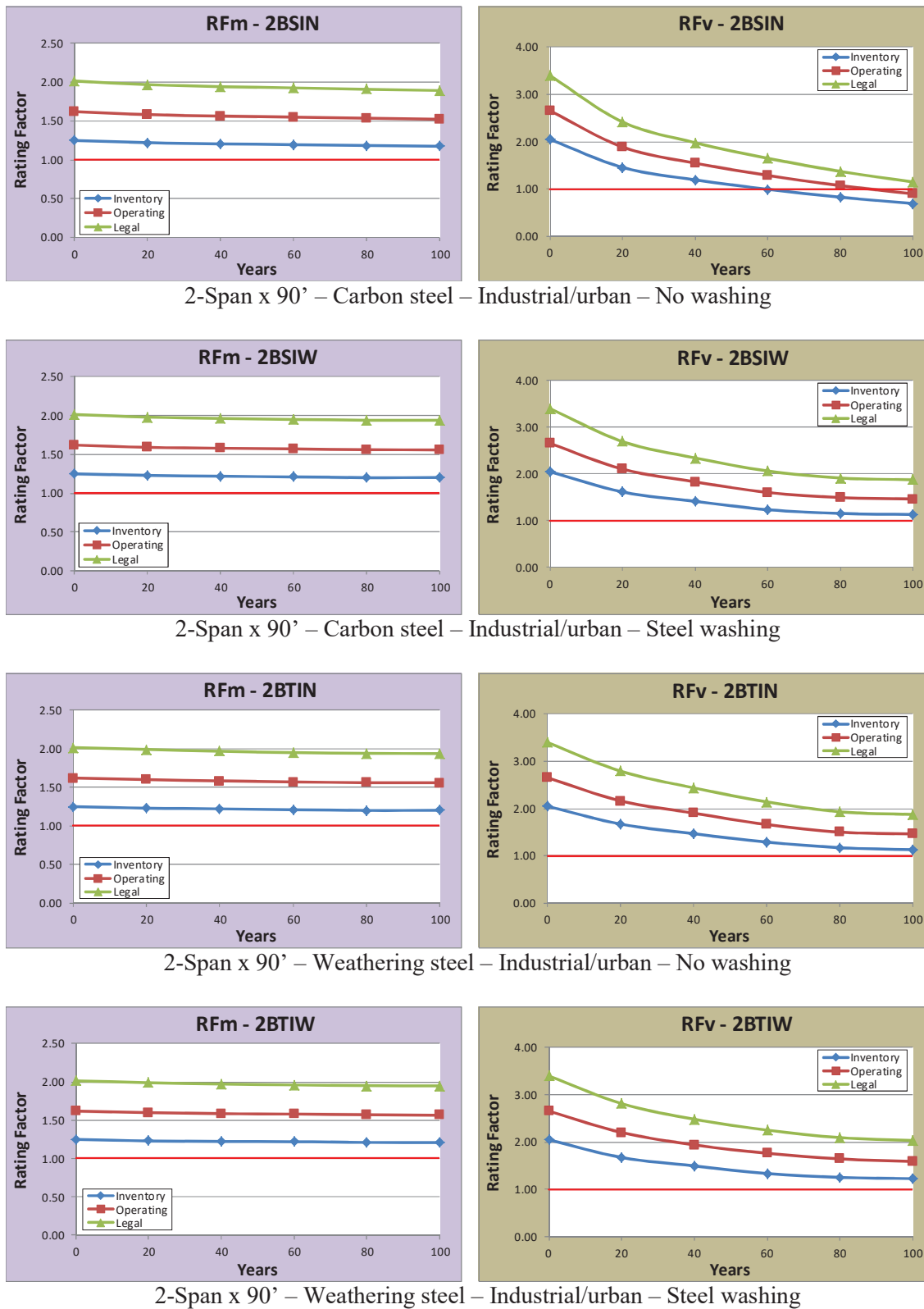


Figure J.6: RfM and RfV versus time for 2-Span x 90', Industrial/urban

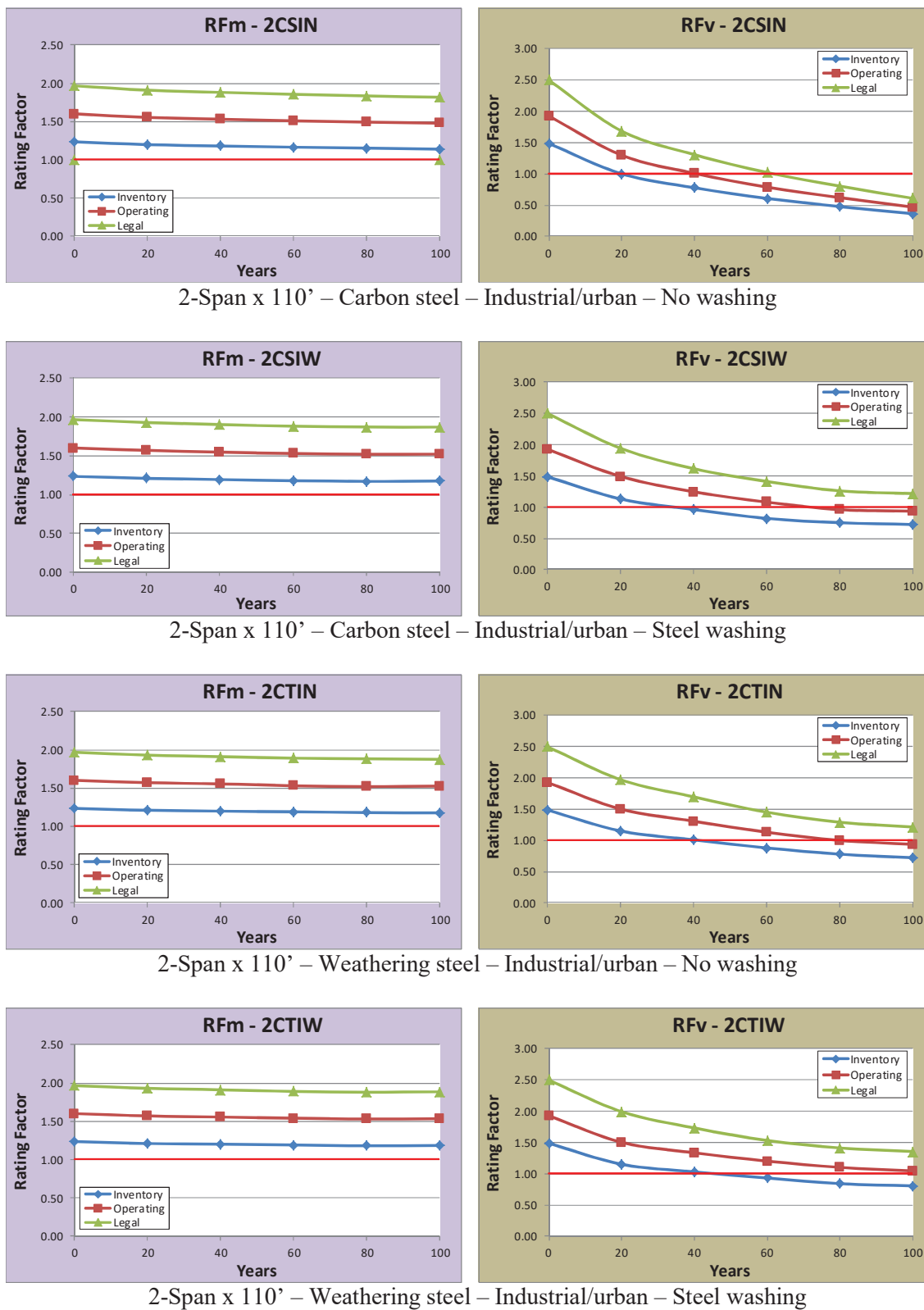


Figure J.7: RFm and RFv versus time for 2-Span x 110', Industrial/urban

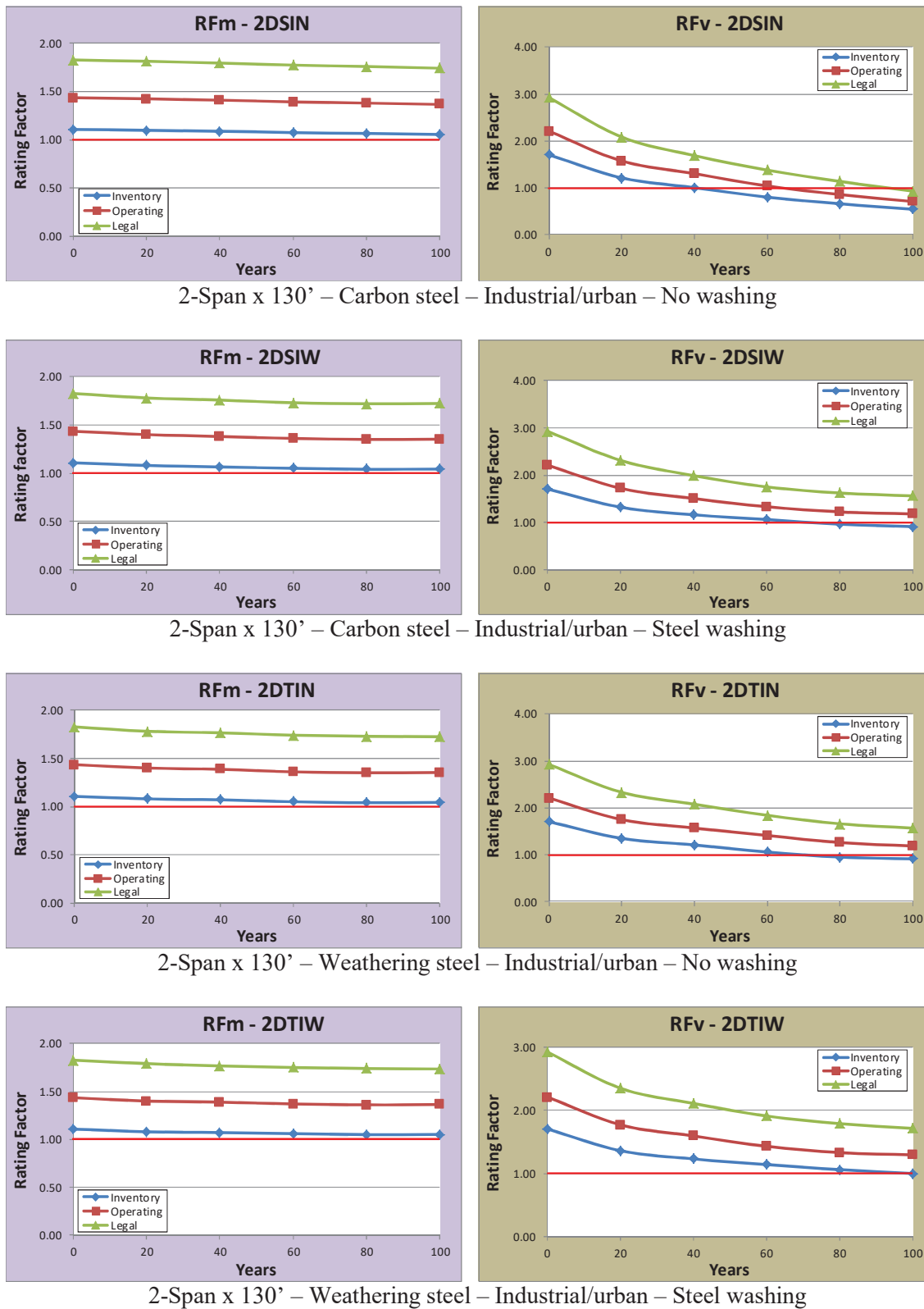
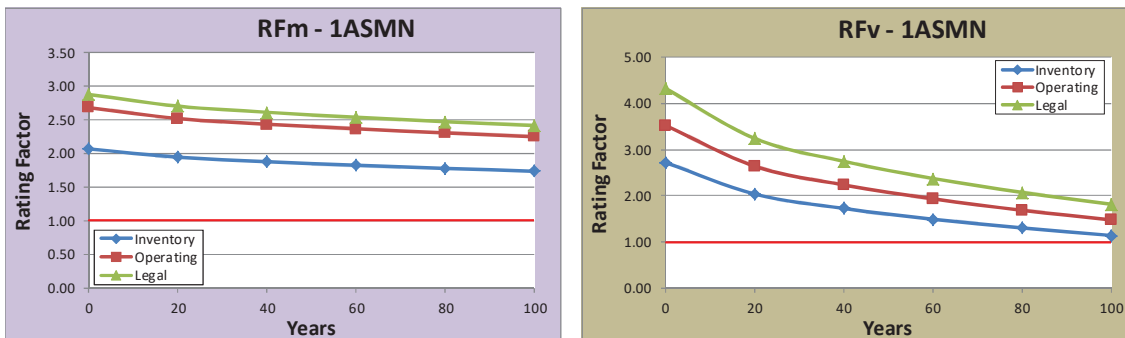
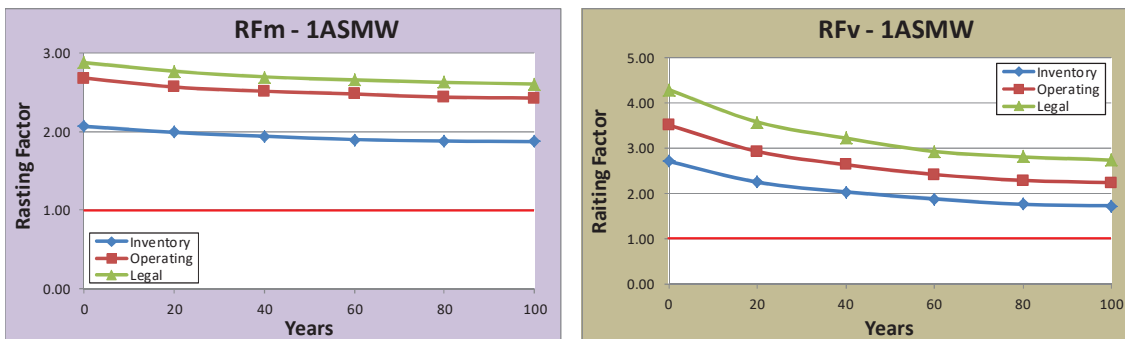


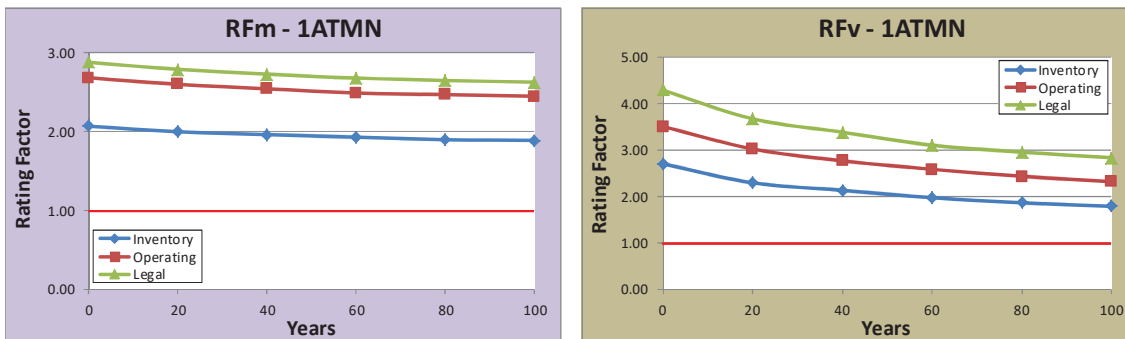
Figure J.8: RFm and RFv versus time for 2-Span x 130', Industrial/urban



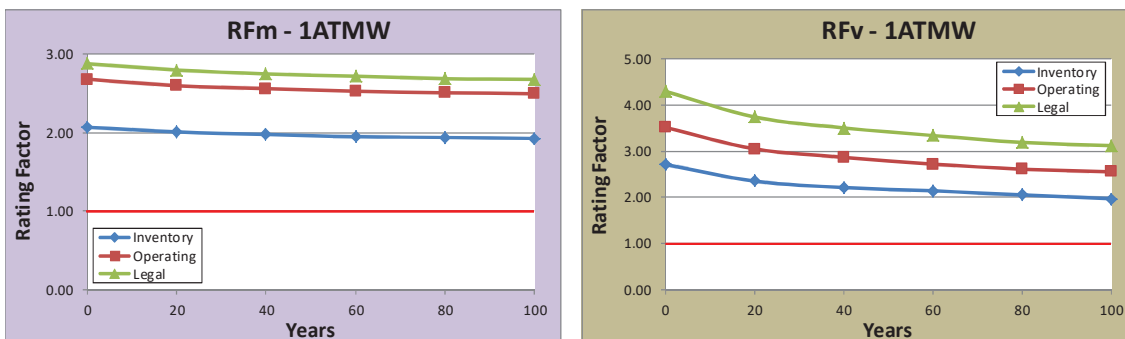
1-Span x 70' – Carbon steel – Marine – No washing



1-Span x 70' – Carbon steel – Marine – Steel washing

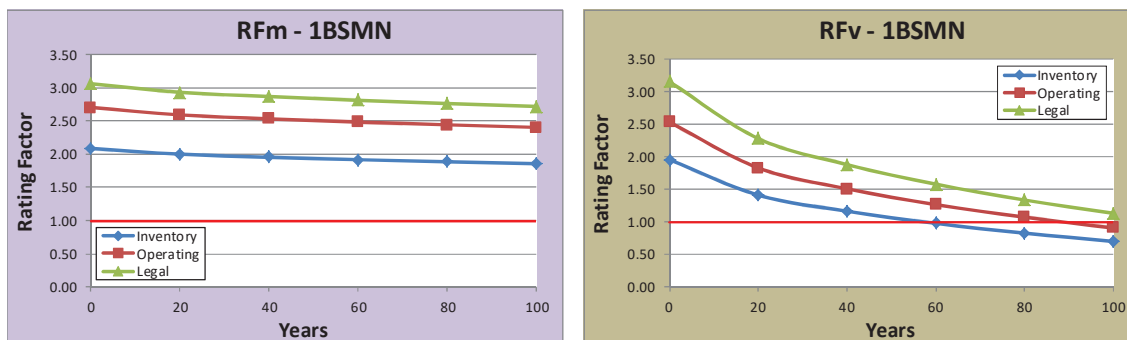


1-Span x 70' – Weathering steel – Marine – No washing

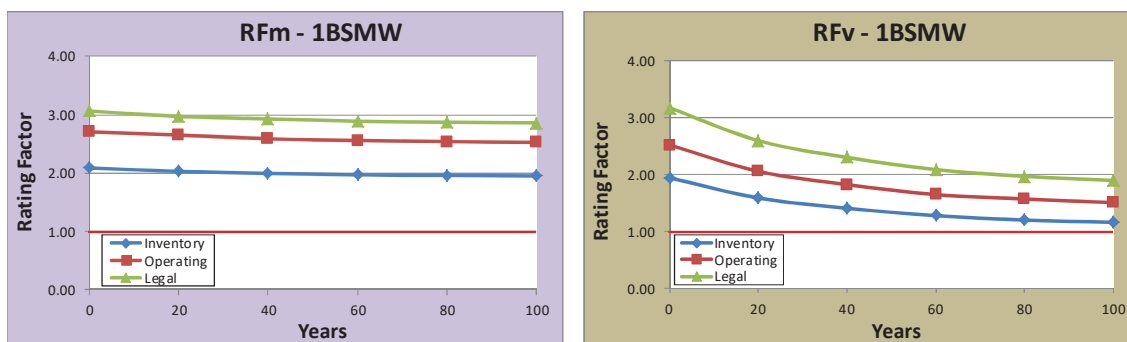


1-Span x 70' – Weathering steel – Marine – Steel washing

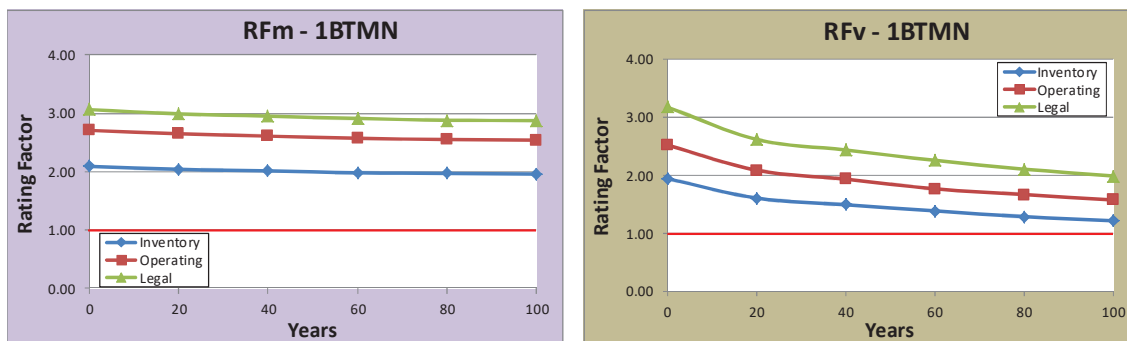
Figure J.9: RFm and RFv versus time for 1-Span x 70', Marine



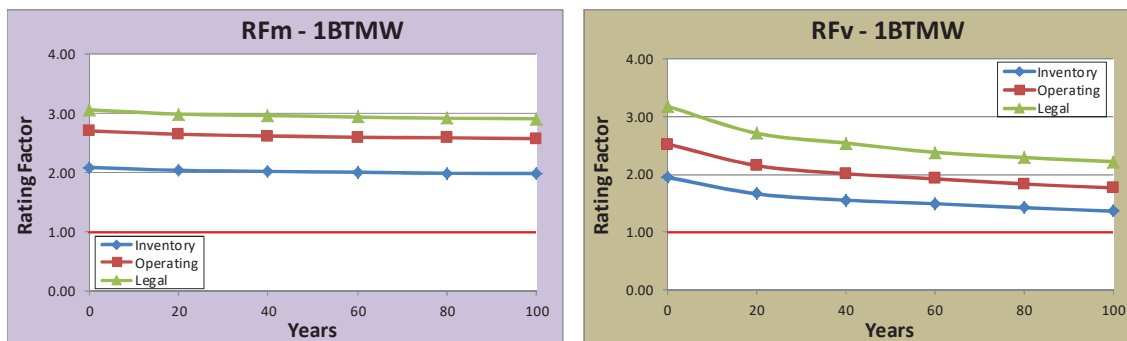
1-Span x 90' – Carbon steel – Marine – No washing



1-Span x 90' – Carbon steel – Marine – Steel washing

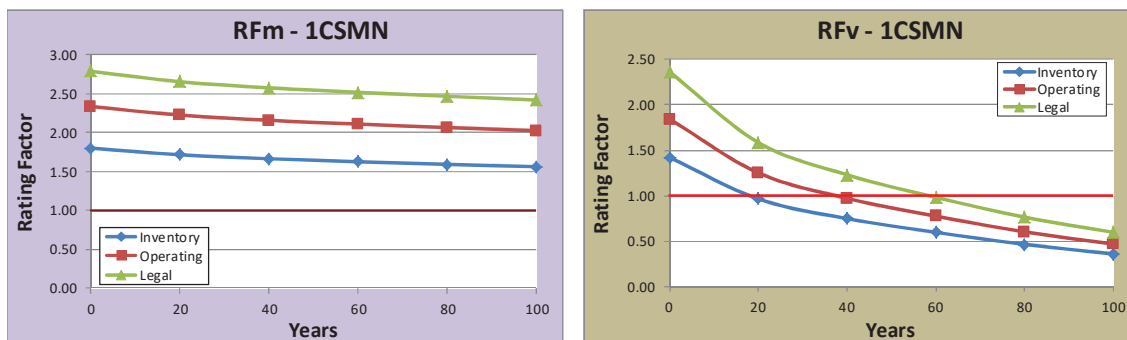


1-Span x 90' – Weathering steel – Marine – No washing

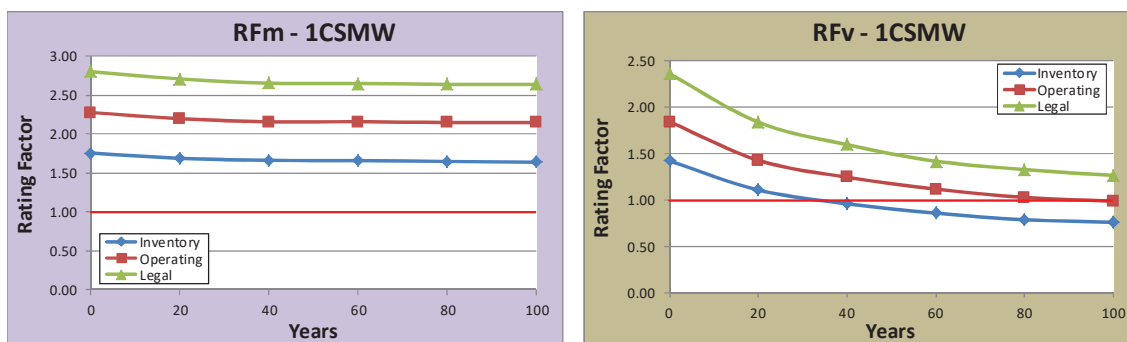


1-Span x 90' – Weathering steel – Marine – Steel washing

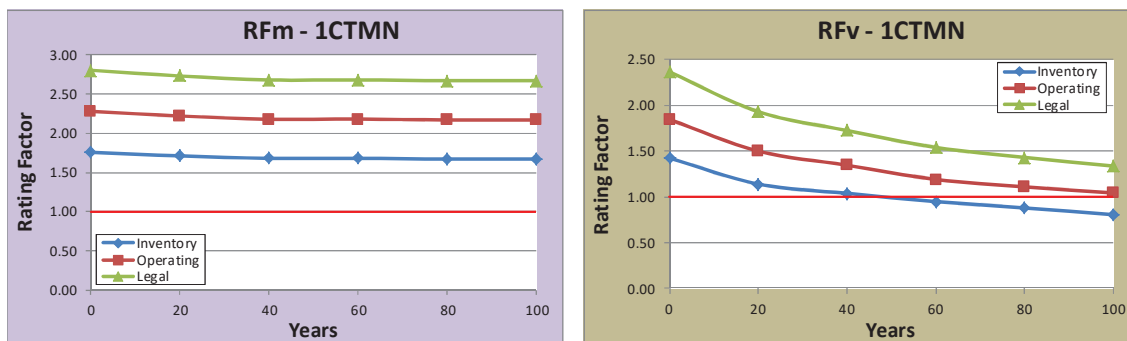
Figure J.10: RFm and RFv versus time for 1-Span x 90', Marine



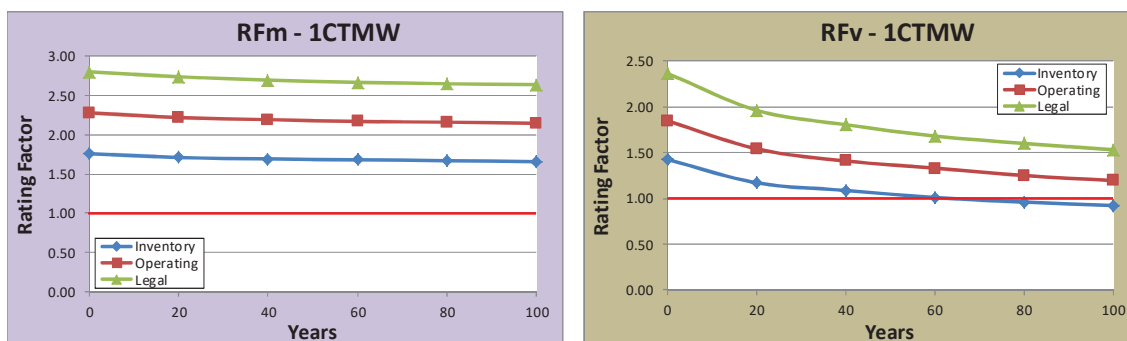
1-Span x 110' – Carbon steel – Marine – No washing



1-Span x 110' – Carbon steel – Marine – Steel washing

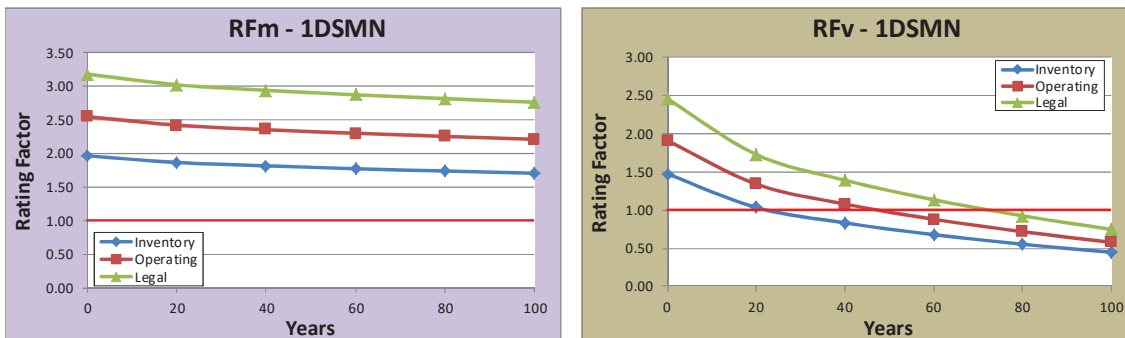


1-Span x 110' – Weathering steel – Marine – No washing

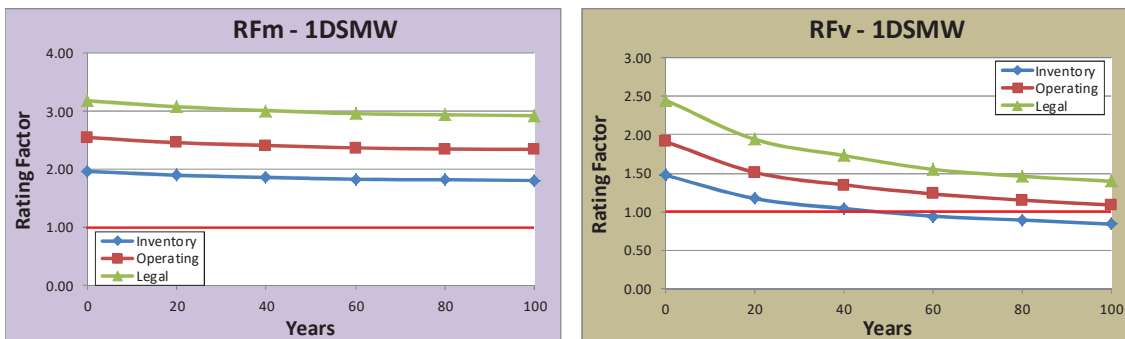


1-Span x 110' – Weathering steel – Marine – Steel washing

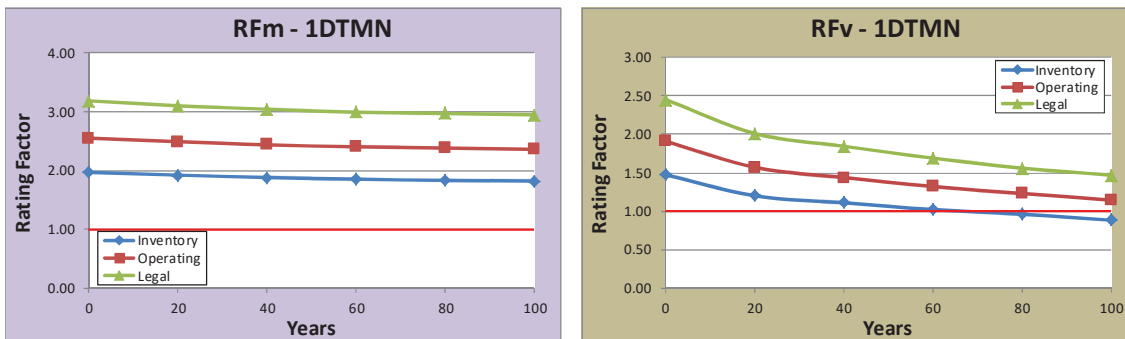
Figure J.11: RFm and RFv versus time for 1-Span x 110', Marine



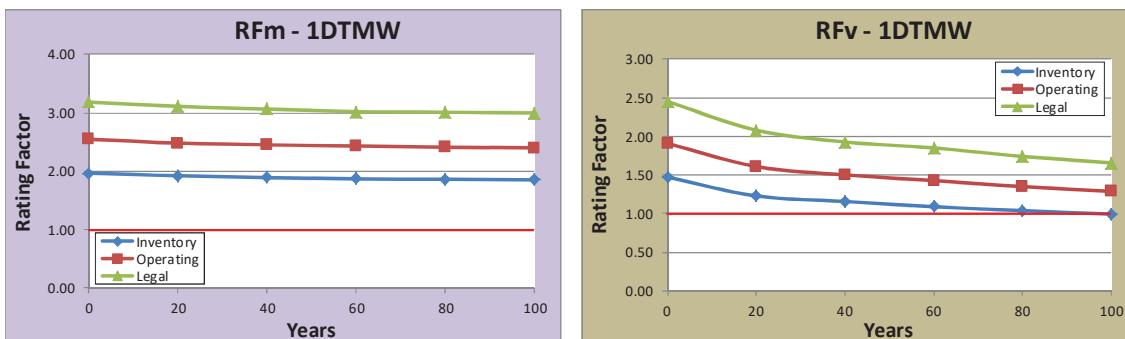
1-Span x 130' – Carbon steel – Marine – No washing



1-Span x 130' – Carbon steel – Marine – Steel washing

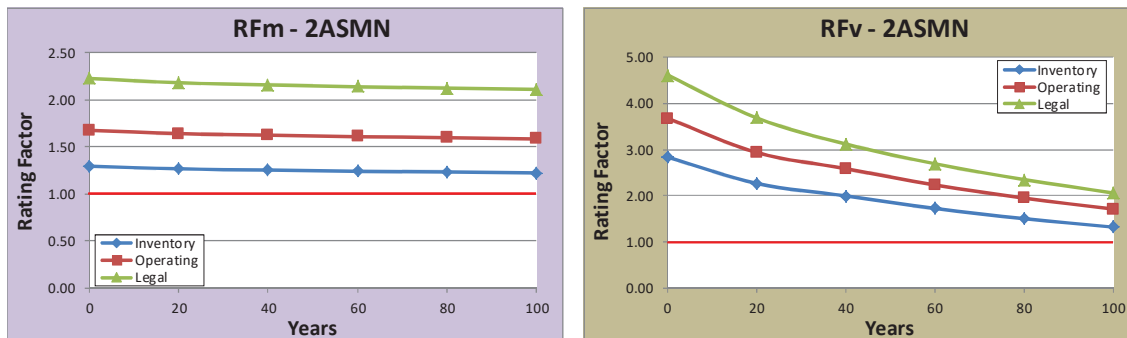


1-Span x 130' – Weathering steel – Marine – No washing

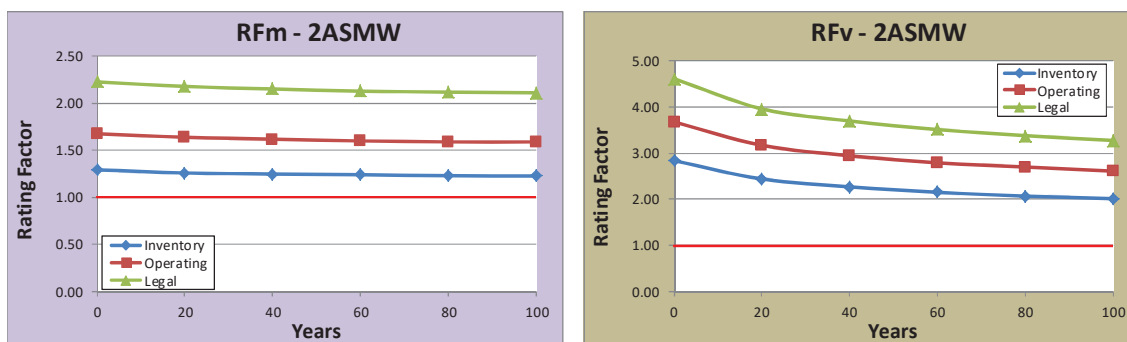


1-Span x 130' – Weathering steel – Marine – Steel washing

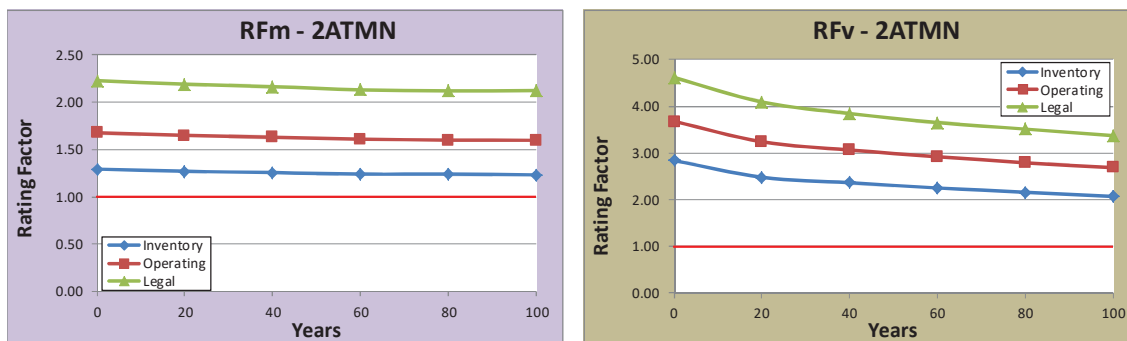
Figure J.12: RFm and RFv versus time for 1-Span x 130', Marine



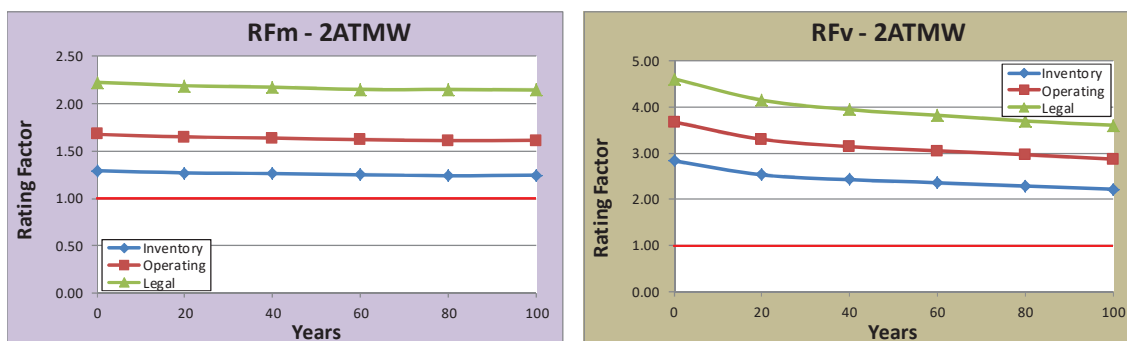
2-Span x 70' – Carbon steel – Marine – No washing



2-Span x 70' – Carbon steel – Marine – Steel washing

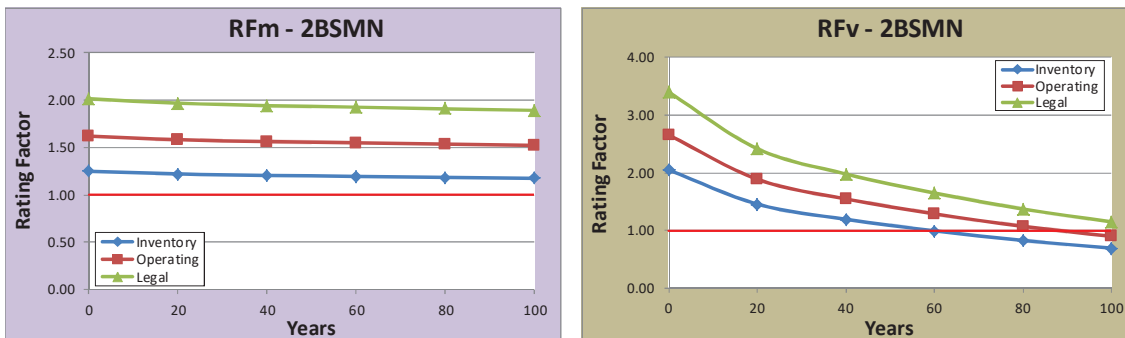


2-Span x 70' – Weathering steel – Marine – No washing

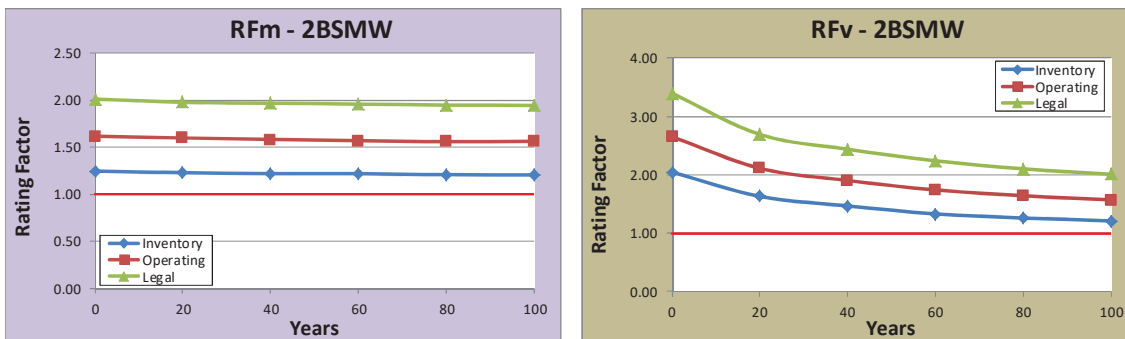


2-Span x 70' – Weathering steel – Marine – Steel washing

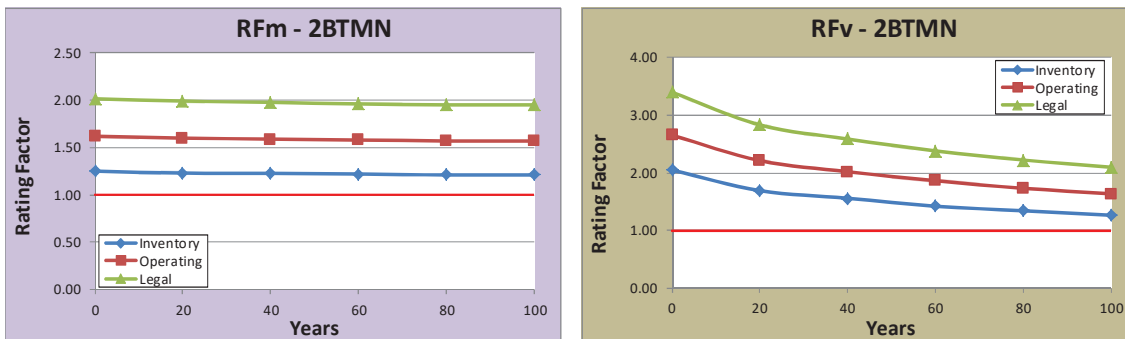
Figure J.13: RFm and RFv versus time for 2-Span x 70', Marine



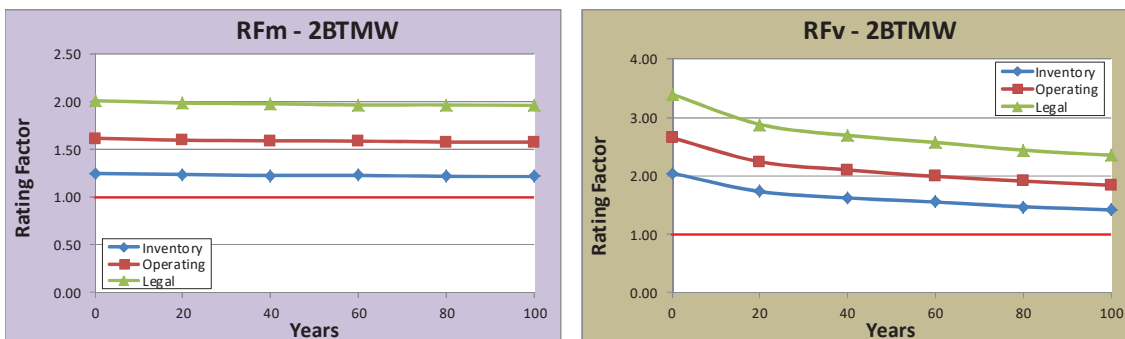
2-Span x 90' – Carbon steel – Marine – No washing



2-Span x 90' – Carbon steel – Marine – Steel washing

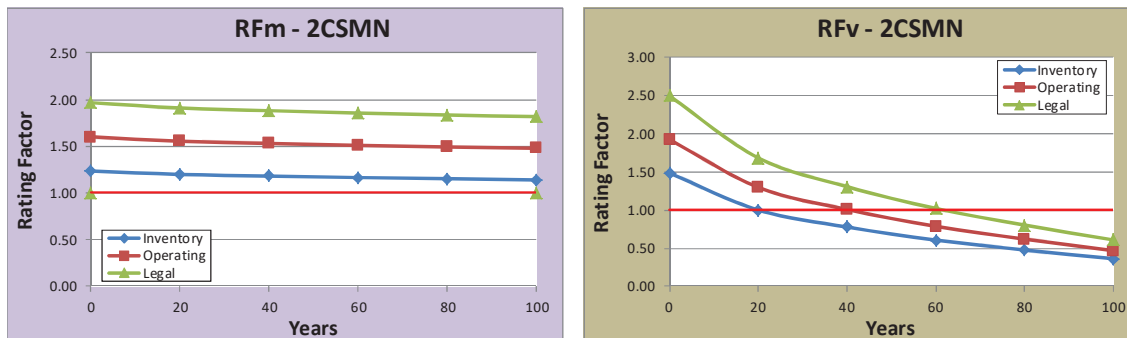


2-Span x 90' – Weathering steel – Marine – No washing

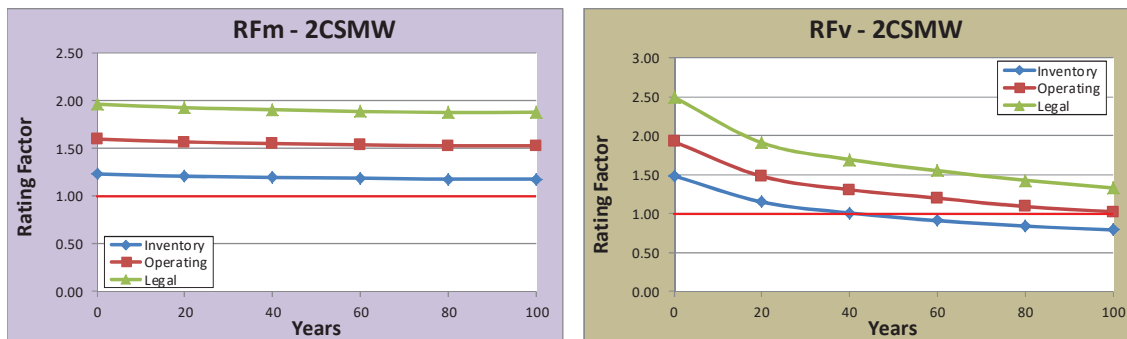


2-Span x 90' – Weathering steel – Marine – Steel washing

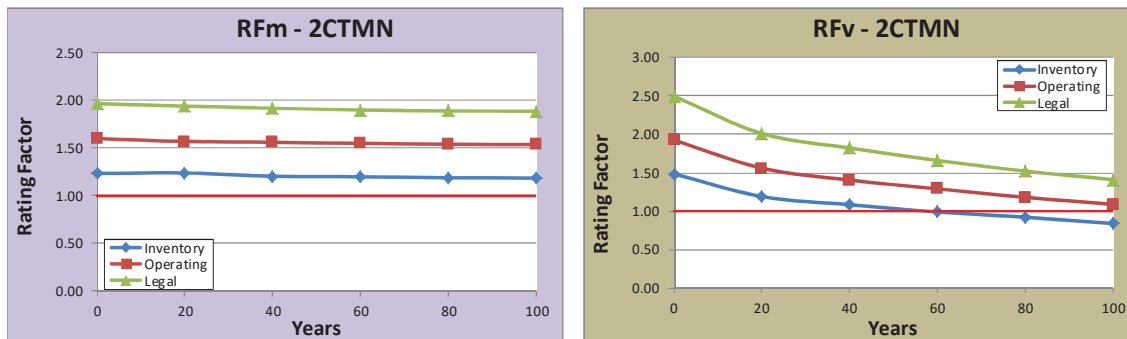
Figure J.14: RFm and RFv versus time for 2-Span x 90', Marine



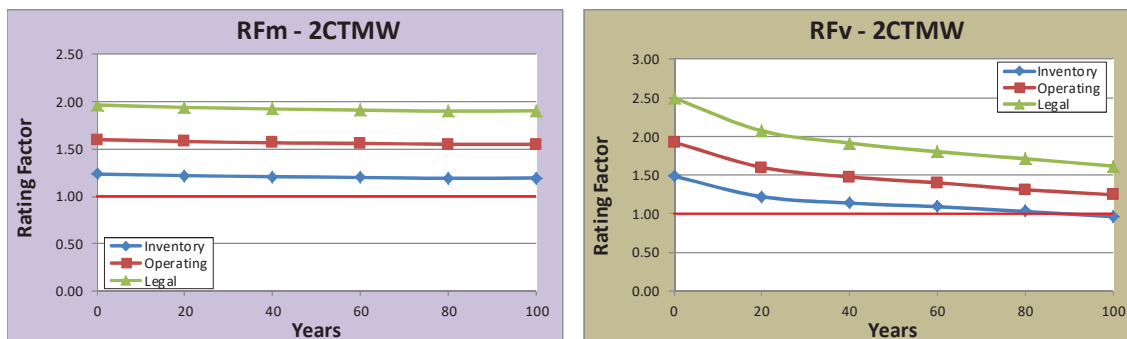
2-Span x 110' – Carbon steel – Marine – No washing



2-Span x 110' – Carbon steel – Marine – Steel washing

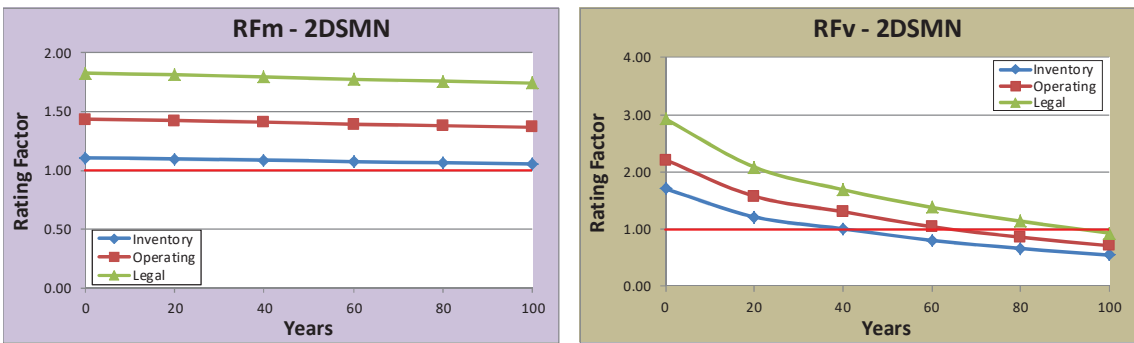


2-Span x 110' – Weathering steel – Marine – No washing

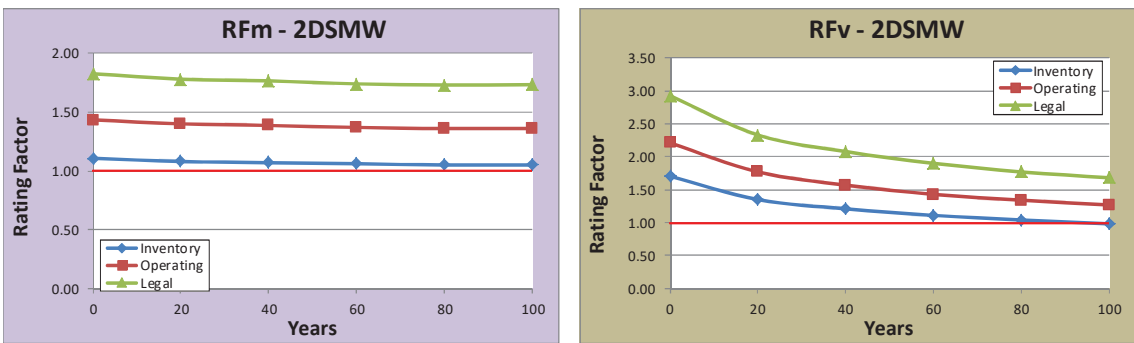


2-Span x 110' – Weathering steel – Marine – Steel washing

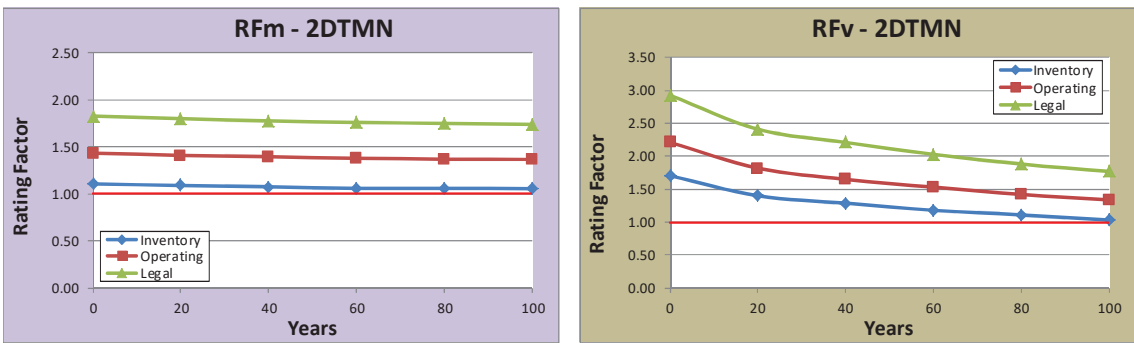
Figure J.15: RFm and RFv versus time for 2-Span x 110', Marine



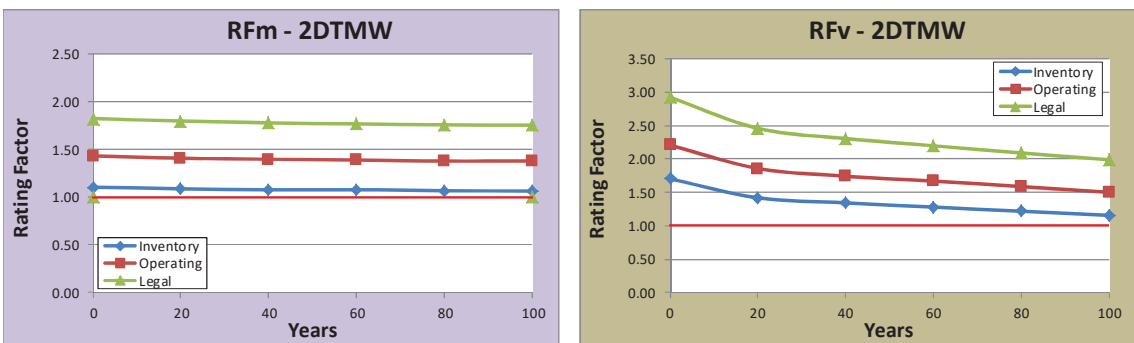
2-Span x 130' – Carbon steel – Marine – No washing



2-Span x 130' – Carbon steel – Marine – Steel washing

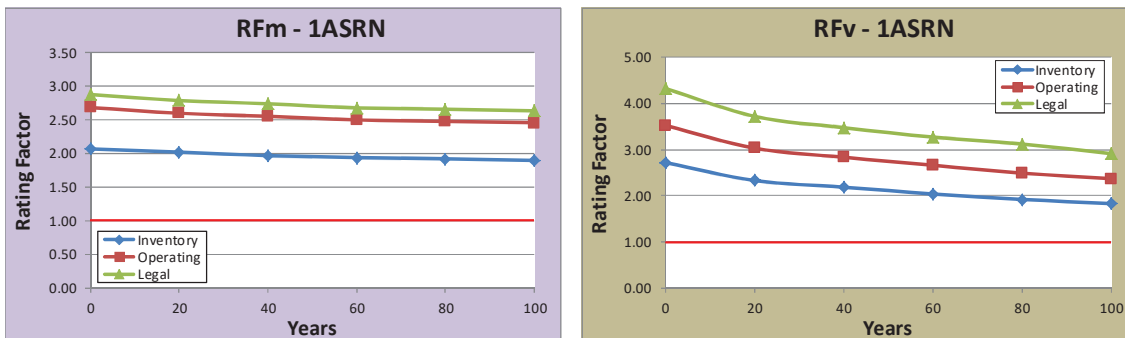


2-Span x 130' – Weathering steel – Marine – No washing

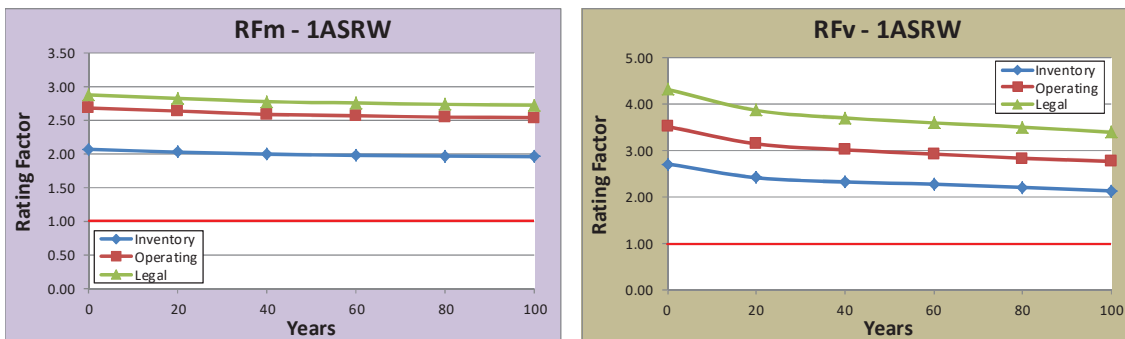


2-Span x 130' – Weathering steel – Marine – Steel washing

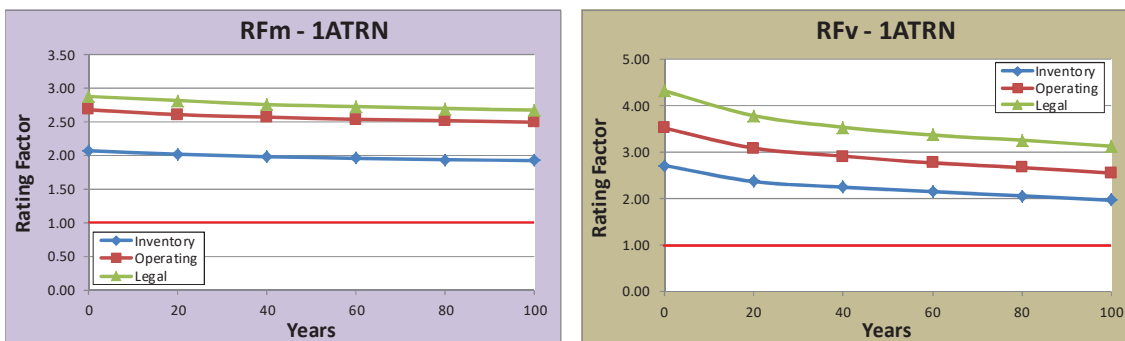
Figure J.16: RFm and RFv versus time for 2-Span x 130', Marine



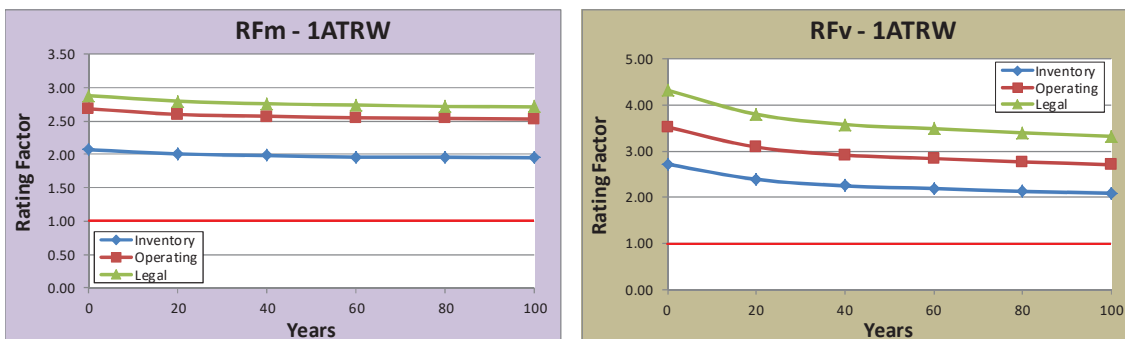
1-Span x 70' – Carbon steel – Rural – No washing



1-Span x 70' – Carbon steel – Rural – Steel washing

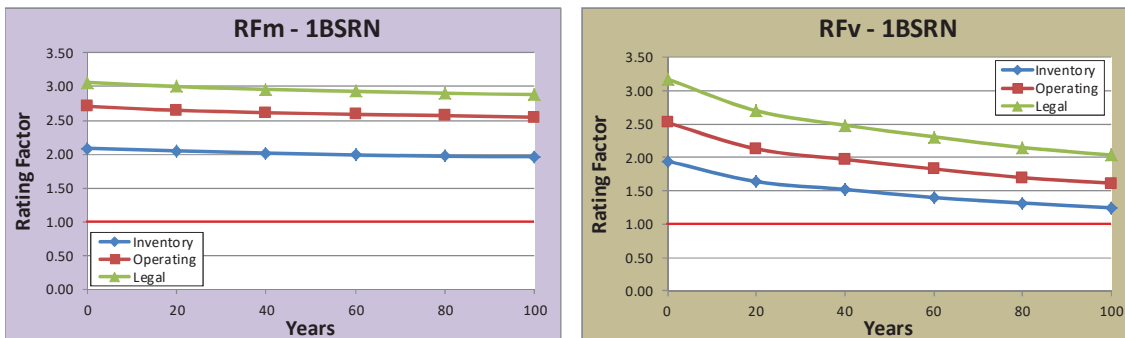


1-Span x 70' – Weathering steel – Rural – No washing

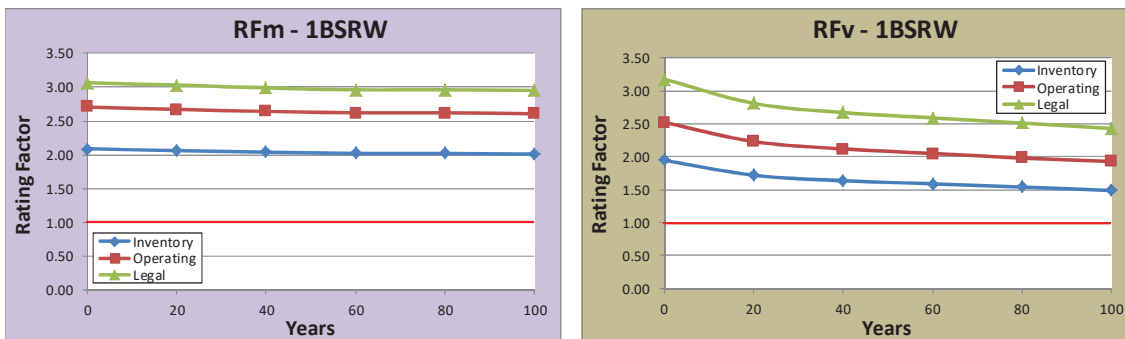


1-Span x 70' – Weathering steel – Rural – Steel washing

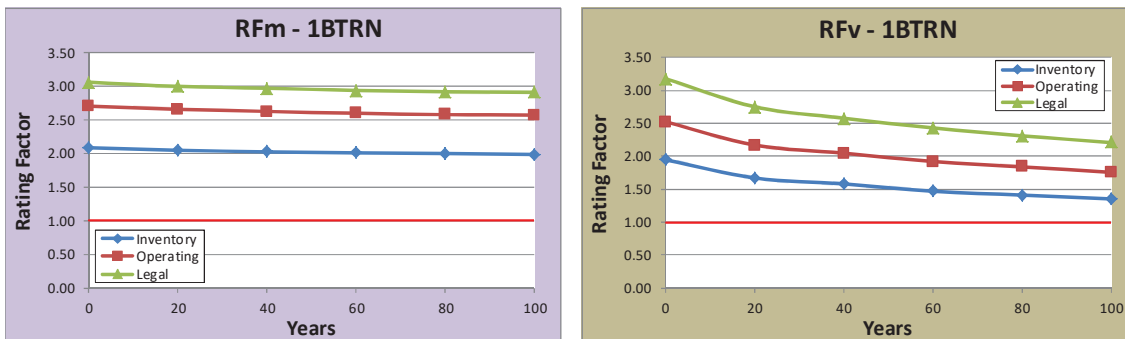
Figure J.17: RFm and RFv versus time for 1-Span x 70', Rural



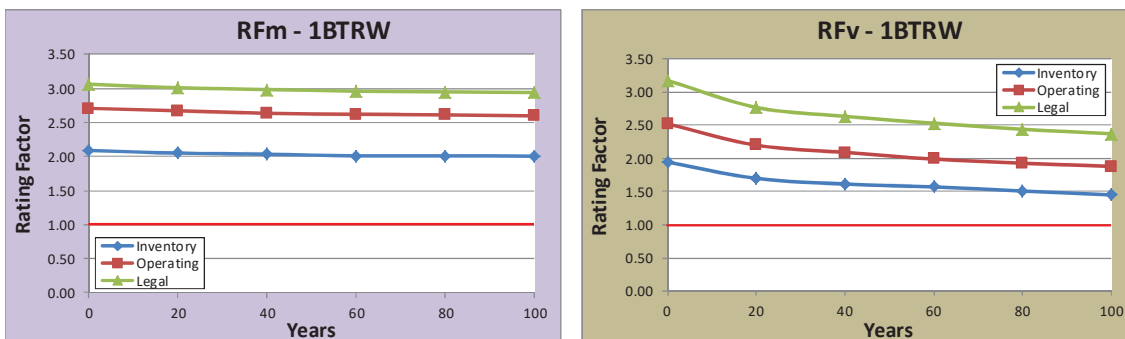
1-Span x 90' – Carbon steel – Rural – No washing



1-Span x 90' – Carbon steel – Rural – Steel washing

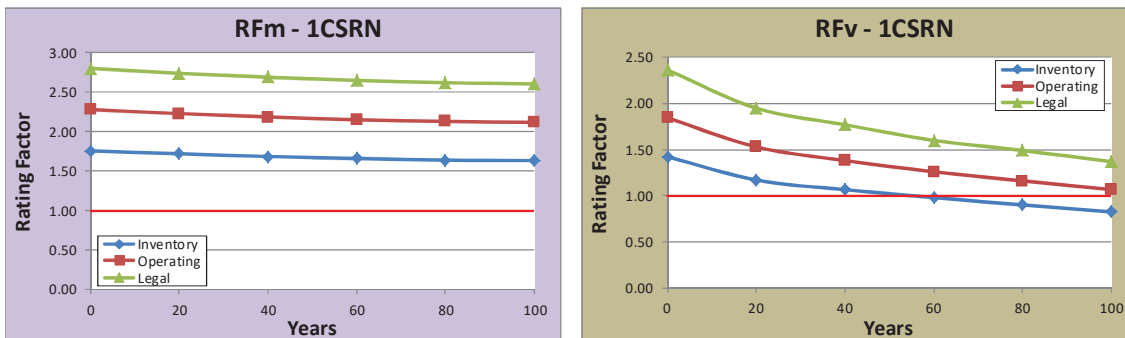


1-Span x 90' – Weathering steel – Rural – No washing

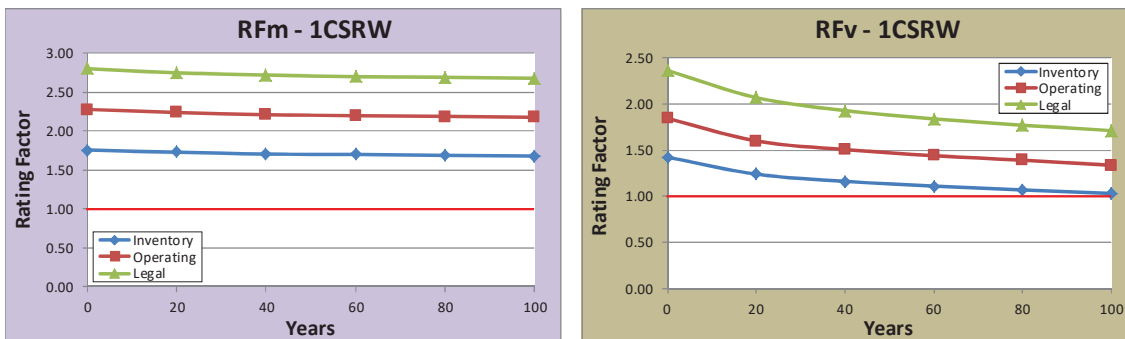


1-Span x 90' – Weathering steel – Rural – Steel washing

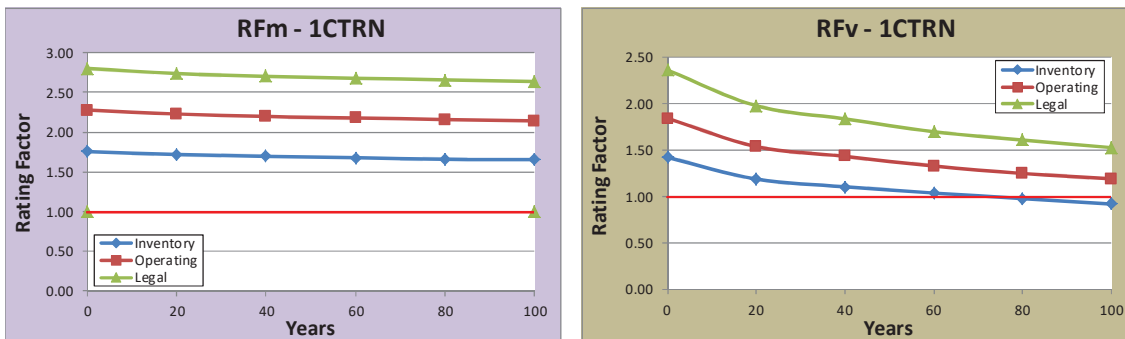
Figure J.18: RFm and RFv versus time for 1-Span x 90', Rural



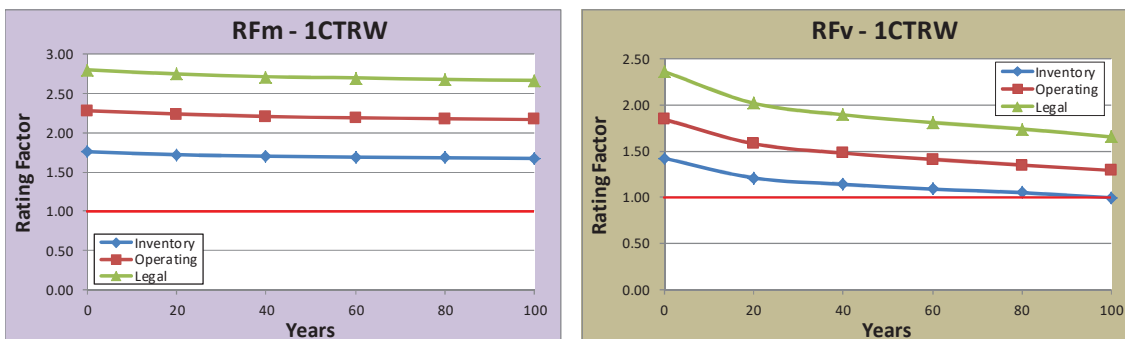
1-Span x 110' – Carbon steel – Rural – No washing



1-Span x 110' – Carbon steel – Rural – Steel washing

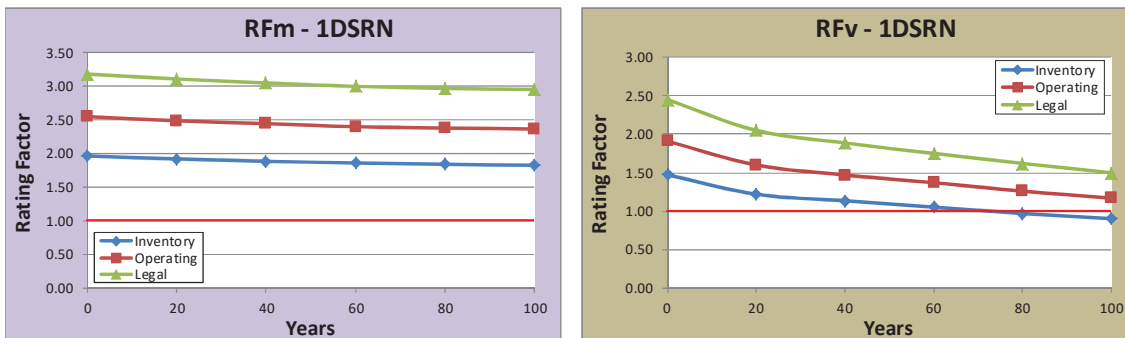


1-Span x 110' – Weathering steel – Rural – No washing

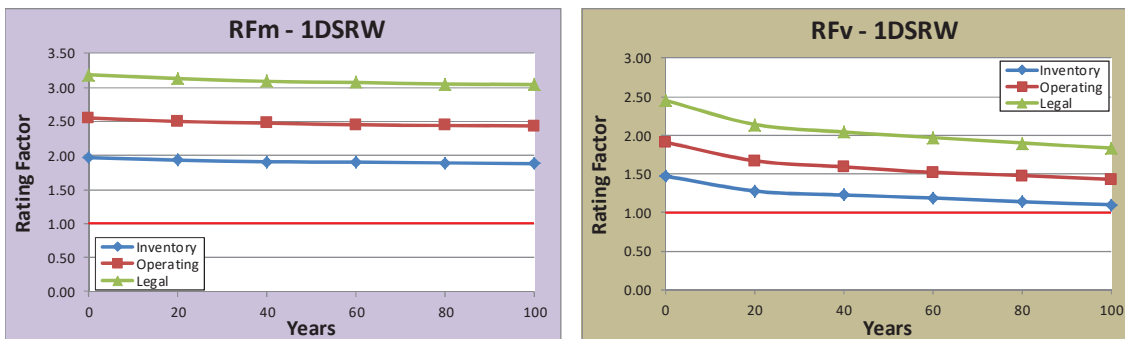


1-Span x 110' – Weathering steel – Rural – Steel washing

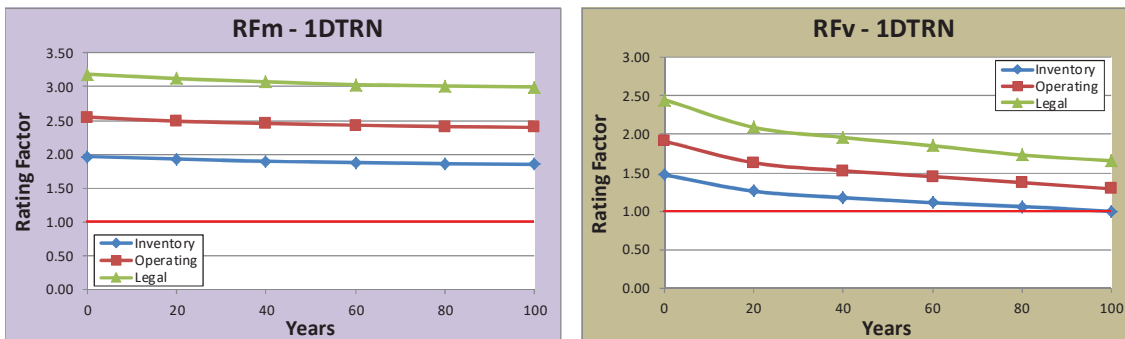
Figure J.19: RFm and RFv versus time for 1-Span x 110', Rural



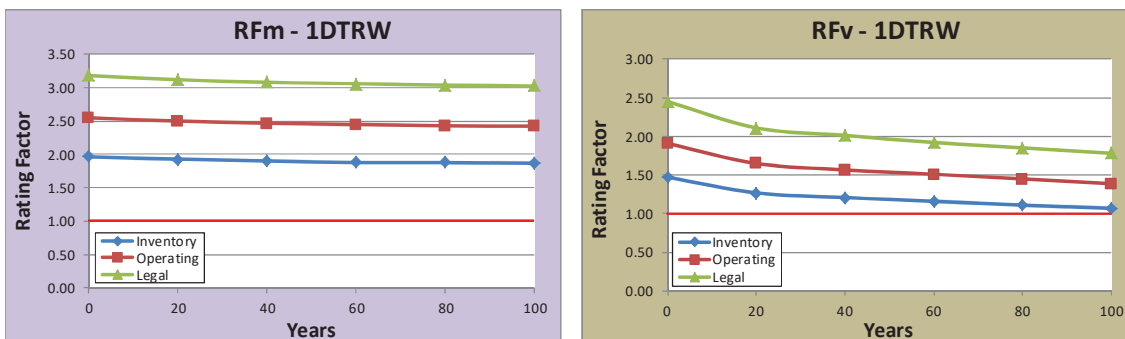
1-Span x 130' – Carbon steel – Rural – No washing



1-Span x 130' – Carbon steel – Rural – Steel washing

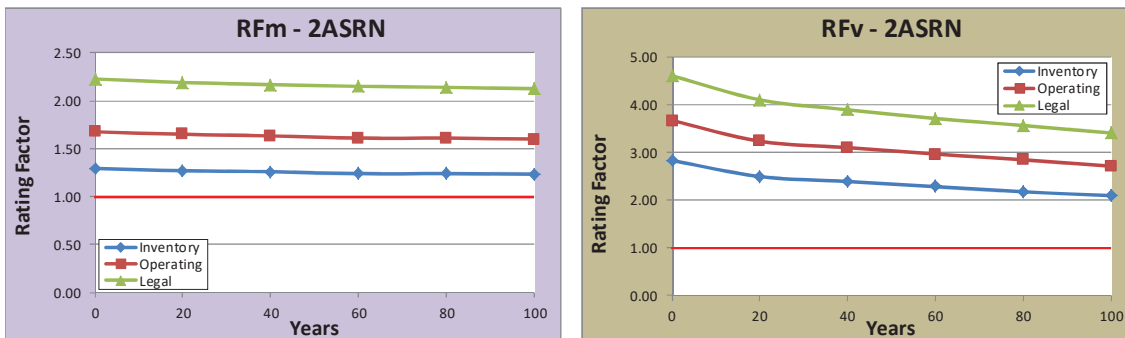


1-Span x 130' – Weathering steel – Rural – No washing

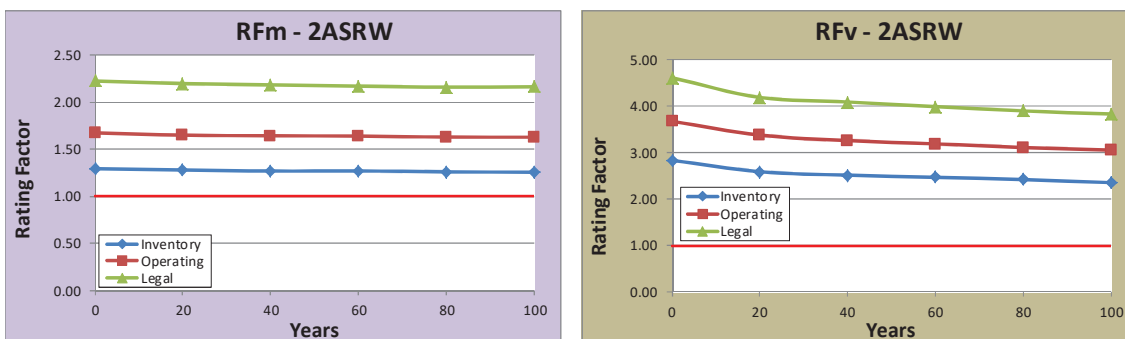


1-Span x 130' – Weathering steel – Rural – Steel washing

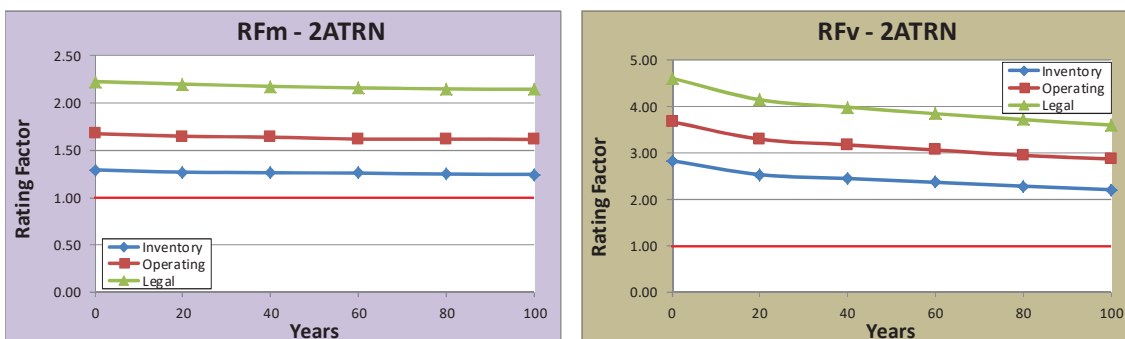
Figure J.20: RFm and RFv versus time for 1-Span x 130', Rural



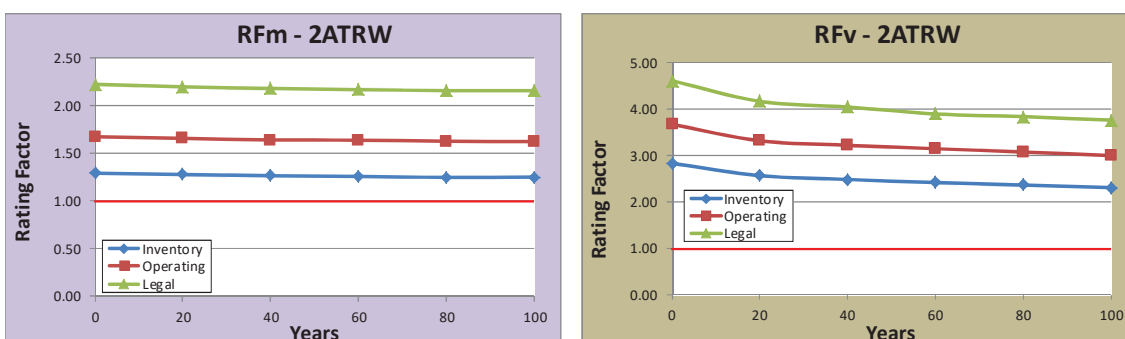
2-Span x 70' – Carbon steel – Rural – No washing



2-Span x 70' – Carbon steel – Rural – Steel washing

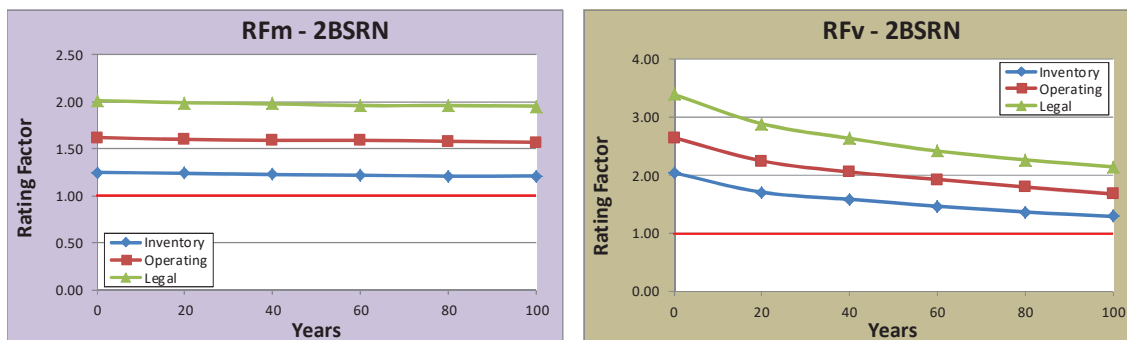


2-Span x 70' – Weathering steel – Rural – No washing

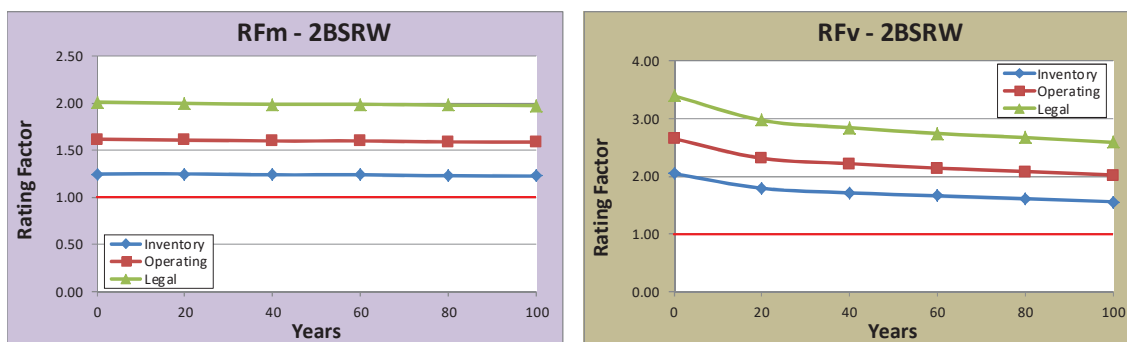


2-Span x 70' – Weathering steel – Rural – Steel washing

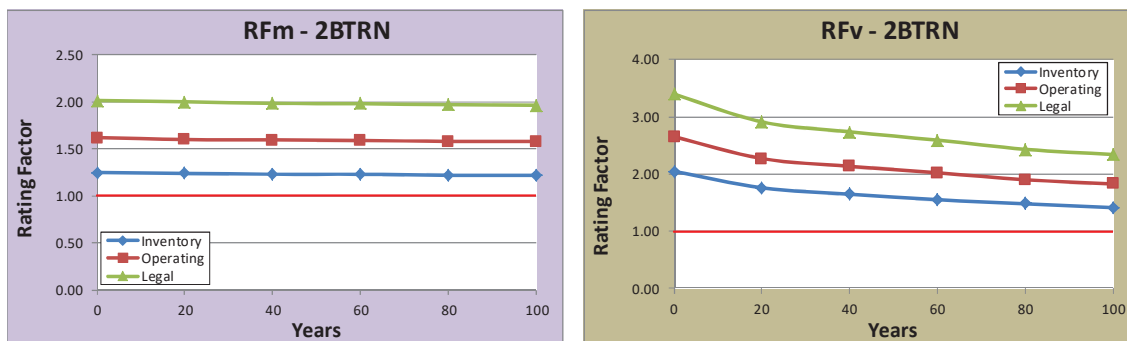
Figure J.21: RFm and RFv versus time for 2-Span x 70', Rural



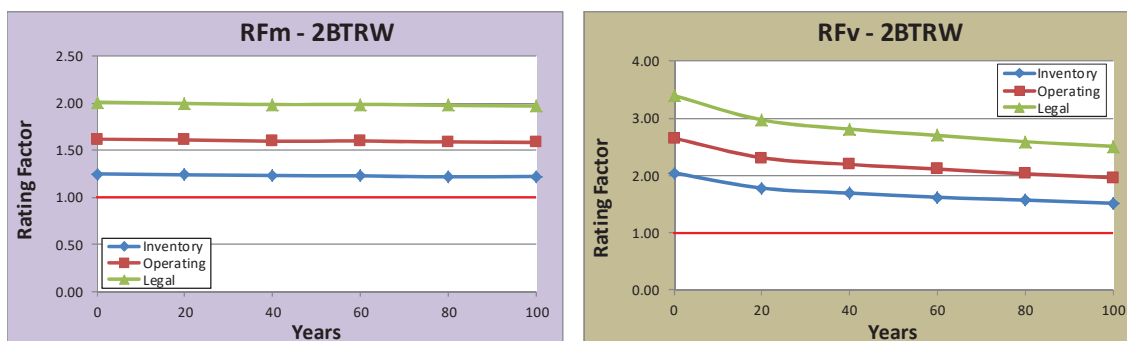
2-Span x 90' – Carbon steel – Rural – No washing



2-Span x 90' – Carbon steel – Rural – Steel washing

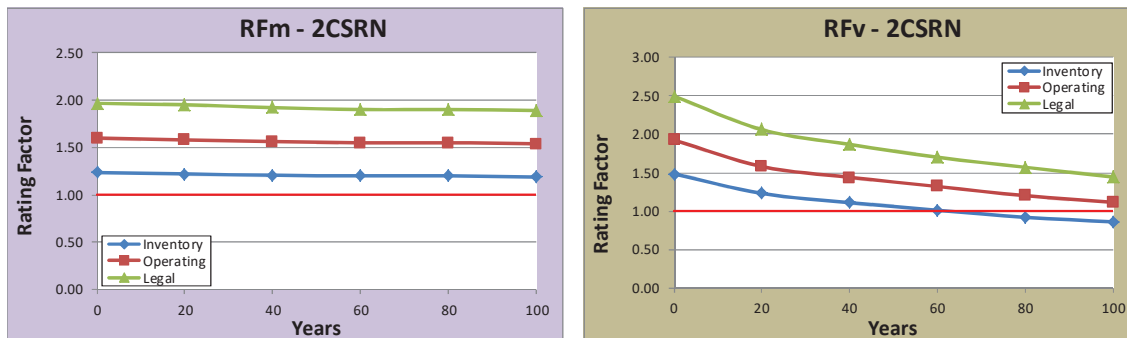


2-Span x 90' – Weathering steel – Rural – No washing

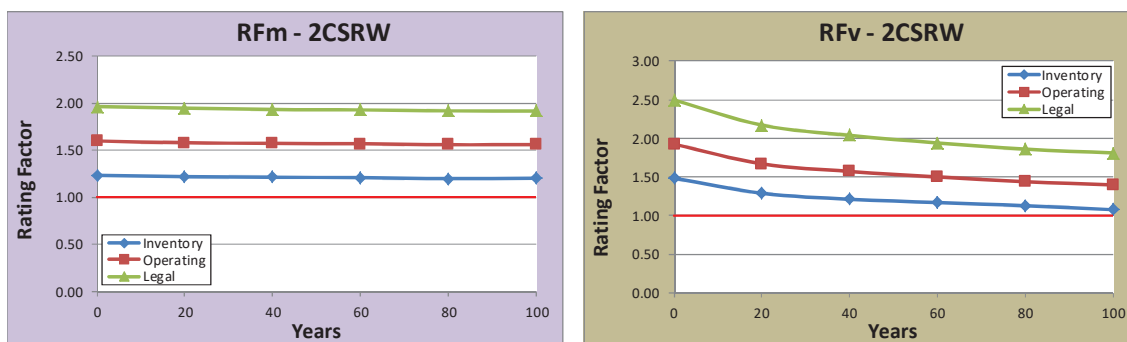


2-Span x 90' – Weathering steel – Rural – Steel washing

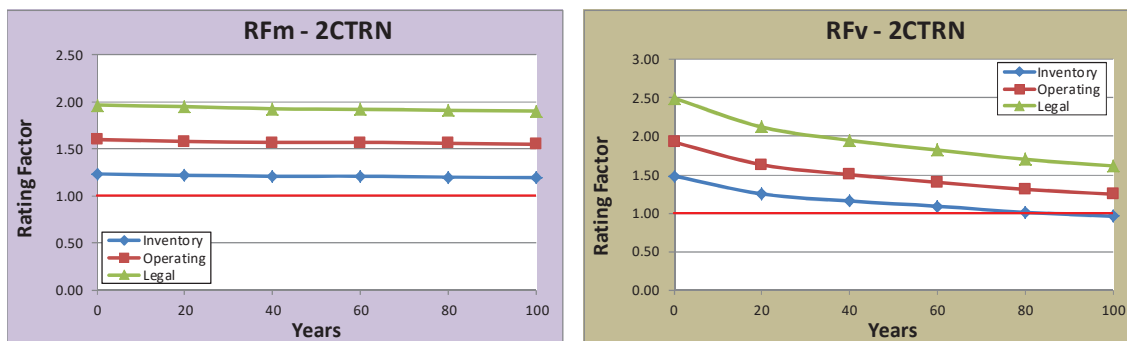
Figure J.22: RFm and RFv versus time for 2-Span x 90', Rural



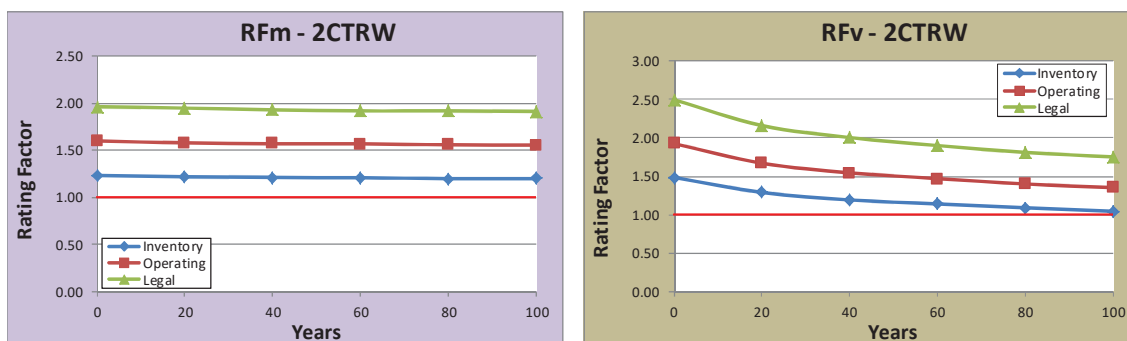
2-Span x 110' - Carbon steel - Rural - No washing



2-Span x 110' - Carbon steel - Rural - Steel washing

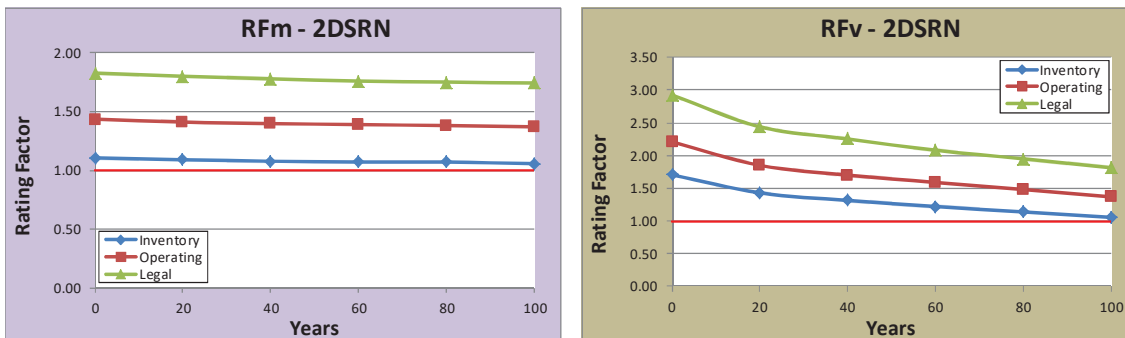


2-Span x 110' - Weathering steel - Rural - No washing

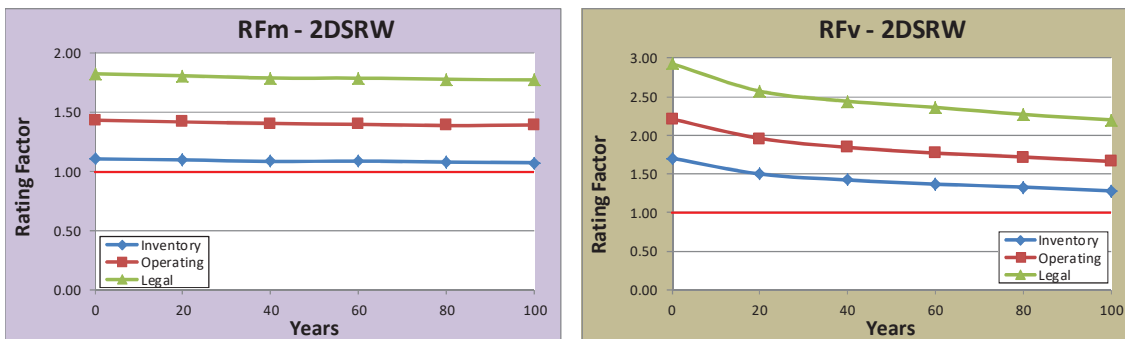


2-Span x 110' - Weathering steel - Rural - Steel washing

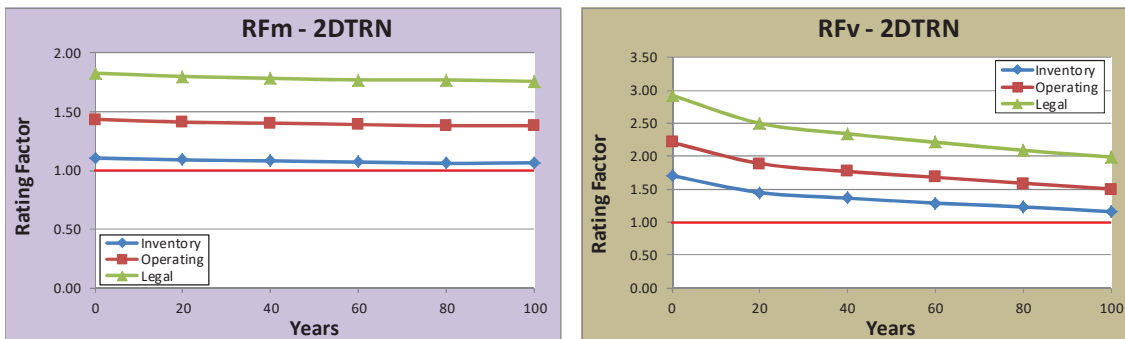
Figure J.23: RFm and RFv versus time for 2-Span x 110', Rural



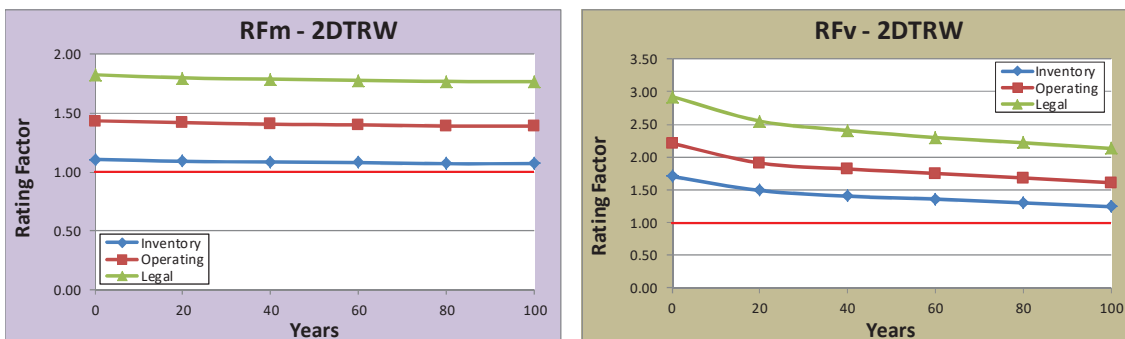
2-Span x 130' – Carbon steel – Rural – No washing



2-Span x 130' – Carbon steel – Rural – Steel washing



2-Span x 130' – Weathering steel – Rural – No washing



2-Span x 130' – Weathering steel – Rural – Steel washing

Figure J.24: RfM and RfV versus time for 2-Span x 130', Rural

VITA

VITA

Luis M. Moran Yanez was born in Lima, Perú on December 16th, 1960. He received his B.S. in Civil Engineering from the Pontifical Catholic University of Peru (Pontificia Universidad Católica del Perú) in 1986 and his M.S. in Civil Engineering from the Imperial College of Science and Technology - University of London, in London in 1991.